TU Delft

Delft University of Technology

Synergetically integrated vertical farms

Reducing energy and resource use through synergies between vertical farms and cities

Blom, T.

DOI
10.71690/abe.2024.17

Publication date
2024

Document Version
Final published version

Citation (APA)
Blom, T. (2024). *Synergetically integrated vertical farms: Reducing energy and resource use through synergies between vertical farms and cities* (24 ed.). [Dissertation (TU Delft), Delft University of Technology]. A+BE | Architecture and the Built Environment. https://doi.org/10.71690/abe.2024.17

Important note
To cite this publication, please use the final published version (if applicable).
Please check the document version above.

Copyright
Other than for strictly personal use, it is not permitted to download, forward or distribute the text or part of it, without the consent of the author(s) and/or copyright holder(s), unless the work is under an open content license such as Creative Commons.

Takedown policy
Please contact us and provide details if you believe this document breaches copyrights.
We will remove access to the work immediately and investigate your claim.

This work is downloaded from Delft University of Technology.
For technical reasons the number of authors shown on this cover page is limited to a maximum of 10.

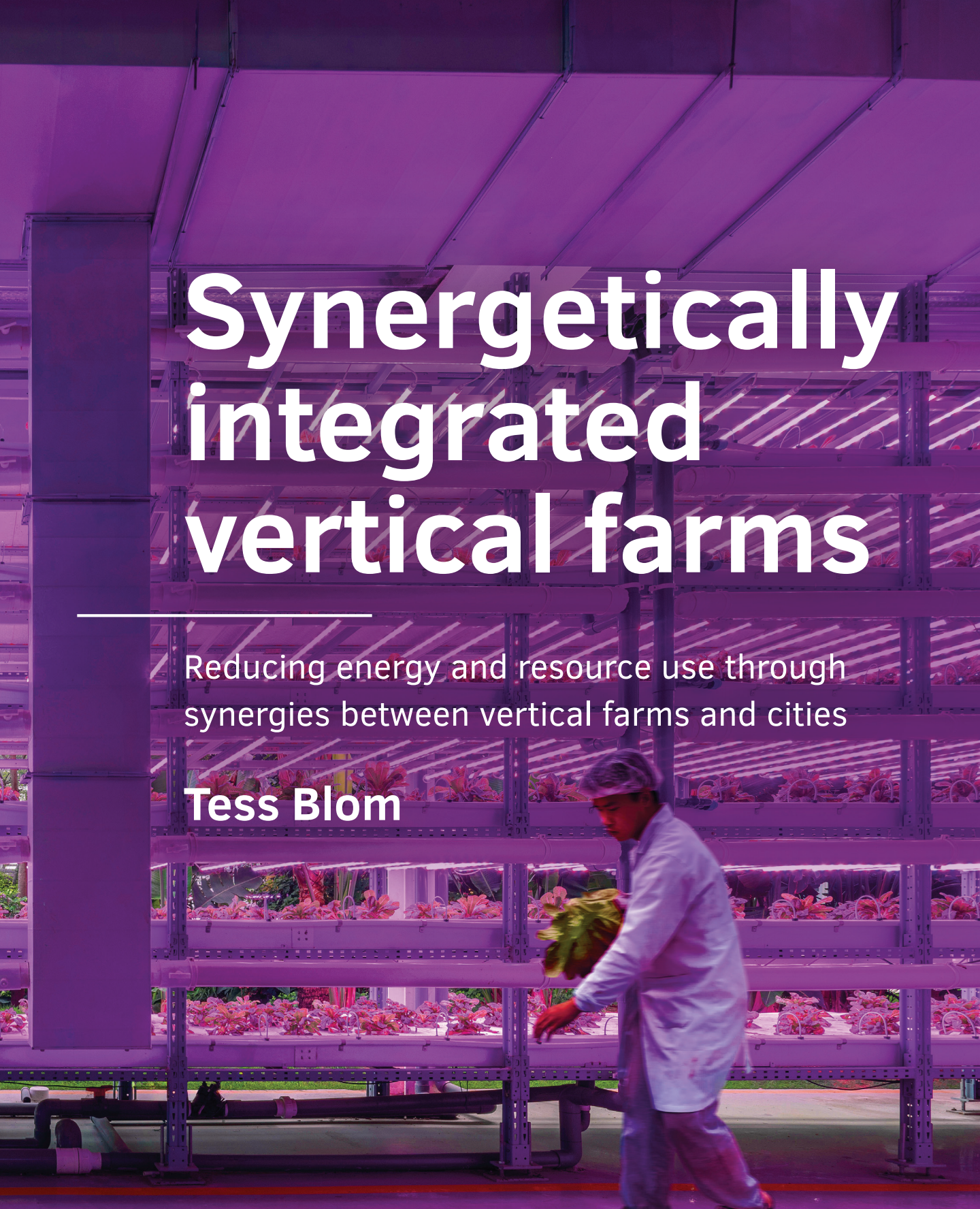

Synergetically integrated vertical farms

Reducing energy and resource use through synergies between vertical farms and cities

Tess Blom

Synergetically integrated vertical farms

Reducing energy and resource use through synergies between vertical farms and cities

Tess Blom

TOC

A+BE | Architecture and the Built Environment | TU Delft BK

24#17

Design | Sirene Ontwerpers, Véro Crickx

Cover photo | van Bergen Kolpa Architects, fotocredit: Jin Weiq

Keywords | carbon footprint, energy transition, residual heat, resource synergies, symbiosis, urban agriculture, vertical farming

ISBN 978-94-6366-938-2
ISSN 2212-3202

© 2024 Tess Blom

This dissertation is open access at https://doi.org/10.7480/abe.2024.17

Attribution 4.0 International (CC BY 4.0)

This is a human-readable summary of (and not a substitute for) the license that you'll find at:
https://creativecommons.org/licenses/by/4.0/

You are free to:
Share — copy and redistribute the material in any medium or format
Adapt — remix, transform, and build upon the material
for any purpose, even commercially.
This license is acceptable for Free Cultural Works.
The licensor cannot revoke these freedoms as long as you follow the license terms.

Under the following terms:
Attribution — You must give appropriate credit, provide a link to the license, and indicate if changes were made. You may do so in any reasonable manner, but not in any way that suggests the licensor endorses you or your use.

Unless otherwise specified, all the photographs in this thesis were taken by the author. For the use of illustrations effort has been made to ask permission for the legal owners as far as possible. We apologize for those cases in which we did not succeed. These legal owners are kindly requested to contact the author.

TOC

Synergetically integrated vertical farms

Reducing energy and resource use through synergies between vertical farms and cities

Dissertation

for the purpose of obtaining the degree of doctor
at Delft University of Technology
by the authority of the Rector Magnificus, prof.dr.ir. T.H.J.J. van der Hagen
chair of the Board for Doctorates
to be defended publicly on
Friday 1 November 2024 at 12:30 o'clock

by

Tess BLOM
Master of Science in Architecture, Urbanism and Building Sciences,
Delft University of Technology, the Netherlands
born in Breda, the Netherlands

TOC

This dissertation has been approved by the promotors.

Composition of the doctoral committee:

Rector Magnificus,	chairperson
Prof.dr.ir. A.A.J.F. van den Dobbelsteen	Delft University of Technology, promotor
Dr. A.J. Jenkins	Delft University of Technology, co-promotor

Independent members:

Prof.dr. L.C.M Itard	Delft University of Technology
Prof.dr.ir. A.L. Nillesen	Delft University of Technology
Dr.ir. C. Stanghellini	Wageningen University & Research
Dr. M.A. Martin	IVL Swedish Environmental Research Institute, KTH Royal Institute of Technology, Sweden
Prof.dr.ir. A.C. Boerstra	Delft University of Technology, reserve member

Non-independent members:

Dr. R.M. Pulselli	Mediterranean University of Reggio Calabria, Italy

This research was part of the TTW Perspectief programme “Sky High”, which is supported by AMS Institute, Bayer, Bosman van Zaal, Certhon, Fresh Forward, Grodan, Growy, Own Greens/Vitroplus, Priva, Philips by Signify, Solynta, Unilever, van Bergen Kolpa Architects, and the Dutch Research Council (NWO).

Acknowledgements

First of all, thanks to my supervisors, Prof.dr.ir. Andy van den Dobbelsteen and Dr. Andy Jenkins. Andy D., you recognised my potential as a researcher six years ago, offering me PhD position 2 years later, and guiding me up to my PhD defense. With your positive support, vast knowledge, and drive to create a more sustainable world, you have always been a great example for me. Thanks for your dedication, often reviewing my work late at night.

Andy J., despite the challenges of working primarily online over the past three years, your clear guidance and critical questions, especially in shaping the research proposal and methodology were greatly appreciated. Special thanks for your enthusiasm for urban agriculture and your positive attitude.

I would also like to thank Dr. Riccardo Pulselli, another key member of the Sky High TUD team. Thanks for your assistance with the carbon footprints and related publications. Thank you for teaching me how to create these carbon footprints even before my PhD journey began.

Many thanks to the independent members of the doctoral committee for taking time to read and assess my thesis. My PhD research was part of the Sky High project, funded by the TTW perspectief programme of NWO. I am grateful to all users and researchers for their support, knowledge, and critical questions during our consortium meetings.

Special thanks go to my family, especially to my parents Lot and Ruud, thank you for your unconditional love and for always supporting and believing in me, Pjotr and Marre with every step we take. This dissertation is dedicated to you.

Last but certainly not least, thanks to you Bart for your love and for being the best home office colleague I could ever ask for. Our endless neighbourhood walks, coffee and lunch breaks, and the cozy home we created together, and creating again. What a great team we make!

Thank you all

TOC

Contents

List of Tables 13
List of Figures 14
List of Definitions 17
List of Abbreviations 21
Summary 23
Samenvatting 27

1 **Introduction** 31

1.1 **Background** 31
1.1.1 Urban symbiosis: a strategy for sustainable cities 31
1.1.2 Urban food production to enhance symbiosis 32
1.1.3 Vertical farming: challenges and opportunities 33
1.1.4 Problem statement: exploring synergies between vertical farms and cities 35

1.2 **Research framework** 36
1.2.1 Research objective and questions 36
1.2.2 Research scope 37
1.2.3 Research approach and thesis outline 38

2 **The carbon footprint of Vertical Farming** 47

2.1 **Introduction** 48
2.1.1 Food security and climate change 48
2.1.2 The carbon footprint of vertical farming 49

2.2 **Methodology** 51
2.2.1 Description of the case studies 51
2.2.2 Carbon footprint assessment 54
2.2.3 Life cycle inventory 58

2.3 **Results** 61

2.4 **Discussion** 64
2.4.1 Farm life cycle 64
2.4.2 Crop life cycle 65
2.4.3 Renewable energy scenario 68
2.4.4 Total footprint with alternative scenarios 70
2.4.5 Comparison to other literature 71

2.5 **Conclusion** 74

3 **Vertical farms integrated into buildings** 81

3.1 **Introduction** 82

3.2 **Methodology** 84
3.2.1 Baseline vertical farm 85
3.2.2 Baseline conditions of buildings 88
3.2.3 Integration strategies for energy synergies 90

3.3 **Results** 94
3.3.1 Energy synergies 94
3.3.2 Crop, water, and nutrient flows 100

3.4 **Discussion** 103
3.4.1 Energy synergies 103
3.4.2 Crop, water, and nutrient flows 106

3.5 **Conclusion** 108

4 **Vertical Farms integrated into urban energy systems** 113

4.1 **Introduction** 115
4.1.1 The urban energy transition 115
4.1.2 The integration of vertical farms into urban energy systems 116
4.1.3 Research aim 117

4.2 **Methodology** 118
4.2.1 Step 1: Context and neighbourhood selection 119
4.2.2 Step 2: Energy profile of the neighbourhood 119
4.2.3 Step 3: Energy profile of the vertical farm 120
4.2.4 Step 4: District heat network configurations 122
4.2.5 Step 5: Energetic performance of the DHN configurations 122
4.2.6 Step 6: Integration with the electricity grid 124
4.2.7 Step 7: Selecting the optimal configuration and calculating the energy savings 127

4.3 **Results** 128
4.3.1 Step 1 to 3: Energy profiles of the neighbourhood and vertical farm 128
4.3.2 Step 4 and 5: District heat network configurations and energetic performance 129
4.3.3 Step 6: Integration with the electricity grid 133
4.3.4 Step 7: Selecting optimal energy systems configuration and determining savings 137

4.4 **Discussion** 138
4.4.1 Integration of the VF with district heating 138
4.4.2 Integration of the VF with the electricity grid 140

4.5 **Conclusion** 143

5 **The carbon footprint of synergetic vertical farms in cities** 149

5.1 **Introduction** 151
5.1.1 Vertical farming: addressing the global challenges in food production 151
5.1.2 The carbon footprint of vertical farming 151
5.1.3 Reducing the energy use of vertical farms 152
5.1.4 Research aim 154

5.2 **Methodology** 154
5.2.1 Step 1: Carbon footprint of standalone farming systems 159
5.2.2 Step 2: Scenario I - Reference city 163
5.2.3 Step 3: Scenario II - Vertical Farm city 164
5.2.4 Step 4: Scenario III - Synergetic Vertical Farm city 164
5.2.5 Step 5: Scenario IV - Attuned Synergetic Vertical Farm city 167

5.3 **Results** 168
5.3.1 Lettuce production in standalone vertical farming systems 168
5.3.2 Vegetable and fruit production in conventional and vertical farming systems 169
5.3.3 Carbon footprint for vegetable and fruit consumption and urban energy use 170

5.4 **Discussion** 172
5.4.1 Lettuce production in standalone vertical farming 172
5.4.2 Vegetable and fruit production in vertical farms 174
5.4.3 Synergetic integration of vertical farms with urban energy systems 175
5.4.4 Other sustainability indicators 177

5.5 **Conclusion** 178

6 **Conclusions** 185

6.1 **Sub-research questions** 186
6.1.1 The carbon footprint of vertical farming 186
6.1.2 Vertical farms integrated into buildings 187
6.1.3 Vertical farms integrated into urban energy systems 188
6.1.4 The carbon footprint of synergetic vertical farms 189

6.2 **Main research question** 190
6.3 **Research contribution** 191
6.4 **Research limitations** 192
6.5 **Recommendations for further research** 194
6.6 **Personal reflection on urban vertical farms** 195

Appendices 199

Appendix A Chapter 2 200
Appendix B Chapter 3 219
Appendix C Chapter 4 241
Appendix D Chapter 5 255

Curriculum Vitae 273
List of publications 275

List of Tables

2.1 Comparison of carbon footprints of VFs in literature and the activities included within those footprints. 50

3.1 Total energy use by the climate systems of one m^2 of one production layer of the VF and the thereby heated areas of the different building typologies when using integration strategies A1, B1, or E2. 96

4.1 Peak loads and operation costs (for 2022) per lighting concept when in fixed operation per m^2 cultivation area of the VF. 134

4.2 Cost flexible operation of the LEDs per m^2 cultivation area of the VF for two specific days in 2022. 136

4.3 Results per assessment criteria 137

5.1 Crop groups and their representative crop as included in this study, including the recommended intake of each crop group as presented by Righini et al. (2023). 157

5.2 Life Cycle Inventory of the production of potato, tomato, strawberry, and cucumber in VFs based on Righini et al. (2023) 162

5.3 Energy use of the City of Amsterdam in 2022 (CBS, 2018a,b; Klimaatmonitor, 2023) 163

5.4 The quantity of mid-temperature heat supplied to buildings using residual heat of VFs that produce different crops, and the energy use by the VF and decentralised energy system. 171

List of Figures

1.1 Impression of a vertical farming system. Image from: Philips Horticulture LED solution by Signify 34

1.2 Examples of synergetic exchanges of energy and resources between a city and vertical farm. 34

1.3 The Green House located within the city of Utrecht, hosting a restaurant, urban farm, and meeting rooms. This VF does not represent the fully enclosed environment as described in Section 1.1.3. Image from: © Lucas van der Wee 37

1.4 Thesis structure 39

2.1 Three-dimensional model of the operational VF case study, including the floor areas of the growth chamber and processing room. 53

2.2 The annual lettuce yields per m2 of gross floor area. 54

2.3 The system boundaries and the life cycle activities of both the farm and the crop as included in the carbon footprint assessment. Activities excluded by this study are depicted in faded grey. 57

2.4 The total carbon footprint of lettuce production within OF, GH(s), GH(a) and VF (please note that the farm end-of life value is not visible at this scale but is still included). 62

2.5 A comparison of the carbon footprint per life cycle stage of the four case studies: the life cycle of the farm including upstream (A) and end-of-life emissions (B), and the life cycle of the crop including upstream (C), core (D), downstream (E) and end-of-life emissions (F). 63

2.6 Carbon sequestration if the gross floor area used to produce one kg FW lettuce was used as a young forest. 65

2.7 Upstream emissions in the baseline scenario versus those when all farming methods use polypropylene packaging. 66

2.8 Downstream emissions in the baseline scenario versus those when all farming methods use polypropylene packaging. 67

2.9 End-of-life emissions of the baseline scenario versus those when all farming methods use polypropylene packaging. 68

2.10 Total core emissions in the baseline scenario versus those in the renewable energy scenario. 68

2.11 The total carbon footprint of lettuce production when considering the use of identical packaging, the transition to renewable energy, and the lost potential of carbon sequestration (please note that the farm end-of life value is not visible at this scale but is still included). 70

2.12 The total carbon footprint of lettuce production in the baseline scenario versus the alternative carbon footprint when considering the use of identical packaging, the transition to renewable energy, and the loss of potential of carbon sequestration. 71

2.13 Comparison of electricity use per kg FW produced by the studied VF and other CBVFs from literature. 72

2.14 Light use efficiency of various vertical farms in g FW produced per mol-1 of incident light. 72

3.1 Structure of the methods (Sections 3.2.1-3.2.3) and that of the results (Sections 3.3.1-3.3.2). 85

3.2 The selected cooling and dehumidification strategy for the VF in which HP1 is used to provide cooling below dew point temperature in HE1, and re-heating in HE2. HE3 removes the abundance of heat produced by the condenser. 87

3.3 The baseline scenario (0) and 5 different direct integration strategies to enable bidirectional exchange of energy between the VF and building (A1-E1). Dashed lines represent air flows, and solid lines represent water flows. 91

3.4 Three different strategies to enable year-round bidirectional exchange of thermal energy between a VF and building using aquifer thermal energy storage (C2-E2). The figure represents the winter season. Dashed lines represent air flows, and solid lines represent water flows. 92

3.5 Floor areas of different typologies that can be heated by creating bidirectional synergy with a vertical farm of one m2 cultivation area, i.e., one m2 of one production layer in the VF. Including the total annual energy use of the climate systems, and the LED systems of the vertical farm in kWh per m2 cultivation area. 98

3.6 Schematic representation of integration strategy HP+HP (E2) with ATES in summer. 100

3.7 The unidirectional flow of lettuce produced by one m2 of one production layer in the VF, that can theoretically be used to supply the annual vegetable consumption of the apartment's residents, the lunches of office employees, or the meals produced in the restaurant. 101

3.8 The unidirectional flows of grey water and nutrient outputs of the host building, that can be used to supply the water and nutrient demands of one m2 of one layer of cultivation area of the vertical farm. The therefore required water and nutrient production is expressed in the number of residents of the apartments, employees of the office, or visitors of the restaurant or swimming pool. 102

4.1 Methodology steps of the research 118

4.2 The cooling and dehumidification system of the VF, using one heat pump (HP1) and three heat exchangers (HE1, HE2, HE3). 121

4.3 Average electricity price per hour of the day for 2022 at day-ahead pricing by EPEX, the Netherlands (ENTSOE, 2023). 125

4.4 Lighting concepts considered for VF integration. 126

4.5 Monthly heating and cooling demands of the Westindische Buurt in 2023 (left) and annual thermal energy balance of the Westindische Buurt in 2023 (right). 128

4.6 Centralised energy system configuration with 4-pipe DHN in winter mode. 130

4.7 Annual electricity use of the Westindische Buurt with integrated VF using the centralised 4-pipe DHN configuration. 131

4.8 Decentralised energy system configuration with 2-pipe DHN in winter mode. 132

4.9 Annual electricity use of the Westindische Buurt with integrated VF using the decentralised 2-pipes DHN configuration. 133

4.10 Lighting concept C16/8(3x) consisting of three segmented VF modules with non-overlapping dark periods. 133

4.11 The baseline profile, and the optimised operation periods of the five alternative lighting concepts in pink. The average hourly electricity prices in 2022 are presented in blue (ENTSOE, 2023). 134

4.12 LED operation I8/4 standard versus flexible operation on January 18th, 2022. 135

4.13 LED operation I8/4 standard versus flexible operation on July 24th, 2022. 135

5.1 Activities included within the carbon footprint of scenario I ‘Reference city’. The vegetables and fruits consumed within the city are produced with conventional farming systems of which both activities within the life cycle of the farm and the crop are included in the carbon footprint. The energy needs of the city are met using existing systems. 155

5.2 Activities included within the carbon footprint of scenario II ‘Vertical farm city’. The vegetables and fruits consumed within the city are produced with vertical farming systems of which both activities within the life cycle of the farm and the crop are included in the carbon footprint. The energy needs of the city are met using existing systems. 156

5.3 Activities included within the carbon footprint of scenario III ‘Synergetic Vertical farm city’ and scenario IV ‘Attuned Synergetic Vertical farm city’. The vegetables and fruits consumed within the city are produced with synergetic vertical farming systems of which both activities within the life cycle of the farm and the crop are included in the carbon footprint. The residual heat of the vertical farm is used to replace the existing fossil-based eating systems. 156

5.4 Methodological steps. 158

5.5 Cooling and dehumidification system of the VF, and the energy systems required to supply the VF heat to the buildings. 165

5.6 Carbon footprints of three vertical farming systems producing lettuce. 168

5.7 Carbon footprints of potatoes, tomatoes, lettuce, strawberries, and cucumbers per kg FW when produced within open-field farming systems (OF), soil-based greenhouse horticulture (GHs), greenhouse horticulture using artificial light (GHa), and standalone vertical farming systems (VFI). ‘Conventional’ represents the average footprint of OF, GHs, and GHa production systems. 169

5.8 Carbon footprints per capita for the city of Amsterdam, including the energy use and the consumption of vegetables and fruits with scenario I-III. 170

List of Definitions

Term	Definition
Vertical farm	A food production system where crops are cultivated within a highly controlled indoor environment using artificial light and climate control systems (Germer et al., 2011; Benke and Tomkins, 2017; Delden et al., 2021). Vertical farms use minimal land by stacking growth systems vertically (Kalantari et al., 2017). This research specifically focusses on closed-box vertical farms, which are highly insulated, opaque, and airtight, minimising external climate and weather influences (Kozai & Nui, 2020; Graamans et al., 2018), and use hydroponic systems.

Term	Definition
Attuned vertical farm	A **vertical farm** designed to synchronise the operation and luminance of its artificial light systems with real-time electricity prices or the hourly share of renewable energy sources in the electricity grid-mix. Through these dynamic adjustments, i.e., **flexible electricity use**, the objectives are to enhance the balance between supplies and demands in the electricity grid, reflected in the electricity prices, or reduce the carbon emissions associated with lighting, respectively.
Attuned synergetic vertical farm	A **vertical farm** of which the generated residual heat is used for building heating purposes, while simultaneously aligning its electricity usage with the real-time electricity prices or the share of renewables in the electricity grid. This concept combines the principles from both the **Synergetic vertical farm** and the **Attuned vertical farm.**
Balanced energy system	This energy system ensures year-round supply of the heating and cooling demands of a given area. To that aim, aquifer thermal energy storage systems are used. These systems achieve an annual equilibrium if the total amount of heat and cold extracted and stored from both warm and cold buffer, i.e., aquifer, are equal.
Carbon footprint	A metric providing insight into the amount of greenhouse gas emissions released during a specific activity. The carbon footprint incorporates the three main greenhouse gas emissions that are released into the atmosphere: carbon dioxide, methane, and nitrous oxide (Pulselli, 2019). This footprint is expressed in kg of carbon dioxide equivalents.
Conventional farming	Traditionally common agricultural practices, including **open-field farming** and **greenhouse horticulture**.
Cultivation area vertical farm	The cumulative area of the **vertical farm** dedicated to crop cultivation, encompassing the different growth layers. The unit per square meter cultivation area specifies the inputs for each square meter of one cultivation layer in the vertical farm.
Greenhouse horticulture using artificial light	A semi-controlled (glazed) greenhouse that supplements natural light with artificial light. Crops are grown in raised beds using drip systems or in hydroponic systems. Climate control involves natural ventilation, solar energy, and, when necessary, mechanical heating and cooling systems.

>>>

Term	Definition
Greenhouse horticulture	Includes practices ranging from soil-based cultivation in uncontrolled environments, such as polytunnel structures, to semi-controlled indoor environments with hydroponic systems. Within this research, we focus on two types of greenhouse cultivation: **soil-based greenhouse horticulture** and **greenhouse horticulture using artificial light**.
Flexible electricity use	In this thesis, flexibility refers to the ability to accelerate or delay the injection or extraction of energy into or from an energy system, typically within time scales of less than a day (Vandermeulen et al., 2018). In the context of an **attuned vertical farm**, this means that increasing and decreasing LED luminance or switching the LEDs on or off. In this way urban energy systems with integrated **attuned vertical farms** can enhance overall energy system flexibility, minimising mismatches between electricity production and demand (Arabzadeh et al., 2023).
Open-field farming	The cultivation of crops directly in soil, exposed to open air, using irrigation in addition to rainfall (Breukers et al,. 2014). Active application of nutrients, pesticides, and herbicides is common practice (Barbossa et al., 2015).
Soil-based greenhouse horticulture	Semi-controlled (glazed) greenhouses in which crops are grown in raised beds with application of water through a drip system. The greenhouse makes use of natural ventilation, and solar energy for heating and for lighting (exclusively). When needed mechanical heating and cooling systems are used to optimise the climate conditions.
Symbiosis	Collaborations between two originally separate entities to create economic, environmental, and/or social benefits for both entities involved. Such symbiosis is established through the use of **synergies**.
Symbiotic integration	The integration of a certain system (e.g., vertical farm) with the energy and/or resource systems of another system (e.g., cities or buildings) to create **symbiosis** between both entities by the use of **synergies**.
Synergetic integration	See the definition of **symbiotic integration**
Synergetic vertical farm	A vertical farm which is in **symbiosis** with the surrounding built environment, using **synergetic** exchanges. In this research such synergetic vertical farm supplies its generation of residual heat to the heating systems of nearby buildings.
Synergy	The exchange of water, energy, and materials by geographical proximity of different objects or entities. Synergies are seen as the key to successful **symbiosis** (Marchi et al., 2018; Lombardi & Laybourn, 2012; Chertow, 2000).
Urban agriculture	The production, processing, and distribution of food, and other products by cultivating plants and/or raising livestock within the city to meet the local demands (Armanda et al., 2019).
Urban symbiosis	Originating from the term industrial symbiosis, it involves collaborations between two originally separate entities to create economic, environmental and/or social benefits for the industries involved (Chertow, 2000). Urban symbiosis aims to close material and energy flows within cities through the use of **synergies** (Vernay & Mulder, 2016).

References

Armanda, D.T., Guinée, J.B., Tukker, A. 2019. The second green revolution: Innovative urban agriculture's contribution to food security and sustainability: A review. Glob. Food Sec., 22, 13-24. https://doi.org/10.1016/j.gfs.2019.08.002.

Barbossa, G.L., Almeida, G.F.D., Kublik, N., Proctor, A., Reichelm, L., Weissinger, L., Wohlleb, G.M., Halden, R.U. 2015. Comparison of land, water, and energy requirements of lettuce grown using hydroponic vs. conventional agricultural methods. Int. J. Environ. Res. Public Health, 12(6), 6879-6891. https://doi.org/10.3390/ijerph120606879.

Benke, K., Tomkins, B. 2017. Future food-production systems: vertical farming and controlled-environment agriculture. Sustainability: Sci. Pract. Policy, 13(1), 13-26. https://doi.org/10.1080/15487733.2017.1394054.

Chertow, M.R. 2000. Industrial symbiosis: literature and taxonomy. Annu. Rev. Energy Environ., 25, 313–337. https://10.1146/annurev.energy.25.1.313.

Germer, J., Sauerborn, J., Asch, F., de Boer, J., Schreiber, J., Weber, G., Müller, J. 2011. Skyfarming an ecological innovation to enhance global food security. J. Verbraucherschutzd Lebensmittelsicherh., 6(2), 237-251. https://doi.org/10.1007/s00003-011-0691-6.

Graamans, L., Baeza, E., van den Dobbelsteen, A., Tsafaras, I., Stanghellini, C. 2018. Plant factories versus greenhouses: Comparison of resource use efficiency. Agric. Syst., 160, 31-42, https://doi.org/10.1016/j.agsy.2017.11.003.

Kalantari, F., Tahir, O. M., Joni, R. A., Fatemi, E. 2017. Opportunities and challenges in sustainability of vertical farming: A review. J. Landscape Ecol., 11(1), 35-60. https://doi.org/10.1515/jlecol-2017-0016.

Kozai, T., Niu, G. 2020. Role of the plant factory with artificial light (PFAL) in urban areas. In: Kozia, T., Takagaki, M., & Niu, G. (Eds.), Plant factory: an indoor vertical farming system for efficient quality food production. Academic Press, London, pp. 129-140. https://doi.org/10.1016/B978-0-12-801775-3.00002-0.

Lombardi, D.R., Laybourn, P. 2012. Redefining Industrial Symbiosis. J. Ind. Ecol., 16, 28-37. https://doi.org/10.1111/j.1530-9290.2011.00444.x.

Marchi, B., Zanoni, S., Pasetti, M. 2018. Industrial Symbiosis for Greener Horticulture Practices: The CO_2 enrichment from Energy Intensive Industrial Processes. Procedia CIRP 2018, 69, 562-567. https://doi.org/10.1016/j.procir.2017.11.117.

Pulselli, R.M., Marchi, M., Neri, E., Marchettini, N., Bastianoni, S. 2019. Carbon accounting for decarbonisation of European city neighbourhoods. J. Clean. Prod., 208, 850-868, https://doi.org/10.1016/j.jclepro.2018.10.102.

Vernay, A.L., Mulder, K. 2016. Organising urban symbiosis projects. Proceedings of the Institutions of Civil Engineers – Engineering Sustainability (online), 169(5), 181-188.

TOC

List of Abbreviations

Abbreviation	Description
ATES	aquifer thermal energy storage
BENG	Bijna energie neutral gebouwen; Dutch abbreviation for nearly zero-energy building
CBVF	closed-box vertical farm
COSP	coefficient of systems performance
COP	coefficient of performance
DHN	district heat network
DHW	domestic hot water
DW	dry weight
DLI	day light integral
EF	emission factor
EPEX	European Power Exchange
ET	Evapotranspiration
FW	fresh weight
GHa	greenhouse horticulture using artificial light
GHG	greenhouse gas emissions
GHs	soil-based greenhouse horticulture
HE	heat exchanger
HP	heat pump
LCA	life cycle assessment
LCI	life cycle inventory
LT	low temperature
LUE	light use efficiency
MT	mid temperature
NFT	nutrient film technique
OF	open-field farming
PPFD	photosynthetic photon flux density
PV	photovoltaic panel
RH	relative humidity
UA	urban agriculture
uLT	ultra-low temperature
VF	vertical farm

TOC

Summary

At present, agriculture is confronted with the significant challenge of increasing production to meet escalating global food demands, while simultaneously dealing with reduced land and resource availability. Moreover, there is an imperative need to lower greenhouse gas emissions for climate change mitigation. In response to these agricultural challenges, vertical farming has emerged as an evolving agricultural method designed to enhance productivity while minimising resource usage and environmental impact. Vertical farms achieve this by cultivating crops in vertically stacked hydroponic systems within an uniformly controlled indoor environment using active climate control systems and artificial light. Through this approach vertical farms operate independent of external climate factors and produce stable year-round yields.

Vertical farming is often advocated as a sustainable food system, as they offer several benefits over conventional farming systems, including efficient land use, high yields, minimal water and nutrient usage, the redundancy of pesticides and herbicides, and the ability to be located within or adjacent to cities where food demands are high. However, a major challenge for vertical farming is the substantial electricity use for artificial lighting and climate control. Despite this drawback, literature recognises vertical farming as a potential strategy to enhance energy and resource use efficiency in both agriculture and cities by creating synergies between both entities.

This study, centred in the Netherlands, addressed the research question:

How can the synergetic integration of vertical farms within cities reduce energy and resource usage as well as carbon emissions of both entities collectively?

The primary focus of the study was the exchange of residual heat produced by VFs with the cold generated when heating buildings in the city, i.e., energetic synergy.

To evaluate the potential of vertical farms to grow food in a sustainable way, this study extended beyond efficient land use and high yields, considering the entire life cycle of the crops cultivated in vertical farms. A carbon footprint assessment compared lettuce produced in an operational vertical farm to open-field farming and greenhouse cultivation in the Netherlands. The findings revealed that the substantial electricity use for artificial light and climate systems outweighed the aforementioned benefits of vertical farming from a carbon footprint perspective.

The high electricity use for artificial light results in the production of substantial quantities of waste heat. Starting at the building scale, we explored how this heat can be captured and reused for building heating. Furthermore, the potential to exchange flows of water and nutrients between the building and the vertical farm (to reduce the need for external inputs) were studied. On the larger urban scale, the possibility to create thermal energetic equilibrium within the local district heat networks using the excess heat from vertical farms was analysed. Moreover, we explored alternative lighting strategies for vertical farms to respond to electricity price fluctuations, addressing imbalances between electricity generation and consumption in the electricity grid, while ensuring the continuous production of fresh vegetables for the city.

Finally, we evaluated the potential benefits of integrating vertical farms with urban energy systems in terms of an overall carbon footprint. To this end, a carbon footprint assessment was performed for four different scenarios for the city of Amsterdam, ranging from a reference city relying on conventional farming methods and existing energy systems, to a city using residual heat from vertical farms that simultaneously attune their electricity use with the availability of renewable energy in the grid. The findings revealed that this attuned and synergetic integration of vertical farms with urban energy systems effectively reduced the collective energy use of both the vertical farm and the city, lowering the carbon footprint of vertical farms in cities. However, despite these carbon savings, the overall carbon footprint of such a synergetic city still surpassed that of cities relying on fossil-based heating and conventional farming for vegetable and fruit consumption. Although the energy used for heating was reduced by the integration of vertical farms, the overall increase was still attributed to the substantial energy use for artificial light to cultivate crops in vertical farms.

Furthermore, the study highlighted the need for careful consideration of location, crop selection, light use efficiency, and the use of residual heat to minimise the additional carbon emissions by the integration of vertical farms into cities. The observed increase in greenhouse gas emissions should be weighed against the potential benefits vertical farms bring to cities, including enhanced food security, self-sufficiency, replacement of fossil-based heating systems, efficient land use, and the flexibility offered to the electricity grid by attuning the LED lighting according to the availability of energy, reflected in the electricity prices.

Finally, the study revealed a trade-off between carbon footprint reduction and the essential need for flexible electricity operations in cities. Attuning LEDs to enhance grid stability, while crucial for cities, increases the carbon emissions of vertical farms. In summary, the synergetic integration of vertical farms presents substantial benefits for cities in terms of crop production, land use, flexible electricity utilisation, and heat supply. However, when focussing on the carbon footprint, vertical farms, even those in synergy with the city, face a significant challenge in competing with conventional farming systems due to the substantial use of electricity for lighting. Further development of effective lighting systems, perhaps hybrid with use of daylight, might leverage this backlash.

TOC

Samenvatting

De agrarische sector staat momenteel voor grote uitdagingen: om aan de wereldwijde groeiende voedselvraag te blijven voldoen moet de voedselproductie worden verhoogd, terwijl de beschikbaarheid van land en grondstoffen drastisch afneemt. Om klimaatverandering tegen te gaan is er tegelijkertijd een dringende noodzaak om de uitstoot van broeikasgassen te reduceren. Als reactie op deze uitdagingen heeft zich een innovatieve landbouwmethode ontwikkeld: verticale landbouw. Verticale landbouw richt zich op het maximaliseren van productiviteit en het minimaliseren van milieueffecten, land- en grondstofgebruik door gewassen te telen in verticaal gestapelde hydrocultuursystemen. Door het gebruik van actieve klimaatregeling en kunstverlichting kan verticale landbouw onafhankelijk van het buitenklimaat opereren en stabiele opbrengsten produceren.

Verticale landbouw wordt vaak gepromoot als een duurzaam voedselproductiesysteem vanwege de diverse voordelen ten opzichte van conventionele landbouw zoals efficiënt landgebruik, hoge opbrengsten, minimaal water- en nutriëntengebruik, afwezigheid van pesticiden en herbiciden, en de mogelijkheid om zich te vestigen binnen of aan de rand van steden waar de vraag naar voedsel hoog is. Een belangrijke uitdaging voor verticale landbouw is echter het aanzienlijke elektriciteitsverbruik voor kunstverlichting en klimaatregeling. Desondanks wordt verticale landbouw vaak gezien als een potentiële strategie om het gebruik van energie en grondstoffen in zowel landbouw als steden te optimaliseren door het realiseren van synergiën tussen beide entiteiten.

Deze studie, gericht op de Nederlandse context, onderzocht daarom de vraag:

Hoe kan de synergetische integratie van verticale landbouw in steden de vraag naar energie en grondstoffen en de uitstoot van CO2 van beide entiteiten gezamenlijk verminderen?

De focus van deze studie lag op het uitwisselen van restwarmte geproduceerd in verticale landbouwsystemen met restkoude geproduceerd tijdens het verwarmen van gebouwen.

Om de potentie van verticale landbouw als duurzaam voedselproductiesysteem te evalueren, werd in eerste instantie de huidige CO_2-voetafdruk van verticale landbouw onderzocht. Hierbij werd de volledige levenscyclus van sla geproduceerd in verticale landbouwsystemen in overweging genomen. Deze CO_2-voetafdruk werd vergeleken met die van sla geproduceerd in conventionele vollegrondsteelt en glastuinbouw in Nederland. De resultaten toonde aan dat het aanzienlijke elektriciteitsverbruik van kunstverlichting en klimaatsystemen de eerder benoemde voordelen van verticale landbouw overschaduwde ten opzichte van conventionele landbouwvormen op het gebied van CO_2-emissies.

Het hoge elektriciteitsverbruik resulteert tevens in de productie van een aanzienlijke hoeveelheid restwarmte. De tweede stap van dit onderzoek analyseerde hoe deze warmte kan worden hergebruikt voor het verwarmen van gebouwen. Daarnaast werd de potentie onderzocht om water en nutriënten tussen een gebouw en verticale landbouw uit te wisselen om het gebruik van externe invoer te verminderen. Als derde stap werd op een grotere stedelijke schaal onderzocht hoe deze restwarmte gebruikt kan worden voor het realiseren van thermisch evenwicht in lokale warmtenetten. Daarnaast onderzochten we alternatieve verlichtingsstrategieën die kunnen reageren op de disbalans tussen elektriciteitsopwekking en -verbruik in het net, welke wordt gereflecteerd in de elektriciteitsprijs. Als voorwaarde moest de continue productie van verse gewassen in verticale landbouw gewaarborgd te blijven.

Ten slotte werden de potentiële effecten van deze integratie van verticale landbouw met stedelijke energiesystemen op de CO_2-voetafdruk van zowel verticale landbouw als steden geëvalueerd. Hiertoe werd een CO_2-voetafdrukstudie uitgevoerd voor vier verschillende scenario's in de stad Amsterdam. Deze scenario's varieerden van een referentiestad, waarin conventionele landbouw- en energiesystemen de stedelijke vraag naar groente, fruit en energie voorzien, tot een stad waar groente, fruit en restwarmte worden geleverd door verticale landbouw die tegelijkertijd het energiegebruik afstemt op de beschikbaarheid van hernieuwbare energie in het net. De resultaten toonden aan dat deze afgestemde en synergetische integratie van verticale landbouw met stedelijke energiesystemen het gezamenlijke energiegebruik van de stad en verticale landbouw effectief verminderde. Dit resulteerde in een verlaging de CO_2-voetafdruk van verticale landbouw in steden. Ondanks deze reductie overtrof de totale CO_2-voetafdruk van deze synergetische stad die van steden die afhankelijk zijn van fossiele verwarmingssystemen en conventionele landbouw. Hoewel het energieverbruik voor het verwarmen van de stad werd verminderd door de integratie van verticale landbouw, was de hogere CO_2-voetafdruk toe te schrijven aan het substantiële energieverbruik van de kunstverlichting.

Om de bijkomende CO_2-emissies door de integratie van verticale landbouwsystemen in steden te minimaliseren is een zorgvuldige afweging van locatie, gewasselectie, efficiëntie van lichtgebruik en het gebruik van restwarmte essentieel. Deze toename in CO_2-emissies moet worden afgewogen tegen de potentiële voordelen die verticale landbouw kan bieden aan steden, waaronder verbeterde voedselzekerheid, restwarmte levering, efficiënt landgebruik en de flexibiliteit die verticale landbouw potentieel aan het elektriciteitsnet kan bieden door het afstemmen van de LED verlichting op de beschikbaarheid van energie in het net.

Daarnaast onthulde deze studie een spanningsveld tussen het verlagen van de CO_2-voetafdruk van verticale landbouw en de essentiële behoefte aan een flexibele elektriciteitsvoorziening in steden. Hoewel het afstemmen van energiegebruik met de vraag en aanbod in het elektriciteitsnet cruciaal is voor de toekomst van onze steden, verhoogde deze aanpak de CO_2-emissies van verticale landbouwsystemen. Samengevat kan de synergetische integratie van verticale landbouw aanzienlijke voordelen leveren voor steden op het gebied van voedselproductie, landgebruik, flexibel elektriciteitsverbruik en alternatieve warmtevoorziening. Echter, wanneer enkel de CO_2-voetafdruk in acht wordt genomen, worden verticale landbouwsystemen geconfronteerd met aanzienlijke concurrentie van de huidige landbouwsystemen, vanwege het hoge elektriciteitsverbruik voor verlichting. Verdere ontwikkelingen van effectieve verlichtingssystemen, wellicht hybridesystemen met gebruik van daglicht, zouden deze voetafdruk potentieel kunnen verlagen.



Philips Horticulture LED solution by Signify

TOC

1 Introduction

1.1 Background

1.1.1 Urban symbiosis: a strategy for sustainable cities

Cities are responsible for 70% of the global greenhouse gas (GHG) emissions (Hirschl, 2018) and present an opportunity and a challenge to combatting climate change. Approximately 90% of the urban resources come from outside their city boundaries (Dobbelsteen et al., 2018). Cities can, thus, be seen as sinks relying on rural areas to meet their energy and resource demands (Hirschl, 2018). The excessive extraction and consumption of resources within cities exceed the earth's capacity to regenerate, leading to environmental degradation and depletion of natural resources (Sanches & Bento, 2020).

Simultaneously, the global population is expected to reach 9.7 billion by 2050 (UN, 2019), of which between 70% and 80% will be living in cities (Lucertini and Musco, 2020). To accommodate this growth within the planetary boundaries, cities must reduce their energy and resource consumption, and the associated GHG emissions drastically. This should not only include the reduction of end-user consumption but also the exchange of waste streams, referring to as the second step of the 'New Stepped Strategy' (Dobbelsteen et al., 2008). This strategy, based on the Trias Energetica, introduces an intermediate step between reducing energy demands and producing renewable energy, focussing on the reuse of residual flows (Tillie et al., 2009).

By reusing waste outputs of one urban function as inputs for another, cities can effectively close resource cycles and minimise waste production (Broekhoven and Vernay, 2018). This concept, known as urban symbiosis, thrives on the collaboration between two originally separate urban systems in geographic proximity (Vernay and

TOC

Mulder, 2016; Chertow, 2000). These collaborations include synergetic exchanges of materials, energy, water, or by-products (Marchi et al., 2018; Lombardi and Laybourn, 2012). Given that all buildings and urban areas generate waste streams, making use of these could significantly reduce energy and resource demands (Tillie et al., 2009). Such exchanges are most cost- and resource-efficient when functions are in close proximity (Lenhart et al., 2015).

1.1.2 Urban food production to enhance symbiosis

An example of urban symbiosis is the exchange of energy, water, materials (Vernay et al., 2010) and nutrients (Jurgilevich et al., 2016) between urban agriculture (UA) and the city. Currently, the agricultural sector is responsible for approximately 11% of global anthropogenic GHG emissions (Smith et al., 2008). Considering the full value chain, from farm-to-fork, agriculture's GHG emissions range from 26% (Poore and Nemecek, 2018) to 37% (Mbow et al., 2019). Agriculture faces increasing challenges as a result of declining resource availability, including decreasing availability of arable land, freshwater supplies, and soil degradation (Kikuchi et al., 2018; Benke and Tomkins, 2017). Simultaneously, global food demands are expected to increase by 70% between 2017 and 2050, driven by population growth and dietary changes (Hunter et al., 2017). To meet this growing demand while reducing the environmental footprint of food production, innovative farming methods, such as urban farming, are needed.

In recent years, UA has gained worldwide popularity for its social, economic, and environmental benefits, including social coherence, improved food security, job creation, and shorter supply chains (Armanda et al., 2019; Sanjuan-Delmás et al., 2018; Kozai and Niu, 2020; Sanyé-Mengual and Montero, 2015). UA is defined as producing, processing, and distributing food and other products from plants grown or livestock raised within cities to meet local demands (Armanda et al., 2019). Despite the numerous benefits, the sustainability of UA in terms of carbon footprint is subject to debate. Local food production can only reduce GHG emissions when its emissions are lower than those of the importable alternatives (Avetisyan et al., 2013) and this can vary significantly per region (Vermeulen et al., 2012).

Urban food production holds the potential to close resource cycles of energy, water, materials (Vernay et al., 2010), and nutrients (Jurgilevich et al., 2016), through synergetic exchanges between urban farms and the city. However, UA is often excluded from the scope of sustainable urban planning, despite the significant inputs of energy, water and land, and the waste implications of food production (Vernay et al., 2010).

Potential synergies include, for example, enhancing crop yields by utilising carbon dioxide from production processes (Marchi et al., 2018) or exhaust air of buildings (Sanjuan-Delmás et al., 2018; Muñoz-Liesa et al., 2022), nutrient recovery from sewage systems (Wielemaker et al., 2018), and reduced heat losses by locating greenhouses on building roofs (Muñoz-Liesa et al., 2020). As such, local food production can enhance the sustainability of both the city and the urban farm (Kozai and Niu, 2020).

1.1.3 Vertical farming: challenges and opportunities

Vertical farming is an evolving urban farming method aimed at addressing the agricultural challenge of enhancing productivity while minimising environmental impacts. Vertical farms (VFs) (Fig. 1.1) produce food within a controlled indoor environment using artificial light and vertically stacked hydroponic systems (Kalantari et al., 2017), ensuring uniform growth conditions independent of external climate factors (Delden et al., 2021). This enables VFs to achieve high yields with minimal land usage (Graamans et al., 2018).

VFs offer several environmental benefits as they increase productivity per unit floor area (Kalantari et al., 2017) and utilise some resources more efficiently than conventional farming methods, including water (Graamans et al., 2018), CO_2 (Kozai et al., 2006), fertilisers (Germer et al., 2011), pesticides, and herbicides (Despommier, 2012). The limited use of these chemicals also minimises the risk of environmental contamination (Germer et al., 2011). Moreover, VFs located within or near cities minimise food miles, food losses (Germer et al., 2011), and storage and packaging requirements (Kalantari et al., 2017). Due to these benefits, vertical farming is frequently advocated as a sustainable food system in literature (Martin et al., 2023).

However, a major challenge for VFs is the substantial use of electricity for artificial lighting and air conditioning, exceeding that of greenhouse systems (Graamans et al., 2018). Electricity use represents the highest share of VF operational costs (Pesch and Louw, 2023), which poses challenges for scaling up VFs (Sørensen et al., 2016). This high electricity use may even outweigh the aforementioned benefits from a carbon footprint perspective (Kikuchi and Kanematsu, 2020). At the initiation of this research, the carbon footprint of vertical farming systems was unknown, necessitating a carbon footprint study to define the capability of VFs to produce sustainable foods when compared to conventional farming systems.



FIG. 1.1 Impression of a vertical farming system. Image from: Philips Horticulture LED solution by Signify

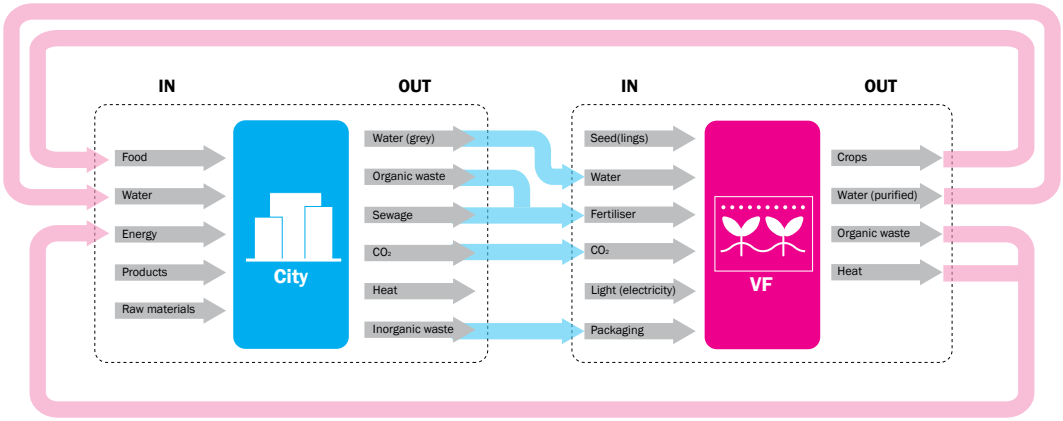

FIG. 1.2 Examples of synergetic exchanges of energy and resources between a city and vertical farm.

TOC

As highlighted in Section 1.1.2, the synergetic exchange of energy and resources between cities and food production systems can enhance the sustainability of both entities (Kozai and Niu, 2020). VFs produce significant quantities of low-temperature heat that could be supplied to district heat networks (Martin et al., 2019; Gentry, 2019; Graamans, 2021) or be used within buildings hosting VFs (Martin et al., 2022). Other examples are presented in Fig. 1.2, and include wastewater purification by VFs through crop transpiration (Kalantari et al., 2017), and increasing CO_2 levels within VFs by integrating these directly in office spaces (Shao et al., 2021).

Furthermore, VFs can contribute to balancing the electricity grid by adjusting the LED lighting according to electricity price fluctuations (Arabzadeh et al., 2023). Given the intermittent and unpredictable nature of renewable energy sources, this adjustment helps to manage the balance between electricity generation and usage, reflected in these price fluctuations (Vandermeulen et al., 2018). Research is needed to quantify the environmental and energetic performance of such symbiosis between the city and local food production (Pulighe and Lupia, 2020; Martin et al., 2019), including VFs.

1.1.4 Problem statement: exploring synergies between vertical farms and cities

In conclusion, this research evolves around two global challenges. First, the urgency for cities to reduce their energy and resource consumption to mitigate greenhouse gas emissions. Second, the need for innovative farming methods that deal with increasing food demands and diminishing resource availability while simultaneously reducing the environmental impacts of food production. Vertical farming is a novel farming system designed to deal with those agricultural challenges by producing food with high yields, minimal resource use, and effective land usage. Existing literature identifies urban food production, including VFs, as a potential strategy to close energy and resource cycles in cities, thereby enhancing resource use efficiency for both entities. However, the environmental performance of vertical farming is unknown, and further research is required to understand how to facilitate and quantify synergies between VFs and cities to evaluate the energetic gains and carbon implications of such a symbiotic relationship.

1.2 Research framework

1.2.1 Research objective and questions

To address the problem statement as highlighted above, the follow research question was formulated:

How can the synergetic integration of vertical farms within cities reduce energy and resource usage, as well as carbon emissions of both entities collectively?

The following sub-questions were defined to answer the main research question, which are aligned to the thesis structure in Section 1.2.3:

1. How does the current carbon footprint of vertical farming systems compare to that of open-field farming and greenhouse horticulture in the Netherlands?
2. How can the integration of vertical farms into the energy and resource systems of a building reduce the energy and resource use of both entities?
3. How can the integration of vertical farms into urban energy systems establish a thermal energy equilibrium with local district heat networks, while responding to fluctuations in electricity supplies by the electricity grid?
4. What carbon reductions can be achieved through the synergetic integration of vertical farms into urban energy systems?



FIG. 1.3 The Green House located within the city of Utrecht, hosting a restaurant, urban farm, and meeting rooms. This VF does not represent the fully enclosed environment as described in Section 1.1.3. Image from: © Lucas van der Wee

1.2.2 Research scope

Resources

This research explores the potential to exchange energy and other resources between vertical farms and the built environment, with a key focus on energetic synergies. These energetic synergies involve the exchange of residual heat produced by vertical farms with the cold produced by heat pumps when heating buildings. In addition to energy, other resources include water and nutrients, and the crops produced within vertical farms.

Context: the Netherlands

The geographical scope of this research is the Netherlands, as the research project was funded by the Dutch Research Council (NWO). Located in climatic zone Cfb according to the Köppen-Geiger classification, the Netherlands has a temperate climate characterised by uniformly distributed precipitation throughout the year and moderate summers.

TOC

Crop selection: butterhead lettuce

Research questions 1 to 3 focus exclusively on the production of butterhead lettuce. Currently, most VFs produce leafy greens due to their rapid growth, short production cycles, and limited height (Voutsinos et al., 2021). Focussing on lettuce crops maximises the availability of data, enhances the relevance of the results for the vertical farming sector, and maximises the transferability of the research findings.

Research field

The author of this dissertation has a background in architecture, urbanism, and building sciences, but is not specialised in plant sciences. Consequently, the indoor conditions of the VF remain unchanged throughout the study, including air temperature, humidity levels, and lighting characteristics, to avoid influencing lettuce yields. The climate systems designed in research questions 2 and 3 are customised to meet these specific requirements.

1.2.3 Research approach and thesis outline

The objective of this research is to investigate how the integration of VFs in cities can reduce energy and resource usage of both entities through synergetic exchanges, to diminish overall carbon emissions. To this end, the study is divided into four sub-research questions (Section 1.2.1). Figure 1.4 presents the thesis outline, starting with the introduction (Chapter 1), and ending with the conclusions and a person reflection from the author on the role of vertical farming systems in sustainable cities (Chapter 6). The four sub-research questions are addressed in Chapters 2 to 5. Chapter 2, 3 and 4 have been published as individual journal articles, and the manuscript of Chapter 5 is has been submitted on March 21st, 2024.

Chapter 2 – The carbon footprint of vertical farming (RQ1)

This chapter presents a quantitative assessment of the carbon emissions associated with lettuce cultivation in vertical farming and conventional farming systems in the Netherlands, including open-field farming and greenhouse horWticulture. The findings serve to establish the baseline environmental performance of vertical farming systems in the Dutch context, while identifying areas for improvement. Within this baseline assessment, the VF has no synergetic relationship with the urban environment.

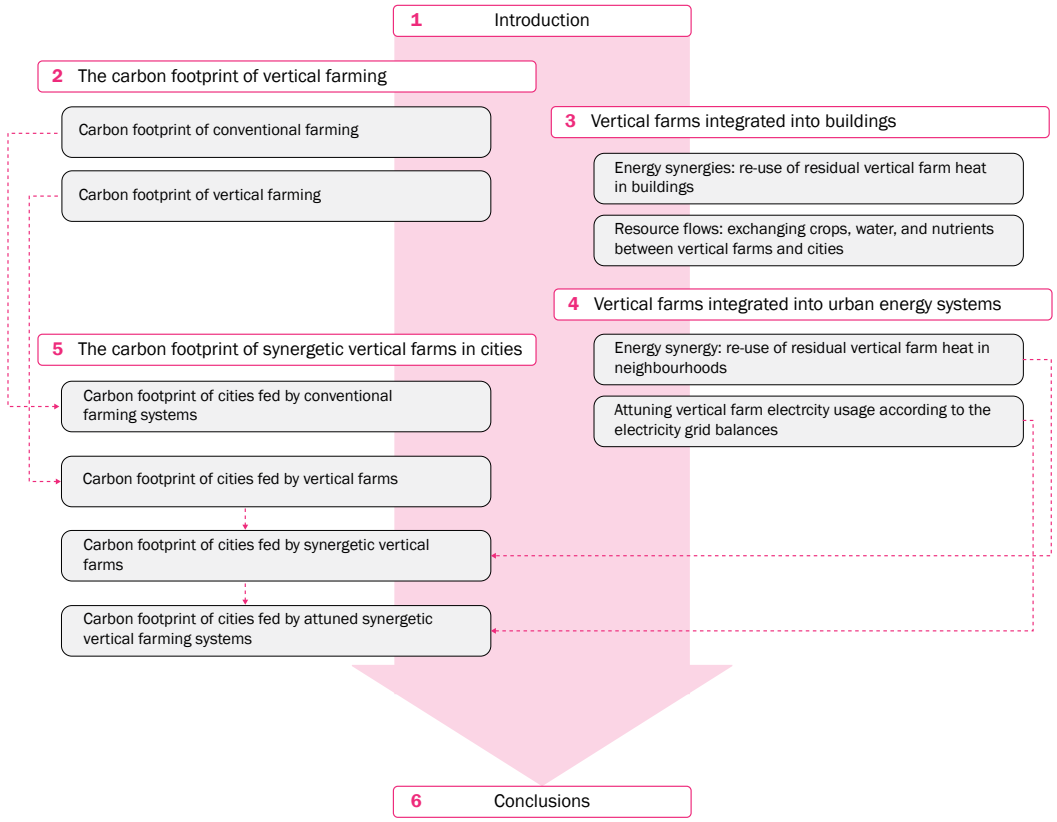

FIG. 1.4 Thesis structure

Chapter 3 – Vertical farms integrated into buildings (RQ2)

Chapter 3 delves into the integration of VFs into the energy and resource systems of their host building, aiming at collectively reducing the energy and resource usage of both entities. The primary focus is to reuse the residual heat produced by the VF for domestic heating, establishing energetic synergy between the VF and building. Therefore, this chapter explores the following aspects: the baseline cooling and dehumidification system used within VFs (1), the quantity of residual heat produced per square meter of cultivation area (2), the energy systems required to facilitate the exchange of heat and cold (3), and the floor area of the building heated with VF heat and the corresponding energy savings, both presented per square meter of cultivation area (4).

TOC

Moreover, the chapter explores the potential resource exchanges between the VF and the building, including the number of building users fed with lettuce produced in the VF, and the required outputs of wastewater and nutrients from the building to sustain the VF.

Chapter 4 – Vertical farms integrated into urban energy systems (RQ3)

In Chapter 4, the study extends from the individual building scale (Chapter 3) towards that of the neighbourhood. This research explores the potential to achieve thermal energy balance in this neighbourhood by facilitating the exchange of heat and cold between VFs and buildings using a district heat network and aquifer thermal energy storage. The chapter calculates the energy savings obtained by replacing the neighbourhood's fossil-based heating systems with heat generated by VFs, considering various district heat network configurations.

Furthermore, the study delves into strategies for operating the VF in a flexible manner to enhance the balance between demands and supplies in the electricity grid. Specifically, these strategies involve attuning the LED lights of the VF with electricity price fluctuations, which reflect the imbalances between renewable electricity generation and demand in the grid.

Chapter 5 – The carbon footprint of synergetic vertical farms in cities (RQ4)

Chapter 5 brings the findings from Chapters 2, 3, and 4 together to evaluate the potential carbon savings achieved through the integration of VFs with urban energy systems. This carbon footprint assessment includes four scenarios, ranging from a city dependent on conventional farming methods and fossil-based energy systems, to a city where synergetic VFs replace fossil-based heating systems and simultaneously attune their lighting systems to minimise disbalances in the electricity grid.

Chapter 6 – Conclusion

The discussion section reflects on the overall findings of the dissertation to answer the main research question. Therefore, the conclusions for each of the sub-research questions are presented first, followed by that of the main research question. Moreover, the research contributions, research limitations, and recommendations for further research area discussed. This chapter concludes with a personal reflection on the role of VFs in sustainable future cities.

References

Armanda, D.T., Guinée, J.B., Tukker, A. 2019. The second green revolution: Innovative urban agriculture's contribution to food security and sustainability: A review. Glob. Food Sec., 22, 13-24. https://doi.org/10.1016/j.gfs.2019.08.002.

Arabzadeh, V., Miettinen, P., Kotilainen, T., Herranen, P., Karakoc, A., Kummu, M., Rautkari, L. 2023. Urban vertical farming with a large wind power share and optimised electricity costs. Appl. Energy, 331, 120416. https://doi.org/10.1016/j.apenergy.2022.120416.

Avetisyan, M., Hertel, T., Sampson, G. 2013. Is local food more environmental friendly? The GHG emission impacts of consuming imported versus domestically produced food. Environ. Resour. Econ., 58, 415-462. https://doi.org/10.1007/s10640-013-9706-3.

Benke, K., Tomkins, B. 2017. Future food-production systems: vertical farming and controlled-environment agriculture. Sustainability: Sci. Pract. Policy, 13(1), 13-26. https://doi.org/10.1080/15487733.2017.1394054.

Broekhoven, S. van, Vernay, A.L. 2018. Integrating Functions for a Sustainable Urban System: A Review of Multifunctional Land Use and Circular Urban Metabolism. Sustainability, 10, 1875. https://doi.org/10.3390/su10061875.

Chertow, M.R. 2000. Industrial symbiosis: literature and taxonomy. Annu. Rev. Energy Environ., 25, 313–337. https://10.1146/annurev.energy.25.1.313.

Delden, S.H. van, SharathKumar, M., Butturini, M., Graamans, L.J.A., Heuvelink, E., Kacira, M., … Marcelis, L.F.M. 2021. Current status and future challenges in implementing and upscaling vertical farming systems. Nature food. https://doi.org/10.1038/s43016-021-00402-w.

Despommier, D. 2012. Advantages of the Vertical Farm. In: Rassia, S., Pardalos, P. (Eds). Sustainable Environmental Design in Architecture, Springer, New York, pp. 259-275. https://doi.org/10.1007/978-1-4419-0745-5_16.

Dobbelsteen, A. van den. 2008. Towards closed cycles – New strategy steps inspired by the Cradle to Cradle approach. 25th Conference on Passive and Low Energy Architecture, Dublin, Ireland.

Dobbelsteen, A. van den, Roggema, R., Tillie, N., Broersma, S., Fremouw, M., Martin, C.L. 2018. Urban Energy Masterplanning: Approaches, Strategies and Methods for the Energy Transition in Cities. In: Droege P. (Ed.), Urban Energy Transition: Renewable Strategies for Cities and Regions. Elsevier, pp. 635-660. https://doi.org/10.1016/B978-0-08-102074-6.00045-0.

Gentry, M. 2019. Local heat, local food: integration vertical hydroponic farming with district heating in Sweden. Energy, 174, 191–197. https://doi.org/10.1016/j.energy.2019.02.119.

Germer, J., Sauerborn, J., Asch, F., de Boer, J., Schreiber, J., Weber, G., Müller, J. 2011. Skyfarming an ecological innovation to enhance global food security. J. Verbraucherschutzd Lebensmittelsicherh., 6(2), 237-251. https://doi.org/10.1007/s00003-011-0691-6.

Graamans, L., Baeza, E., van den Dobbelsteen, A., Tsafaras, I., Stanghellini, C. 2018. Plant factories versus greenhouses: Comparison of resource use efficiency. Agric. Syst., 160, 31-42, https://doi.org/10.1016/j.agsy.2017.11.003.

Graamans, L.J.A. 2021. Stacked: the building design, systems engineering and performance analysis of plant factories for urban food production [Doctoral dissertation, Delft University of Technology]. A+BE | Architecture and the Built Environment. https://doi.org/10.7480/abe.2021.05.

Hirschl, H. 2018. The Urban Energy Transition: Pathways to Climate Neutrality in Our Cities. In: Droege P. (Ed.), Urban Energy Transition: Renewable Strategies for Cities and Regions. Elsevier, pp. 245-254. https://doi.org/10.1016/B978-0-08-102074-6.00027-9.

Hunter, M.C., Smith, R.G., Schipanski, M.E., Atwood, L.W., Mortensen, D.A. 2017. Agriculture in 2050: recalibrating targets for sustainable intensification. Biosci. 67(4), 386–391. https://doi.org/10.1093/biosci/bix010.

Jurgilevich, A., Birge, T., Kentala-Lehtonen, J., Korhonen-Kurki, K., Pietikäinen, J., Saikku, L., & Schösler, H. 2016. Transition towards Circular Economy in the Food System. Sustainability, 8(69). https://doi.org/10.3390.su8010069.

Kalantari, F., Tahir, O. M., Joni, R. A., Fatemi, E. 2017. Opportunities and challenges in sustainability of vertical farming: A review. J. Landscape Ecol., 11(1), 35-60. https://doi.org/10.1515/jlecol-2017-0016.

Kikuchi, Y., Kanematsu, Y., Yoshikawa, N., Okubo, T., Takagaki, M. 2018. Environmental and resource use analysis of plant factories with energy technology options: a case study in Japan. J. Clean. Prod. 186, 703–717. https://doi.org/10.1016/j.jclepro.2018.03.110.

Kikuchi, Y., Kanematsu, Y., 2020. Life cycle assessment. In: Kozia, T., Takagaki, M., Niu, G. (Eds.), Plant factory: an indoor vertical farming system for efficient quality food production. Academic Press, London, pp. 321–329. https://doi.org/10.1016/B978-0-12-816691-8.00027-3.

Kozai, T., Ohyama, K., Chun, C. 2006. Commercialized closed systems with artificial lighting for plant production. Acta Hortic., 711, 61–70. https://doi.org/10.17660/actahortic.2006.711.5.

Kozai, T., Niu, G. 2020. Role of the plant factory with artificial light (PFAL) in urban areas. In: Kozia, T., Takagaki, M., & Niu, G. (Eds.), Plant factory: an indoor vertical farming system for efficient quality food production. Academic Press, London, pp. 129–140. https://doi.org/10.1016/B978-0-12-801775-3.00002-0.

Lenhart, J., van Vliet, B., Mol, A.P.J. 2015. New roles for local authorities in a time of climate change: the Rotterdam Energy Approach and Planning as a case of urban symbiosis. J. Clean. Prod., 107, 593–601. http://dx.doi.org/10.1016/j.jclepro.2015.05.026.

Lombardi, D.R., Laybourn, P. 2012. Redefining Industrial Symbiosis. J. Ind. Ecol., 16, 28–37. https://doi.org/10.1111/j.1530-9290.2011.00444.x.

Lucertini, G., Musco, F. 2020. Circular Urban Metabolism Framework. One Earth, 2, 138–142. https://doi.org/10.1016/j.oneear.2020.02.004.

Marchi, B., Zanoni, S., Pasetti, M. 2018. Industrial Symbiosis for Greener Horticulture Practices: The CO_2 enrichment from Energy Intensive Industrial Processes. Procedia CIRP 2018, 69, 562–567. https://doi.org/10.1016/j.procir.2017.11.117.

Martin, M., Poulikidou, S., Molin, E. 2019. Exploring the environmental performance of urban symbiosis for vertical hydroponic farming. Sustainability (Switserland), 11 (23), 6724. https://doi.org/10.3390/su11236724.

Martin, M., Weidner, T., Gullström, C. 2022. Estimating the potential of building integration and regional synergies to improve the environmental performance of urban vertical farming. Front. Sustain. Food Syst. 6, 849304. https://doi.org/10.3389/fsufs.2022.849304.

Martin, M., Elnour, M., Siñol, A.C. 2023. Environmental life cycle assessment of a large-scale commercial vertical farm. Sustainable Prod. Consumption, 40, 182–103. https://doi.org/10.1016/j.spc.2023.06.020.

Mbow, C., Rosenzweig, C., Barioni, L.G., Benton, T.G., Herrero, M., Krishnapillai, M., Liwenga, E., Pradhan, P., Rivera-Ferre, M.G., Sapkota, T., Tubiello, F.N., Xu, Y., 2019. Food security. In: Shukla, P.R., Skea, J., Calvo Buendia, E., Masson-Delmotte, V., Pörtner, H.O., … Malley, J. (Eds.), Climate change and land: an IPCC special report on climate change, desertification, land degradation, sustainable land management, food security, and greenhouse gas fluxes in terrestrial ecosystems. In Press. https://www.ipcc.ch/srccl/chapter/chapter-5/

Muñoz-Liesa, J., Royapoor, M., López-Capel, E., Cuerva, E., Rufí-Salís, M., Gassó-Domingo, S., Josa, A. 2020. Quantifying energy symbiosis of building-integrated agriculture in a mediterranean rooftop greenhouse. Renew. Energy, 156, 696–709. https://doi.org/10.1016/j.renene.2020.04.098. https://doi.org/10.1016/j.buildenv.2021.108585.

Muñoz-Liesa, J., Royapoor, M., Cuerva, E., Gassó-Domingo, S., Gabarrell, X., Josa, A. 2022. Building-integrated greenhouses raise energy co-benefits through active ventilation systems. Build. Environ. 208. https://doi.org/10.1016/j.buildenv.2021.108585.

Pesch, H., Louw, L. 2023. Evaluating the Economic Feasibility of Plant Factory Scenarios That Produce Biomass for Biorefining Processes. Sustainability. 15(2), 1324. https://doi.org/10.3390/su15021324.

Poore, J., Nemecek, T., 2018. Reducing food's environmental impacts through producers and consumers. Science. 360, 987–992. https://doi.org/10.1126/science.aaq0216.

Pulighe, G. Lupia, F. 2020. Food first: COVID-19 outbreak and cities lockdown a booster for a wider vision on urban agriculture. Sustainability, 12(12). https://doi.org/10.3390/su12125012.

Sanches, T.L., Bento, N.V.S. 2020. Urban Metabolism: A Tool to Accelerate the Transition to a Circular Economy. In: Filho, W.L., Azul, A.M., Brandli, L., Özuyar, P.G., Wall, T. (Eds.), Sustainable Cities and Communities Springer, Chambridge, pp. 860–876. https://doi.org/10.1007/978-3-319-95717-3_117.

Sanjuan-Delmás, D., Llorach-Massana, P., Nadal, A., Ercilla-Montserrat, M., Munoz, P., Montero, J.I., Josa, A., Gabarrell, X., Rieradevall, J. 2018. Environmental assessment of an integrated rooftop greenhouse for food production in cities. J. Clean. Prod., 177(10), 326-337. https://doi.org/10.1016/j.jclepro.2017.12.147.

Sanyé-Mengual, E., Oliver-Solà, J., Montero, J.I., Rieradevall, J. 2015. An environmental and economic life cycle assessment of rooftop greenhouse (RTG) implementation in Barcelona, Spain. Assessing new forms of urban agriculture from the greenhouse structure to the final product level. Int. J. Life Cycle Assess., 20(3), 350-366. https://doi.org/10.1007/s11367-014-0836-9.

Shao, Y., Li, J., Zhou, Z., Hu, Z., Zhang, F., Cui, Y. 2021. The effects of vertical farming on indoor carbon dioxide concentration and fresh air energy consumption in office buildings. Build. Environ., 195, 107766. https://doi.org/10.1016/j.buildenv.2021.107766.

Smith, P., Martino, D., Cai, Z., Gwary, D., Janzen, H.H., 2008. Global estimations of the inventory and mitigation potential of methane emissions from rice cultivation conducted using the 2006 intergovernmental panel on climate change guidelines. Glob. Biogeochem. Cycles, 23.

Sørensen, J.C., Kjaer, K.H., Ottosen, C.O., Jørgensen, B.N. 2016. DynaGow – Multi-Objective Optimization for Energy Cost-efficient Control of Supplemental Light in Greenhouses. Proceedings of the 8th International Joint Conference on Computational Intelligence, 1, 41-48. https://doi.org/10.5220/0006047500410048.

Tillie, N., van den Dobbelsteen, A., Doepel, D., de Jager, W., Joubert, M., Mayenburg, D. 2009. REAP Rotterdam Energy Planning Towards CO2-neutral Urban Development. REAP: Rotterdam, The Netherlands.

United Nations. 2019. World Population Prospects 2019: Highlights (ST/ESA/SER.A/423). United Nations, Department of Economic and Social Affairs, Population Division.

Vandermeulen, A., van der Heijde, B., Helsen, L. 2018. Controlling district heating and cooling network to unlock flexibility: A review. Energy, 151, 103-115. https://doi.org/10.1016/j/energy.2018.03.034.

Vermeulen, S.J., Campbell, B.M., & Ingram, J.S.I. 2012. Climate Change and Food Systems. Annu. Rev. Environ. Resour., 37, 195-222. https://doi.org/10.1146/annurev-environ-020411-130608.

Vernay, A.L., Salcedo Rahola T.B., Ravesteijn, W. 2010. Growing food, feeding change: Towards a holistic and dynamic approach of eco-city planning. 3rd Annual Conference NG-Infra on Next generation infrastructure systems for eco-cities, Shenzhen, 11-13. https://doi.org/10.1109/INFRA.2010.5679234.

Vernay, A.L., Mulder, K. 2016. Organising urban symbiosis projects. Proceedings of the Institutions of Civil Engineers – Engineering Sustainability (online), 169(5), 181-188.

Voutsinos, O., Mastoraki, M., Ntatsi, G., Liakopoulos, G., Savvas, D. 2021. Comparative assessment of hydroponic lettuce production either under artificial lighting, or in a Mediterranean greenhouse during wintertime. Agriculture, 11, 503. https://doi.org/10.3390/agriculture11060503.

Wielemaker, R.C., Weijma, J., & Zeeman, G. 2018. Harvest to harvest: Recovering nutrients with New Sanitation systems for reuse in Urban Agriculture. Resour. Conserv. Recycl., 128,426-437. https://doi.org/10.1016/j.resconrec.2016.09.015.



Philips Horticulture LED solution by Signify

TOC

2 The carbon footprint of Vertical Farming

The content of this chapter was published as:
The embodied carbon emissions of lettuce production in vertical farming, greenhouse horticulture, and open-field farming in the Netherlands
Blom, T., Jenkins, A., Pulselli, R.M., van den Dobbelsteen, A.A.J.F.
Journal of Cleaner Production, 2022, 337. DOI: 10.1016.j.clepro.2022.134443

Supplementary material for this chapter is provided in Appendix A
The datasets of this chapter are available at the repository 4TU Research Data.
DOI: 10.4121/19487078

Over the past decades, various farming methods have evolved in response to the global challenges of increasing food demands, decreasing availability of arable land, and climate change. One of these new farming methods is vertical farming (Section 1.1.3). To understand the potential contributions of vertical farms to future sustainable food production, it is important to consider the resources utilised throughout the entire life cycle of the crops cultivated in vertical farms, to provide greater detail beyond the realms of efficient land-use and high yields. Therefore, it is crucial to assess the present state of vertical farms in terms of their carbon footprint. In response to this aim, this chapter addresses the first research question of the dissertation:

How does the current carbon footprint of vertical farming systems compare to that of open-field farming and greenhouse horticulture in the Netherlands?

To answer this research question, Chapter 2 evaluates the current carbon footprint of lettuce produced in an operational vertical farm in comparison to that of open-field farms and greenhouse horticulture in the Netherlands. This assessment includes the greenhouse gas emissions of the life cycle of the farm and the crop, from cradle-to-grave. Finally, an alternative scenario is explored to include the lost carbon sequestration potential due to land-use change, uniform packaging materials across all farming methods, and the use of renewable energy sources.

2.1 Introduction

2.1.1 Food security and climate change

Climate change and food security are inextricably linked and are both factors that endanger the future health and wellbeing of people across the globe. Agriculture is one of the major contributors to climate change, emitting ~11% of total anthropogenic greenhouse gas (GHG) emissions (Smith et al., 2008) and between 26% (Poore and Nemecek, 2018) and 37% (Mbow et al., 2019) of GHG emissions when considering the full value chain. Food production will be greatly impacted in the future by the globally decreasing availability of agricultural land (Benke and Tomkins, 2017) and declining yields due to adverse weather and increased food spoilage as direct consequence of climate change (Edwards et al., 2011). This creates great challenges as global food production will need to increase by up to 70% between 2017 and 2050 due to a growing global population and changing diets (Hunter et al., 2017). To produce the extra food required by 2050 without further destruction of natural landscapes to provide new arable land, the environmental impact of food production systems needs to be reduced and new methods of cultivating crops are desperately needed.

A farming technique that has been developed to reduce the environmental impacts of agriculture whilst maximising productivity is vertical farming. Vertical farms (VFs) are indoor growth systems that use artificial light and air treatment systems exclusively alongside multi-layer hydroponic systems; creating uniform growing conditions independent of the outdoor climate (Delden et al., 2021). This allows VFs to achieve year-round production with maximum density and productivity (Graamans et al., 2018). Kalantari et al. (2017) performed a literature survey on the benefits of vertical farming; literature frequently suggested that VFs reduce the use of water, pesticides and herbicides, whilst increasing productivity per unit area. Benke and Tomkins (2017) state that VFs potentially require less fertilisers and Germer et al. (2011) note that the limited use of pesticides, herbicides, and fertilisers minimises the risk of discarding these chemicals into the environment. Germer et al. (2011) also draw attention to the capability of VFs to reduce food waste due to controlled growth environments and shorten food miles by placing such facilities within or adjacent to cities. The creation of short supply chains can also reduce the need for storage and packaging (Kalantari et al., 2017). Considering these benefits, it could be concluded that the environmental impact of VFs is lower than that of conventional agricultural practices for crop cultivation; in this research referred to as open-field farming

and green- house horticulture. The advantages of VFs, however, result in higher electricity demands for artificial lighting and air conditioning (Delden et al., 2021). This electricity demand exceeds the energy consumption of greenhouse systems (Graamans et al., 2018) to such an extent that, in terms of carbon footprint, it could outweigh the aforementioned benefits altogether (Kikuchi and Kanematsu, 2020).

2.1.2 The carbon footprint of vertical farming

To explore the potential role of VFs as a component of future sustainable food production, a greater depth of knowledge is required to determine the environmental impact of the practice relative to conventional farming systems. Three carbon footprints of VFs were found in existing literature (Table 2.1). The most comprehensive analysis, performed by Kikuchi et al. (2018), did not only include the carbon emissions released during crop cultivation – the core emissions – but also the emissions produced by both pre-production and post-production processes of the crop, i.e., upstream, downstream, and end-of-life emissions of the crop life cycle. The life cycle of the farm was also taken into account. Considering that 75% (Kikuchi et al., 2018), 85% (Benis et al., 2017), and 90% (Li et al., 2020) of the carbon footprints represent artificial light, the electricity consumption per kg fresh weight (FW) varies greatly (Table A.1, #1–3) and results in a large dispersion between the carbon footprints. These data also suggest that the emissions to produce a kWh of electricity differs significantly between countries. To put this into perspective the electricity use of these three VFs were compared to that of other VFs studied in existing literature, which mostly represent simulated farms. The electricity use for artificial light variated greatly between 3.1 and 31.5 kWh per kg FW produced (Table A.1, #4–8), suggesting a wide range of carbon footprints. The carbon footprint of the lettuce producing CBVF located in Kashiwa, Japan, was compared to that of conventional cultivation within plastic tunnel greenhouses without artificial light. Kikuchi et al. (2018) also studied hydroponic greenhouse production with both artificial and natural light relative to conventional horticulture, focussing on tomato production. Both studies focus on different crops, making it difficult to compare the carbon footprints. The GHG emissions of the VF in Kashiwa were reduced by 60% by using more efficient and sustainable technologies, such as implementing photovoltaic (PV) production on the VF roof and using a hydrogen powered combined heat and power system. These technologies were not applied to the conventional farming methods, resulting in an unfair comparison. Table A.1 also presents details on the energy use for artificial lighting in relation to crop yields of these VFs. The carbon footprint studies (Table A.1, #1–3) did not document all data, such as photoperiods and yields, which made it difficult to validate the findings presented or compare them to the other VFs in a robust manner.

TABLE 2.1 Comparison of carbon footprints of VFs in literature and the activities included within those footprints.

Carbon footprint $kgCO_{2\text{-}eq}\ kg^{-1}$	Life cycle farm	Life cycle crop				Reference
		Upstream	Core	Downstream	End-of-life	
1.32	-	-	Water, Electricity	Transport	-	Benis et al., 2017
1.44	-	Fertilisers, Seeds	Water, Electricity, CO_2	-	-	Li et al., 2020
~25.0*[1]	Construction and decommissioning of buildings and devices	Fertilisers, Pesticides, Seedlings, Culture media, Packaging	Water, Electricity, Fuels, CO_2	Transport	Waste treatment	Kikuchi et al., 2018

1. Value taken from Figure 4B in Kikuchi et al., 2018

The quantity of energy used (Avetisyan et al., 2013), the source of energy (Delden et al., 2021), the local climate conditions affecting resource use efficiency (Graamans et al., 2018), and local farm typologies (Benis and Ferrão, 2018) make the sustainability of food systems context specific, meaning that the emissions vary per region. To the authors' knowledge, no quantitative comparison of carbon emissions associated with both the life cycle of the farm and the crop, from cradle to grave, exist for VFs relative to open-field farming and both soil-based and hydroponic greenhouse horticulture within the Dutch context.

The goal of the study presented is, therefore, to evaluate the carbon footprint of vertical farming in comparison to conventional farming systems to determine the potential role of VF as a sustainable cultivation method in the Netherlands. To this aim, this study performs a quantitative carbon footprint assessment of lettuce cultivation in open-field farming (OF), soil-based greenhouse horticulture (GHs), hydroponic greenhouse horticulture using artificial light (GHa) and vertical farming (VF) in the Netherlands, including the upstream, core, downstream, and end-of-life emissions of both the farm life cycle and crop life cycle, from cradle-to-grave. The discussion section proposes three alternative scenarios to include the lost carbon sequestration potential by land-use change, identical packaging, and renewable energy usage across all case studies to provide a fair basis of comparison across the four food systems analysed. Finally, the energy use and light use efficiency of the studied VF is presented relative to other VFs from literature to provide an opportunity to contextualise the results.

2.2 Methodology

2.2.1 Description of the case studies

This study presents the carbon footprint assessment of butterhead lettuce grown in four different farming systems in the Netherlands: OF, GHs, GHa, and VF. A typical farm is defined for open-field farming and both forms of greenhouse horticulture, based on existing databases. An operational commercial VF located in the Netherlands was used as a case study as it is not yet possible to define a typical VF due to the breadth of approaches. Butterhead lettuce was used as the sole crop of comparison in this study as it is one of the most important leafy vegetables worldwide due to their fast growth and short production cycles, which also makes them an interesting proposition for vertical farmers (Voutsinos et al., 2021).

2.2.1.1 Open-field farming

OF is defined as the cultivation of crops in soil, open to the air, with the application of nutrients, pesticides, and herbicides (Barbosa et al., 2015). European crops grown in open-field farming systems are rainfed (Portmann et al., 2010) and use additional irrigation (Breukers et al., 2014). OF requires machinery, such as tractors, buildings for storage, and vast areas of land to achieve the economy of scale required to generate profit. Within the Dutch context, the average lettuce producing OF is 15 ha gross in size (CBS, 2021) and produces 84,300 butterhead lettuce crops per ha per growth cycle (Schreuder et al., 2009). On average, open-field lettuce farms have three growth cycles per year (Snoek, 1985) and a crop FW of 350 g. This FW corresponds with Snoek (1985), suggesting that lettuce crops are harvested when 100 crops have a FW of approximately 35 kg in total. Resulting in the production of 253,000 heads of lettuce per ha, i.e., 8.9 kg FW m^{-2} y^{-1}.

2.2.1.2 Soil-based greenhouse horticulture

Greenhouse horticulture includes a wide range of different approaches from soil-based, uncontrolled environments in polytunnels through to hydroponic, semi-closed, controlled environments in glasshouses. In this study, GHs refers to soil-based cultivation of lettuce crops in the semi-closed growth environment of a Venlo greenhouse with active application of nutrients, pesticides, and herbicides, along- side drip-fed irrigation. The growing conditions are achieved and maintained through a combination of mechanical and passive strategies, where sunlight is used as the primary source for heating and exclusively for lighting (Graamans et al., 2018). On average, the heating temperature is 8 °C above ambient and the maximum relative humidity is 92% (Raaphorst and Benninga, 2019). Natural ventilation is used for passive cooling, ventilation, and dehumidification. GHs requires an active supply of carbon dioxide (CO_2) to compensate the losses of CO_2 into the atmosphere by natural ventilation and maintain CO_2 levels of 800 ppm (Graamans et al., 2018). In the Netherlands, the average greenhouse covers an area of 4 ha and produces 830,000 lettuce heads per ha of 350 g each (Raaphorst and Benninga, 2019), i.e., 29.05 kg FW m^{-2} y^{-1}.

2.2.1.3 Hydroponic greenhouse horticulture using artificial light

GHa has the same indoor environment as described for GHs but includes the use of artificial light with LED systems of 87 µmol m^{-2} s^{-1} for 2000 h y^{-1} in addition to natural light. The heat dissipated by these LED systems results in a slightly higher average indoor temperature of 10 °C above ambient. Furthermore, GHa uses hydroponic lettuce cultivation with nutrient film technique (NFT), in which roots partially hang in a sloped channel through which a thin layer of nutrient solution is pumped (Lennard and Leonard, 2006). The crops are harvested at 220 g FW, producing 241.8 lettuce heads per m^2, i.e., 53.2 kg FW m^{-2} y^{-1} (Raaphorst and Benninga, 2019).

2.2.1.4 Vertical farm

The operational VF used in this study occupies two rooms in an existing office building: a growing room and a processing room (Fig. 2.1). The growth chamber of the VF is not airtight and consists of an opaque façade with a single covered window and an access door. The VF produces basil, butterhead lettuce, and multi-

TOC

leaf lettuce crops in a hydroponic system. Within this hydroponic system, each crop is grown in individual plastic containers filled with nutrients and water. These containers are placed in moveable, multiple-layer trollies equipped with built-in LED lights. An air conditioning unit and a dehumidifier maintain the climate conditions in the VF. The growing chamber is not enriched with CO_2 because it is not a sealed compartment. Any enriched CO_2 added to the growth chamber would simply leak into the processing room and the rest of the building.

The VF produces 2068 kg FW basil and 4550 kg FW lettuce annually with a total cultivation area of 122 m^2 and a total floor area of 90 m^2, inclusive of the processing room. Lettuce is produced within ten 7-layer trollies and basil within ten 6-layer trolleys. The VF achieves 14.6 growth cycles a year by rearranging growth densities throughout each growth cycle and by harvesting the lettuce crops at a relatively low FW of 110 g. In total, 50% of the floor area is assigned to lettuce and 54% of the cultivation area, resulting in a lettuce production of 101 kg FW y^{-1} per m^2 floor area.

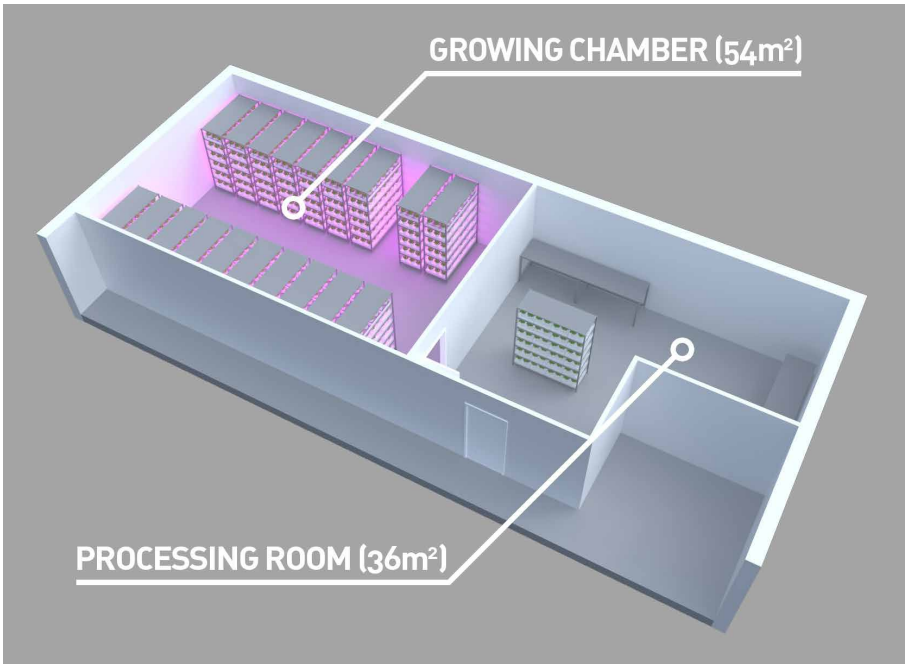

FIG. 2.1 Three-dimensional model of the operational VF case study, including the floor areas of the growth chamber and processing room.

Figure 2.2 presents the yields of the four farming methods in kg FW per m^2 gross floor area per year, including the floor areas used for crop cultivation and other processes, e.g., seeding and storage. Despite the minimal FW per crop produced, the VF has a significantly higher yield per m^2 due to its vertical arrangement, the optimised indoor growth conditions, and year-round production.

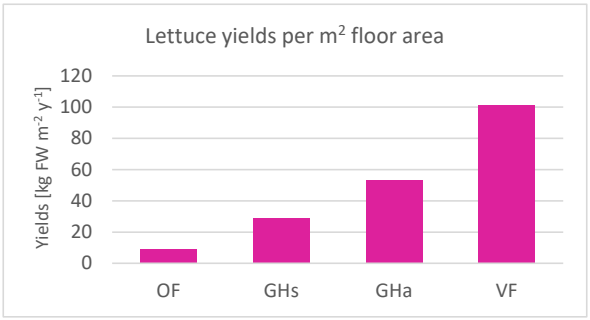

FIG. 2.2 The annual lettuce yields per m2 of gross floor area.

2.2.2 Carbon footprint assessment

2.2.2.1 Functional unit

Within the datasets selected to define the carbon footprint of butterhead lettuce produced in an average OF, GHs, or GHa (Section 2.2.3), no data was available on the dry weight of the crops. Similarly, in the running VF used as case study, dry weight was not measured. Consequently, the functional unit (FU) for this carbon footprint assessment is 1 kg FW butterhead lettuce.

Dry matter content is, however, a critical factor in LCAs as it reflects the efficiency in which resources such as light and nutrients are converted into dry matter. The addition of water finally determines the fresh weight achieved. The dry matter content directly impacts the carbon footprint, as it indicates how much of the plants fresh weight is composed out of water. For instance, 1 kg FW lettuce with a dry matter content of 5% will have a lower carbon footprint in terms of dry weight than lettuce with a 4% dry matter content. Combing our data with dry matter content

TOC

data of other literature or datasets would significantly affect the carbon footprint per kg of dry weight. Therefore, we did not consider the carbon footprint per kg fry weight in this study.

In addition to data availability, we chose to use the FU per kg FW instead of dry weight for two other reasons. First, this unit better reflects market relevance, as lettuce is typically sold and consumed in fresh form. Assessing the carbon footprint in kg FW aligns with the form in which lettuce is actually produced, distributed, and consumed. Second, previous studies as shown in Table 2.1 have also presented the carbon footprint of vertical farming in kg FW produced, enhancing the comparability of our study. The emissions of greenhouse gasses are therefore represented as kg of carbon dioxide equivalent (CO2-eq) per kg FW butterhead lettuce (kg CO_2-eq kg-1 FW).

2.2.2.2 Category indicator

The unit $CO_{2\text{-eq}}$ is the category indicator of the impact category for Global Warming Potential (GWP100) of an LCA, i.e., the carbon footprint. The $CO_{2\text{-eq}}$ includes the GHG emissions released into the atmosphere by human activities: mainly carbon dioxide (CO_2), methane (CH_4), and nitrous oxide (N_2O) (Pulselli et al., 2019).

2.2.2.3 System boundaries

This study includes the upstream, core, downstream, and end-of-life emissions of both the farm life cycle and crop life cycle, from cradle-to-grave. Figure 2.3 represents the different life cycle activities assessed in this study, including the life cycle of the farm on the left, and the life cycle of the crop on the right. The far-left and far-right of the figure present the inputs and outputs from each life cycle stage, respectively.

The upstream emissions of the farm life cycle include the extraction, processing, manufacturing and transportation of the materials of built structures, and the replacement of these materials after their useful lifespan. The end-of-life emissions of the farm materials include the transportation of the materials to a treatment site but not the process of material recycling, as this is considered part of the upstream emissions of a new production chain.

Due to the lack of robust and scientific data in some key areas, a few emissions are not included in this study. These include the emissions associated with the materials used in machinery, climate installations and auxiliary equipment, the energy used to construct and disassemble the farm, and land-use change, i.e., the emissions from energy used to transform land from one type of usage into another, in this case agricultural land. Later in the study, the lost potential for carbon sequestration is included to account for some of the impacts, subsequent to converting land for agricultural purposes. This considers the CO_2 that could be sequestered if the land occupied by agriculture was a forest instead.

The upstream emissions of the crop life cycle include the extraction, processing, and manufacturing of fertilisers, pesticides, herbicides, growing media, packaging materials and pressurised CO_2 for carbon enrichment, the energy and resources used to produce seeds and seedlings, and the emissions related to the transportation of these inputs to the farm. The core emissions are emissions released to extract, process, and produce the energy and resources needed to sow and plant seeds, irrigate crops, and maintain growing conditions, such as temperature and humidity, where necessary. These core emissions also include the lubricants used for agricultural machinery.

The downstream emissions include the emissions from transporting the crops to the wholesale or retail location. The emissions released during incineration of growth and packaging materials, composting of food lost during cultivation, distribution and consumption, and transportation of this waste to a treatment facility are part of the end-of-life emissions.

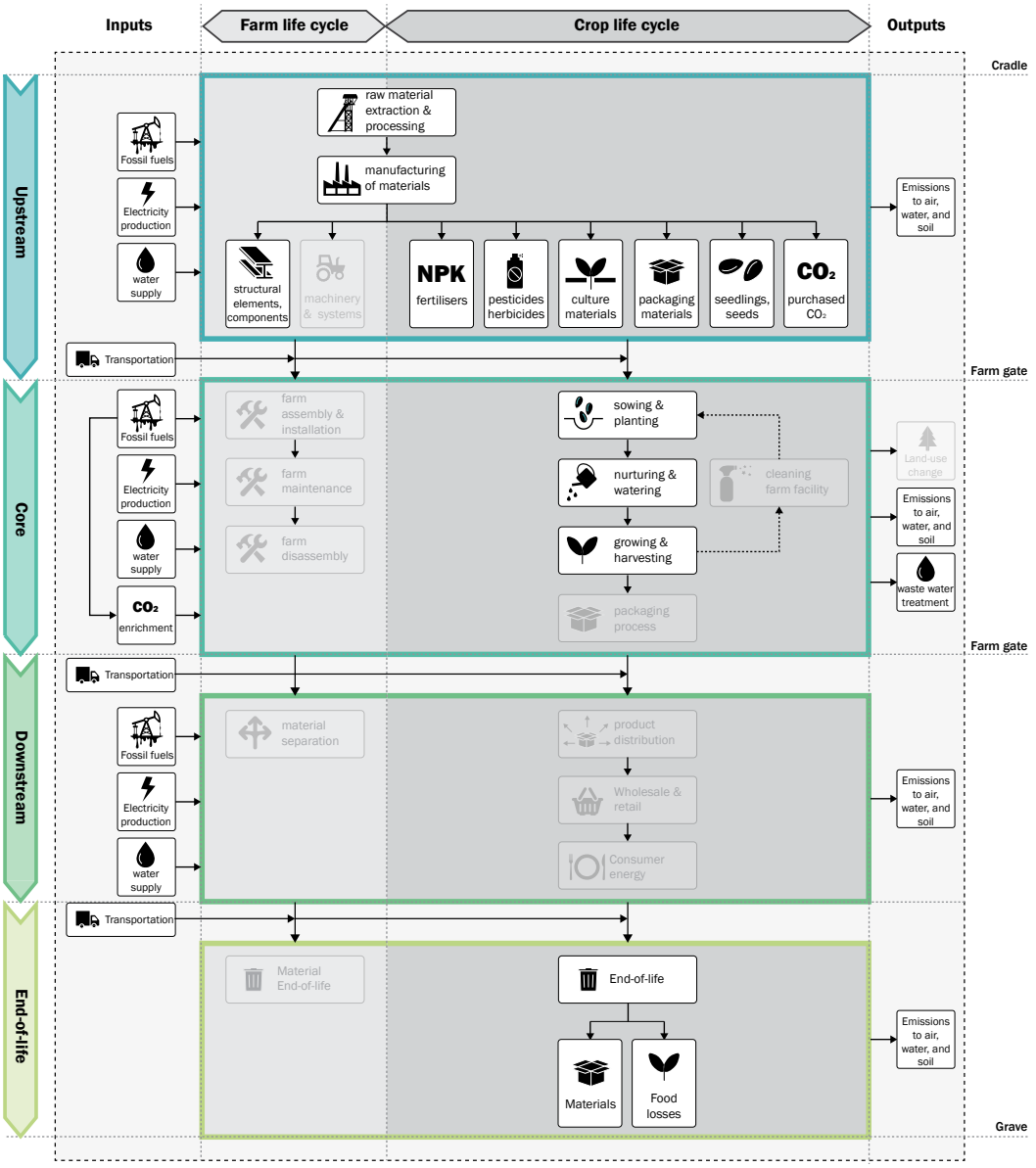

FIG. 2.3 The system boundaries and the life cycle activities of both the farm and the crop as included in the carbon footprint assessment. Activities excluded by this study are depicted in faded grey.

TOC

Due to the lack of scientific data, the crop life cycle does not include the energy used to package the crops, clean the farming facility and refrigerate the crop by the consumer, and the energy and resources needed in the food supply chain after the food reaches the retail or wholesale location, such as on-site refrigeration. These activities are depicted grey in Figure 2.3.

2.2.2.4 Life cycle inventory data and emissions factors

The carbon footprint of each case study is calculated by accounting for all the GHG emissions from life cycle activities within the system boundaries (Fig. 2.3). These GHG emissions were calculated as follows:

$$CO_{2\text{-eq}} = \text{activity data} \times EF \qquad \text{(Eq. 2.1)}$$

where $CO_{2\text{-eq}}$ is the carbon footprint of the activity in kg $CO_{2\text{-eq}}$ and EF the emission factor of the activity in kg $CO_{2\text{-eq}}$ per unit of the activity data. These EFs are assessed by the IPCC GWP100a characterisation method in SimaPro 9.0.0, which is based on the Ecoinvent 3.6 database. Appendix Table A.2 provides an overview of the references of the EF used within this study. Country-specific EFs for the Netherlands were used for natural gas and electricity consumption to reflect the correct energy mix (CO_2 emissiefactoren, 2021).

2.2.3 Life cycle inventory

The life cycle inventory (LCI) data, their references, and the assumptions made for each case study are discussed in the subsequent sections. The following assumptions were applied to all case studies, except for instances where specific data were available. The transportation of the crop inputs to greenhouse facilities varies between 55 and 200 km (Montero et al., 2011a, 2011b); a distance of 100 km was assumed for all case studies (1). As no data were available on the distance travelled between the farm and retail location of lettuce crops produced and consumed in the Netherlands, green beans with an average transportation distance of 160 km (Pegge et al., 2006) were taken as a reference (2). For both the transportation of the crops and the crop inputs, diesel lorry transportation between 3.5 and 7.5 t was selected (3). Food losses in Dutch supermarkets are approximately 1.7% of the food they stock, of which potatoes, vegetables, and fruits form 34.5% (WUR, 2020) (4). Once sold, 9.5% of the food is, on average, lost by

TOC

Dutch households (Dooren, 2019) (5). A distance of 50 km was assumed for the transportation of all end-of-life materials to a treatment facility (6).

2.2.3.1 Open-field farming

The LCI data of the upstream and core processes of the crop life cycle were obtained from the KWIN database for open-field farming (Table A.3). The KWIN database provides an insight into the average crop-specific inputs per ha of open-field butterhead lettuce production in the Netherlands (Schreuder et al., 2009). The application of nitrogen (N) fertilisers to soil-based crop production systems results in both direct and indirect emission of N_2O–N. Nitrogen fertiliser application directly results in denitrification of the soils of approximately 0.01 kg N_2O–N per kg synthetic N applied to the crop. Indirectly, it results in both N_2O emissions from volatilization (0.001 kg N_2O–N kg^{-1} N) and leaching (0.002 kg N_2O–N kg^{-1} N) (Klein et al., 2006; Table A.3).

To define the materiality of the buildings of the OF, a theoretical model was created as no sources of information were found that categorically identify the nature, type, and number of agricultural buildings that were required by an open-field farm of a specific size. A farm of 15 ha is assumed that grows only butterhead lettuce crops, consisting of two steel-framed and steel-clad sheds for storing fertilisers, pesticides, herbicides, machinery, and harvested crops, with a total floor area of 1400 m^2 (Appendix A.4). The operational lifespan of these buildings is 50 y (Nemecek and Kägi, 2007).

2.2.3.2 Soil-based greenhouse horticulture

The LCI data for the life cycle of the crop of soil-based greenhouses were obtained from the KWIN database for greenhouse production (Raaphorst and Benninga, 2019) (Table A.4). This lettuce-producing greenhouse uses natural gas for heating (5.6 m^3 m^{-2} y^{-1}) as well as soil steaming to remove pests and pathogens between growth cycles (5 m^3 m^{-2} y^{-1}) (Raaphorst and Benninga, 2019). GHs uses natural light exclusively. The exhaust gases produced when burning natural gas on-site are used for carbon enrichment of greenhouses (Li et al., 2018) and result in 1.78 kg CO_2 per m^3 natural gas combusted (Smit, 2010). The average demands for CO_2 enrichment of vegetable production in Dutch greenhouses without artificial light is 10 kg CO_2 m^{-2} y^{-1} (Velden and Smit, 2019). In GHs these demands are fully covered by

on-site natural gas combustion. Italian values from Ecoinvent 3.6 were applied for fertiliser, pesticide, and herbicide use as no data were available for Dutch GHs lettuce farms.

The LCI data on farm materiality was obtained from Montero et al. (2011a; 2011b), which described the materiality of a 4 ha, Dutch, Venlo greenhouse structure in detail, including the quantities of each material used. Although most greenhouse growers use their facility longer, their useful lifespan was set to 15 years for all structural elements, in accordance with the European code CEN 2001 (Montero et al., 2011a). The activity data per FU were achieved by assuming year-round production in a greenhouse that grows only butterhead lettuce.

2.2.3.3 Greenhouse horticulture using artificial light

The KWIN database for greenhouse horticulture provided the data related to the life cycle of the crop (Table A.5). The use of fertilisers, pesticides and herbicides was expressed in average money spend for both GHs and GHa. Per kg produce, GHa growers use 43% of the fertiliser, and 41% of the pesticide budget spend by GHs growers (Raaphorst and Benninga, 2019). To estimate the quantities used these ratios were applied to the consumption of these chemicals by GHs (Section 2.2.3.2).

Within a hydroponic growth environment the water surface open to air is limited, minimising evaporation (Benke and Tomkins, 2017). The water usage was estimated by including the minimal evapotranspiration (ET) rate to avoid tip burn of 1.4 L per 5 g DW lettuce (Ciolkosz et al., 1998) and nutrient flushing of 1.1 times the minimal ET requirements (Barbosa et al., 2015). A dry weight (DW) of 5% was used for butterhead lettuce production in GHa (Monsees et al., 2019). In total, 18.7 kg CO_2 m^{-2} y^{-1} is supplied to GHa to enrich the growing atmosphere (Raaphorst and Benninga, 2019) of which 45% is produced with on-site natural gas combustion, using the calculation method cited in Section 2.2.3.2. The remaining 55% is purchased as liquefied CO_2, which is a widely used carbon enrichment source for greenhouses (Li et al., 2018).

GHa uses the same 4 ha Venlo greenhouse as GHs, however, it has a greater yield per m^2 floor area, resulting in significantly lower quantities of materials used per kg FW produced. PVC CropKing's Classic channels of 3.7 m with 24 plant spaces (CropKing, 2022) and Rockwool substrates were selected for the NFT system.

2.2.3.4 Vertical farm

An operational commercial VF in the Netherlands, which produces multi-leaf lettuce, butterhead lettuce, and basil provided the LCI data of the VF (Table A.6). This VF is currently not operational on its full capacity, thus the measured inputs and outputs, based on several thousands of crops grown and sold, were extrapolated to achieve data for full operation. The water, nutrients, and seed inputs were specified for basil and lettuce separately, together with growth and packaging materials.

As stated by the manufacturer, both 6- and 7-layer trolleys use 600 W of LED and a photoperiod of 20 h, resulting in an electricity use of 9.7 kWh per kg FW lettuce. The remaining electricity demands were provided for the farm as whole and required assumptions to determine the allocation between lettuce and basil. The electricity demands for cooling and fan usage were allocated according to the electricity consumption of the LEDs (50% lettuce), as heat dissipated by artificial light leads to most of the cooling demands (Graamans et al., 2018). Propagation light was assigned according to the number of seeds, for each lettuce seeds, 15 basil seeds were propagated. To allocate dehumidification of mainly leaf transpired vapour, fresh weight was used (65% lettuce). These allocations resulted in a total electricity demand of 14.7 kWh per kg FW lettuce.

The crops produced never travel more than 15 km to the point of sale, as the VF is located very close to retailers. The transportation also includes for the weight of water within the sales pot of 5.45 L kg^{-1} lettuce. The materiality of the farm only considers components and materials up to, but not including, the walls, ceilings and floors of the rooms utilised by the farm due to its integration within an existing room in an existing building.

2.3 Results

Figure 2.4 presents the total carbon footprint of lettuce cultivation within the four farming typologies: OF, GHs, GHa, and VF. The carbon footprint of the VF is 8.177 $kgCO_{2\text{-}eq}$ kg^{-1} FW, 16.7 times greater than that of the OF (0.490 kg $CO_{2\text{-}eq}$ kg^{-1} FW), 6.8 times greater than GHs (1.211 kg $CO_{2\text{-}eq}$ kg^{-1} FW), and 5.6 times greater than GHa (1.451 kg $CO_{2\text{-}eq}$ kg^{-1} FW). The performance of the VF is specific to the case study used and is not representative of every VF operation. Other VFs, which employ different technologies and operational methods, may have differing results.

TOC

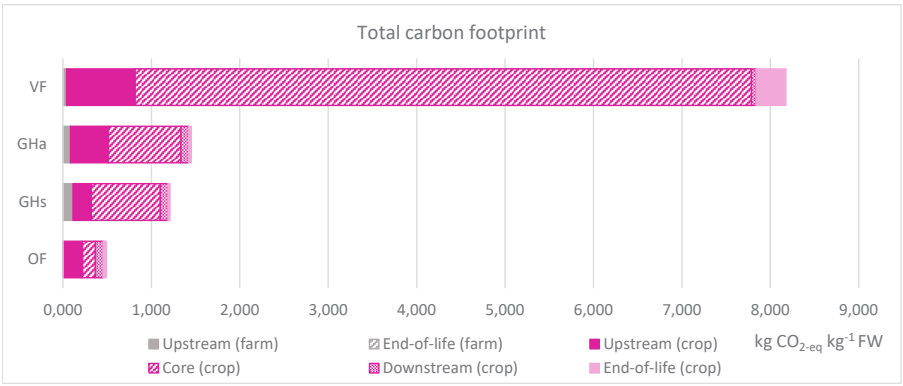

FIG. 2.4 The total carbon footprint of lettuce production within OF, GH(s), GH(a) and VF (please note that the farm end-of life value is not visible at this scale but is still included).

The carbon emissions of the different life cycle stages of the farm (Fig. 2.5A and B) and the crop (Fig. 2.5C–F) were compared between the case studies. GHs has the highest emissions relating to the farm itself, both for upstream and end-of-life emissions (Fig. 2.5A and B). Regarding the crop life cycle, the VF has the highest upstream (Fig. 2.5C), core (Fig. 2.5D), and end-of-life emissions (Fig. 2.5F), which results in the highest crop life cycle emissions overall.

The core emissions accounted for 85% of the total footprint of the VF, 56% of GHa, 65% of GHs, and 30% of OF. These emissions mostly related to electricity and fuel use, which represent the largest share of the total carbon footprint in GHs, GHa and VF. Carbon enrichment to enhance plant growth accounted for 38% of the upstream emissions of GHa, however, it did not result in emissions for GHs (Fig. 2.5C) as they were already accounted for in the core emissions due to on-site natural gas combustion (Section 2.2.3.2).

The upstream emission were primarily attributed to the energy and resources used for seedlings production within OF, GHs and GHa, representing 65%, 62%m and 46% of their respective carbon footprints. The VF propagates seedlings on-site, incorporating the energy and resources used in both upstream and core emissions of the crop life cycle. Finally, the transportation of the crop to the retail location accounted for relatively high downstream emissions in conventional farming methods (Fig. 2.5E), representing between 5.9% and 17.3% of their total carbon footprints.



FIG. 2.5 A comparison of the carbon footprint per life cycle stage of the four case studies: the life cycle of the farm including upstream (A) and end-of-life emissions (B), and the life cycle of the crop including upstream (C), core (D), downstream (E) and end-of-life emissions (F).

TOC

2.4 Discussion

The baseline scenario (Section 2.3) examined and compared empirical data between the four farming systems. Three alternative scenarios are proposed to improve the comparability of the data and include prospective improvements to the carbon footprints of all farming systems through the use of renewable energy. These scenarios include the lost potential of carbon sequestration by of land-use change (1), an alternative packaging scenario where all farms use polypropylene bags (2), and a scenario where all energy needs are met through renewable energy and bio-based fuels (3). The electricity use of the studied VF is later compared to that of existing literature to obtain a better understanding of its performance.

2.4.1 Farm life cycle

The farm life cycle of the GHs structure, with a lifespan of 15 y, emits 2.7 times more $CO_{2\text{-eq}}$ than the VF, and 23 times more than the OF (Fig. 2.5A). GHa uses NFT channels to produce lettuce within the exact same greenhouse as GHs. The annual yields of GHa are 1.8 times greater than GHs, resulting in 25% less upstream emissions. The OF, with a total building footprint of 1400 m^2, uses significantly larger quantities of materials than the VF. The lower emissions are explained by the total OF area of 15 ha gross (CBS, 2021) and the 50 y lifespan of the agricultural buildings (Nemecek and Kägi, 2007), compared to the 8–10 y lifespan of the VF components. If the studied VF was not integrated within an existing building it would require additional materials to construct the enclosure around the farm, leading to greater emissions. It should be emphasised that the materiality of the OF was based on assumptions made in a theoretical model (Appendix A.4) and the materials used in auxiliary equipment, climate installations, and machinery were not included both due a lack of robust data (Section 2.2.2.3).

2.4.1.1 The indirect impacts of land-use change

The indirect impacts of land-use change are explored by considering the potential capacity of agricultural land to sequester CO_2 if it was a forest instead. Figure 2.6 presents the potential for carbon uptake if the land used for agriculture was a young European forest, which is equivalent to 0.78 kg CO_2 m^{-2} (COM, 2021).

TOC

The potential for carbon sequestration that is lost by using land for the farming practice is significantly smaller for the VF due to its increased productivity and vertical arrangement. Furthermore, VFs are unlikely to occupy space that would otherwise be forest due to their location within urban environments. Therefore, the equivalent loss of carbon uptake presented in Figure 2.6 is not representative for VF.

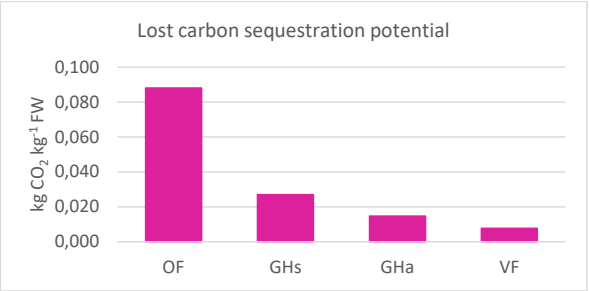

FIG. 2.6 Carbon sequestration if the gross floor area used to produce one kg FW lettuce was used as a young forest.

The lost potential for carbon sequestration by the studied VF, specifically, is considered to be zero as it is a form of zero-acreage farming, characterised by the non-use of land (Thomaier et al., 2014). This farming approach uses existing space within or upon buildings, differing from farming systems that occupy space at ground-level (Specht et al., 2015). For each ton of FW lettuce produced in the VF, the land freed up elsewhere would allow 15 to 88 kg CO_2 to be sequestered, if that land was to converted into a young forest.

2.4.2 Crop life cycle

2.4.2.1 Upstream

The literature reviewed in Section 2.1.1. suggested that VFs, compared to greenhouse horticulture and open-field farms, reduce the use of water, fertilisers, pesticides, and herbicides. The VF studied consumes no pesticides and herbicides, however, it consumes the highest concentration of nutrients. These nutrients are applied in tablet form to the growth containers, limiting dosing options. At the end of the growth cycle, 20% of these nutrients are discarded, which could easily be addressed and reduced. It is also a possibility that a recirculating system, as opposed to a closed system, would lead to additional nutrient efficiencies (Son et al., 2020).

The nutrient consumption of the VF does not solely explain the high upstream emissions; another aspect is the use of growth and packaging materials, which represent 42% and 48% of these emissions respectively (Fig. 2.5C). The VF studied uses a growth container (clear plastic), and sales container (bamboo paper with PE coating) to allow the plant to survive once purchased. This is seen as a unique selling point by the farmers. An alternative scenario was created where all lettuce crops from all case studies are packaged in polypropylene bags, as is already the case for conventionally grown lettuce. This scenario decreases the upstream emissions of the VF by 46% (Fig. 2.7). It was not possible to create uniformity across growth materials of the different case studies as these are an essential characteristic of each farming practice, i.e., the use of soil by OF and GHs, Rockwool and NFT channels by GHa, and growth containers with Rockwool plugs by VF.

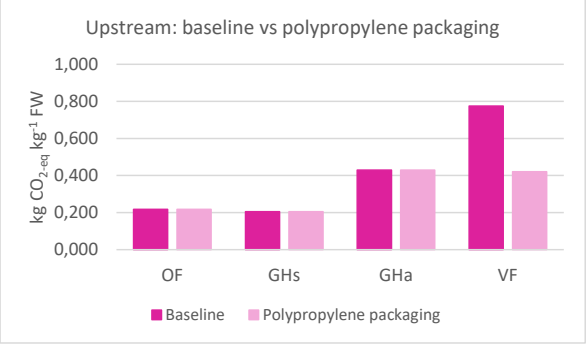

FIG. 2.7 Upstream emissions in the baseline scenario versus those when all farming methods use polypropylene packaging.

2.4.2.2 Core

Within the baseline scenario, electricity use from the national grid represented 85% of the total footprint of the VF. LED lights of 91 W m^{-2} and a 20-h photoperiod attributed to 65% of this electricity. To put the electricity use of the VF into perspective, it was compared to that of other VFs in Section 2.4.5.

The hydroponic systems of GHa and VF minimised evaporation of water by the limited surface open to air. The VF uses 9.1 L water per kg FW produced, when excluding the water discarded at the end of each growth cycle, compared to 1.5 L kg^{-1} FW by GHa. This indicates a high transpiration rate in the VF. Majid et al. (2021) confirmed this finding by stating that the transpiration rate of deep-water culture - in some ways comparable to the growth pots of the VF - is significantly higher than that of a NFT

TOC

system. Changing to a hydroponic NFT system could potentially reduce the water use of the studied VF. However, these savings will not be reflected in the carbon footprint as the current contribution of water in both GHa and VF is below 1%. It is important to not that the water usage of GHa was estimated based on three assumptions due to a lack of specific data: a 5% dry matter content for lettuce production, a minimal ET rate of 1.4 L per 5 g DW lettuce, and nutrient flushing of 1.1 times the minimal ET requirements (Section 2.2.3.3).

2.4.2.3 Downstream

The lettuce cultivated in the VF travels no further than 15 km to its selling location, in contrast to conventionally cultivated lettuce, which travels 160 km (Section 2.2.3). In the baseline scenario, the reduction in carbon footprint is limited to 37% as it considers the transportation of the crop, the sales container, and the water within it (5.45 L kg^{-1} FW). The alternative packaging scenario diminishes these emissions to 0.008 $kgCO_{2\text{-eq}}$ kg^{-1} FW, a significant 90% reduction compared to the conventional supply chain (Fig. 2.8). Despite this, the overall reduction in the VF's footprint is limited to 1%.

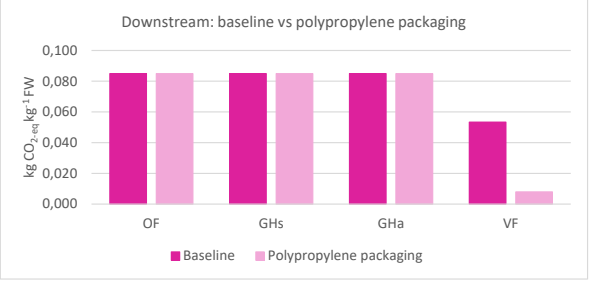

FIG. 2.8 Downstream emissions in the baseline scenario versus those when all farming methods use polypropylene packaging.

2.4.2.4 End-of-life

VFs have the potential to reduce food losses during cultivation, transportation, and consumption due to optimised growth conditions, reduced food miles (Grewal and Grewal, 2012), and improved shelf life (Benke and Tomkins, 2017). Given the lack of data on food losses in the supply chain and consumption phase, it was not possible to confirm the reduced food losses with the studied VF. The cumulative food losses

TOC

represent a small fraction of the total end-of-life emission of the VF, as the packaging and growth materials are responsible for 86% of these emissions (Fig. 2.5F). Although switching to polypropylene packaging decreases the end-of-life emissions of the VF by 56% (Fig. 2.9), the emissions remain significantly higher than those of conventional farming methods due to the use of individual plastic growth containers. As explained in Section 2.4.2.1, achieving uniformity across the growth materials in the different case studies was not feasible, as this is a specific characteristic of the farming practice and altering it would potentially affect lettuce yields.

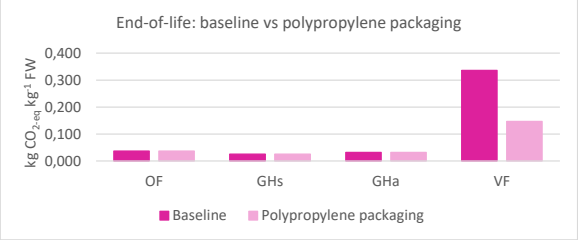

FIG. 2.9 End-of-life emissions of the baseline scenario versus those when all farming methods use polypropylene packaging.

2.4.3 Renewable energy scenario

The transition to renewable energy usage would significantly reduce the contribution of energy use to the carbon footprint of the farming practices. In this scenario, the electrification of heating with a ground source heat pump, steam production with an electric boiler, biodiesel use for agricultural machinery, and electricity production with PV panels were considered (Appendix A.5). This transition reduces the core emissions of OF, GHs, GHa, and VF by 23%, 75%, 85% and 83%, respectively (Fig. 2.10).

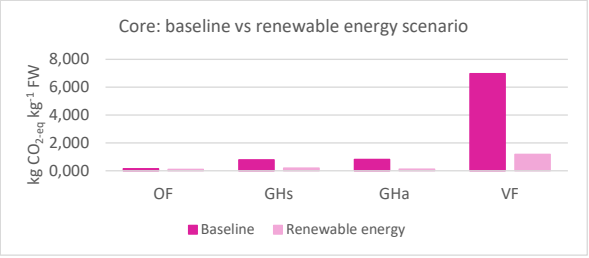

FIG. 2.10 Total core emissions in the baseline scenario versus those in the renewable energy scenario.

TOC

The remaining core emissions of GHs, GHa, and VF are explained by the EF used for electricity production with grid-connected PV panels in the Netherlands (Ecoinvent 3.6). This EF includes for the extraction of the materials of the PV panel, the electric components and mounting systems, the transportation of these materials to the production site, the production of the PV panel, waste treatment, and the installation. To translate these emissions into kg $CO_{2\text{-eq}}$ kWh^{-1}, country-specific yields based on local irradiation levels and current PV efficiencies are included (Jungbluth et al., 2007). Therefore, electricity production with PV panels still resulted in carbon emissions of 0.167, 0.125 and 1.173 kg $CO_{2\text{-eq}}$ kg^{-1} FW for GHs, GHa and VF, respectively.

To produce all electricity required by 1 m^2 VF cultivation area, 5.1 m^2 of south facing, 40° inclined, PV cells are needed, corresponding to about 6.8 m^2 of land (Appendix A.5). A significant area compared to the 0.69 m^2 floor area used per m^2 cultivation area. If the VF was a standalone structure with PV panels covering the entire south, east and west facades, and the roof, each m^2 cultivation area would still require 3.8 m^2 of PV cell area at ground level. The land-use of these PV panels would most likely result in a lost potential for carbon sequestration; however, this falls beyond the intended scope of this research.

Furthermore, due to the transition to renewable energy usage, external sources of CO_2 have to be sought for greenhouse horticulture as no CO_2 will be produced on-site when using all-electric heating. These sources would need to be of biogenic origin, e.g., biogas, biomass, or carbon capture and storage (Li et al., 2018). In this research, biogas was selected as the primary source of greenhouse carbon enrichment. Biogas consists of 55% methane (CH_4), and 43% CO_2. The remaining 2% includes impurities that are not useful. When upgrading biogas to the quality of natural gas, CH_4 is separated from CO_2. After separation, the CO_2 mixture is purified to remove impurities before using it as carbon enrichment of crops (Dijk et al., 2014). To represent emissions from CO_2 production, 44% of the EF for biogas was allocated to carbon enrichment. This reflects the pro- portion of gaseous content that is CO_2 as well as a proportional share of the impurities that need to be removed.

Therefore, the emissions from carbon enrichment in GHs increase from zero to 0.139 kg $CO_{2\text{-eq}}$ kg^{-1} FW in the renewable energy scenario, and that of GHa reduce from 0.429 to 0.407 kg$CO_{2\text{-eq}}$ kg^{-1} FW. It should be noted that the energy transition will reduce the availability of CO_2 drastically due to the limited availability of biogas and biomass worldwide (Beuchelt and Nassl, 2019).

2.4.4 Total footprint with alternative scenarios

Figure 2.11 presents the total carbon footprint when considering the use of identical packaging, the transition to renewable energy usage, and the loss of potential carbon sequestration altogether. The use of PV panels reduced the core emissions of the VF by 83%, however, electricity use still represents 66% of this alternative carbon footprint.

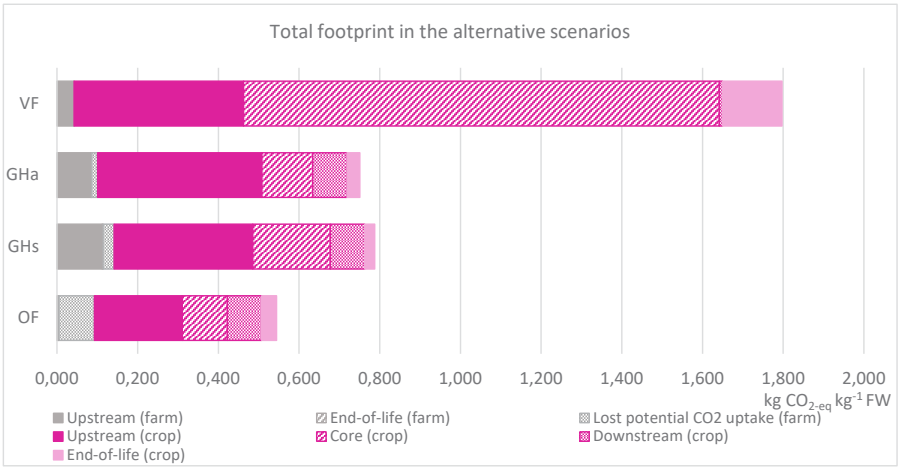

FIG. 2.11 The total carbon footprint of lettuce production when considering the use of identical packaging, the transition to renewable energy, and the lost potential of carbon sequestration (please note that the farm end-of life value is not visible at this scale but is still included).

The carbon footprints of GHs, GHa and VF are reduced by 35%, 48%, and 78%, respectively, when compared to the baseline scenarios (Fig. 2.12). Conversely, due to its extensive land-use, the carbon footprint of the OF increases with 11% when including the lost carbon sequestration potential. By considering the three alternative scenarios together, the substantial differences in carbon footprints the conventional farming methods and the VF observed in the baseline scenario are reduced from a factor of 16.7 to a factor of 3.3, narrowing the gap between OF and VF.

TOC

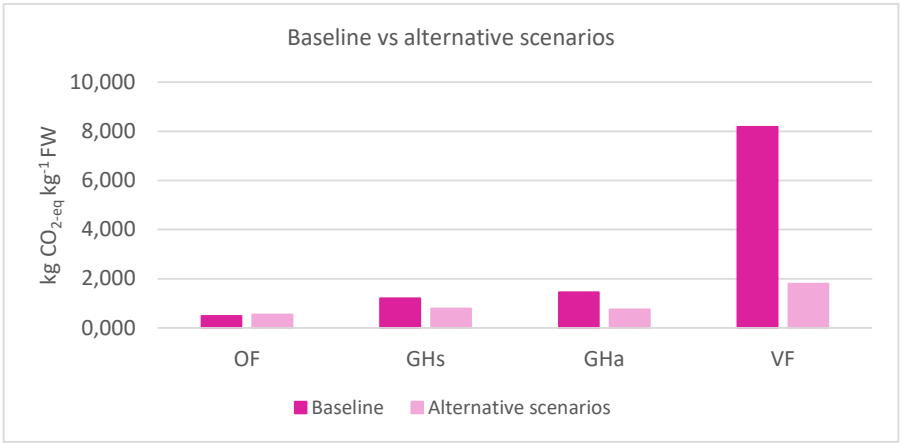

FIG. 2.12 The total carbon footprint of lettuce production in the baseline scenario versus the alternative carbon footprint when considering the use of identical packaging, the transition to renewable energy, and the loss of potential of carbon sequestration.

2.4.5 Comparison to other literature

The electricity use was the largest contributor to the carbon footprint of the VF in both the baseline and alternative scenario. Table A.1, #1–8 represents the diverging electricity use per kg FW of CBVFs from literature and includes details on yields and light characteristics. The VF studied is added to this comparison in Fig. 2.13 (and Table A.1, #9) and uses relatively little electricity with a lower proportion allocated to artificial light.

The amount of FW produced per kWh electricity depends on many factors, including the photosynthetic photon flux density (PPFD) and the photoperiod. The relation between PPFD (µmol m^{-2} s^{-1}) and power of the light (W m^{-2}) is the molar efficacy, which currently ranges between 2.1 and 3.5 µmol J^{-1} for LED (Weidner et al., 2021). The VF simulated by Benis et al. (2017) uses the least amount of kWh kg^{-1} FW, however, the data are too optimistic as the molar efficacy is 9.1 µmol J^{-1} (47 W m^{-2}; 427 µmol m^{-2} s^{-1}). The studied VF uses 91 W m^{-2} LED with a PPFD of 140 µmol m^{-2} s^{-1}, resulting in a very low molar efficacy of 1.54 µmol J^{-1}.

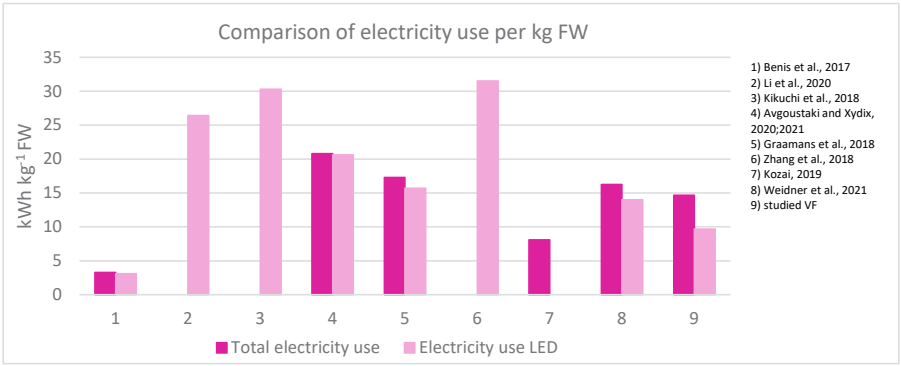

FIG. 2.13 Comparison of electricity use per kg FW produced by the studied VF and other CBVFs from literature.

The best performance for lettuce production, in terms of quality and yield, requires approximately a PPFD of 240 µmol m^{-2} s^{-1} and a 16 h photoperiod (Matysiak et al., 2022). This corresponds to a daily light integral (DLI) of 13.8 mol m^{-2} d^{-1} compared to 10.1 mol m^{-2} d^{-1} observed in the studied VF. To gain more insight into the VF's performance, the light use efficiency (LUE) of the studied VF was compared to that of VFs in existing literature (Fig. 2.14). The LUE presents the sellable FW produced per mol of incident light provided to the crops (Carotti et al., 2021).

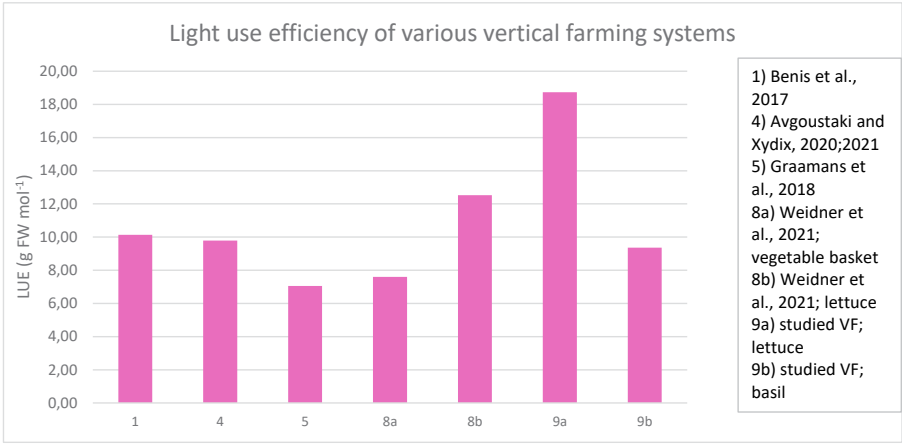

FIG. 2.14 Light use efficiency of various vertical farms in g FW produced per mol-1 of incident light.

TOC

Matsyiak et al. (2022) noted significantly more cases of tip burn above the optimal DLI of 13.8 mol m^{-2} d^{-1}. Similar findings were noted by Sago (2016) stating that an increase of PPFD from 150 to 300 µmol m^{-2} s^{-1} resulted in significantly more cases of tip burn. Both studies of Graamans et al. (2018) and Li et al. (2020) used a PPFD far above this level. PPFDs between 200 and 300 µmol m^{-2} s^{-1} were applied by Zhang et al. (2018), Avgoustaki and Xydis (2021; 2021) and Weidner et al. (2021). Figure 2.14 did not include the studies of Zhang et al. (2018) and Li et al. (2020) as no data on their yields were provided. Kikuchi et al. (2018) did not present data on yield, photoperiod, DLI and PPFD, making it hard to compare the measured data of this CBVF with that of the studied VF.

Aside from lettuce production, the LUE of basil production in the studied VF was included in Fig. 2.14. The LUE of basil was significantly lower than that of lettuce, as the FW of the basil produced was significantly lower while using similar lighting properties. Comparing basil production in Avgoustaki and Xydis (2020; 2021) and lettuce in Weidner et al. (2021) gives similar findings, as the DLI of basil is higher.

The studied VF consumes relatively little electricity for artificial light to produce a kg of lettuce, whilst the molar efficacy and the PPFD are low. This suggests that the lettuce crops produced in the studied VF convert moles of incident light very efficiently into FW. To put this in perspective relative to findings from other studies, the LUE of lettuce produced in the simulated VF of Weidner et al. (2021) was applied to the studied VF. A DLI of 15.06 mol m^{-2} d^{-1}, a photoperiod of 20 h and a molar efficacy of 2.1 µmol J^{-1} results in 99.6 W m^{-2} LED with an electricity usage of 10.6 kWh kg^{-1}. Using this value increases the baseline carbon footprint by 4% and the alternative footprint with 3%.

2.5 Conclusion

This study performed a quantitative carbon footprint assessment of lettuce cultivation within a typical open-field farm, soil-based green- house, hydroponic greenhouse, and an operational VF in the Netherlands to evaluate the current carbon footprint of vertical farming systems. The assessment included the emissions related to both the life cycle of the farm and the crop, from cradle-to-grave. The baseline empirical data showed that the carbon footprint of the VF (8.177 kg $CO_{2\text{-eq}}$ kg^{-1} FW) was 16.7 times greater than OF (0.490 kg $CO_{2\text{-eq}}$ kg^{-1} FW), 6.8 times greater than GHs (1.211 kg $CO_{2\text{-eq}}$ kg^{-1} FW) and 5.6 times greater than GHa (1.451 kg $CO_{2\text{-eq}}$ kg^{-1} FW).

Three alternative scenarios were considered to improve the comparability of the baseline data as well as present potential carbon savings in all case studies by using renewable energy. These scenarios included: the lost carbon sequestration potential as a result of land-use change (1), identical packaging for all farming systems (2), and the transition to renewable energy usage (3). When these scenarios were considered collectively, the carbon footprint of the VF (1.797 kg $CO_{2\text{-eq}}$ kg^{-1} FW) reduced to 3.3 times greater than OF (0.544 kg $CO_{2\text{-eq}}$ kg^{-1} FW), 2.3 times greater than GHs (0.788 kg $CO_{2\text{-eq}}$ kg^{-1} FW) and 2.4 times greater than GHa (0.751 kg $CO_{2\text{-eq}}$ kg^{-1} FW).

Even with the use of PV panels, the largest contributor to the VF's carbon footprint was electricity usage, representing 66% of the overall alternative carbon footprint. Artificial light accounted for 65% of this electricity. To put this electricity use into perspective, the kWh of electricity used to produce a kg of lettuce and LED characteristics of the VF were compared to that of other VFs from literature. This literature review showed that most of the existing vertical farming data are based on simulated farms and often not all data on the light characteristics and yields are presented, which makes it difficult to make a fair comparison. This lack of data applied in particular to the studies that presented the carbon footprint of vertical farming. The studied VF used a low amount of electricity for artificial light and still had high yields. Using light use efficiency values from literature to improve its representation of an average VF resulted in a slight increase in the baseline and alternative carbon footprint by 4% and 3% respectively.

This illustrates that VFs, as they exist today, are not able to provide a sustainable solution to the global issues of decreasing availability of arable land and increasing food demands, even though they offer great benefits when compared to conventional farming methods. To become a sustainable solution, VFs need to decrease their energy use drastically to significantly reduce their carbon footprint and compete with conventional farming techniques from an environmental perspective.

The upstream and end-of-life emissions of the growth materials represented the second largest carbon emissions in the alternative scenario. Suggesting that, simultaneously reducing the use of these growth materials and the electricity demands will greatly improve the carbon footprint of the practice. Further research is required to determine how these reductions might be achieved and whether it is a possibility that vertical farming might one day compete with greenhouse horticulture from a carbon footprint perspective. If this can be achieved, vertical farming could form part of a sustainable, low carbon, and secure future food system as a result of its efficient use of land, high yields, minimal use of water and nutrients, the redundancy of pesticides and herbicides, and the ability to be located within or adjacent to cities where demands for food are highest.

References

Avetisyan, M., Hertel, T., Sampson, G. 2013. Is local food more environmental friendly? The GHG emission impacts of consuming imported versus domestically produced food. Environ. Resour. Econ. Times 58, 415–462. https://doi.org/10.1007/s10640- 013-9706-3.

Avgoustaki, D.D., Xydis, G. 2020. Indoor vertical farming in the urban Nexus content: business growth and resource savings. Sustainability, 12. https://doi.org/10.3390/su12051965.

Avgoustaki, D.D., Xydis, G, 2021. Energy cost reduction by shifting electricity demand in indoor vertical farms with artificial lighting. Biosyst. Eng., 211, 219–229. https://doi.org/10.1016/j.biosystemseng.2021.09.006.

Barbosa, G.L., Almeida, G.F.D., Kublik, N., Proctor, A., Reichelm, L., Weissinger, L., Wohlleb, G.M., Halden, R.U. 2015. Comparison of land, water, and energy requirements of lettuce grown using hydroponic vs. conventional agricultural methods. Int. J. Environ. Res. Publ. Health, 12 (6), 6879–6891. https://doi.org/10.3390/ijerph120606879.

Benis, K., Ferrao, P. 2018. Commercial farming within the urban built environment; taking stock of an evolving field in northern countries. Global Food Secur., 17, 30–37. https://doi.org/10.1016/j.gfs.2018.03.005.

Benis, K., Reinhart, C., Ferrao, P. 2017. Development of a simulation-based decision support workflow for the implementation of building-integrated agriculture (BIA) in urban contexts. J. Clean. Prod., 147, 589–602. https://doi.org/10.1016/j.jclepro.2017.01.130.

Benke, K., Tomkins, B. 2017. Future food-production systems: vertical farming and controlled-environment agriculture. Sustain. Sci. Pract. Policy, 13 (1), 13–26. https://doi.org/10.1080/15487733.2017.1394054.

Beuchelt, T.D., Nassl, M. 2019. Applying a sustainable development lens to global biomass potentials. Sustainability, 11 (5078). https://doi.org/10.3390/su11185078.

Breukers, A., Stokkers, R., Spruijt, J., Roelofs, P., de Haan, J. 2014. Teelt de grond uit in perspectief: prestaties van teeltsystemen op het gebied van integrale duurzaamheid. Praktijkonderzoek Plant & Omgeving, WUR, Wageningen.

Carotti, L., Graamans, L., Puksic, F., Butturini, M., Meinen, E., Heuvelink, E., Stanghellini, C. 2021. Plant factories are heating up: Hunting for the best combination of light intensity, air temperature and root-zone temperature in lettuce production. Front. Plant Sci. 11. https://doi.org/10.3389/fpls.2020.592171.

Centraal Bureau voor de Statistiek. 2021. Landbouw: gewassen, dieren en grondgebruik naar bedrijfstype, nationaal. https://opendata.cbs.nl/statline/#/CBS/nl/dataset/ 80782ned/table?ts=1642524024433.

Ciolkosz, D.E., Albright, L.D., Both, A.J. 1998. Characterizing evapotranspiration in a greenhouse lettuce crop. Acta Hortic. 456, 255–261.

CO2 emissiefactoren. 2021. CO2 emissiefactoren. https://www.co2emissiefactoren.nl/. (Accessed December 6, 2021).

COM. 2021. Commission staff working document: the 3 billion tree planting pledge for 2030 (651 final). European Commission, Brussel. https://ec.europa.eu/environment/3-billion-trees_en.

CropKing. 2022. CropKing. https://cropking.com/sites/default/files/2022-02/Catalo g_Web.pdf. (Accessed April 25, 2022).

Delden, S.H. van, SharathKumar, M., Butturini, M., Graamans, L.J.A., Heuvelink, E., Kacira, M., Marcelis, L.F.M. 2021. Current status and future challenges in implementing and upscaling vertical farming systems. Nature food, https://doi. org/10.1038/s43016-021-00402-w.

Dijk, C.J. van, Meinen, E., Dueck, T.A. 2014. Kwaliteit biogas-CO2 voor toepassing in de glastuinbouw: research report (GTB-1310). Wageningen UR Glastuinbouw, Wageningen.

Dooren, C. van, 2019. Factsheet Voedselverspilling Bij Huishoudens in Nederland in 2019. Stichting Voedingscentrum Nederland, Den Haag.

Ecoinvent. 2015. The Ecoinvent Database. V.3.6

Edwards, F., Dixon, J., Friel, S., Hall, G., Larsen, K., Lockie, S., Wood, B., Lawrence, M., Hanigam, I., Hogan, A., Hattersleyl, L. 2011. Climate change adaptation at the intersection of food and health. Asia. Pac. J. Publ. Health 23, 91–104. https://doi. org/10.1177/1010539510392361.

Forster, P., Storelvmo, T., Armour, K., Collins, W., Dufresne, J.L., Frame, D., Lunt, D.J., Mauritsen, T., Palmer, M.D., Watanabe, M., Wild, M., Zhang, H. 2021. The earth's energy budget, climate feedbacks, and climate sensitivity. In: Masson-Delmotte, V., Zhai, P., Pirani, A., Connors, S.L., Pean, C., Berger, S., Caud, N., Chen, Y., Goldfarb, L., Gomis, M.I., Huang, M., Leitzell, K., Lonnoy, E., Matthews, J.B.R., Maycock, T.K., Waterfield, T., Yelekçi, O., Yu, R., Zhou, B. (Eds.), Climate Change 2021: the Physical Science Basis. Contribution of Working Group I to the Sixth Assessment Report of the Intergovernmental Panel on Climate Change. Cambridge University Press, Cambridge, United Kingdom and New York, NY, USA, pp. 923–1054. https://doi.org/10.1017/9781009157896.009.

Germer, J., Sauerborn, J., Asch, F., de Boer, J., Schreiber, J., Weber, G., Müller, J. 2011. Skyfarming an ecological innovation to enhance global food security. J. Verbrauch. Lebensm., 6 (2), 237–251. https://doi.org/10.1007/s00003-011-0691-6.

Graamans, L., Baeza, E., van den Dobbelsteen, A., Tsafaras, I., Stanghellini, C. 2018. Plant factories versus greenhouses: comparison of resource use efficiency. Agric. Syst., 160, 31–42. https://doi.org/10.1016/j.agsy.2017.11.003.

Grewal, S.S., Grewal, P.S. 2012. Can cities become self-reliant in food? Cities, 29, 1–11. https://doi.org/10.1016/j.cities.2011.06.03.

Hunter, M.C., Smith, R.G., Schipanski, M.E., Atwood, L.W., Mortensen, D.A. 2017. Agriculture in 2050: recalibrating targets for sustainable intensification. Bioscience, 67 (4), 386–391. https://doi.org/10.1093/biosci/bix010.

Jungbluth, N., Dones, D., Frischknecht, R. 2007. Life cycle assessment of photovoltaics: update of the ecoinvent database. Mater. Res. Soc. Symp. Proc., https://10.155 7/PROC-1041-R01-03.

Kalantari, F., Tahir, O.M., Joni, R.A., Fatemi, E. 2017. Opportunities and challenges in sustainability of vertical farming: a review. J. Landsc. Ecol., 11 (1), 35–60. https:// doi.org/10.1515/jlecol-2017-0016.

Kikuchi, Y., Kanematsu, Y. 2020. Life cycle assessment. In: Kozia, T., Takagaki, M., Niu, G. (Eds.), Plant Factory: an Indoor Vertical Farming System for Efficient Quality Food Production. Academic Press, London, pp. 321–329.

Kikuchi, Y., Kanematsu, Y., Yoshikawa, N., Okubo, T., Takagaki, M. 2018. Environmental and resource use analysis of plant factories with energy technology options: a case study in Japan. J. Clean. Prod. 186, 703–717. https://doi.org/10.1016/j.jclepro.2018.03.110.

Klein, C. de, Novoa, R.S.A., Ogle, S., Smith, K.A., Rochette, P., Wirth, T.C., McConkey, B. G., Mosier, A., Rypdal, K. 2006. N2O emission from managed soils, and CO2 emissions from lime and urea application. In: Eggleston, S., Buendia, L., Miwa, K., Ngara, T., Tanabe, K. (Eds.), IPPC Guidelines for National Greenhouse Gas Inventories Volume 4: Agriculture, Forestry and Other Land Use. IPPC, pp. 11.1–11.54.

Kozai, T. 2019. Towards sustainable plant factories within artificial lighting (PFALs) for achieving SDGs. Int. J. Agric. Biol. Eng. 12, 28–37. https://doi.org/10.25165/j. ijabe.20191205.5177.

Lennard, W.A., Leonard, B.V. 2006. A comparison of three different hydroponic sub- systems (gravel bed, floating, and nutrient film technique) in an aquaponic test system. Aquac. Bar Int. 14 (6), 539–550. https://doi.org/10.1007/s10499-006-9053-2.

Li, Y., Ding, Y., Li, D., Miao, Z. 2018. Automatic carbon dioxide enrichment strategies in the greenhouse: a review. Biosyst. Eng. 171, 101–119. https://doi.org/10.1016/j. biosystemseng.2018.04.018.

Li, L., Li, X., Chong, C., Wang, C.H., Wang, X. 2020. A decision support framework for the design and operation of sustainable urban farming systems. J. Clean. Prod. 268, 1–15. https://doi.org/10.1016/j.jclepro.2020.121928.

Majid, M., Khan, J.N., Shad, Q.M.A., Masoodi, K.Z., Afroza, B., Parvaze, S. 2021. Evaluation of hydroponic systems for the cultivation of lettuce (lactuca sativa L., var. Longifolia) and comparison with protected soil-based cultivation. Agric. Water Manag. 23, 156–162. https://doi.org/10.31830/2348-7542.2022.022.

Matysiak, B., Ropelewska, E., Wrzodak, A., Kowalski, A., Kaniszewski, S. 2022. Yield and quality of romaine lettuce at different daily light integral in an indoor controlled environment. Agronomy 12 (1026). https://doi.org/10.3390/agronomy12051026.

Mbow, C., Rosenzweig, C., Barioni, L.G., Benton, T.G., Herrero, M., Krishnapillai, M., Liwenga, E., Pradhan, P., Rivera-Ferre, M.G., Sapkota, T., Tubiello, F.N., Xu, Y. 2019. Food security. In: Shukla, P.R., Skea, J., Calvo Buendia, E., Masson- Delmotte, V., Po¨rtner, H.O., Malley, J. (Eds.), Climate Change and Land: an IPCC Special Report on Climate Change, Desertification, Land Degradation, Sustainable Land Management, Food Security, and Greenhouse Gas Fluxes in Terrestrial Ecosystems. In Press. https://www.ipcc.ch/srccl/chapter/chapter-5/.

Monsees, H., Suhl, J., Paul, M., Kloas, W., Dannehl, D., Würtz, S. 2019. Lettuce (Lactuca Sativa variety Salanova) production in decoupled aquaponic system: same yield and similar quality as in conventional hydroponic systems but drastically reduced greenhouse gas emissions by saving inorganic fertilizer. PLoS One 14(6). https://doi.org/10.1371/journal.pone.0218368.

Montero, J.I., Anto´n, A., Torrellas, M., Ruijs, M., Vermeulen, P. 2011a. Environmental and Economic Profile of Present Greenhouse Production Systems in Europe: EUPHOROS Deliverable N 5 Final Report (No. Deliverable 5 Final Report). European Commission, Cabrils/Wageningen.

Montero, J.I., Anto´n, A., Torrellas, M., Ruijs, M., Vermeulen, P. 2011b. Environmental and Economic Profile of Present Greenhouse Production Systems in Europe: Annex (No. Deliverable 5 Final Report). European Commission, Cabrils/Wageningen.

Nemecek, T., Kägi, T. 2007. Life Cycle Inventories of Agricultural Production Systems: Data v2.0. Agroscope Reckenholz-Tänikon Reseach Station ART. https://db.ecoinve nt.org/reports/15_Agriculture.pdf.

Pegge, S.M., van der Heijden, C.H.T.M., Duineveld, M.P.J. 2006. Food Miles: eindrapporatage behorend bij de Food Mile Evalator. Agrotechnology and Food Sciences Group, Wageningen.

Poore, J., Nemecek, T. 2018. Reducing food's environmental impacts through producers and consumers. Science 360, 987–992. https://doi.org/10.1126/science.aaq0216.

Portmann, F.T., Siebert, S., Doll, P. 2010. MIRCA2000-global monthly irrigated and rainfed crop areas around the year 2000: a new high-resolution data set for agricultural and hydrological modelling. Global Biogeochemi. Cycles 24 (1). https://doi.org/10.1029/2008GB003435.

Pulselli, R.M., Marchi, M., Neri, E., Marchettini, N., Bastianoni, S. 2019. Carbon accounting for decarbonisation of European city neighbourhoods. J. Clean. Prod. 208, 850–868. https://doi.org/10.1016/j.jclepro.2018.10.102.

Raaphorst, M.G.M., Benninga, J. 2019. Kwantitatieve informatie voor de glastuinbouw 2019: kengetallen voor groenten-, snijbloemen-, pot- en perkplanten teelten. Wageningen UR, Wageningen, 26.

Sago, Y. 2016. Effects of light intensity and growth rate on tipburn development and leaf calcium concentration in butterhead lettuce. Hortscience 51, 1087–1091. https:// doi.org/10.21273/HORTSCI10668-16.

Schreuder, R., van Leeuwen, M., Spruijt, J., van der Voort, M., van Asperen, P., Hendriks- Goossens, V. 2009. Kwantitatieve informatie akkerbouw en vollegrondsteelt 2009. Wageningen UR, Lelystad.

Smit, P.X. 2010. CO2-voorziening Glastuinbouw 2008-2020: Vooruitblik Bij Toepassing 20% Duurzame Energie. LEI Wageningen UR, Den Haag.

Smith, P., Martino, D., Cai, Z., Gwary, D., Janzen, H.H. 2008. Global estimations of the inventory and mitigation potential of methane emissions from rice cultivation conducted using the 2006 intergovernmental panel on climate change guidelines. Global Biogeochem. Cycles 23.

Snoek, N.J. 1985. Teelt van sla. Consultentschap in algemene dienst voor akkerbouw en de groenteteelt in de vollegrond, Lelystad.

Son, J.E., Kim, H.J., Ahn, T.I. 2020. Hydroponic Systems. In: Kozia, T., Takagaki, M., Niu, G. (Eds.), Plant Factory: an Indoor Vertical Farming System for Efficient Quality Food Production. Academic Press, London, pp. 273–283.

Specht, K., Siebert, R., Thomaier, S., Freisinger, U.B., Sawicka, M., Dierich, A., Henckel, D., Busse, M. 2015. Zero-acreage farming in the city of Berlin: an aggregated stakeholder perspective on potential benefits and challenges. Sustainability 7, 4511–4523. https://doi.org/10.3390/su7044511.

Thomaier, S., Specht, K., Henckel, D., Dierich, A., Siebert, R., Freisinger, U., Sawicka, M. 2014. Farming in and on urban buildings: present practice and specific novelties of zero-acreage farming (zfarming). Renew. Agric. Food Syst. 1–12. https://doi.org/ 10.1017/S1742170514000143.

Velden, N.J.A. van der, Smit, P.X. 2019. CO2-behoefte Glastuinbouw 2030: Research Report (2019-074). Wageningen UR, Wageningen.

Wada, T. 2019. Theory and technology to control the nutrient solution of hydroponics. In: Anpo, M., Fukuda, H., Wada, T. (Eds.), Plant Factory Using Artificial Light: Adapting to Environmental Disruption and Clues to Agriculture Innovation. Elsevier, Amsterdam, pp. 5–14. https://doi.org/10.1016/C2017-0-00580-3.

Wageningen University and Research. 2020. Dutch supermarkets provide insights into food waste. https://www.wur.nl/en/Research-Results/Research-Institutes/food-biobased-research/show-fbr/Dutch-supermarkets-provide-insights-into-food-waste-F00DWa5.htm.

Weidner, T., Yang, A., Hamm, M.W. 2021. Energy optimisation of plant factories and greenhouses for different climatic conditions. Energy Convers. OR Manag. 243 (114336) https://doi.org/10.1016/j.enconman.2021.114336.

Zhang, X., He, D., Niu, G., Yan, Z., Song, J. 2018. Effects of environmental lighting on the growth, photosynthesis, and quality of hydroponic lettuce in a plant factory. Int. J. Agric. Biol. Eng. 11 (2), 33–40. https://doi.org/10.25165/j.ijabe.20181102.3420.



© Lucas van der Wee

TOC

3 Vertical farms integrated into buildings

The content of this chapter was published as:
Synergetic integration of vertical farms in buildings: reducing the use of energy, water, and nutrients
Blom, T., Jenkins, A., van den Dobbelsteen, A.A.J.F.
Frontiers in Sustainable Food Systems, 2023, 29. DOI: 10.3389/fsufs.2023.1227672

Supplementary material for this chapter is provided in Appendix B
The datasets of this chapter are available at the repository 4TU Research Data.
DOI: 10.4121/adca348c-49a6-4e2f-a1c7-6f2b3d40c16b.v3

In the previous chapter, the baseline carbon footprint of vertical farming systems was calculated in comparison to that of conventional farming systems in the Netherlands. Vertical farming offers several benefits over conventional farming systems, including efficient land-use, high yields, minimal water and nutrient usage, the redundancy of pesticides and herbicides, and the ability to be located within or adjacent to cities where food demands are high. However, the result of this carbon assessment demonstrated that the substantial electricity use for artificial lighting outweighed these benefits from a carbon footprint perspective. These findings suggest that vertical farms, in their current state, are not able to provide a sustainable solution to the global challenges of increasing food demands, decreasing availability of arable land, and climate change. To become a sustainable solution, vertical farms must make substantial reductions in their energy usage. In addition, the high electricity use for artificial lighting results in the production of substantial quantities of waste heat.

Chapter 3 delves into the potential to integrate vertical farming systems within buildings. The main focus of this study is to reduce the energy usage of both the vertical farm and building by leveraging energy synergies between both entities. Furthermore, the study explores the potential to exchange flows of water and nutrients between the building and the vertical farm to reduce the need for external inputs. Consequently, Chapter 3 addresses the second research question posed in this dissertation:

How can the integration of vertical farms into the energy and resource systems of a building reduce the energy and resource use of both entities?

3.1 Introduction

In 2021, the energy used for building heating purposes represented 23% of the global energy consumption (IEA, 2022). The total energy use by buildings is responsible of 28% of the global greenhouse gas (GHG) emissions (World Green Building Council, 2019), creating the need to drastically reduce building energy use to curtail these GHG emissions. The 'New Stepped Strategy' can be applied to achieve this aim, which adds an intermediate step between reducing demands and using renewable sources to the well-known Trias Energetica strategy. This step includes the use of available waste flows (van den Dobbelsteen et al., 2011).

The integration of urban agriculture in cities can help to better close resource cycles of energy, water, materials (Vernay et al., 2010), and nutrients (Jurgilevich et al., 2016) by creating synergies between the farm and other urban functions, i.e., reusing the waste streams of urban agriculture as a resource for the city and vice versa. Examples of these synergies include nutrient recovery from the sewage system (Wielemaker et al., 2018), and the use of carbon dioxide (CO_2) from production processes to increase crop yields (Marchi et al., 2018).

At the building scale, bidirectional synergies between a rooftop greenhouse and an office building with laboratories have been identified and quantified by Muñoz-Liesa et al. (2020, 2022). The greenhouse functioned as a heat and cold sink by reusing the building's exhaust air for heating during colder months and cooling during warmer months, and as a solar collector that supplied excess heat to the building. Furthermore, this greenhouse reduced heat losses through the building's roof (Muñoz-Liesa et al., 2020), and the CO_2-concentration of the greenhouse was increased using the building's exhaust air (Sanjuan-Delmás et al., 2018). Using these principles, urban agriculture can increase the sustainability of cities, buildings, and food systems (Kozai and Niu, 2020).

An recent typological addition to urban agriculture is vertical farming; a food production system within a controlled environment that uses vertically stacked hydroponic systems and artificial light (Kalantari et al., 2017) to achieve year-round production of crops with maximum density and high yields (Graamans et al., 2018). Vertical Farms (VFs) use water, pesticides, herbicides (Kalantari et al., 2017), CO_2 (Kozai et al., 2006), and fertilisers (Germer et al., 2011) highly efficiently. The electricity use for artificial light and climate systems is, however, substantial and outweighs the aforementioned benefits altogether when comparing the carbon footprint of a VF to that of conventional agriculture systems in the Netherlands

(Chapter 2). Furthermore, the electricity use represents the highest share of the operational costs (Pesch and Louw, 2023), especially when considering recent high energy prices.

The artificial lights within a VF produce excess heat, which has been identified as a potential low-temperature heat source for district heat networks by various researchers (Thomaier et al., 2014; Gentry, 2019; Martin et al., 2019). VFs may also contribute to a balanced renewable energy system by producing food and residual heat when there is excess electricity production during sunny or wind days. The heat produced by VFs can be stored in seasonal thermal energy storage systems to bridge energy imbalances (Graamans, 2021). Martin et al. (2022) explored a bidirectional energy synergy between a VF and a residential building. This synergy exchanged waste heat produced by the VF with the cold produced when heating the building to reduce the total energy use of the building. One other study identified a synergy between VFs and buildings through the direct integration of VFs in office spaces to reduce indoor CO_2 levels, and the energy used by ventilation systems (Shao et al., 2021).

Although the potential to minimise resource use in cities through the integration of urban agriculture had been recognized by literature, little research had been done on creating synergies between urban agriculture and buildings, and even less on the integration of VFs. The goal of this study is to investigate how the integration of VFs into the energy and resource systems of a building can reduce the energy and resource use of both entities collectively.

This chapter focuses on the integration of VFs within apartments, offices, restaurants, supermarkets, and swimming pools. The baseline conditions of the VF and building typologies are discussed first in Sections 3.2.1 and 3.2.2. As energy represents the largest share of the carbon footprint of VFs (Chapter 2), the main focus is to exchange residual energy between the VF and the building, creating bidirectional synergies. To explore the potential to enlarge these synergies through the use of seasonal energy storage, the study investigates the integration of VF within buildings with and without seasonal storage (Section 3.2.3). Unidirectional flows are also studied, including the potential to reuse water and nutrients outputs from the building within the VF, and the production of crops for the building users.

The results present the ratios required between the cultivation area of the VF and floor area of the building to supply the thermal energy demands using bidirectional synergies, including the calculated energy savings (Section 3.3.1). Section 3.3.2 discusses the unidirectional flows of water and nutrient outputs from the building to the VF. This section also calculates the number of building users that

can be fed by the crops produced within the VF. Finally, the results and assumptions are discussed in greater detail in Section 3.4, including the identification of future research opportunities, leading to the final conclusions of the research in Section 3.5.

3.2 Methodology

This chapter investigates the potential for bidirectional energy exchange between VFs and buildings. Furthermore, three unidirectional flows are studied: the production of crops for consumption by the building users (1), the reuse of treated grey water outputs from the building for crop irrigation (2), and the recovery of nutrients from urine to replace synthetic fertilisers (3).

The research method is separated into three subsections (Fig. 3.1). Section 3.2.1 describes the baseline conditions of the VF, including the climate setpoints, cooling and dehumidification strategy, and the inputs and outputs of crops, water, and nutrients. Section 3.2.2 defines the baseline heating and cooling systems of the buildings, and the inputs and outputs of vegetables, water, and nutrients. The potential strategies to enable bidirectional exchange of energy are defined in Sections 3.2.3.1 and 3.2.3.2. Finally, the performance of these strategies are assessed and the potential energy savings are calculated (Section 3.2.3.3).

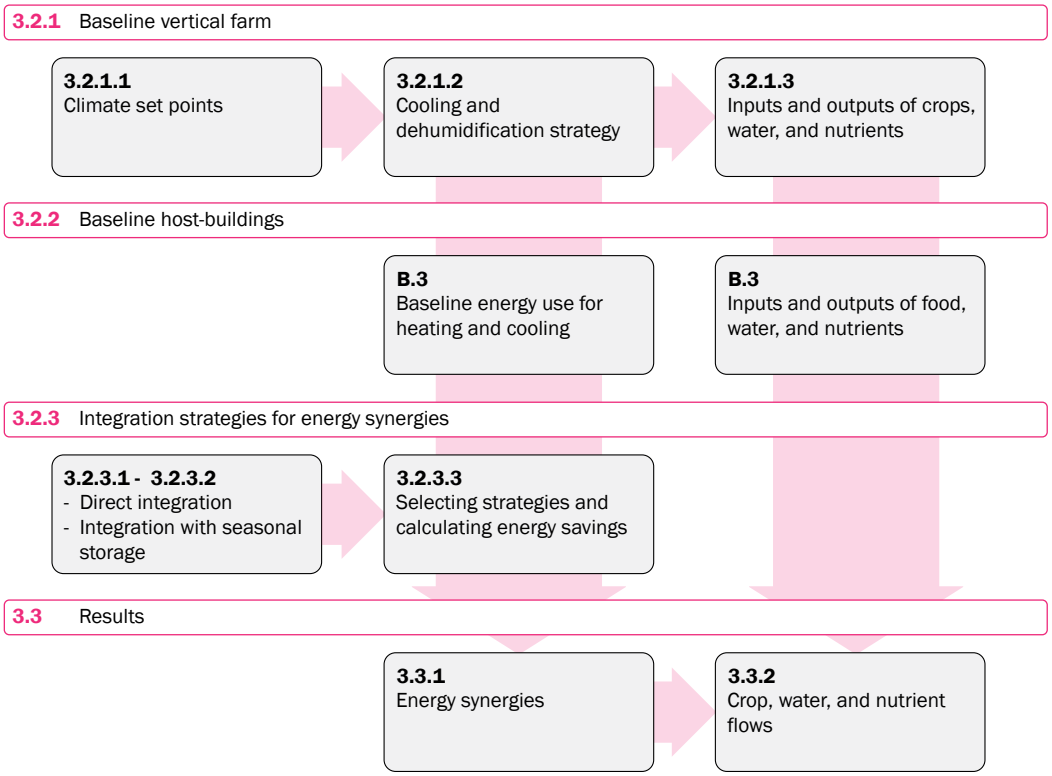

FIG. 3.1 Structure of the methods (Sections 3.2.1–3.2.3) and that of the results (Sections 3.3.1–3.3.2).

3.2.1 Baseline vertical farm

In contrast to Chapter 2, this study focuses on a hypothetical VF located in the Netherlands. This VF can be defined as a closed-box VF, which is hermetically sealed to create uniform growth conditions that are independent from the outdoor climate (Van Delden et al., 2021). This includes uniform lighting, temperature, CO_2 levels, and relative humidity (Graamans, 2021). To maintain these constant conditions, air is reconditioned and recirculated, and the infiltration of outdoor air is avoided as much as possible. Hydroponic nutrient film technique is used to produce butterhead lettuce.

TOC

To date, there are many different approaches to growing food in VFs, e.g., the growth method, the number of growth layers, cultivation height, and automation. This makes it impossible to define a typical VF layout (Section 2.2.1). To maximise the transferability of the results, we focused on the outputs and inputs per m^2 cultivation area within the VF. When we refer to the one m^2 cultivation area in this research, this means one m^2 of one production layer of the VF.

3.2.1.1 Climate set points

The climate set points of the hypothetical VF studied were based on that of a commercial VF located in the Netherlands. This VF produces a mix of leafy greens within multiple container sized closed-box growth environments. During the photoperiod, the exhaust air of the VF has a temperature of 26°C, and a relative humidity (RH) of 72%. The return air, after cooling and dehumidification, is 24°C and 76% RH. To produce butterhead lettuce, the VF studied uses a Photosynthetic Photon Flux Density (PPFD) of 200 µmol m^{-2} s^{-1} and a photoperiod of 16 h d^{-1}, resulting in a Day Light Integral of 11.5 mol m^{-2} d^{-1}. With a LED molar efficacy of 3.5 µmol J^{-1} (Weidner et al., 2021), the electricity use of the LEDs is 334 kWh m^{-2} y^{-1}. During the dark period (8 h), the temperature was approximately 2°C lower, and the RH about 10% higher (Graamans et al., 2017). For simplification, this research only includes the photoperiod.

The cooling demands in a closed-box VF are the result of the heat dissipated by fans, pumps, auxiliary equipment, and most significantly, the LED lights. Currently, LEDs have a wall-plug-efficiency of 60–65%, meaning that 60–65% of the energy input is emitted as optical energy and 35–40% as sensible heat (Personal communication Signify). Crops only convert a few percent of the optical energy into chemical energy, i.e., biomass. As a result, most optical energy in converted into sensible and latent heat. Therefore, approximately 95–98% of the electrical energy consumed by LEDs has to be cooled away (Personal communication Signify). When assuming some heat losses through the thermal envelope of the VF, approximately 90% of the LEDs' electricity input needs to be dissipated by dehumidification and cooling systems. This number was confirmed by the commercial vertical farmer that provided the climate set points. Therefore, the cooling demand is approximately 300 kWh m^{-2} y^{-1}.

TOC

3.2.1.2 Cooling and dehumidification strategy

Current cooling and dehumidification systems for VFs were discussed with five companies in the Dutch VF sector. A cooling and dehumidification system was selected for the baseline VF that uses one water-to-water heat pump (HP1) for cooling, dehumidification, and reheating (see Fig. 3.2). The evaporator of HP1 is used to cool the exhaust air of the VF below its dew point temperature in heat exchanger 1 (HE1) to reject moisture from the air. The condenser of HP1 reheats the air in heat exchanger 2 (HE2) to obtain the required return temperature of 24°C. The condenser produces more heat than is required by HE2, this abundance of heat is rejected to the atmosphere via a water-to-air heat exchanger (HE3). A cold and warm buffer tank are included together with mixing values to allow temperature variations within the system whilst maintaining uniform VF conditions. More details are presented in Appendix B.1.1.

The total energy use of the cooling and dehumidification system (Fig. 3.2), and the residual heat removed by HE3 were calculated using mathematical simulations. The total heat produced by the VF is specified in Appendix B.1.2. The HP calculations are discussed step-by-step in Appendix B.2, together with the energy calculations of the heat exchangers, mixing valves, fans, and pumps within the climate system. In additional to the electricity use of 334 kWh m^{-2} y^{-1} for LEDs, the cooling and dehumidification system of the VF used 84 kWh m^{-2} y^{-1}. As the total cooling demands of the VF were 300 kWh_{th} m^{-2} y^{-1} (Section 3.2.1.1), this resulted in an overall efficiency of the climate systems of 360%, i.e., a coefficient of systems performance (COSP) of 3.6. In total, 353 kWh_{th} m^{-2} y^{-1} residual heat of 25°C on average is removed by HE3.

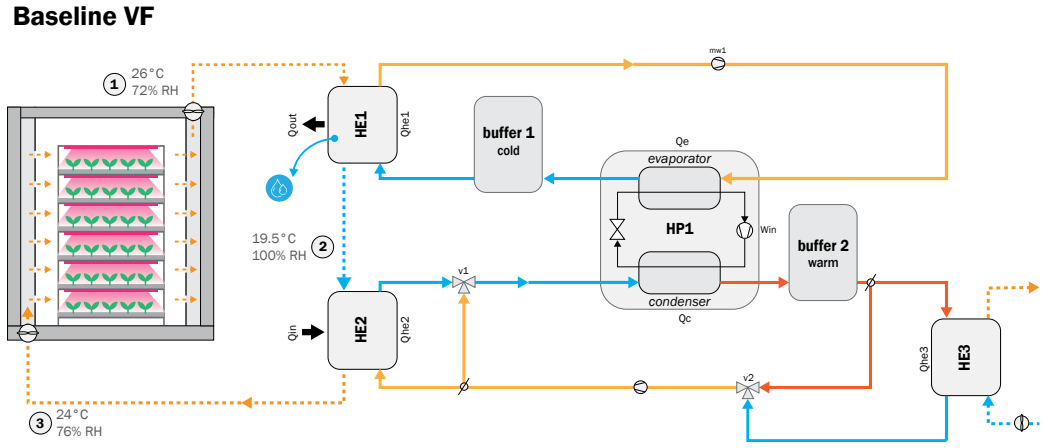

FIG. 3.2 The selected cooling and dehumidification strategy for the VF in which HP1 is used to provide cooling below dew point temperature in HE1, and re-heating in HE2. HE3 removes the abundance of heat produced by the condenser.

TOC

3.2.1.3 Inputs and outputs of crops, water, and nutrients

The VF described in Chapter 2 was used as reference for nutrient consumption and crop production. This VF produces butterhead lettuce with a light use efficiency of 18.7 g fresh weight lettuce per mol incident light (Section 2.4.5). When using the light recipe presented, this results in an annual lettuce production of 78.8 kg fresh weight per m^2 cultivation area. The quantity of water vapour removed by dehumidification in HE1 was calculated with the following formula:

$$\dot{m}w = \dot{m}a \times Dw \qquad \text{(Eq. 3.1)}$$

where $\dot{m}w$ is the water removal in kg s^{-1}, $\dot{m}a$ is the air flow rate in the VF in kg s^{-1}, and Δw the difference in humidity ratio across HE1 (Appendix B.1). The water demand of the VF is the sum of the water vapour removed by dehumidification (Eq. 3.1), and the water content of the crop. Using a dry matter content of 4% for lettuce (Jin et al., 2021), the total water demand is 309 L y^{-1} per m^2 of cultivation area. The hypothetical VF will reuse the water vapour recovered by dehumidification, where we assumed an overall loss of 5%. This results in an actual water usage of 87 L m^{-2} y^{-1}. The nutrient use is 2.1 kg per m^2 cultivation area annually, including the uptake of 26 g synthetic fertiliser per kg of lettuce produced (Appendix A, Table A.6) and a 5% loss during nutrient circulation.

3.2.2 Baseline conditions of buildings

This research considers apartments, offices, restaurants, indoor and outdoor swimming pools, and supermarkets located in the Netherlands. To obtain a high density of heating demand, single-family housing were excluded from this research. For each building typology, data was collected on the average heating and cooling demands (Appendix B.3.1) and the inputs and outputs of food, water, and nutrients (Appendix B.3.3– B.3.5).

The energy demands of the apartments are based on the average energy use of 75 to 100 m^2 apartments in the Netherlands. Office energy demands are included for smaller (250–2,500 m^2) and larger (2,500–5,000 m^2) offices. Three energy labels are considered for apartment and offices: BENG-label (nearly zero-energy building code) to represent new apartments, and A- and C-labels for renovations. Energy labels inform potential buyers or renters about the energy efficiency of the building (Van Den Brom et al., 2018). After the BENG-label, A-labels represent the highest energy efficiency and G-labels the lowest. Energy labels lower than C

TOC

were not included as we assumed that the integration of VFs within buildings would require deep renovations. In 2021, 64% of the apartments in the Netherlands had an energy label, of which 68% was a labelled as C or higher (RVO, 2022). Lower energy labels can still be renovated to improve the energy label. All office buildings in the Netherlands need to have an energy label of C or higher since January 2023 (RVO, 2023). There were no data available about the energy labels of restaurants, swimming pools, and supermarkets, therefore, we used the average energy use of these typologies (CBS, 2018; Stimular, 2022).

A reversible air-source HP system was assumed as the baseline heating and cooling system across the building typologies (Appendix B.3.2). BENG and A-labelled apartments and offices, the restaurant, and supermarket were heated with low-temperature floor heating of 40°C supply, and C-labels with mid-temperature radiators of 70°C. The return temperature of floor heating was 10°C lower than the supply temperature, and the return temperature of radiators decreased by 20°C (Maivel and Kurnitski, 2015). The coefficient of performance (COP) of these HPs were 4.4 for low-temperature heating, and 2.4 for mid-temperature heating. To avoid condensation, we used floor cooling with a supply temperature of 18°C and a return temperature of 23°C for all building typologies. Domestic hot water (DHW) was excluded from this study. The average water temperature of the swimming pools was 23°C (Koppejan, 2016). The indoor swimming pool was heated year-round, whilst the outdoor pool was opened and heated between May and September. This resulted in a COP of 4.8 for the indoor pool, and 5.5 for the outdoor pool.

Besides the electricity use of the HP, the overall energy use of the heating and cooling system included the electricity used by the outdoor fan. The energy use of the pumps that distribute the heat and cold through the building strongly depends on the head difference between the HP and heat delivery system, i.e., the design of the building. The distribution pump of the floor heating system studied by Hwang and Jeong (2021), used less than 1% of the total electricity used by the air-sourced HP system. The distribution energy of the heating system was, therefore, excluded from this research. This also applies to the performance calculations of the integration strategies.

3.2.3 Integration strategies for energy synergies

3.2.3.1 Direct integration

In the baseline non-integrated approach, residual heat was removed from the VF by HE3 (Fig. 3.2). To enable bidirectional energy exchange between the VF and building, HE3 was replaced by one or two components that connect the VF to the building's heating system (Fig. 3.3). These components included a HE (A1), a HP (B1), a HE combined with a HP at the building-side (C1), a HP connected to a HE at the building-side (D1), and two HPs (E1). These five strategies supply the heat produced by the VF to the building where it was used directly for space heating or stored within a storage vessel for short periods of 1–3 days. Outside of the building's heating season the VF switches back to the baseline cooling and dehumidification system and the residual heat is dissipated via HE3, and the building is cooled by the air-source HP (section 3.2.2).

3.2.3.2 Integration with seasonal energy storage

To further enhance the symbiosis between the VF and the building, the potential to include an aquifer thermal energy storage (ATES) system as part of the integration strategies A1-E1 was explored. The Netherlands has a high potential for ATES systems (Bloemendal et al., 2018). ATES systems can overcome the discrepancy between times of heat surplus and heat shortage by seasonally storing and recovering heat (Bloemendal et al., 2018) in the underground, at a depth of 100–250 m. ATES systems store heat at a maximum of 25°C, and a minimum of 5°C (IF Technology, 2019). As such, heat produced by the VF during summer can be stored and extracted during winter.

This year-round bidirectional energy exchange would require the simultaneous cooling of both VF and building during summer, which is not possible for strategies HE (A1) and HP (B1) even when integrating an ATES system. Figure 3.4 schematically presents strategies C1, D1, and E1 combined with ATES during the winter months when heating is required by the building, we refer to these strategies as C2, D2, and E2, respectively.

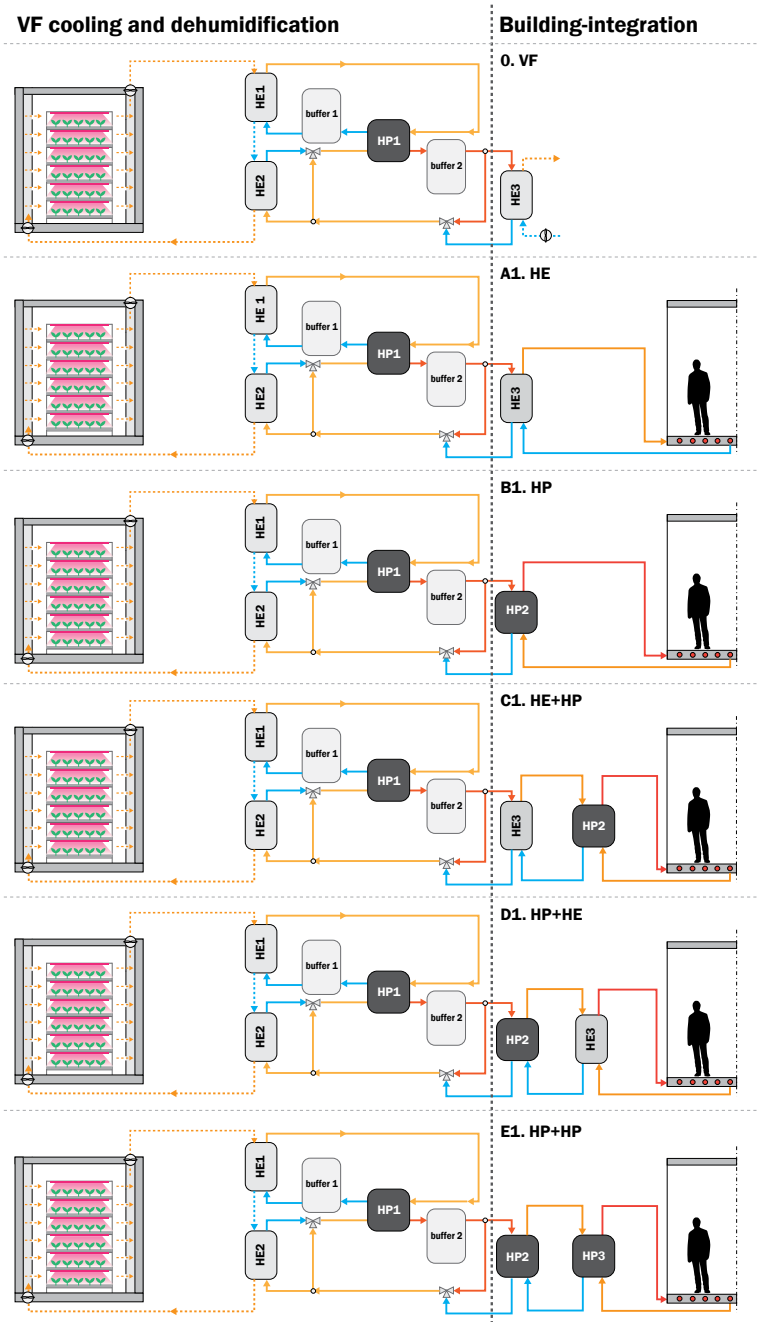

FIG. 3.3 The baseline scenario (0) and 5 different direct integration strategies to enable bidirectional exchange of energy between the VF and building (A1–E1). Dashed lines represent air flows, and solid lines represent water flows.

TOC

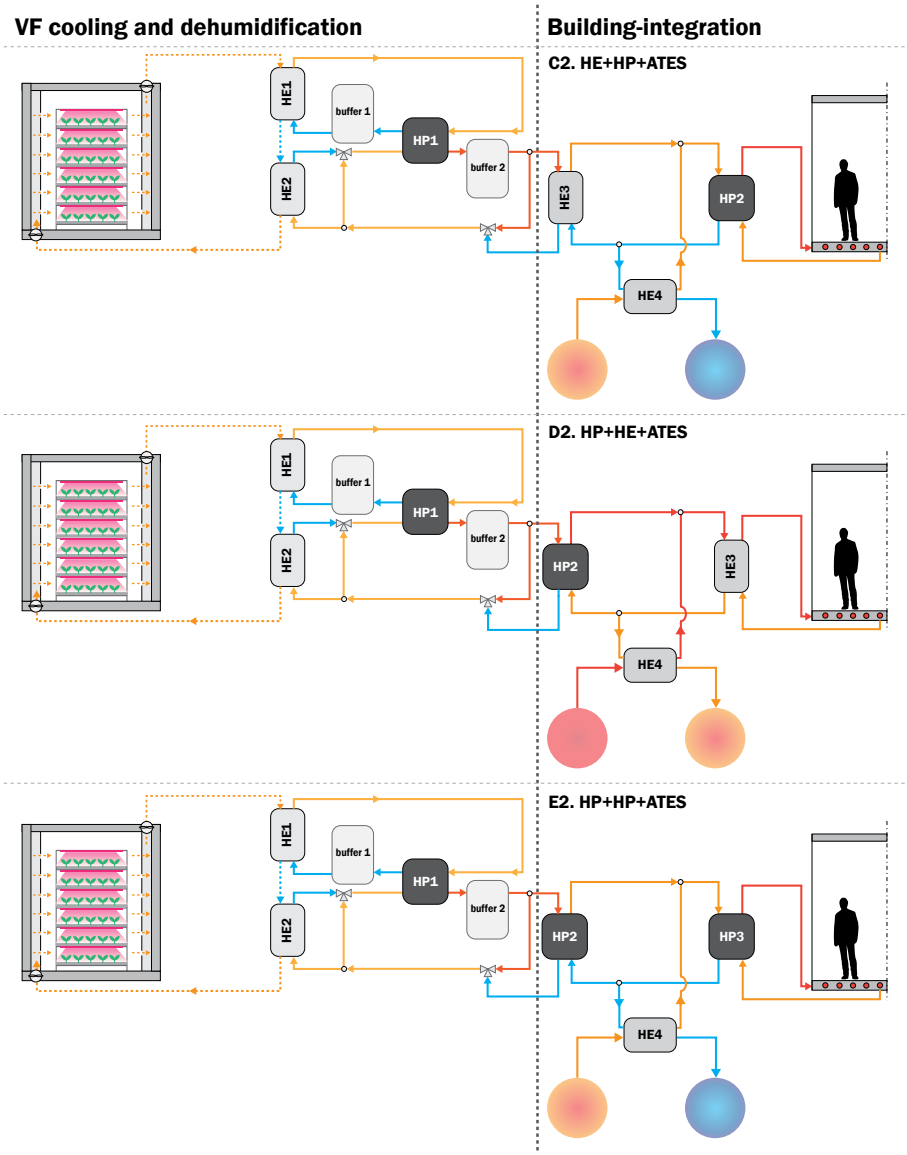

FIG. 3.4 Three different strategies to enable year-round bidirectional exchange of thermal energy between a VF and building using aquifer thermal energy storage (C2-E2). The figure represents the winter season. Dashed lines represent air flows, and solid lines represent water flows.

TOC

In winter, direct heat from the VF and the heat stored in the ATES system during summer are supplied to the building. While the cold produced by heating the building is supplied to the VF or stored in the ATES system. In summer, cold is extracted from the ATES system to cool the VF and the building, and the heat produced by the cooling systems is stored. To avoid exhaustion of the aquifers, thermal energy extraction and storage should be balanced over the year (Bloemendal et al., 2018).

3.2.3.3 Selecting integration strategies and calculating the energy savings

To define the potential energy savings as a result of the bidirectional exchange of energy between the VF and the different building typologies, the most applicable energy strategies had to be selected first. The integration strategies were selected on three criteria. The ability to produce the required heating temperatures (1), i.e., 23°C heating of swimming pools, 40°C low-temperature heating, and mid-temperature heating of 70°C (Section 3.2.2). The potential to comply with storage temperature restrictions of 25°C maximum, and 5°C minimum when using ATES (2). Finally, the energy efficiency of the applicable strategies were calculated (3).

The energy efficiency of the strategies was calculated for the integration with low-temperature heating. This energy efficiency indicates the quantity of 40°C heat (kWh_{th}) that can be produced per kWh of electricity used by the climate systems of the integration. The electricity use of the climate systems that enable the bidirectional exchange of thermal energy between the VF and building include: the energy used by the HP, fans and pumps of the VF's cooling and dehumidification system (Fig. 3.2), the energy used by the HP(s) and pump(s) that supply the VF heat to the building's heating system at the right temperature, and where applicable the energy used by the ATES pump. The energy use of these components was calculated according to the methods described in Appendix B.2. The energy used by the distribution pumps of the building's heating system were excluded (Section 3.2.2.).

Finally, we calculated the energy savings achieved as a result of the bidirectional thermal energy exchange between the VF and the different host building typologies, and the floor area of the building that could be heated via this exchange. The energy savings are presented in kWh per m^2 cultivation area, and for the floor area of the building that was heated with this synergy. The energy savings compare the energy use of the climate systems of the integration with that of the baseline VF and building in isolation. The baseline scenario adds together the energy used for cooling and dehumidification of one m^2 cultivation area, and the baseline energy used to heat

and cool the building's floor area defined for the integration. For these calculations Microsoft Excel was used as a way to create dynamic relationships between changing conditions of building typologies, the VF, and the different integration strategies. The dataset can be downloaded via 4TU Research Data, and a step-by-step description of these calculations is found in Appendix B.

3.3 Results

The following sections describe the results of this study. The selected energy strategies to facilitate the bidirectional exchange of heat and cold between the VF and the different buildings are described first, including direct integration (Section 3.3.1.1) and integration with ATES (Section 3.3.1.2). These sections also present the floor area of each building typology that can be heated with one square meter cultivation area in the VF, and the energy savings. Section 3.3.2 discusses the unidirectional flows of crops, water, and nutrients. All results are presented per one m^2 of one production layer within the VF, i.e., one m^2 cultivation area.

3.3.1 Energy synergies

This section describes the energy savings obtained by creating bidirectional synergies between the VF and various building typologies. These savings include the baseline energy use of the cooling and dehumidification system of one m^2 cultivation area of VF in isolation and that of the heating and cooling system of the building for the area heated by the synergy, in comparison to the total energy use of the integrated energy system cooling one m^2 cultivation area and heating the specified area of the connected building. The elements included within the total energy use of the integrated climate system were specified in Section 3.2.3.3. The total energy use of these climate systems is presented in kWh per m^2 cultivation area of the VF. This also includes for the floor area of the building heated by this synergy.

3.3.1.1 Direct integration

Two strategies were selected for direct integration without seasonal energy storage: HE (A1), and HP (B1). Strategy A1 was most efficient for heating of 20–30°C as no additional HPs was needed, i.e., heating was done passively. The limitation of 20–30°C heating in strategy A1 was the result of the fixed temperatures required by HE2 to reheat the VF air to 24°C. This temperature could not be obtained when supplying 40°C heat to the host building. Therefore, strategy HE (A1) was only applicable for integration with swimming pools, using temperatures of 30°C supply and 23°C return. One m^2 VF supplied the heat demands of an indoor swimming pool with a water surface of 0.17 m^2, and an outdoor pool of 1.04 m^2 (Table 3.1; Fig. 3.5). The annual savings obtained by the climate systems of the synergy between the VF and the outdoor pool are 27%, which is significantly smaller than the savings of 51% when integrating the VF with an indoor pool. The outdoor pool is closed in winter and the VF will switch to the baseline strategy; dissipating excess heat to the environment.

Direct integration strategies B1 through to E1 can supply heating of 40°C and higher, as active systems can upgrade the heat produced by the VF. The COSP represents the ratio between the amount of heat supplied to the host building's heating system, and the total energy use of the system (as specified in Section 3.2.3.3). When connected to a building with a floor heating system of 40°C, the COSP of strategies B1, C1, D1, and E1 were respectively, 7.4, 7.1, 7.2, and 6.8. Therefore, strategy B1 (HP) was selected as the most efficient active direct integration strategy in this study.

Integration strategy B1 (HP) was used to heat the building. When there was no heating demand, the VF and building were cooled independently according to their baseline systems. By using strategy B1 (HP), each m^2 cultivation area of the VF could supply the heating demands of between 2.8 m^2 and 4.1 m^2 of an apartment (C-, A-, BENG-label), between 2.7 m^2 and 11.1 m^2 of an office (A-, C-, BENG-label), 0.9 m^2 of a restaurant, 0.2 m^2 water of an indoor swimming pool, or 1.1 m^2 water of an outdoor swimming pool (Table 3.1; Fig. 3.5).

TABLE 3.1 Total energy use by the climate systems of one m^2 of one production layer of the VF and the thereby heated areas of the different building typologies when using integration strategies A1, B1, or E2.

			Heating season			Year-round		
	Integration strategy	Area per m^2 VF	E_{tot} baseline	E_{tot} synergy	Savings	E_{tot} baseline	E_{tot} synergy	Savings
	-	$m^2\ m^{-2}$ VF	kWh m^{-2} VF	kWh m^{-2} VF	%	kWh m^{-2} VF	$m^2\ m^{-2}$ VF	%
Apartment	HP (**B1**)	4.1	76	55	28	126	105	17
BENG-label	HP+HP+ATES (**E2**)	15.6	-	-	-	244	216	12
Apartment	HP (**B1**)	3.0	76	55	28	126	105	17
A-label	HP+HP+ATES (**E2**)	11.2	-	-	-	239	210	12
Apartment	HP (**B1**)	2.8	126	98	22	177	149	16
C-label	HP+HP+ATES (**E2**)	11.4	-	-	-	462	363	21
Small office	HP (**B1**)	11.1	97	55	44	155	113	27
BENG-label	HP+HP+ATES (**E2**)	86.3	-	-	-	633	433	32
Small office	HP (**B1**)	2.7	97	55	44	156	113	27
A-label	HP+HP+ATES (**E2**)	24.8	-	-	-	749	501	33
Small office	HP (**B1**)	2.9	172	98	43	231	157	32
C-label	HP+HP+ATES (**E2**)	41.1	-	-	-	2139	1399	34
Large office	HP (**B1**)	7.4	97	55	44	115	113	27
BENG-label	HP+HP+ATES (**E2**)	57.7	-	-	-	637	436	32
Large office A-label	HP (**B1**)	3.7	97	44	44	161	119	26
Large office C-label	HP (**B1**)	3.7	172	98	43	236	162	31
Restaurant	HP (**B1**)	0.9	76	55	28	131	110	16
	HP+HP+ATES (**E2**)	5.3	-	-	-	370	270	27
Indoor	HE (**A1**)	0.2*	159	79	51	159	79	51
swimming pool	HP (**B1**)	0.2*	165	108	35	164	108	35
Outdoor	HE (**A1**)	1.0*	62	33	47	111	82	27
swimming pool	HP (**B1**)	1.1*	65	45	30	114	94	17
Supermarket	-	-	-	-	-	-	-	-

** Area of swimming pool represented per m^2 water surface.*

TOC

Typology	Direction	VF	HE (A1)	HP (B1)	HP+HP+ATES (E2)
Apartment BENG		 **1.0 m²**	-	 **4.1 m²** kWh m⁻²y⁻¹ 105 334	 **15.6 m²** kWh m⁻²y⁻¹ 216 334
Apartment A-label		 **1.0 m²**	-	 **3.0 m²** kWh m⁻²y⁻¹ 105 334	 **11.2 m²** kWh m⁻²y⁻¹ 210 334
Apartment C-label		 **1.0 m²**	-	 **2.8 m²** kWh m⁻²y⁻¹ 149 334	 **11.4 m²** kWh m⁻²y⁻¹ 363 334
Small office BENG		 **1.0 m²**	-	 **11.1 m²** kWh m⁻²y⁻¹ 113 334	 **86.3 m²** kWh m⁻²y⁻¹ 433 334
Small office A-label		 **1.0 m²**	-	 **2.7 m²** kWh m⁻²y⁻¹ 113 334	 **24.8 m²** kWh m⁻²y⁻¹ 501 334
Small office C-label		 **1.0 m²**	-	 **2.9 m²** kWh m⁻²y⁻¹ 157 334	 **41.1 m²** kWh m⁻²y⁻¹ 1399 334
Large office BENG		 **1.0 m²**	-	 **7.4 m²** kWh m⁻²y⁻¹ 113 334	 **57.7 m²** kWh m⁻²y⁻¹ 436 334
Large office A-label		 **1.0 m²**	-	 **3.7 m²** kWh m⁻²y⁻¹ 119 334	-
Large office C-label		 **1.0 m²**	-	 **3.7 m²** kWh m⁻²y⁻¹ 162 334	-

>>>

Typology	Direction	VF	HE (A1)	HP (B1)	HP+HP+ATES (E2)
Restaurant		 **1.0 m²**	-	**0.9 m²** kWh m⁻²y⁻¹ 110 334	 **5.3 m²** kWh m⁻²y⁻¹ 270 334
Indoor swimming pool		 **1.0 m²**	**0.2 m²** kWh m⁻²y⁻¹ 79 334	**0.2 m²** kWh m⁻²y⁻¹ 108 334	-
Outdoor swimming pool		 **1.0 m²**	**1.0 m²** kWh m⁻²y⁻¹ 82 334	**1.1 m²** kWh m⁻²y⁻¹ 94 334	-

FIG. 3.5 Floor areas of different typologies that can be heated by creating bidirectional synergy with a vertical farm of one m2 cultivation area, i.e., one m2 of one production layer in the VF. Including the total annual energy use of the climate systems, and the LED systems of the vertical farm in kWh per m2 cultivation area.

The year-round energy savings varied between 16 and 35%, and savings within the heating season between 22 and 44%. The savings within the heating season refer to the period when the synergetic exchange of heat and cold between the VF and building are active. Within the annual savings we also include the energy used by the baseline systems during periods without heat demands of the host building, i.e., when no synergy occurred. The synergy between a VF and a supermarket was not beneficial from an energy perspective as the cooling demands of the supermarket were significantly higher than its heating demands (Table B.2). If the supermarket and VF would be integrated an abundance of heat would be produced as both functions require cooling throughout the year.

3.3.1.2 Integration with seasonal energy storage

Integration strategies C1, D1, and E1 could be combined with an ATES system (Section 3.2.3.2). HE4 connects the ATES system to the water circuit between HE3 and HP2 (C2), HP2 and HE3 (D2), and HP2 and HP3 (E2), see Figure 3.4. In the Netherlands, ATES temperatures are restricted to 25°C maximum, and 5°C minimum. To produce supply air with a temperature of 24°C and RH of 76% for the VF, the

TOC

water temperature leaving HE3 (C2) or HP2 (D2/E2) towards HE2 should be higher than 27.3°C. Due to the maximum temperature of 25°C in the ATES hot source, this cannot be achieved when using integration strategy C2.

The floor heating supply and return temperatures were at least 40 and 30°C. The connection of HE3 to the floor heating system in strategy D2, therefore, resulted too high temperatures for storage in the ATES system. Integration strategy E2 (HP + HP) overcomes both difficulties of C2 and D2, as the temperatures produced by HP2 and HP3 were adjustable. Integration strategy HP + HP (E2) was, therefore, selected when using ATES.

In contrast to the direct integration strategies not using ATES, bidirectional synergies between the VF and host building occur year-round due to the integration with seasonal storage. During the building's heating season, the amount of heat supplied to the building was the sum of the heat produced by the VF, the amount of heat extracted from the ATES hot source, and the electricity input of HP3. By heating the building, HP3 produces cold that was used for VF cooling by HP2, and the remainder was stored in the ATES cold source (Fig. 3.4). Outside of the building's heating system (Fig. 3.6), this cold is extracted from the ATES cold source and used to remove heat from the VF whilst simultaneously cooling the building. The heat generated by HP2 and HP3 was stored within the ATES hot source for later usage. The amount of heat extracted and stored within both hot and cold source of the ATES system was balanced over the year.

To achieve the thermal balance described above by using strategy E2 (HP + HP + ATES), each m^2 of VF should be combined with between 11.2 m^2 and 15.6 m^2 of an apartment (A, C-, or BENG-label), between 24.8 m^2 and 86.3 m^2 of a small office (A, C-, or BENG-label), 57.7 m^2 of a large BENG-labelled office, or 5.3 m^2 of a restaurant (Table 3.1; Fig. 3.5). These synergies resulted in total annual energy savings of between 12 and 35%.

Large, A- and C-labelled offices were not suitable for integration with VFs when using ATES. When cooling large offices with ATES systems, enough heat is generated during the summer months to supply the heating demands during the colder and intermediate months without the need for additional VF heat. The indoor swimming pool would not benefit from the ATES system either as it uses the heat produced by the VF year-round. The outdoor pool had a heat demand in summer, when other functions had no heat demand, e.g., apartments and restaurants. In the heating season of these buildings, the outdoor pool is closed. Therefore, the integration of a VF with an outdoor pool and an apartment or restaurant could create year-round symbiosis without the need for ATES. Finally, as described in Section 3.3.1.1 the synergy between the VF and supermarket was not beneficial due to the high cooling demands by the supermarket.

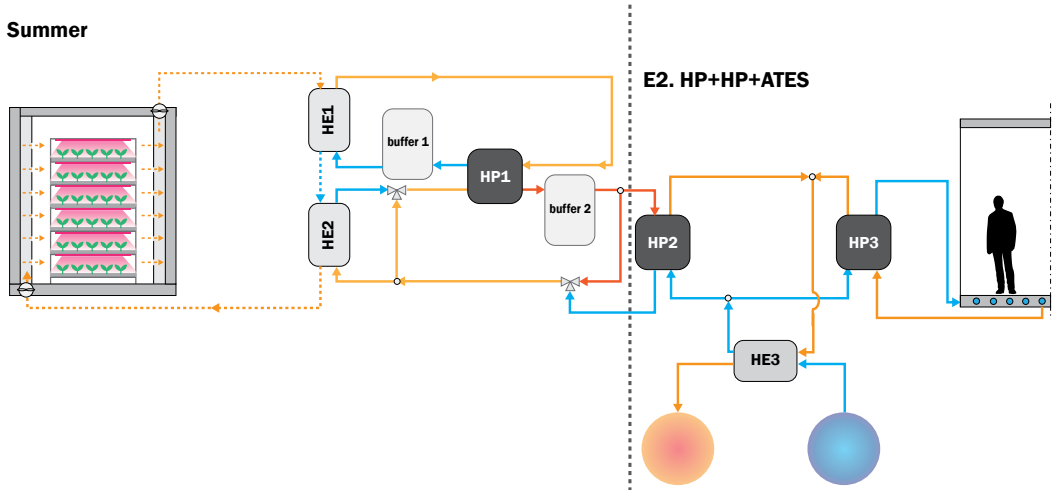

FIG. 3.6 Schematic representation of integration strategy HP+HP (E2) with ATES in summer.

The results indicate that one m^2 cultivation area of the VF can heat a larger floor area of small C-label offices, and C-label apartments with ATES than A-labels (Fig. 3.5). This was not expected due to the higher heating demands of C-labels (Appendix B.3.1). The COP value for mid-temperature heating was lower than for low-temperature heating, thus the HP of C-labels used more electricity, and the condenser produced more heat. The ratios between the heating demands of these A- and C-label offices and apartments were smaller than the ratios between the electricity inputs of these HPs. Therefore, the C-labelled offices and apartments with ATES required less cultivation area than the A-labels.

3.3.2 Crop, water, and nutrient flows

Besides the bidirectional exchange of heat and cold using integration strategies A1, B1, or E2, unidirectional flows between the VF and the building could be established. These include the production of lettuce in the VF for consumption by the building users, and the reuse of grey water and nutrients from the building in the VF.

TOC

3.3.2.1 Crop production

We assumed that each person consumed 250 g of vegetables per day, and for simplification of the study all vegetables consumed were lettuce. The lettuce demands per person for each building typology are described in Appendix B.3.3. One m^2 of cultivation area produces enough lettuce annually to feed 0.9 person living in the apartment, to provide the lunch of 1.4 full time employees working in an office, or to produce the vegetables for 315 meals in the restaurant (Fig. 3.7). Furthermore, each m^2 of cultivation area could produce 79 kg of lettuce for a supermarket annually. We assumed swimming pool visitors consume minimal quantities of vegetables, and this flow was thus excluded for this typology.

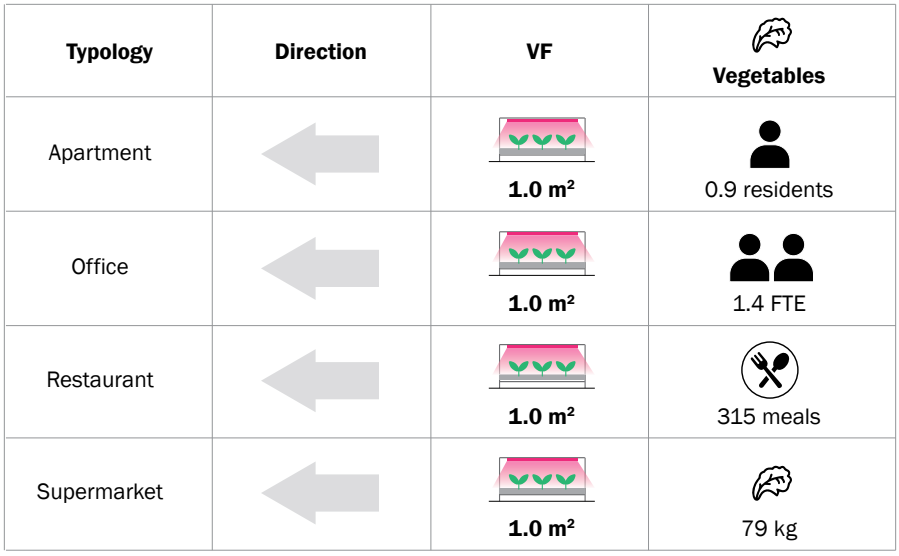

FIG. 3.7 The unidirectional flow of lettuce produced by one m2 of one production layer in the VF, that can theoretically be used to supply the annual vegetable consumption of the apartment's residents, the lunches of office employees, or the meals produced in the restaurant.

3.3.2.2 Grey water use

Grey water output of host building can be filtered and reused for toilet flushing or to water the crops of the VF. The reuse of grey water for toilet flushing was prioritized, the remaining grey water was supplied to the VF. As the grey water production of the offices was smaller than the water used for toilet flushing, no grey water was

TOC

supplied to the VF (Appendix B.3.4). The grey water production of apartments, restaurants, and swimming pools was higher than the water required for toilet flushing, and therefore the remaining grey water could be reused for crop watering in the VF. Each m^2 of cultivation area annually consumes the grey water outputs produced by 0.004 residents in the apartments. One m^2 of cultivation area could also be watered by the grey water output of 10 visitors to the restaurant or one visitor to the swimming pool assuming each visitor uses the toilet once. There were no data available on the water consumption of the supermarket, thus the supply of grey water to the VF was excluded in Fig. 3.8.

3.3.2.3 Nutrient recovery

Nutrients recovered from human urine could be used to replace synthetic fertilisers in the VF (Appendix B.3.5). The annual nutrient demands of one m^2 cultivation area in the VF could be supplied with the nutrients recovered from urine of 0.3 residents in the apartments, 1.7 full time employees, or 344 visitors of the restaurant or swimming pool (Fig. 3.8). For the latter, we assumed each visitors uses the toilet once.

Typology	Direction	VF	Water	Nutrients
Apartment	→	**1.0 m²**	0.004 residents	0.3 residents
Office	→	**1.0 m²**	-	1.7 FTE
Restaurant	→	**1.0 m²**	10 visitors	344 visitors
Swimming pool	→	**1.0 m²**	1 visitor	344 visitors

FIG. 3.8 The unidirectional flows of grey water and nutrient outputs of the host building, that can be used to supply the water and nutrient demands of one m2 of one layer of cultivation area of the vertical farm. The therefore required water and nutrient production is expressed in the number of residents of the apartments, employees of the office, or visitors of the restaurant or swimming pool.

TOC

3.4 Discussion

Section 3.4.1 discusses the results related to the bidirectional energy synergies in more detail and in relation to other studies, identified some of the research limitations, and makes suggestions for further study. Section 3.4.2 provides further discussion on the unidirectional flows of crops, water, and nutrients and makes suggestions for further studies on resource flows other than energy.

3.4.1 Energy synergies

3.4.1.1 Residual heat production by vertical farms

Within existing literature, two studies calculated the residual heat production by VFs. Graamans (2021) defined the annual residual heat production of a non-integrated VF of 1,037 kWh per m^2 cultivation area during a 16-h photoperiod, and 64 kWh m^{-2} y^{-1} during the 8-h dark period. The LEDs used 973 kWh m^{-2} y^{-1}, with a PPFD of 500 µmol m^{-2} s^{-1}, a DLI of 28.8 mol m^{-2} d^{-1}, and a molar efficacy of 3.0 µmol J^{-1}. The studied non-integrated (baseline) VF produced 353 kWh m^{-2} y^{-1} of residual heat (Section 3.2.1.2). The LEDs had a DLI of 11.5 mol m^{-2} d^{-1}, and a molar efficacy of 3.5 µmol J^{-1}. The electricity used for artificial light per m^2 cultivation area is thereby 34% of the electricity used by LEDs in Graamans (2021). This explains the significant difference in heat production between both studies. According to Matysiak et al. (2022), the best performance in terms of quality and yield for lettuce production is achieved with a DLI of approximately 13.8 mol m^{-2} d^{-1}, which is closer to that used in the current study. This study excluded the dark period from the research. The results of Graamans (2021), indicate a minimal increase of heat production when including dark period in the calculations.

Martin et al. (2022) studied the direct integration of VFs within the energy system of an apartment building in Sweden, i.e., without seasonal energy storage. In total, 107 MWh_{th} of heat was supplied to this apartment by a VF that uses 130 MWh y^{-1} for LEDs (DLI of 12.46 mol m^{-2} d^{-1}), and 45 MWh y^{-1} for climate systems. This results in a heat production of 0.82 kWh_{th} per kWh of electricity for LEDs in comparison to 1.2 kWh_{th} per kWh of LED in this research using strategy B1 (HP). Both VFs used a different baseline strategy for cooling and dehumidification. A study

TOC

of different cooling and dehumidification strategies for VFs including energy use and residual heat production is needed to further increase the energy efficiency of VF integration with building energy systems. Such a study could also include water-cooled LEDs that diminishes heat dissipation into the VF by cooling the LEDs directly with water (Xiaoying et al., 2015). As the removal of latent heat requires air-cooled systems (Graamans, 2021) such a strategy would require both water- and air-cooled systems.

3.4.1.2 Energy savings by building-integration

The results suggest that the bidirectional exchange of energy between a VF and a building can decrease total annual energy use of the climate systems collectively by between 12% and 51% when compared to the cumulative baseline approaches of both functions. This positive effect of energy synergies between urban agriculture and buildings was also found in previous studies that investigated energy exchange between rooftop greenhouses and buildings (Muñoz-Liesa et al., 2020, 2022; Jans-Singh et al., 2021; Ledesma et al., 2022).

The energy synergy in this research was most effective when the building contrasted the VF in terms of energy demand. Therefore, the highest annual savings of 51% were achieved when creating synergy between the VF and the indoor swimming pool that requires heating year- round. For the same reason, supermarkets with year-round cooling demand and minimal heating demand did not benefit from this synergy (Section 3.3.1.1). This suggest that the use of residual heat from a VF within the energy systems of buildings offers most benefits within cold and temperate climates, and less for warm climates where buildings have minimal heating demands. This thought was confirmed by Graamans (2021) stating that the integration of VFs in urban energy systems has little value for locations dominated by cooling demands. This finding did not apply to the broader perspective of Muñoz-Liesa et al. (2022) and urban agriculture, which concluded that bidirectional energy exchanges between a rooftop greenhouse and office building in a warmer Mediterranean climate resulted in energy savings for heating and cooling both entities.

Buildings without continuous heating demands obtained year-round energy symbiosis with the VF by including an ATES system for seasonal heat and cold storage. The synergy between a VF and a BENG-label office, or a small A- or C-label office resulted in annual energy savings from the climate systems of 32, 33, and 34%, respectively, when using strategy E2 (HP + HP + ATES). For these functions, strategy E2 resulted in higher savings than for the direct

integration with strategy B1 (HP), which reduced the energy for climate systems by between 27 and 32%. In addition to the energy used for climate systems, each m^2 cultivation area of the VF used 334 kWh of electricity for LEDs. The floor areas of these offices heated by one m^2 cultivation area were between 7.8 and 14.2 times larger for the integration of offices with ATES than without, resulting in relatively low electricity use for artificial light per m^2 of office space for strategy E2. Integration strategy E2 also reduced the electricity use of the climate systems of the C-label apartments and restaurants by 21 and 27% respectively, in comparison to 16% for both functions when using strategy B1. Furthermore, one m^2 cultivation area could heat 4.1 and 5.9 times more floor area of the C-label apartment and restaurant for E2 in comparison to B1.

Direct integration without seasonal storage also resulted in energy savings although the VF and building switched to their baseline strategies when there was no demand for heat; i.e., during warmer months. The year-round energy savings by the climate systems when using strategy B1 (HP) were 16–17% for the apartments, 26–27% for BENG- and A-label offices, 31–32% for C-label offices, and 16% for restaurants. The year-round savings were higher for BENG and A-label apartments when using integration strategy B1 than for strategy E2. However, the floor areas heated per one m^2 cultivation area of the VF were about 3.7 times larger for strategy E2 than for B1.

3.4.1.3 Research limitations and suggestions for further study

The energy savings in this chapter were calculated in comparison to the baseline energy use of the VF and building typologies: the sum of the energy used by the cooling and dehumidification systems of one m^2 cultivation area of a VF, and the energy used by the baseline heating and cooling systems of the building's floor area heated by of one layer cultivation area of the VF. These savings are sensitive to the choice of the replaced energy system (Martin et al., 2022). In this research, the baseline buildings used air-sourced HPs, while most existing buildings in the Netherlands are heated with natural gas. Such comparison would result in higher energy savings than calculated.

The study did not include the energy used by the distribution pumps of the building's heating system, and the production of DHW. The production of DHW would require an additional HP to produce water of 60°C and would decrease the floor area of the building that can be heated with one m^2 cultivation area. The symbiosis between the VF and building would, however, be improved as the residual heat could partly be used for DHW production in summer (Martin et al., 2022).

The floor areas of BENG-label apartments and offices that could be heated with one m^2 cultivation area were significantly larger than that of the A-label equivalents (Fig. 3.5). The energy demands of the BENG-labels were based on simulated data, whilst the A- and C-labels used empirical data from a real-world setting. The difference between actual and simulated energy is the energy-performance gap. In the Netherlands, the actual energy use is significantly higher than the simulated energy use for heating energy efficient residential buildings (Van Den Brom et al., 2018) and heating and cooling energy efficient office buildings (Sipma, 2019). This suggests that the indicated cultivation areas to heat BENG-labelled apartments and offices would be higher in a real-world setting.

The results indicated that the integration of a VF and ATES system (E2) was not possible for larger A- and C-label offices as their HPs produced enough heat for winter by cooling the office in summer. The integration of a VF would thus result in an abundance of heat in the ATES system. However, no specific data were available on the cooling demands of offices in the Netherlands, and they were approximated by appointing 17% of the electricity use to the cooling installations with a COP of 4 (KWA, 2016). This indicates that the appropriateness to integrate VFs with offices and ATES should be considered for each office specifically. Besides building energy patterns, the integration with ATES may not be possible as a result of underground characteristics or project budgets.

To maximise transferability of the results, we focused on the inputs and outputs of one m^2 cultivation area of a VF, i.e., one m^2 of one production layer of the VF. To date, it is not possible to define a typical VF layout as many different approaches of food production exist, e.g., growth method, number of growth layers, cultivation height, and automation. If a certain food production system within the VF is selected this will have a big impact on the overall floor areas required within the building as a result of production efficiency and the overall number of cultivation layers. To increase replicability of the research for other VF configurations, the Supplementary material provide a step-by-step description of the different calculations made to support the dataset provided in the data availability statement.

3.4.2 Crop, water, and nutrient flows

The results presented that each m^2 cultivation area of the VF can produce sufficient lettuce to fulfil the vegetable demands of 0.9 residents, 1.4 office employees, or 315 restaurant visitors (Fig. 3.7). This indicates that an abundance of crops may be produced when sizing the VF to according to the building's heat demands. The

yields were calculated using a light use efficiency of 19 g fresh weight lettuce per mol of incident light. Carotti et al. (2021) noted a light use efficiency of 44 g fresh weight per mol within a lettuce producing VF. This light use efficiency increases the yields from 78.8 to 185 kg fresh weight m^{-2} y^{-1} and reduces cultivation area to produce 1 kg fresh weight lettuce by 43%. In that case, food should partially be sold when the goal is to supply the building with heat from the VF. In this study, the VF only produces lettuce, whilst an assorted range of vegetables is required to provide a healthy diet. The production of various vegetables would affect the quantity of fresh weight and heat produced as each crop has its specific requirements, e.g., temperature, RH, PPFD, photoperiod, and growth density.

The VF used water highly efficiently due to the reuse of water vapour from dehumidification. This could be further improved by replacing tap water inputs with the filtered grey water outputs of apartments, restaurants and swimming pools. Fig. 3.8 indicates that the annual grey water outputs of 0.004 residents, or the water outputs of 10 restaurants visitors or 1 swimming pool visitor collectively are sufficient to supply the water demands of the VF. This suggest that when sizing a VF according to the heat or vegetable demands of the building, large quantities of grey water will remain unused. Evapotranspiration of crops could be used to purify grey water or rainwater (Kalantari et al., 2017). Reusing this filtered water within the building could reduce tap water inputs and grey water outputs of the building. Nutrient recovery from urine to replace synthetic fertilisers in the VF is less effective than water reuse but offers a significant potential to reduce inputs from external sources in the VF.

Other resource flows might be explored to further increase symbiosis between the VF and building. Human respiration is the main source of indoor CO_2. CO_2-levels can reach up to 2,500 ppm in office building depending on the ventilation rate (Shao et al., 2021). Studies presented that the CO_2-levels of rooftop greenhouses can be increased by reusing the ventilation exhaust air of offices (Sanjuan-Delmás et al., 2018) or classrooms (Ledesma et al., 2022). This could effectively replace the need for pressurised CO_2 in VFs in a sustainable matter. However, the closed-box environment of the VF adds another level of complexity as the growth conditions should remain uniform and independent from the building and outdoor climate.

Furthermore, the integration of VFs within urban areas will unlock an array of future synergies as a wider range of resources in higher quantities will be available. Finally, further research is required to better understand the potential of bidirectional energy flows, and unidirectional water and nutrient flows, to reduce the environmental impacts of VFs and buildings. Besides the resource savings, this study should include the impacts related to the technical systems and infrastructure required for these resource exchanges.

3.5 Conclusion

This research showed that the bidirectional exchange of thermal energy between VFs and buildings can reduce the total combined energy use of both entities. Furthermore, it indicates that the VF's inputs of water and nutrients from external sources can be diminished by using waste flows from the building, whilst the crops produced within the VF can provide vegetables to the building users. If the goal of the integration is to provide all heating demands of the building by the residual heat produced within the VF, the energy used by the climate systems of both entities could be reduced by between 12 and 51%. When sizing the VF to produce all heating demands of an apartment with a floor area of between 75 and 100 m^2, the water and nutrient requirements of the VF can be fully supplied by the waste outputs of one or more resident(s). The VF will produce all vegetables consumed by these residents. These findings apply to energy labels BENG, A, and C when using a HP as direct integration strategy, or two HPs in combination with seasonal thermal energy storage. The cultivation area required to heat a certain size office (of any energy label) using the integration strategy with two HPs and ATES is too small to provide all vegetables for the lunches of the employees, but ample nutrients will be produced to sustain the VF. When using a HP for direct integration, sufficient food will be produced, however, too little employees will be available to produce for the nutrient inputs, and the electricity use for the climate systems and LEDs will increase significantly. In all situations, not enough grey water is produced by the offices to sustain the VF. The restaurant and swimming pool will supply the water inputs of the VF, when the latter is sized to according to the building's heat demands. Replacing all synthetic fertilisers will be challenging for these integrations. Finally, the exchange of resources between the VF and supermarket is limited to the production of lettuce for the supermarket.

The results of this study provide a first step in quantifying the potential energy savings and resource synergies between VFs and buildings. Further research is required to investigate the influences of other baseline strategies to heat, cool, and dehumidify the VF, inclusion of DHW demands, the production of an assorted range of vegetables, and to study other potential synergies between VF and buildings. Although there are many variables and potential implications of the different strategies and approaches that have been investigated, this research shows that the integration of VF in an array of different buildings with different functions offers a great potential to reduce the environmental impacts of both VFs and buildings, whilst producing food within cities.

References

Bloemendal, M., Jaxa-Rozen, M., Olsthoorn, T. 2018. Methods for planning of ATES systems. Appl. Energy 216, 534–557. https://doi.org/10.1016/j.apenergy.2018.02.068.

Brom, P. van den, Meijer, A., Visscher, H. 2018. Performance gaps in energy consumption: household groups and building characteristics. Build. Res. Inf. 46, 54–70. https://doi.org/10.1080/09613218.2017.1312897.

Carotti, L., Graamans, L., Puksic, F., Butturini, M., Meinen, E., Heuvelink, E. Stanghellini, C. 2021. Plant factories are heating up: hunting for the best combination of light intensity, air temperature and root-zone temperature in lettuce production. Front. Plant Sci. 11. https://doi.org/10.3389/fpls.2020.592171.

CBS. 2018. Energiekentallen utiliteitsbouw dienstensector: oppervlakte klasse. Available at: https://opendata.cbs.nl/statline/#/CBS/nl/dataset/83374NED/ table?ts=1642090250137 (Accessed June 20, 2023).

Delden, S.H. van, SharathKumar, M., Butturini, M., Graamans, L.J.A., Heuvelink, E., Kacira, M., … Marcelis, L.F.M. 2021. Current status and future challenges in implementing and upscaling vertical farming systems. Nature Food. https://doi.org/10.1038/s43016-021-00402-w.

Dobbelsteen A. van den, Tillie, N., Kürschner, J., Mantel, B., Hakvoort, L. 2011. The Amsterdam guide to energetic urban planning. Management and Innovation for a Sustainable Built Environment; MISBE 2011, (June 20-23) CIB International Conference, Amsterdam.

Gentry, M. 2019. Local heat, local food: integration vertical hydroponic farming with district heating in Sweden. Energy 174, 191–197. https://doi.org/10.1016/j. energy.2019.02.119.

Germer, J., Sauerborn, J., Asch, F., de Boer, J., Schreiber, J., Weber, G. (2011). Skyfarming an ecological innovation to enhance global food security. J. Verbr. Lebensm. 6, 237–251. https://doi.org/10.1007/s00003-011-0691-6.

Graamans, L.J.A. 2021. Stacked: the building design, systems engineering and performance analysis of plant factories for urban food production [doctoral dissertation, Delft University of Technology]. A+BE | architecture and the built environment.

Graamans, L., Baeza, E., van den Dobbelsteen, A., Tsafaras, I., Stanghellini, C. 2018. Plant factories versus greenhouses: comparison of resource use efficiency. Agric. Syst. 160, 31–43. https://doi.org/10.1016/j.agsy.2017.11.003.

Graamans, L., van den Dobbelsteen, M., Meinen, E., Stanghellini, C. 2017. Plant factories; crop transpiration and energy balance. Agric. Syst. 153, 138–147. https://doi.org/10.1016/j. agsy.2017.01.003.

Hwang, Y. J., Jeong, J. W. 2021. Energy saving potential of radiant floor heating assisted by an air source heat pump in residential buildings. Energies 14(132). https://doi.org/10.3390/en14051321.

IEA. 2022. Heating. Available at: https://www.iea.org/reports/heating (Accessed March 21, 2023).

IF Technology. 2019. Hamerkwartier Amsterdam: bodemenergieplan. Available at: https://openresearch.amsterdam/nl/page/81174/hamerkwartier-interferentiegebied (Accessed March 14, 2023).

Jans-Singh, M., Ward, R., Choudhary, R. 2021. Co-simulating a greenhouse in a building to quantify co-benefits of different coupled configurations. J. Build. Perform. Simul. 14, 247–276. https://doi.org/10.1080/19401493.2021.1908426.

Jin, W., Lopez, D. F., Heuvelink, E., Marcelis, L.F.M. 2021. Light use efficiency of lettuce cultivation in vertical farms compared with greenhouse and field. Food Energy Secur. 12, 1–10. https://doi.org/10.1002/fes3.391.

Jurgilevich, A., Birge, T., Kentala-Lehtonen, J., Korhonen-Kurki, K., Pietikäinen, J., Saikku, L., Schösler, H. 2016. Transition towards circular economy in the food system. Sustain. 8 (69). https://doi.org/10.3390.su8010069.

Kalantari, F., Tahir, O. M., Joni, R. A., Fatemi, E. 2017. Opportunities and challenges in sustainability of vertical farming: a review. J. Landsc. Ecol. 11, 35–60. https://doi.org/10.1515/jlecol-2017-0016

Koppejan, J. 2016. Inventarisatie van markttoepassingen van biomassaketels en bio- wkk. Available at: https://www.rvo.nl/sites/default/files/2017/04/Rapportage- Marktkansen-bioketels.pdf (Accessed September 23, 2022).

Kozai, T., Niu, G. 2020. Role of the plant factory with artificial light (PFAL) in urban areas. In: Kozia, T., Takagaki, M., & Niu, G. (Eds.), Plant factory: an indoor vertical farming system for efficient quality food production. Academic Press, London, pp. 129-140. https://doi.org/10.1016/B978-0-12-801775-3.00002-0.

Kozai, T., Ohyama, K., Chun, C. 2006. Commercialized closed systems with artificial lighting for plant production. Acta Hortic. 711, 61–70. https://doi.org/10.17660/ actahortic.2006.711.5.

KWA. 2016 Het elektrisch energieverbruik en het warmteaanbod van koelinstallaties voor een veertigtal bedrijfssectoren. RVO, The Hague.

Ledesma, G., Nikolic, J., Pons-Valladares, O. 2022. Co-simulation for thermodynamic coupling of crops in buildings. Case study of free-running schools in Quito, Ecuador. Buid. Environ. 207. https://doi.org/10.1016/j.buildenv.2021.108407.

Maivel, M., Kurnitski, J. 2015. Heating system return temperature efficiency effect on heat pump performance. Energy Build. 94, 71–79. https://doi.org/10.1016/j. enbuild.2015.02.048.

Marchi, B., Zanoni, S., Pasetti, M. 2018. Industrial symbiosis for greener horticulture practices: the CO2 enrichment from energy intensive industrial processes. Procedia CIRP 2018, 562–567. https://doi.org/10.1016/j.procir.2017.11.117

Martin, M., Poulikidou, S., Molin, E. 2019. Exploring the environmental performance of urban symbiosis for vertical hydroponic farming. Sustainability 11. https://doi.org/10.3390/su11236724.

Martin, M., Weidner, T., Gullström, C. 2022. Estimating the potential of building integration and regional synergies to improve the environmental performance of urban vertical farming. Front. Sustain. Food Sys. 6:849304. https://doi.org/10.3389/ fsufs.2022.849304.

Matysiak, B., Ropelewska, E., Wrzodak, A., Kowalski, A., Kaniszewski, S. 2022. Yield and quality of romaine lettuce at different daily light integral in an indoor controlled environment. Agronomy, 12. https://doi.org/10.3390/agronomy12051026.

Muñoz-Liesa, J., Royapoor, M., López-Capel, E., Cuerva, E., Rufí-Salís, M., Gassó-Domingo, S., Josa, A. 2020. Quantifying energy symbiosis of building-integrated agriculture in a mediterranean rooftop greenhouse. Renew. Energy, 156, 696-709. https://doi.org/10.1016/j.renene.2020.04.098.

Muñoz-Liesa, J., Royapoor, M., Cuerva, E., Gassó-Domingo, S., Gabarrell, X., Josa, A. 2022. Building-integrated greenhouses raise energy co-benefits through active ventilation systems. Build. Environ. 208. https://doi.org/10.1016/j.buildenv.2021.108585.

Pesch, H., Louw, L. 2023. Evaluating the economic feasibility of plant factory scenarios that produce biomass for biorefining processes. Sustainability 15. https://doi.org/10.3390/su15021324

RVO 2022. Energielabel woningen naar woningtype, 1 januari 2020. Available at: www.clo.nl/nl055608 (Accessed July 18, 2023).

RVO 2023. Energielabel C kantoren. Available at: https://www.rvo.nl/onderwerpen/ wetten-en-regels-gebouwen/energielabel-c-kantoren (Accessed July 18, 2023).

Sanjuan-Delmás, D., Llorach-Massana, P., Nadal, A., Ercilla-Montserrat, M., Munoz, P., Montero, J.I., Josa, A., Gabarrell, X., Rieradevall, J. 2018. Environmental assessment of an integrated rooftop greenhouse for food production in cities. J. Clean. Prod. 177 (10), 326-337. https://doi.org/10.1016/j.jclepro.2017.12.147.

Shao, Y., Li, J., Zhou, Z., Hu, Z., Zhang, F., Cui, Y. 2021. The effects of vertical farming on indoor carbon dioxide concentration and fresh air energy consumption in office buildings. Build. Environ. 195:107766. https://doi.org/10.1016/j. buildenv.2021.107766.

Sipma, J.M. 2019. Het daadwerkelijk energieverbruik van gelabelde en niet-gelabelde restaurants. Available at: www.tno.nl (Accessed February 28, 2022).

Stimular. 2022. Gemiddelde milieubelasting zwembaden. Available at: www. milieubarometer.nl (Accessed March 02, 2023).

Thomaier, S., Specht, K., Henckel, D., Dierich, A., Siebert, R., Freisinger, U., Sawicka, M. 2014. Farming in and on urban buildings: present practice and specific novelties of zero-acreage farming (ZFarming). Renew. Agric. Food Syst. 1-12. https://doi.org/10.1017/S1742170514000143.

Vernay, A.L., Salcedo Rahola, T.B., Ravesteijn, W. 2010. Growing food, feeding change: towards a holistic and dynamic approach of eco-city planning. Next generation infrastructure systems for eco-cities, Shenzhen. 1-6. https://doi.org/10.1109/INFRA.2010.5679234.

Weidner, T., Yang, A., Hamm, M. W. 2021. Energy optimisation of plant factories and greenhouses for different climatic conditions. Energy Convers. Manag. 243:114336. https://doi.org/10.1016/j.enconman.2021.114336.

Wielemaker, R. C., Weijma, J., Zeeman, G. 2018. Harvest to harvest: recovering nutrients with new sanitation systems for reuse in urban agriculture. Resour. Conv. Recycl. 128, 426–437. https://doi.org/10.1016/j.resconrec.2016.09.015

World Green Building Council. 2019. Bringin embodied carbon upfront: coordinated action for building and construction sector to tackle embodied carbon. Available at: www.worldgbc.org (Accessed July 06, 2023).

Xiaoying, L., Xuelei, J., Xuyang, Y., Zhigang, X. 2015. Design and test of LED surface light source used in plant factory with water-cooling system. Nongye Gongcheng Xuebao/Trans. Chin. Soc. Agric. 31, 244–247. https://doi.org/10.11975/j.issn.1002-6819.2015.17.032.



van Bergen Kolpa Architects, fotocredit: Jin Weiqi

TOC

4 Vertical Farms integrated into urban energy systems

The content of this chapter was published as:
Synergetic urbanism: a theoretical exploration of a vertical farm as local heat source and flexible electricity user
Blom, T., Jenkins, A., van den Dobbelsteen, A.A.J.F.
Sustainable Cities and Society, 2024, 103. DOI: 10.1016.j.scs.2024.105267

Supplementary material for this chapter is provided in Appendix C
The datasets of this chapter are available at the repository 4TU Research Data.
DOI: 10.4121/8b67deea-aa93-4284-adda-464cc285f45b

Chapter 3 highlighted the potential to reduce external inputs of energy, water, and nutrients by facilitating the exchange of energy and residual flows between various building typologies and integrated vertical farming systems. This chapter builds upon the research presented in Chapter 3 by extending the scope from individual buildings to urban neighbourhoods. Here, we investigate how vertical farms can contribute to local district heat networks by generating (waste) heat. Furthermore, this chapter explores the possibilities for vertical farms to use electricity in a flexible manner. This approach allows vertical farms to address two major challenges in the urban energy transition: the need for alternative heat sources, and fluctuating electricity supplies. Thus, Chapter 4 addresses the third research question of the dissertation:

How can the integration of vertical farms into urban energy systems establish a thermal energy equilibrium within local district heat networks, while responding to fluctuations in electricity supplies by the electricity grid?

A stepped approach was used to design energy systems that achieve thermal energy balance through the exchange of heat and cold between the vertical farm and buildings within a specific neighbourhood in the Netherlands. Furthermore, we explored alternative lighting strategies for vertical farms to respond to electricity price fluctuations, reflecting imbalances between renewable electricity generation and consumption, while ensuring the continuous production of fresh vegetables for the city.

4.1 Introduction

4.1.1 The urban energy transition

To limit the impacts of global warming, cities must achieve energy neutrality through the transition to renewable energy systems. One approach to realise energy-neutral cities is the 'New Stepped Strategy' introduced by Dobbelsteen (2008). At the urban scale, this strategy was elaborated as the 'Rotterdam Energy Approach and Planning' methodology (Tillie et al., 2009), and the 'Amsterdam Guide to Energetic Urbanism' (Dobbelsteen et al., 2011). The essence of the New Stepped Strategy lies in its structured steps: 0. Research the local circumstances; 1. Reduce energy demand; 2. Reuse residual energy flows; 3. Produce renewable energy. Research by Pulselli et al. (2021) and Caat et al. (2021) found great potentials in cities for energy savings (step 1), and residual heat usage by attuning, exchanging and storage of heat (step 2). In these studies, residual heat is exchanged between different urban functions based on geographic proximity. All buildings and urban areas generate residual heat and/or cold flows that could be employed, and making use of these could significantly reduce primary energy demands (Tillie et al., 2009). When in proximity, these exchanges are often cost-efficient, resource-efficient, and logistically manageable (Lenhart et al., 2015).

Traditional energy systems relied on the centralised supply of electricity, natural gas, and/or high-temperature district heating. These centralised and high-temperature characteristics of these district heat networks (DHNs) have posed challenges in integrating low-temperature (LT) waste heat sources (Gjoka et al., 2023). Recent developments have shifted towards low-temperature and smaller scales at neighbourhood and district levels, thereby facilitating the potential to exchange energy between the different buildings (Jansen et al., 2021a). These systems are called fifth-generation DHNs, which make use of decentralised heat and cold generation from multiple sources (Gjoka et al., 2023).

The use of lower temperatures in these DHN enables heat pumps, operating either in heating or cooling mode, to use the DHN as heat source or sink, and promote energy exchange in the network (Saini et al., 2023). Consequently, the exchange of warm return flows from cooling processes and the cold return flows from heating processes contribute significantly to covering thermal energy demands in the neighbourhood (Boesten et al., 2019; Saini et al., 2023). Ideally, the heat and cold demands are

balanced throughout this neighbourhood to eliminate the need for additional heat or cold sources. However, in instances where equilibrium is not achieved, the ultra-low temperature of DHN allows for direct integration of renewable sources, such as solar heat and aquathermal energy (Boesten et al., 2019; Jansen et al., 2021b).

Despite these advantages of these low temperatures, they make the DHN unsuitable for direct heating, in contrast to the conventional high-temperature DHNs. Therefore, centralised or decentralised water source heat pumps must be included to deliver the required temperature levels for building heating (Jansen et al., 2021a).

The exchange of residual flows from heating and cooling processes is particularly interesting in urban environments, as cities accommodate diverse functions with different energy patterns. These functions demand varying quantities of heat, cold, and electricity at different times of the day, week, or year (Dobbelsteen et al., 2023). By attuning functions energetically, exchanging redundant waste heat or cold, and storing these diurnally, weekly or inter-seasonally, cities will achieve energy-neutrality more effectively than a sole focus on renewable energy production. Under high densities, after all, sufficient generation of renewable energy (e.g., from sun or wind) to fulfil our needs becomes more complicated (Jansen et al., 2021a).

4.1.2 The integration of vertical farms into urban energy systems

When considering synergetic urban energy systems, a novel function can be introduced that not only generates heat but also produces food: vertical farming. These highly controlled indoor farms produce year-round crops with minimal land usage (Kalantari et al., 2017) using artificial LED lights (Delden et al., 2021). As a consequence of artificial lighting, vertical farms (VFs) produce significant quantities of low-temperature heat. The study presented in Chapter 3 and by Martin et al. (2022) presented the potential to capture and reuse this heat for building heating purposes. Martin et al. (2019) proposed to use this heat within DHNs to enhance the synergetic relationship between VFs and the built environment. This opportunity was also highlighted by Gentry (2019). The use of residual heat from VFs mostly offers benefits within colder and temperate climates where buildings have significant heating demands (Section 3.4.1.2). Graamans (2021) used residual heat produced by VFs to balance urban energy systems reliant on renewable energy. In this study, the VFs supplied heat to the DHNs and responded to fluctuations in renewable electricity production by adjusting the LEDs according to the availability of electricity in the grid, i.e., demand response operation by switching LEDs on and off.

Demand response operations can also offer a promising solution to high electricity costs, which is currently a limiting factor to scale up VFs and offers a big challenge to growers (Sørensen et al., 2016). On this basis, VFs can schedule their lighting periods according to the cheapest hours (Arabzadeh et al., 2023; Avgoustaki and Xydis 2021) and growers can determine the balance between operational costs and revenue by adjusting the growth parameters (Pimentel et al., 2023).

The transition to renewable electricity, and the electrification of transport and energy systems introduce new challenges, such as increased peak loads and bidirectional electricity flows (Voulis et al., 2018). Grid congestion occurs when the demand for electricity transportation in a certain area exceed the grid's capacity (Liander, 2019). As renewable energy sources are intermittent, this complicates the balance between renewable production and usage, leading to increased price fluctuations (Vandermeulen et al., 2018). System flexibility is crucial to counteract this effect (Arabzadeh et al., 2023). Flexibility, in this context, refers to the ability to accelerate or delay the injection or extraction of energy into or from an energy system, typically within time scales of less than a day (Vandermeulen et al., 2018). When operating the VF in a flexible manner, by increasing or decreasing LED luminance or switching the LEDs on or off, energy systems with integrated VFs can enhance overall energy system flexibility, limiting the mismatch between electricity production and demand (Arabzadeh et al., 2023).

4.1.3 Research aim

The energy transition requires the development of novel heating and cooling systems, as well as enhanced flexibility in electricity usage. Within the existing body of literature, VFs have been identified as a potential low-temperature heat source for urban environments, whilst allowing for flexible electricity usage. However, to date, the design and potential energy savings of the energy systems facilitating the exchange of residual heat and cold between VFs and urban functions remain unexplored. Additionally, the extent to which such systems can unlock flexibility within the electricity grid while sustaining food production levels remains unknown. Therefore, this research aims to investigate how the integration of VFs in cities can improve the daily and seasonal energy balances of heat and cold in a neighbourhood while enhancing flexibility for the electricity grid. To achieve this, a theoretical case study is employed, examining the integration of VFs into a neighbourhood in the Netherlands.

4.2 Methodology

Figure 4.1 represents the steps followed to design the optimal configuration of the DHN that integrates VFs into urban energy systems to balance heat and cold within a theoretical case study area. Concurrently, strategies are formulated to enhance the flexibility of electricity use in the VF. Step 1 to 5 and step 7 were adapted from the steps developed by Jansen et al. (2021b) to design optimal DHN configurations and estimate their energy efficiency. Step 6 was added to include for the integration with the electricity grid. The following sections describe each step of the methodology.

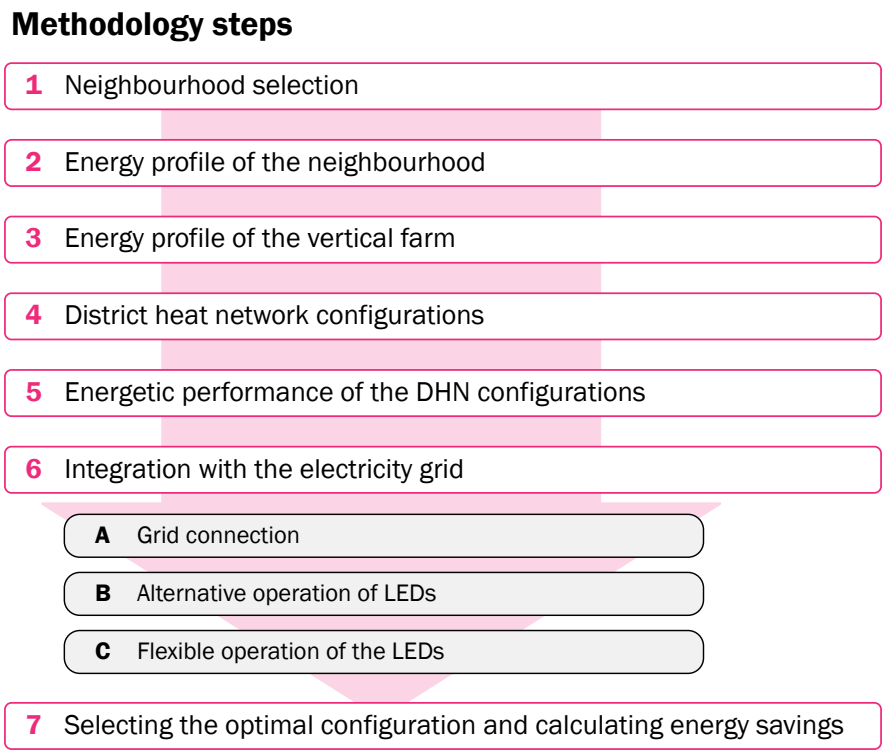

FIG. 4.1 Methodology steps of the research

TOC

4.2.1 Step 1: Context and neighbourhood selection

As highlighted in the introduction, the use of residual VF heat for building heating purposes is particularly advantageous in cold and temperate climates. Therefore, this study focusses on the Westindische Buurt, a residential neighbourhood in Amsterdam, the Netherlands Situated in climatic zone Cfb according to the Köppen-Geiger classification, the Netherlands experiences a temperate climate characterised by evenly distributed precipitation throughout the year and moderate summers.

The neighbourhood consists of 3,632 multi-family houses of on average 93 m^2 gross floor area, and accommodates 1,245 company registrations (CBS, 2022). Non-residential functions include restaurants, cafes, retail, offices, and four large supermarkets. The majority of the buildings were constructed between 1920 and 1940, with 83% of the residences possessing an energy label C or lower. This study focusses on the predicted energy use of the neighbourhood in 2025 and assumes minimal to no building renovations within this time frame. In the upcoming years, the municipality of Amsterdam is planning to introduce a DHN within the Westindische Buurt (Gemeente Amsterdam, 2023).

4.2.2 Step 2: Energy profile of the neighbourhood

To minimise the need for external heat or cold, the exchange of heat and cold between the different building functions within the neighbourhood should be maximised. To define to what extent the energy system can rely on this exchange, the thermal energy balance of the neighbourhood shall be defined initially. This thermal energy balance illustrates the monthly and annual heat and cold demands, with space heating and domestic hot water (DHW) collectively represented as positive values on the vertical axis and cooling demands as negative values.

A positive disbalance between heat and cold demands requires the connection of alternative heat sources to the energy system, such as residual heat from a VF. Seasonal energy storage should be considered to address seasonal mismatches between heat and cold demands. Moreover, heating and cooling demands were defined for the warmest and coldest day of the year: January 18th and July 24th, averaging 2.3 °C and 22.3 °C respectively (mean value over 24 hours) between 2012 and 2022 (KNMI, 2023). Additionally, monthly electricity usage is defined for January 18th and July 24th.

Assuming no significant renovations by 2025, buildings will maintain their current energy performance, relying on natural gas for heating. Data on natural gas and electricity usage in the Westindische Buurt were collected from national statistics CBS (2021a;b) and Klimaatmonitor (2023) for the year 2022. Monthly and daily gas and electricity use profiles were generated using MMFBAS (2023), providing hourly gas and electricity use profiles for various user profiles. Cooling demands were estimated due to a lack of reliable data of electricity for cooling purposes. This study also includes for neighbourhood electric vehicle charging and user-related electricity. Appendix C.1 provides further details on data collection and the conversion into monthly and hourly profiles for heating, cooling, and electricity usage.

4.2.3 Step 3: Energy profile of the vertical farm

This study builds upon the previous work of this dissertation, which delved into the potential integration of VFs with the energy and resource systems of buildings (Chapter 3). Further details regarding the VF, such as climate setpoints, and the cooling and dehumidification systems, can be found in Section 3.2.1. In summary, the study focusses on a closed-box VF that produces butterhead lettuce with a Photosynthetic Photon Flux Density (PPFD) of 200 µmol m^{-2} s^{-1} and a 16-hour photoperiod. A closed-box VF is characterised by highly insulation and airtightness.

In this study, the VF conditions are maintained using one heat pump (HP1) and two air-to-water heat exchangers (HE1 and HE2) to cool and dehumidify the VF air (Fig. 4.2). HE1 cools the air below dew point temperature, while HE2 re-heats the air to the desired return temperature using the evaporator and condenser of HP1. Excess heat generated by the condenser is removed via HE3 and supplied to the DHN.

The LEDs used in this study have a molar efficacy of 3.5 µmol J^{-1} (Weidner et al., 2021), and approximately 90% of their electricity usage results in both sensible and latent heat consistently throughout the year (section 3.2.1.1). Differing from the approach in Chapter 3, this study accounts for heat production during both light and dark periods.

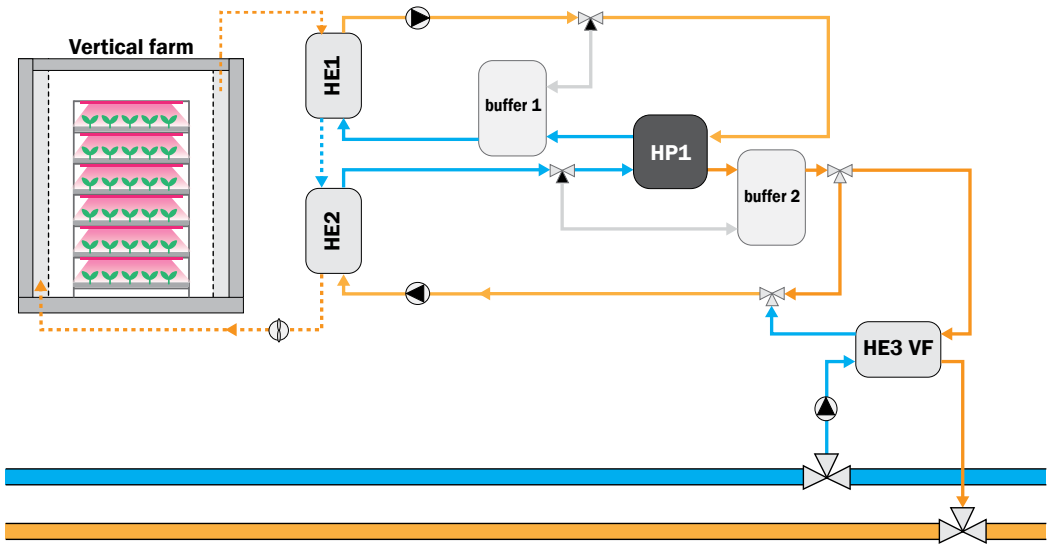

FIG. 4.2 The cooling and dehumidification system of the VF, using one heat pump (HP1) and three heat exchangers (HE1, HE2, HE3).

Throughout the 16-hour photoperiod, the exhaust air from the VF entering HE1 has a temperature of 26°C and a 72% relative humidity. The return air provided by HE2 is 24°C with 76% RH. During the dark period, the temperatures decrease by between 1–2°C, and the relative humidity increases by 10%, with no sensible heat production as the LEDs are turned off. The latent heat demand at 23°C is estimated to be approximately 32.8 W m^{-2} (Graamans et al., 2021), assuming a constant air flow rate during both dark and light periods.

The total cultivation area of VF to obtain thermal energy balance within Westindische Buurt (step 2) will be determined in this study. The exact dimensions and the location of the VF remain unknown at this stage due to the wide range of approaches for food production in VFs, including number of growth layers, cultivation height, and level of automation. Consequently, it is presently impossible to define a typical VF layout. Therefore, electrical inputs and heat outputs are specified per m^2 of cultivation area, representing one m^2 of a growth layer in the VF.

4.2.4 Step 4: District heat network configurations

The energy system configurations considered in this study can be categorised as centralised and decentralised. Centralised systems use a central HP to obtain the desired temperature levels for heating and/or cooling, and distribution is done via DHNs and individual heat exchangers in each building. This eliminates the need for individual HPs in each building, which is beneficial for small apartments (Jansen et al., 2021b). In contrast, the decentralised configuration employs individual HPs in each building within the neighbourhood to adjust the temperatures of the DHN. DHN configurations can have 2, 3, or 4 pipes, with three-pipe DHNs being significantly more expensive and hydraulically complex (Jansen et al., 2021b). In this research, temperature levels are defined as cold when ranging from 5°C to 15°C, ultra-low-temperature (uLT) when between 15°C and 30°C, low-temperature (LT) when from 30°C to 55°C, mid-temperature when from 55°C to 75°C, and above 75°C as high-temperature.

Aquifer thermal energy storage (ATES) will be implemented in all configurations to maximise the exchange of heat and cold among various building functions. The Netherlands exhibits a high potential for ATES systems (Bloemendal et al., 2018). The warm and cold aquifer temperatures for heat storage and cold storage were set at 24°C and 7°C, respectively. The ATES system is connected to a DHN using an 80% efficient water-to-water heat exchanger, determining the DHN temperatures (Appendix C.2.1). The amount of thermal energy extracted and stored from the aquifers should be balanced annually to prevent exhaustion (Bloemendal et al., 2018).

4.2.5 Step 5: Energetic performance of the DHN configurations

The designed energy system configurations were assessed on six criteria:

1 The cultivation area of the VF: the cultivation area required to meet the heat demands of the neighbourhood under both centralised and decentralised configurations. The cultivation area is affected by several factors:

   a The heating and cooling demands of the neighbourhood, which are the same for both configurations.
   b Heat losses in the DHN. Modern DHNs experience heat losses ranging from 15% to 20% (Energy Transition Model, 2023), which were estimated at 15% in this research.
   c Heat from cooling processes. A share of the heating demands will be provided by the heat generated from cooling processes within the neighbourhood.
   d Heat from compressors. The compressors of both the centralised and decentralised HPs will produce an additional quantity of heat beyond what is supplied to the HP. The heat produced by these HPs is the sum of the heat supplied via the DHN and the electrical input of the HP.

   The preference for a smaller cultivation area arises from the challenge to spatially integrate sufficient VF cultivation area to meet the heating demands of the Westindische Buurt.

2 The ability to balance the ATES aquifers annually to prevent exhaustion (Section 4.2.4).

3 The quantity of thermal energy stored within these aquifers.

4 The total annual electricity use of the configuration, including electricity use of the neighbourhood (user-related electricity and electric vehicle charging), the VF (LEDs, HP, fans, and pumps), and the energy systems themselves. The latter includes the energy used to produce mid-temperature heat for space heating and DHW using centralised or decentralised HPs (1), to produce space and product cooling (2), and to pump energy through the DHN (3) and ATES system (4). The calculation methods for these four components are described in Appendix C.3. The electricity used to distribute heat or cold within the buildings is excluded.

5 Spatial requirements for energy systems within buildings. Buffer tanks for DHW storage in residences are not required when using mid-temperature DHNs but are needed for buildings connected to (u)LT DHNs. For each apartment, these buffer tanks have an approximate volume of 0.14 m^3 alongside individual HPs of 0.25 m^3 (Meerkerk, 2022).

6 Future readiness, using the following considerations.

   a (u)LT DHNs are better suited to connect other sustainable heat sources. The number of (u)LT heat sources in the built environment are also more readily available than mid-temperature heat sources (Meerkerk, 2022).
   b (u)LT DHNs are capable of direct delivery of passive or high-efficient cooling, whilst cooling demand will increase in the future due to climate change.
   c (u)LT DHNs allow for future building renovations that lower heating temperature requirements. When using individual HP systems, these temperature levels can be attuned to the individual requirements without affecting the other households.

4.2.6 Step 6: Integration with the electricity grid

Step 6 addresses the integration of VFs with the electricity grid, while maintaining the thermal energy balance. Two aspects are essential to enhance the electricity balance between supply and demand in the grid, to meet its transportation capacity, and to reduce costs for growers: minimising grid connections, and optimising production usage according to the hourly day-ahead electricity prices (Avgoustaki and Xydis, 2021).

Given that LEDs represent approximately 80% of the VF's electricity use (Section 4.2.3), we focus on exploring alternative lighting concepts to minimise grid connections and to adapt to price fluctuations. The following sections explore the average hourly electricity prices in the Netherlands (Section 4.2.6.1), alternative operation concepts for LEDs (Section 4.2.6.2), and flexibility concepts for LEDs (Section 4.2.6.3).

4.2.6.1 Average hourly electricity prices

Since 2015, the Dutch electricity prices have been determined one day-ahead at the European Power Exchange (EPEX) market, i.e., the day-ahead market. These prices are established based on expected demands and supplies. Large electricity consumers (above 100 MWh) pay for their electricity consumption in accordance with these EPEX prices. The electricity prices drop significantly at times of high inflexible generation that meet low electricity demands.

Figure 4.3 presents the average hourly day-ahead electricity price in the Netherlands for 2022 in euro per MWh. The graph indicates peak prices at 06:00 and 17:00. Due to the high penetration of solar energy during the day and low demands at night, the electricity prices are the lowest around noon and mid night.

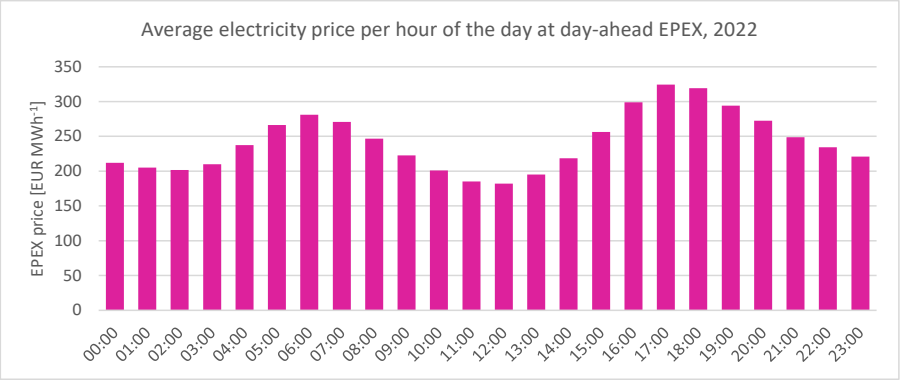

FIG. 4.3 Average electricity price per hour of the day for 2022 at day-ahead pricing by EPEX, the Netherlands (ENTSOE, 2023).

4.2.6.2 Alternative operation of LEDs

In general, lettuce cultivation involves continuous light with a 16-hour photoperiod and a PPFD of 200 µmol m^{-2} s^{-1} (Blom et al., 2023), resulting in a daily light integral of 11.52 mol m^{-2} d^{-1}. The photoperiod typically aligns with working hours, operating between 06:00 and 22:00 (Pimentel et al,. 2023). This lighting schedule is referred to as the 'baseline scenario' in this study. Five alternative lighting concepts (Fig. 4.4) were considered to minimise grid connection and respond to the electricity price profile defined in Figure 4.3. C-strategies refer to one continuous and uninterrupted photoperiod each day, while I-strategies involve multiple intermittent photoperiods. Each of these attempts aims to reduce lighting costs while sustaining plant yields (Arabzadeh et al., 2023).

Firstly, the operational hours of the baseline lighting strategy were adjusted, a concept referred to as 'C16/8'. Secondly, considering lettuce's tolerance for constant 24-hours lighting (Velez-Ramirez et al., 2011), a strategy involving continuous 24-h light (C24/0) was considered. In this approach, a PPFD of 133 µmol m^{-2} s^{-1} was used to maintain the daily light integral at 11.52 mol^{-2} d^{-1}.

TOC

Besides continuous lighting, intermittent light periods can be provided to lettuce crops. Chen and Yang (2018) conducted experiments comparing lettuce growth under a continuous 16-h photoperiod to intermittent lighting concepts while maintaining the daily light integral. Their findings indicate that lettuce fresh weights could increase by 111% to 118% when adopting intermittent lighting, compared to the C16/8 concept, without increasing overall energy consumption. The intermittent light concepts had a total photoperiod of 16-h and a PPFD of 200 µmol m^{-2} s^{-1}. These concepts included two cycles of 8 h of light and 4 h of darkness (I8/4), four cycles of 4 h of light and 2 h of dark ness (I4/2), and six cycles of 3 h of light and 1 h of darkness (I3/1). The increased yield when using I8/4 over C16/8 was also observed by Kondrateva et al. (2021), and Chen and Yang (2018) noted improved taste in terms of crispness and sweetness.

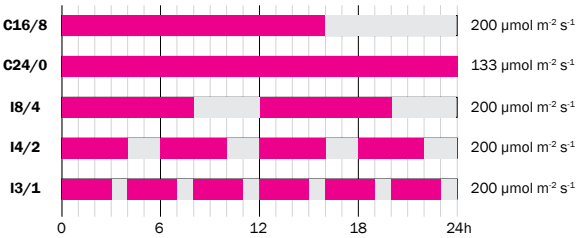

FIG. 4.4 Lighting concepts considered for VF integration.

4.2.6.3 Flexible operation of LEDs

The actual day-ahead electricity prices will differ from that of the average day as depicted in Figure 4.3. To avoid high electricity costs, adapting the VF's electricity consumption from its regular routine is essential (Arabzadeh et al., 2023). Consequently, we explored the potential to adjust LED schemes to real-time price fluctuations by varying light intensity. This concept involves exposing crops to bright light during periods with low electricity prices and dimming the light during peak price hours (Pimentel et al., 2023).

This approach is based on the idea that the PPFD received by the plants does not need to be uniform throughout the day, as long as the number of photons remain constant during the photoperiod. The experiment conducted by Bhuiyan and van Iersel (2021) indicated that PPFD fluctuations between 400 and 0 µmol s^{-1} m^{-2}, and 360 and 40 µmol s^{-1} m^{-2}, result in lettuce crops with fewer and smaller leaves compared to treatments with smaller variations. They concluded

TOC

that lettuce tolerates fluctuating PPFDs as long as the differences are not too extreme. Building on this study, Pimentel et al. (2023) selected a PPFD that varied between 80 and 320 µmol s^{-1} m^{-2} stating that the growth conditions and lettuce yields were unaffected as long as the daily light integral remained constant throughout the photoperiod. Although, the effects of fluctuating light intensities on lettuce yields require study, PPFD variations in the range of 320 to 80 µmol s^{-1} m^{-2} were selected, ensuring a consistent daily light integral within each photoperiod. The cost savings resulting from these PPFD variations will be determined for January 18th and July 24th, 2022, using the hourly electricity prices (ENTSOE, 2023).

4.2.7 Step 7: Selecting the optimal configuration and calculating the energy savings

The evaluation of the two configurations will be based on the six criteria defined in step 5. In addition, the performance of the configurations for integrating the VF within the electricity grid will be assessed according to two specific criteria. First, the required grid connection for the VF related to the peak loads. Second, the annual electricity cost savings by selecting an alternative LED operation in comparison the baseline, and/or the daily cost savings by PPFD fluctuations using day-ahead electricity prices. Finally, the energy savings achieved by the selected configuration will be calculated in comparison to those of the current energy system.

4.3 Results

4.3.1 Step 1 to 3: Energy profiles of the neighbourhood and vertical farm

The total baseline energy use of the Westindische Buurt was 44,388 MWh y^{1}, of which 76% was natural gas used for DHW and space heating. The remaining 24% was used for user-related energy, electric vehicle charging and cooling. The heating and DHW demands were 30,212 MWh_{th} y^{-1}, and the cooling demands were 4,038 MWh_{th} y^{-1}. Appendix C.4.1 presents more details on the daily heat, cold and electricity profiles of the Westindische Buurt. The thermal energy balance is presented in Figure 4.5. The heat and cold demands indicated a significant disbalance of 26,129 MWh annually when exchanging heat and cold between the different building functions.

The VF used 434 kWh y^{-1} of electricity per m^2 cultivation area and produced 462 kWh m^{-2} y^{-1} of LT residual heat (Appendix C.4.2).

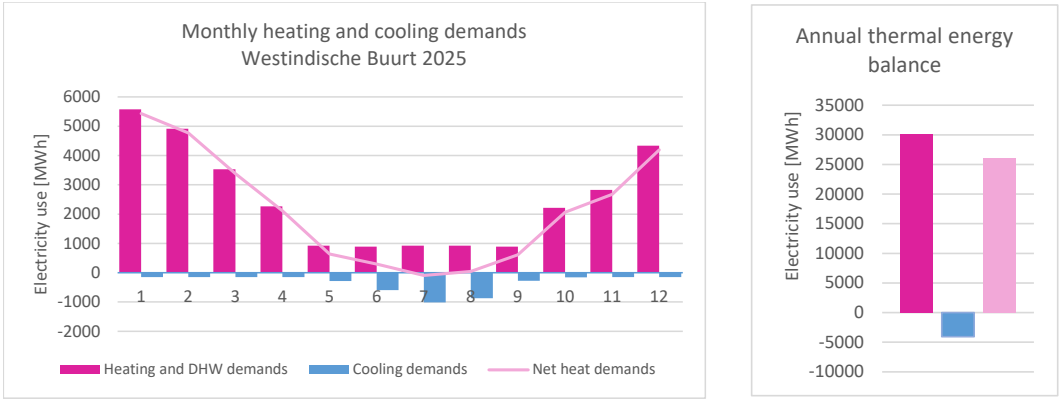

FIG. 4.5 Monthly heating and cooling demands of the Westindische Buurt in 2023 (left) and annual thermal energy balance of the Westindische Buurt in 2023 (right).

TOC

4.3.2 Step 4 and 5: District heat network configurations and energetic performance

4.3.2.1 Centralised: 4-pipes DHN with central heat pump

The centralised configuration (Fig. 4.6) makes use of a central HP (HP2) that upgrades the LT heat produced during the cooling of the VF (via HE3), buildings (via HE6) and supermarkets (via HP3) to mid-temperature heat. This mid-temperature heat is used for space heating and DHW applications (via HE5). The centralised HP2 is connected to a 4-pipe DHN, including cold, ultra-low, low, and mid-temperature levels. An ATES system is integrated via HE4 to address timing issues between heat and cold production and demand.

The energy system operates in 'winter mode' when the total heat produced (by HE3, HE6, and HP3) is insufficient to meet the heat demands and losses in the DHN. Therefore, additional heat is extracted from the warm aquifer during winter mode. Simultaneously, centralised HP2 generates more excess cold than used (by HE3, HE6, and HP3), which is then stored in the cold aquifer. Conversely, in 'summer mode' (Appendix C.4.3.1), when heat production exceeds heat demands, the surplus heat is stored in the warm aquifer. The cold produced by centralised HP2 is supplemented with cold extracted from the cold aquifer.

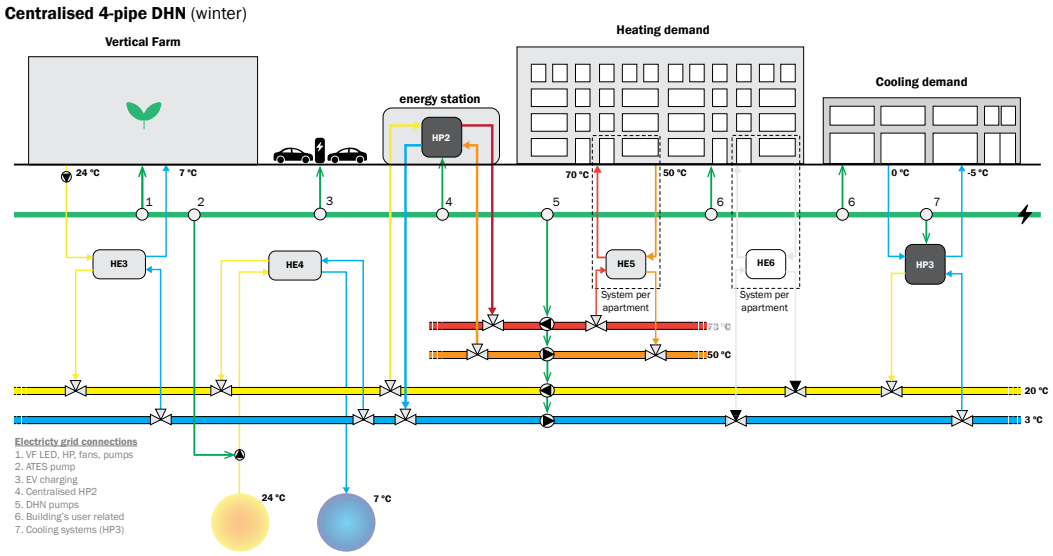

FIG. 4.6 Centralised energy system configuration with 4-pipe DHN in winter mode.

The total electricity use of the configuration amounted 44,738 MWh y^{-1} (Fig. 4.7). This total comprised 11,091 MWh for user-related electricity and electric vehicle charging, 18,385 MWh for the VF, and 15,262 MWh for the energy system. The central HP2 accounted for 31% of the total electricity use, primarily due to its relatively low coefficient of performance (COP) ranging between 2.4 and 3.0.

To achieve thermal energy balance within the neighbourhood, the VF required a cultivation area of 42,385 m^2. The annual heat and cold balances are detailed in Appendix C.4.3.1 (Fig. C.4 and C.5). The compressor of the central HP2, the VF, and the cooling processes within the supermarkets and buildings fulfilled respectively 37%, 52% and 12% of the heating demands. Due to the 4-pipe system, heat losses within the DHN were relatively high, contributing an additional 7,661 MWh to the building's heat demand of 30,212 MWh. During winter, 7,701 MWh of heat was extracted from the ATES warm aquifer, while the same quantity of heat was stored again in the summer. This process was reversed for the cold aquifer.

TOC

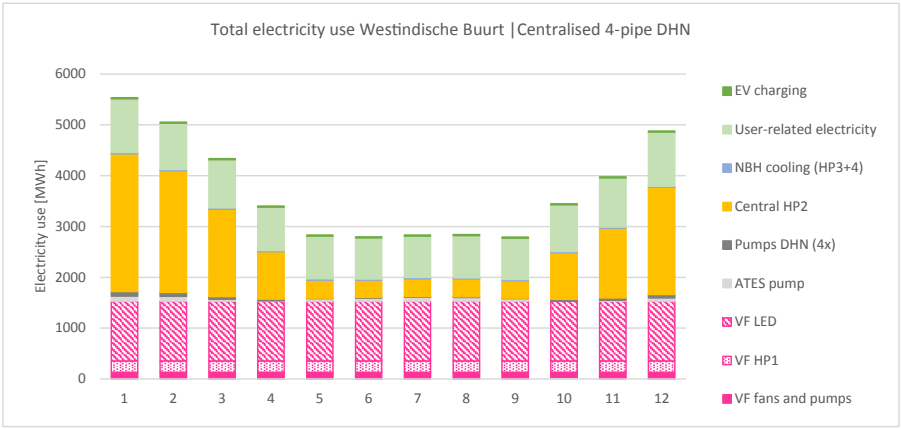

FIG. 4.7 Annual electricity use of the Westindische Buurt with integrated VF using the centralised 4-pipe DHN configuration.

4.3.2.2 Decentralised: 2-pipes DHN with decentralised heat pumps

The decentralised configuration (Fig. 4.8) uses a 2-pipe DHN with individual HPs to generate mid-temperature heat (HP4) from LT waste heat derived from cooling the VF (via HE3), supermarkets (via HP3), and the buildings (via HP4 in cooling mode). The DHN consist of one uLT and one cold pipe. Similar to the centralised system, an ATES system is integrated to overcome timing issues between heat and cold production and demand.

During winter mode, the amount of heat produced (by HE3, HP3, and HP4) is insufficient to meet the heat demands (HP4 and losses DHN). Consequently, heat is extracted from the warm aquifer. The surplus of cold produced by HP4 is stored in the cold aquifer during this mode. In summer mode (Appendix C.4.3.2), heat production exceeds the demands and is stored within the warm aquifer. The cold generated by decentralised HP4 is supplemented by cold extracted from the cold aquifer to meet cooling requirements.

TOC

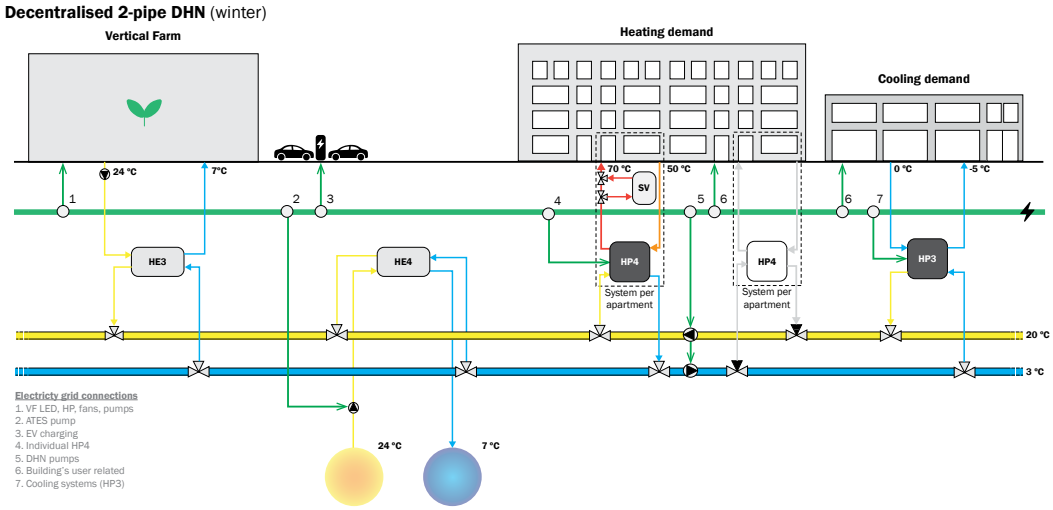

FIG. 4.8 Decentralised energy system configuration with 2-pipe DHN in winter mode.

The decentralised configuration used 39,702 MWh annually (Fig. 4.9). Again, 11,091 MWh was allocated to user-related electricity and electric vehicle charging. To achieve thermal energy balance in the neighbourhood, a VF with a cultivation area of 38,547 m^2 was required, consuming 16,720 MWh y^{-1}. The energy systems used 11,891 MWh y^{-1}.

The individual HPs for building heating exhibited COPs ranging between 2.6 and 3.8 throughout the year, contributing to 27% of the configuration's electricity use. These decentralised HPs generated 32% of the total annual heat demands of 30,212 MWh y^{-1}. The cooling processes of the VF and neighbourhood provided the remaining 54% and 14% of the annual heat demands, respectively. Losses within the 2-pipe DHN represented 15% of these heat demands.

To balance the DHN seasonally, 7,390 MWh was extracted from the ATES hot source in winter, with the same quantity being stored in summer. The cold source operated inversely. The heat and cold balances are presented in Appendix C.4.3.2 (Figures C.7 and C.8).

TOC

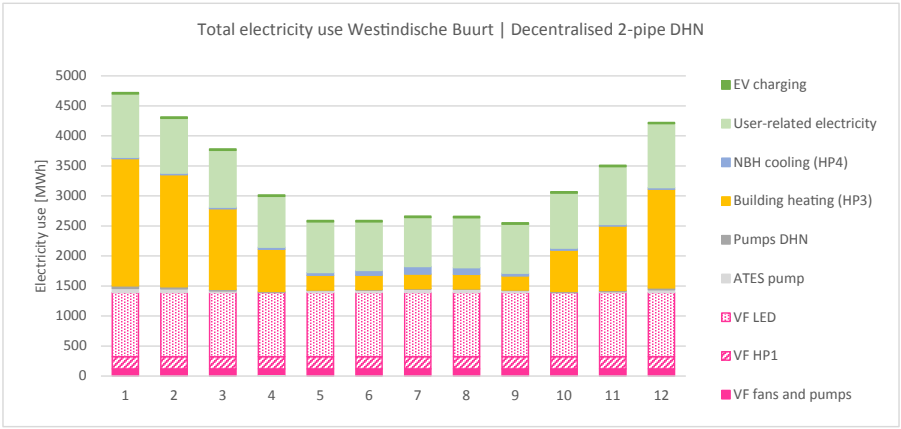

FIG. 4.9 Annual electricity use of the Westindische Buurt with integrated VF using the decentralised 2-pipes DHN configuration.

4.3.3 Step 6: Integration with the electricity grid

4.3.3.1 Grid connection

Given that 80% of the VF's electricity use was attributed to LEDs, their optimisation offers the highest potential to reduce peak loads and subsequent grid connection in both the centralised and decentralised systems. The LEDs generated a peak load of 57.1 W m^{-2} when using the baseline profile or alternative strategies C16/8, I8/4, I4/2, and I3/1. A reduction of 33% was achieved by using 24-h continuous light (C24/0), or by segmenting the VF in three modules with non-overlapping dark periods. The latter approach was applied to concepts C16/8, I8/4, and I4/2, referred to as '3x'. Figure 4.10 illustrates the segmented VF concept for C16/8(3x).

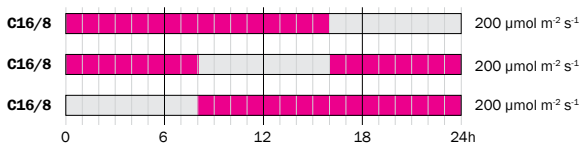

FIG. 4.10 Lighting concept C16/8(3x) consisting of three segmented VF modules with non-overlapping dark periods.

TOC

4.3.3.2 Alternative operation of the LEDs

The annual electricity costs of the baseline scenario, operating the VF lights from 06:00 to 22:00, was 83.8 EUR per m^2 of cultivation area in 2022. Each of the five lighting concepts (Fig. 4.4) were optimised for reduced electricity costs based on the hourly electricity prices in 2022 (ENTSOE, 2023). Table 4.1 presents the peak loads and annual costs per m^2 cultivation area for each lighting concept.

TABLE 4.1 Peak loads and operation costs (for 2022) per lighting concept when in fixed operation per m^2 cultivation area of the VF.

		Base-line	C16/8	C24/0	I8/4	I4/2	I3/1	C16/8 (3x)	I8/4 (3x)	I4/2 (3x)
Peak loads	W m^{-2}	57.1	57.1	38.1	57.1	57.1	57.1	38.1	38.1	38.1
Annual costs	EUR m^{-2} y^{-1}	83.8	75.6	80.7	73.3	79.5	90.6	80.7	80.7	80.7

In comparison to the baseline scenario (C16/8 06:00-22:00), alternatives C16/8, C24/0, I8/4, and I4/2 reduced the electricty costs by 11%, 4%, 14%, and 5% respectively when using the operational hours as presented in Figure 4.11. Alternatives C16/8(3x), I8/4(3x), and I4/2(3x) demonstrated similar performance to C24/0. Profile I3/1 increased the electricity costs by 7%. Operating the LED lights from 04.00 to 08.00 and from 16.00 to 20.00 (I8/4) resulted in the lowest annual electricity costs of 73.3 EUR m^{-2} for 2022.

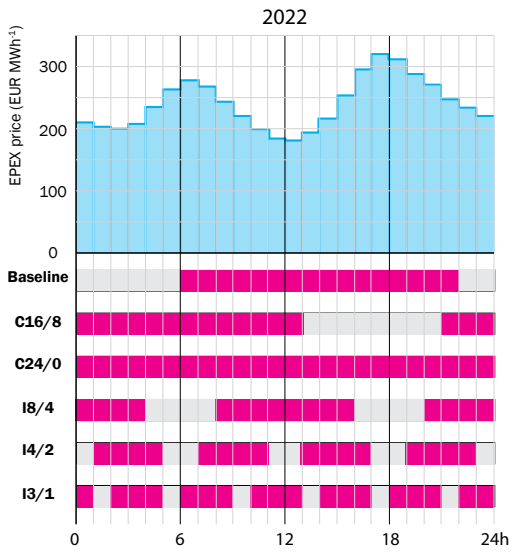

FIG. 4.11 The baseline profile, and the optimised operation periods of the five alternative lighting concepts in pink. The average hourly electricity prices in 2022 are presented in blue (ENTSOE, 2023).

TOC

4.3.3.3 Flexible operation of the LEDs

Hourly variations of light intensities between 80 and 320 µmol m^{-2} s^{-1} were applied to alternatives I8/4 and C16/8(3x). The moles of incident light within each photoperiod remained the constant as in the non-flexible concept: 5.76 mol m^{-2} for each 8-h photoperiod in I8/4, and 11.52 mol m^{-2} for the 16-h photoperiod in C16/8(3x).

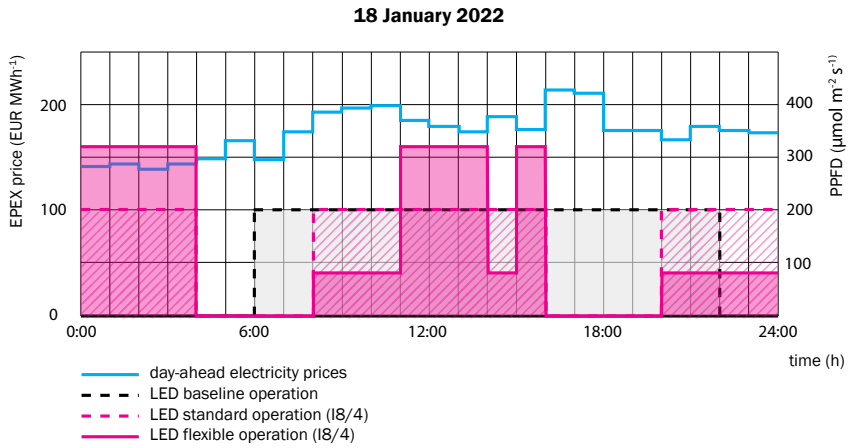

FIG. 4.12 LED operation I8/4 standard versus flexible operation on January 18th, 2022.

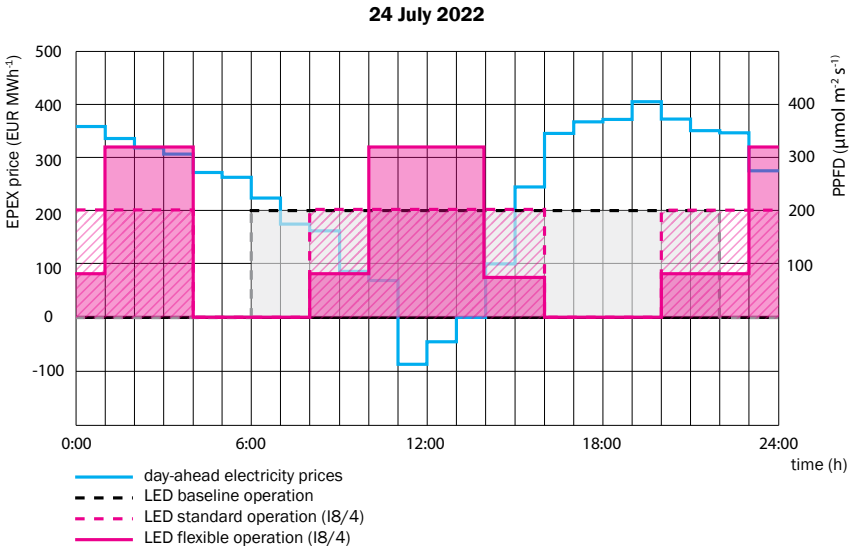

FIG. 4.13 LED operation I8/4 standard versus flexible operation on July 24th, 2022.

TOC

On January 18th, 2022, flexible operation of both I8/4 and C16/8(3x) reduced cost by 11% compared to the baseline. On July 24th, 2022, I8/4's flexible operation resulted in 3% lower costs than for C16/8(3x), and reduced the electricity cost by 15% in comparison to the baseline. Comparing flexible operation with standard operation in I8/4, cost savings were 4% for the winter day, and 16% for the summer day. Figure 4.12 and 4.13 present the hourly day-ahead electricity prices on the left axis (ENSTOE, 2023), and the PPFD for both standard and flexible operation of I8/4 on the right axis. The daily costs per m^2 cultivation area are presented in Table 4.2.

TABLE 4.2 Cost flexible operation of the LEDs per m^2 cultivation area of the VF for two specific days in 2022.

		Baseline	I8/4	C16/8 (3x)	I8/4 (3x)
January 18th, 2022	EUR m^{-2} d^{-1}	0.173	0.154	0.163	0.154
July 24th, 2022	EUR m^{-2} d^{-1}	0.179	0.153	0.157	0.176

4.3.3.4 Effects on thermal energy balance

When employing the baseline LED operation (C16/8, 06:00-22:00), the ATES system effectively managed seasonal timing issues between heat and cold production and usage. Aquifer exhaustion was avoided as the heat and cold extracted and stored in the aquifers remained balanced throughout the year (see thermal balances in Appendix C.4.3).

In the alternative lighting strategy I8/4, whether in standard or in flexible operation, the total light energy provided to the crops remained constant throughout each photoperiod, ensuring consistent heat production. Hourly fluctuations in heat production were effectively covered by ATES system. For example, when the PPFD is reduced to 80 µmol s^{-1} m^{-2} for 4 hours, heat production decreased. However, with daily light integral remaining constant, the subsequent 4 hours use a PPFD of 320 µmol s^{-1} m^{-2}, compensating for heat production. In winter, this translates into a 4-hour increased heat extraction from the warm aquifer, followed by a 4-hour decrease. In summer, there is a 4-hour reduction in heat storage, which is compensated in the next 4 hours. Consequently, flexible LED operation does not affect the annual thermal energy balance of the system.

4.3.4 Step 7: Selecting optimal energy systems configuration and determining savings

The optimal energy system configuration for integrating VFs within the urban DHNs and the electricity grid was selected based on eight criteria: VF cultivation area to achieve thermal energy balance (1), aquifer balancing capability (2), quantity of energy stored (3), annual energy use (4), spatial requirements within buildings for HPs, buffers, and HEs (5), future readiness (6), grid connection (7), and cost savings by LED operations (8).

As highlighted in Section 4.3.2, the decentralised configuration excelled in criteria 1, 3, and 4. Both configurations effectively managed to balance the aquifers year-round and obtained equal percentage cost-savings through alternative LED operations. The centralised system required less apartment space since no individual HPs and buffer tanks were needed. Concerning future readiness, both configurations allowed for the integration of (u)LT heat sources and passive or highly efficient cooling via the (u)LT DHN. However, the decentralised configuration offered greater flexibility in adjusting heating temperature during scattered building renovations.

The decentralised energy configuration was selected as the most optimal energy system for integrating VFs in the Westindische Buurt, reducing the energy use for heat, DHW, and cooling by 65% compared to the current system based on natural gas. Even when accounting for VF electricity use, the energy savings reached 15%, while simultaneously producing 3037 kg fresh weight lettuce annually (Section 3.2.1.3). These findings are summarised in Table 4.3.

TABLE 4.3 Results per assessment criteria

Assessment criteria	Unit	Centralised 4-pipe DHN + centralised HP	Decentralised 2-pipe DHN + decentralised HP
1. VF cultivation area	m^2	42,385	38,547
2. Annual aquifer balance	[-]	*yes*	*yes*
3. Q_{stored} hot/cold aquifers $Q_{extracted}$ hot/cold aquifers	MWh MWh	7,701 7,701	7,390 7,390
4. Annual energy use a. Energy systems configuration b. VF c. Neighbourhood	MWh MWh MWh MWh	44,738 15,262 18,385 11,091	39,702 11,891 16,720 11,091
5. Spatial requirements in building	[-]	+	-
6. Future readiness	[-]	-	+
7. Grid connection LED I8/4	kW	2422	2203
8. Annual savings by LED I8/4	%	14	14

TOC

4.4 Discussion

The following section discusses the results in more detail and in relation to other studies, identifies research limitations, and makes suggestions for further research. Section 4.4.1 focusses on the integration of VFs within the neighbourhood to create thermal energy balance, and Section 4.4.2 on the integration of VFs with the electricity grid.

4.4.1 Integration of the VF with district heating

4.4.1.1 Centralised versus decentralised configuration

Compared to the centralised configuration, the decentralised configuration use 11% less energy, required a 9% smaller cultivation area to obtain thermal energy balance, minimised aquifer thermal energy storage by 4%, and enabled future-ready temperature control for the buildings. However, spatial integration, particular for apartments and small non-residential units, may be challenging due to the need for individual HPs and buffer tanks, and could lead to the choice of collective systems.

These results align with Jansen et al. (2021b), concluding that the energy system is more efficient when the energy station (HP) is closer to the end-users, as temperatures can be matched precisely with the demands and distribution losses are minimised. The heat losses within each 2-pipes DHN were assumed to be 15% (Section 4.2.5). In the 4-pipes DHN, 20% of the total heat produced was lost, compared to 9% in the 2-pipes configuration (Appendix C.4.3). The increased heat losses in the centralised system contributed to a larger cultivation area requirement to maintain thermal balance.

Both configurations reached annual equilibrium within the ATES aquifers. The Netherlands generally has a high potential for ATES systems (Bloemendal et al., 2018). Factors such as aquifer sizing, spatial well distancing, energy losses, and temperature variations during storage were not considered in this study. Approximately 23-24 kWh of thermal energy should be stored annually per square meter land of the Westindische Buurt. In a case study in Amstelveen, the Netherlands, an annual storage capacity of 40 kWh m^{-2} was planned (Bloemendal et al., 2018). Although more research is needed to determine the storage capacity in the Westindische Buurt, this comparison suggest it is feasible.

4.4.1.2 Vertical farm size

Significant cultivation areas of 42,385 m^2 and 38,547 m^2 were necessary to achieve thermal energy balance within the Westindische Buurt when utilising the centralised and decentralised configurations, respectively. This study did not address the spatial integration of these large VFs in the Westindische Buurt, as numerous factors influence the floor areas needed by VFs. These factors make it impossible to define a typical VF layout, e.g., growth method and the number and height of growth layers. Nevertheless, integrating such substantial cultivation areas poses a significant challenge. Even with multi-layer stacking, incorporating VFs in existing neighbourhoods will be difficult. Possible (combinations of) solutions include situating VFs on the outskirts of the city, spreading multiple small-scale VFs throughout the neighbourhood (e.g., building-integrated farms, Chapter 3), utilising alternative (u)LT heat sources (e.g., PV-thermal, and heat extraction from water or ground sources), and building renovations to reduce heat demands. Further research is required to understand the spatial integration of VF in urban settings.

4.4.1.3 Energy efficiency

In the Westindische Buurt, gas boilers currently provide space heating and DHW, and air conditioning units are used for space cooling. Integrating VFs into this neighbourhood with the decentralised configuration resulted in a total energy saving of 15% for heating, DHW, and cooling compared to the baseline system. This calculation includes energy used by the energy systems (individual HPs for heating and cooling, DHN pumps, and ATES pumps), and the VF (LED, HP, fans, and pumps). When excluding the energy use of the VF, savings increased to 64% compared to the current system. The VF significantly affects the energy system efficiency, but also produces 3037 t of lettuce annually, which not only meets the vegetable needs of the Westindische buurt but allows for significant sales to surrounding neighbourhoods. To fully assess the potential benefits of integrated VFs in urban energy systems, a carbon footprint assessment is needed. This assessment should compare the carbon footprint of a city with integrated VFs for heat and vegetable production with that of a baseline city relying on natural gas for heating and importing food.

Datacentre heat is an alternative LT residual heat source that is commonly studied. Similar to VFs, datacentres consistently generate heat throughout year (Li et al., 2021). Approximately 90% (Oltmanns et al., 2020) to 97% (Lu et al., 2011) of the electrical input of IT equipment in datacentres is converted into heat, compared to around 90% of the electrical inputs of LEDs in VFs (Section 3.2.1.1).

The electrical input of IT equipment in datacentres accounts for 52% (Nadjahi et al., 2018) to 75% (Lu et al., 2011) of the total electricity use, while LEDs in the VF consume about 80% of the electricity inputs (Section 3.2.1.2). This suggests that VFs and datacentres exhibit similar efficiency in terms of residual heat production. However, there are distinctions; datacentres produce heat at 45 °C (Oltmanns et al. 2020) in contrast to the approximately 25 °C produced by VFs (Section 3.2.1.2). Conversely, VFs offer the potential to adapt their operation based on the availability in the electricity grid, while datacentres necessitate non-flexible operation to ensure a secure and reliable environment for IT equipment (Nadjahi et al., 2018).

4.4.1.4 Geographical location

This study focussed on a case study in the Netherlands, characterised by a temperate climate and a high potential for ATES systems. The temperate climate results in relatively high heating demands, making it suitable for VFs to supply their residual heat. The integration of VFs and urban thermal energy systems will, however, offer little value for locations primarily characterised by cooling demands (Graamans, 2021; Section 3.4.1.2). Furthermore, countries with ample heat demand but limited potential for ATES systems will require significantly larger cultivation areas. This is because the heat produced by the VF during the summer cannot be stored for usage in the winter, and is dissipated into the outdoor environment.

4.4.2 Integration of the VF with the electricity grid

4.4.2.1 Alternative lighting concepts

This study presents a significant potential to reduce operational costs associated with artificial lighting in VFs. This potential lies within the adaptation of the lighting recipe to align with the annual average hourly electricity prices and, additionally, adjusting this profile to the day-ahead price fluctuations. These price fluctuations are a direct reflection of the availability of electricity in the grid. The alternative lighting concepts, therefore, enhance the system's flexibility, limiting the mismatch between electricity production and demand.

Five alternative lighting concepts were considered (Fig. 4.4), all of which existing studies have demonstrated no adverse effects on lettuce yields (Velez-Ramirez et

TOC

al., 2011; Chen and Yang, 2018; Kondrateva et al., 2021). In this study, the intermittent light concept including two cycles of 8 h of light d 4 h of darkness (I8/4) achieved the highest annual cost savings of 14% compared to the baseline concept with 16 h of continuous light when using Dutch hourly day-ahead electricity prices for 2022.

Avgoustaki and Xydis (2021) conducted a similar comparison between 16-hours of continuous light and an intermittent lighting concept for lettuce production. The intermittent concept involved three four-hours photoperiods during the cheapest electricity hours, within the remaining 12 hours 10 minutes of light was provided during each hour of darkness. By employing this intermittent concept, annual costs were reduced by 16% to 26%. Although this VF was located in Denmark, its suggests that additional cost-savings might be obtained when considering more granular lighting concepts.

Additionally, this study explored potential cost savings by varying light intensities between 80 and 320 μmol s^{-1} m^{-2} while maintaining a constant daily light integral within each photoperiod. Operating I8/4 in this manner reduced the electricity costs by 11% on January 18th, 2022, and 15% on July 24th, 2022, compared to I8/4 with a constant PPFD of 200 μmol s^{-1} m^{-2}. The chosen light intensity range was based on preliminary findings of Bhuiyan and van Iersel (2021), suggesting that such variations would not adversely affect lettuce crop yields as long as the daily light integral remains constant within the photoperiod.

Pimentel et al. (2023) conducted a similar study on costs savings through light intensity fluctuations within the presented range for lettuce production in Hungary, using a baseline scenario identical to that of our study. Pimentel et al. (2023) obtained annual cost savings of 16%, exceeding the daily savings obtained in this study. This difference may be explained by the focus on Hungary, which has another electricity price profile due its different electricity mix and climate conditions. However, Pimentel et al. (2023) concluded that further research is necessary to understand crop performance under changing photoperiods and alternating light intensities.

Further research is thus needed to explore alternative lighting concepts and the effects of varying light intensities on crop yields, aiming to determine the optimal balance between crop yields and annual electricity costs. These experiments should include various crop types, considering that each crop has specific light intensity and photoperiod requirements, allowing for a broader range of light intensity fluctuations. For instance, Arabzadeh et al. (2023) found that plants with shorter photoperiods achieve higher electricity cost savings due to their increased flexibility in avoiding peak prices. Furthermore, each crop has unique requirements for PPFD, photoperiod, temperature, and relative humidity, which affects the quantity of residual heat produced by the VF.

4.4.2.2 Additional flexibility

To address structural capacity issues in the electricity grid through flexible consumption, a range of users and suppliers should participate (Steman et al., 2021). Load shifting according to the day-ahead hourly electricity prices should thus extend beyond the VF. In winter, the HPs producing mid-temperature heat represent a significant share of the total electricity use. For instance, on January 18th, these HPs represented between 39% and 89% of the hourly peak loads in the centralised configuration, and between 35% and 87% in the decentralised configuration. Flexible operation of these HPs, in addition to the VF, in response to the day-head electricity prices would enhance grid stability even further and results in cost savings for energy consumption.

One way this can be achieved is by using thermal inertia of buildings for short-term flexibility, under the condition that the indoor comfort is maintained (Vandermeulen et al., 2018). This can be achieved by temporarily overheating and underheating buildings, with room temperature variations limited to ±0.5°C (Kensby et al.,2015) and ±2°C (Dreau and Heiselberg, 2016). In this way, short-term distributed storage divided over all buildings connected to the DHN is created (Romanchenko et al., 2018). Hong et al. (2021) shifted HP usage for heating of existing houses in the UK by one to two hours without causing discomfort. Employing these strategies allows for the adjustment of HP operation times, enhancing flexibility during periods of grid congestion or low renewable energy production (Hong et al., 2012; Bos et al., 2022). The use of thermal inertia presents a significant potential to gain flexibility and is cost effective, however, it requires collaboration with the end-users (Kensby et al., 2015; Dreau and Heiselberg, 2016). Future research should quantify the additional flexibility potential and cost savings associated with the use of thermal inertia in both DHN configurations.

In 2025, 10 percent of the vehicles in the Westindische Buurt are projected to be electric (Refa et al., 2019). The city of Amsterdam set the ambitious goal of complete electrification of all vehicles in Amsterdam by 2030. Consequently, the total annual electricity use of the Westindische Buurt will increase with 6% in the decentralised scenario. This growth could lead to severe peak loads if not attuned with the capacity of the electricity grids. To address this challenge, electric vehicles could be used as batteries to store excess electricity during periods of low prices and subsequently release this stored energy during times of scarcity, providing additional flexibility to the grid.

4.5 Conclusion

This study demonstrates that VFs can establish year-round thermal energy balance within the district heat networks of neighbourhoods, whilst concurrently offering flexibility to the electricity grid through adaptive LED operation. Two configurations were designed for the Westindische buurt in the Netherlands that enabled the exchange of residual heat and cold between the buildings and the VF: a 4-pipes DHN with a centralised HP, and a 2-pipes DHN with decentralised HPs. Both configurations included ATES to address timing issues between heat and cold supplies and demands. The decentralised configuration proved to be most effective in terms of VF size, energy storage requirements, and overall energy usage. Furthermore, it enabled individual temperature control to allow for future building renovations. However, spatial integration of individual HPs and required buffer tanks may pose challenges at building level.

In comparison to the baseline systems using natural gas systems for heating and DHW, and air-conditioning for cooling, the decentralised configuration achieved a 15% reduction in energy consumption when including for VF energy usage. A substantial cultivation area of 38,547 m^2 was needed to produce sufficient heat for thermal energy balance. The integration of such area within existing neighbourhood might pose a significant challenge. The cultivation area could be reduced through the inclusion of alternative LT heat sources, e.g., PV-thermal and surface water heat, and through building renovations. The spatial integration of VFs, whether placed on the outskirts of the city or scattered small-scale farms within the city, requires further study.

Due to the substantial cultivation area of the VF, a significant electricity load is added to the neighbourhood. When excluding the VF's energy usage and considering only the energy systems of the decentralised configuration, the total savings increased to 64% compared to the baseline system. This suggests that VFs produce heat inefficiently, however, the ratio between electricity input and LT heat production is comparable to that of datacentres. Additionally, VFs can provide flexibility to the electricity grid, minimising additional loads by attuning its lighting schedules in response to the day-ahead electricity price fluctuations. Implementing intermittent lighting in two cycles of 8 hours of light, followed by 4 hours of darkness, reduced the electricity cost for lighting by 14% in 2022. Further savings could be achieved by varying light intensities between 80 and 320 µmol s^{-1} m^{-2} while maintaining a consistent daily light integral. Although further research is needed to explore the impacts of alternative lighting concepts and the impacts of varying light intensities

on the crop yields, the findings indicate the potential of adaptive LED operation to reduce operational costs for VFs. This is of significant importance given the high electricity prices that limit VF scalability (Sørensen et al., 2016). In near future, flexible operation of LEDs will become even more important as the growing share of renewables in the grid will increase electricity cost fluctuations.

In conclusion, the integration of VFs into energy systems can balance DHNs with residual heat from the farm. Although this requires a substantial VF cultivation area, resulting in significant electricity loads, the use of dynamic LED operation in response to day-ahead electricity pricing can minimise these peaks and enhance stability in the electricity grid. Through these contributions, VFs can play a valuable role within the ongoing energy transition, while simultaneously providing fresh vegetables for the city.

References

Arabzadeh, V., Miettinen, P., Kotilainen, T., Herranen, P., Karakoc, A., Kummu, M., Rautkari, L. 2023. Urban vertical farming with a large wind power share and optimised electricity costs. Appl. Energy, 331, 120416. https://doi.org/10.1016/j.apenergy.2022.120416.

Avgoustaki, D.D., Xydis, G. 2021. Energy cost reduction by shifting electricity demand in indoor vertical farms with artificial lighting. Biosyst. Eng., 211, 219-229. https://doi.org/10.1016/j.biosystemseng.2021.09.006.

Bhuiyan, R., van Iersel., M.W. 2021. Only extreme fluctuations in Light Levels Reduce Lettuce Growth Under Sole Source lighting. Front. Plant Sci., 12. https://doi.org/10.3389/fpls.2021.619973.

Bloemendal, M., Jaxa-Rozen, M., Olsthoorn. T. 2018. Methods for planning of ATES systems. Appl. Energy, 216, 534-557. https://doi.org/10.1016/ j.apenergy.2018.02.068.

Boesten, S., Ivens, W., Dekker, S.C., Eijdems, H. 2019. 5th generation district heating and cooling systems as a solution for renewable urban thermal energy supply. ADGEO, 49, 129-136. https://doi.org/10.5194/adgeo-49-129-2019.

Bos, B., Hoes, P.J., van Prooijen, I., Papachristou, C. 2022. Flexibility deployment of a heating system with heat pump in residential towers. CLIMA 2022 The 14th REHVA HVAC World Congress. https://doi.org/10.34641/clima.2022.295.

Caat, ten, N., Graamans, L., Tenpierik, M., van den Dobbelsteen, A. 2021. Towards Fossil Free Cities: A Supermarket, Greenhouse & Dwelling Integrated Energy System as an Alternative to District Heating: Amsterdam Case Study. Energies, 14, 347. https://doi.org/10.3390/en14020347.

CBS Statline. 2021a. Elektriciteitslevering vanuit het openbare net; woningkenmerken, bewoners, 2019. Opendata.cbs.nl/statline

CBS Statline. 2021b. Energieverbruik particuliere woningen; woningtype, wijken en buurten, 2020. Opendata.cbs.nl/statline

CBS Statline. 2022. Kerncijfers wijken en buurten 2021. Opendata.cbs.nl/statline

Chen, X.L., Yang, Q.C. 2018. Effects of intermittent light exposure with red and blue light emitting diodes on growth and carbohydrate accumulation of lettuce. Sci. Hortic., 234, 220-226. https://doi.org/10.1016/j.scienta.2018.02.055.

Delden, S.H. van, SharathKumar, M., Butturini, M., Graamans, L.J.A., Heuvelink, E., Kacira, M., … Marcelis, L.F.M. 2021. Current status and future challenges in implementing and upscaling vertical farming systems. Nat. Food. https://doi.org/10.1038/s43016-021-00402-w.

Dobbelsteen, A. van den. 2008. 665: Towards closed cycles – New strategy steps inspired by the Cradle to Cradle approach. PLEA 2008- 25th Conference on Passive and Low Energy Architecture, 22-24 October 2008, Dublin, Ireland.

Dobbelsteen, A. van den, Tillie, N., Kürschner, J., Mantel, B., Hakvoort, L. 2011. The Amsterdam Guide to energetic urban planning. Proceedings of Management and Innovation for Sustainable Built Environment Conference, 20-23 June 2011, Amsterdam, Netherlands.

Dobbelsteen, A., van den, Chen, H.C., Dang, M., Voskuilen, P. 2023. From nuisance to nurture – using residual heat for low-temperature local heating systems in cities. 18th SDEWES Conference, 24-29 September 2023, Dubrovnik, Croatia.

Dreau, J. le, Heiselberg, P. 2016. Energy flexibility of residential buildings using short term heat storage in the thermal mass. Energy, 111, 991-1002. DOI: 10.1016/j.energy.2016.05.076.

ENTSOE. 2023. Day Ahead Prices [dataset]. https://transparency.entsoe.eu.

Gemeente Amsterdam. 2023. Aardgasvrij buurten. Maps.amsterdam.nl (retrieved at 18-10-2023).

Gentry, M. 2019. Local heat, local food: Integration vertical hydroponic farming with district heating in Sweden. *Energy, 174, 191-197*. https://doi.org/10.1016/j.energy.2019.02.119.

Gjoka, K., Rismanchi, B., Crawford, R.H. 2023. Fifth-generation district heating and cooling systems: a review of recent advancements and implementation barriers. Renew. Sust. Energ. Rev. 171. https://doi.org/10.1016/j.rser.2022.112997.

Graamans, L.J.A. 2021. Stacked: the building design, systems engineering and performance analysis of plant factories for urban food production [Doctoral dissertation, Delft University of Technology]. A+BE | Architecture and the Built Environment. https://doi.org/10.7480/abe.2021.05.

Hong, J., Kelly, N.J., Richardson, I., Thomson, M. 2023. Assessing heat pumps as flexible load. Sage Journal. https://doi.org/10.1177/0957650912454830.
Jansen, S., Mohammadi, S., Bokel, R. 2021a. Developing a locally balanced energy system for an existing neighbourhood, using the 'Smart Urban Isle' approach. Sustain. Cities and Soc., 64. https://doi.org/10.1016/j.scs.2020.102496.
Jansen, S., Verhoeven, R., Elswijk, M. 2021b. KoWaNet: Technisch handboek koele warmtenetten. www.kowanet.net
Kalantari, F., Tahir, O. M., Joni, R. A., & Fatemi, E. 2017. Opportunities and challenges in sustainability of vertical farming: A review. J. Landsc. Ecol., 11(1), 35-60. https://doi.org/10.1515/jlecol-2017-0016.
Kensby, J., Truschel, A., Dalenback, J.O. 2015. Potential of residential buildings as thermal energy storage in district heating systems – Results from a pilot test. Appl. Energy, 137, 773-781. http://dx.doi.org/10.1016/j.apenergy.2014.07.026.
Klimaatmonitor. 2023. Gemeente Amsterdam: rapportage wijken en buurten. Klimaatmonitor.databank.nl
KNMI. 2023. https://daggegevens.knmi.nl/klimatologie/uurgegevens.
Kondrateva, N., Filatov, D., Bolshin, R., Krasnolutskaya, M., Shishov, A., Ovchukova, S., Mikheev, G. 2021. Determination of the effective operating hours of the intermittent lighting system for growing vegetables. International AgroScience Conference: Earth and Environmental Science, 935. https://dx.doi.org/10.1088/1755-1315/935/1/012004.
Lenhart, J., van Vliet, B., Mol, A.P.J. 2015. New roles for local authorities in a time of climate change: the Rotterdam Energy Approach and Planning as a case of urban symbiosis. J. Clean. Prod., 107, 593-601. https://dx.doi.org/10.1016/j.jclepro.2015.05.026.
Liander. 2019. Innovatieve flexoplossingen om congestie in het net te verminderen. https://www.liander.nl/partners/energietransitie/dynamo-flexmarktontwikkeling/innovatieve-flexoplossingen
Li, H., Hou, J., Hong, T., Ding, Y., Nord, N. 2021. Energy, economic, and environmental analysis of integration of thermal energy storage into district heating systems using waste heat from data centres. Energy, 219. https://doi.org/10.1016/j.energy.2020.119582
Lu, T., Lu, X., Remes, M., Viljanen, M. 2011. Investigation of air management and energy performance in a data center in Finland: Case study. Energy and Build., 43, 12, 3360-3372. https://doi.org/10.1016/j.enbuild.2011.08.034.
Martin, M., Poulikidou, S., Molin, E. 2019. Exploring the environmental performance of urban symbiosis for vertical hydroponic farming. Sustainability (Switserland), 11(23), 6724. https://dx.doi.org/10.3390/su11236724.
Martin, M., Weidner, T., Gullström, C. 2022. Estimating the potential of building integration and regional synergies to improve the environmental performance of urban vertical farming. Front. Sustain. Food Sys. 6, 849304. https://doi.org/10.3389/fsufs.2022.849304.
Meerkerk, M, van., Pothof, I., van Vossen, B. 2022. Criteria voor onderlinge vergelijking van warmtenetten en configuraties. Deltares. Topsectorenergie.nl/kennisbank
MFFBAS. 2023. https://www.mffbas.nl/documenten/.
Nadjahi, C., Louahlia, H., Lemasson, S. 2018. A review of thermal management and innovative cooling strategies for data center. SUSTAIN COMPUT-INFOR., 19, 14-28. https://doi.org/10.1016/j.suscom.2018.05.002.
Oltmanns, J., Sauerwein, D., Dammel, F., Stephan, P., Kuhn, C. 2020. Potential for waste heat utilization of hot-water-cooled data centers: A case study. Sci. Eng., 8(5), 1793-1810. https://doi.org/10.1002/ese3.633.
Pimentel, J., Balazs, L., Friedler, F. 2023. Optimization of vertical farms energy efficiency via multiperiodic graph-theoretical approach. J. Clean. Prod., 416. https://doi.org/10.1016/j.jclepro.2023.137938.
Pulselli, R.M., Broersma, S., Martin, C.L., Keeffe, G., Bastianoni, S., van den Dobbelsteen, A. 2021. Future city visions. The energy transition towards carbon-neutrality: lesson learned from the case of Roeselare, Belgium. Renew. Sust. Energ. Rev., 137. https://doi.org/10.1016/j.rser.2020.110612.
Refa, N., Speel, P., van Bokhoven, P., van der Poel, G., Noordijk, R., de Croon, R. 2019. Waar rijden en laden EV's in de toekomst?: de ontwikkeling van elektrische voertuigen en laadpunten in Nederland t/m 2035. https://elaad.nl.
Romanchenko, D., Kensby, J., Oldenberger, M., Johnsson, F. 2018. Thermal energy storage in district heating: Centralised storage vs. Storage in thermal inertia of buildings. Energy Convers. Manag., 162, 26-38. https://doi.org/10.1016/j.enconman.2018.01.068.

Saini. P., Huang, P., Fiedler, F., Volkova, A., Zhang X. 2023. Techno-economic analysis of a 5th generation district heating system using thermo-hydraulic model: A multi-objective analysis for a case study in heating dominated climate. Energy Build. 296. https://doi.org/10.1016/j.enbuild.2023.113347

Steman, B., Nieuwesteeg, P., Friele, K. 2021. Verbeteren netinpassingen zonne-energieprojecten: netinpassingen zonne-energie. Royal Haskoning BV. Amersfoort, Nederland.

Sørensen, J.C., Kjaer, K.H., Ottosen, C.O., Jørgensen, B.N. 2016. DynaGow – Multi-Objective Optimization for Energy Cost-efficient Control of Supplemental Light in Greenhouses. Proceedings of the 8th International Joint Conference on Computational Intelligence, 1, 41-48. https://doi.org/10.5220/0006047500410048.

Tillie, N., van den Dobbelsteen, A., Doepel, D., de Jager, W., Joubert, M., Mayenburg, D. 2009. REAP Rotterdam Energy Planning Towards CO2-neutral Urban Development. REAP: Rotterdam, The Netherlands.

Vandermeulen, A., van der Heijde, B., Helsen, L. 2018. Controlling district heating and cooling network to unlock flexibility: A review. Energy, 151, 103-115. https://doi.org/10.1016/j/energy.2018.03.034.

Velez-Ramirez. A.I., van Ieperen, W., Vreugdenhil, D., Millenaar, F.F. 2011. Plants under continuous light. Trends in Plant Sci., 16(6), 310-318. https://doi.org/10.1016/j.tplants.2011.02.003.

Venkatachalam, R., Ilamurugu, K. 2009. Crop Physiology: lecture 15 Photoperiodism. http://www.eagri.org/eagri50/PPHY261. Assessed on: 05-09-2023.

Voulis, N., Warnier, M., Brazier, F.M.T. 2018. Understanding spatio-temporal electricity demand at different urban scales: A data-driven approach. Appl. Energy, 230: 1157-1171. https://doi.org/10.1016/j.apenergy.2018.08.121.

Weidner, T., Yang, A., Hamm, M.W. 2021. Energy optimisation of plant factories and greenhouses for different climatic conditions. Energy Convers. Manag. 243, 114336. https://doi.org/10.1016/j.enconman.2021.114336.



Philips Horticulture LED solution by Signify

TOC

5 The carbon footprint of synergetic vertical farms in cities

The content is under review as:
Synergetic Urban Agriculture: life cycle based design of vertical farms integrated with urban energy systems
Blom, T., Jenkins, A., Pulselli, R.M., van den Dobbelsteen, A.A.J.F.
Frontiers in Built Environment and Urban Science doi:-

Supplementary material for this chapter is provided in Appendix D
The datasets of this chapter are available at the repository 4TU Research Data.
DOI: 10.4121/126df61b-3fa8-4a23-8125-7a66494947a8

Chapter 2 defined the baseline carbon footprint of vertical farming systems in comparison to conventional farming systems in the Netherlands. The carbon footprint of vertical farming systems was significantly higher than that of the conventional farming systems. The main contributor to this high footprint was the electricity use, which outweighed the benefits of reduced resource usage from a carbon footprint perspective. Furthermore, the use of artificial light within the enclosed environment of the vertical farm led to the generation of significant quantities of residual heat.

The subsequent chapters delved into the potential to capture and reuse this heat for building heating purposes. Initially this was explored at the building scale in Chapter 3, in addition to the reuse of building's wastewater and nutrient outputs within the vertical farm. Later, in Chapter 4, the residual heat produced by the vertical farm was used to establish equilibrium within local district heat networks. In addition, electricity grid stability was enhanced by employing dynamic LED operation in response to day-ahead hourly electricity prices.

To evaluate the potential benefits of integrating vertical farms with urban energy systems, a carbon footprint assessment is required. This assessment should quantify the environmental performance of these energy synergies between the city and the vertical farm. Therefore, this chapter focusses on the fourth research question of the dissertation:

What carbon reductions can be achieved through the synergetic integration of vertical farms into urban energy systems?

To this end, a carbon footprint assessment was performed for four different scenarios for the city of Amsterdam, ranging from a reference city relying on conventional farming methods and existing energy systems, to a city using residual heat from vertical farms that simultaneously attune their electricity use with to the electricity prices to minimise grid imbalances.

5.1 Introduction

5.1.1 Vertical farming: addressing the global challenges in food production

In the past decade, vertical farming has emerged in response to the global challenges of climate change, increasing food demands, and decreasing availability of arable land and agricultural resources. Vertical farms (VFs) seek to achieve year-round, crop production with high yields, limited land use (Graamans et al., 2018) and minimal resource consumption, including nutrients (Germer et al., 2011), CO_2 for carbon enrichment (Kozai et al., 2006), water, pesticides, and herbicides (Kalantari et al., 2017. This is accomplished through vertical stacking of growth layers within a highly controlled indoor environment utilising hydroponic systems and artificial lighting (Kalantari et al., 2017).

VFs are typically placed within or adjacent to urban areas to minimise food miles (Germer et al., 2011), and to reduce storage and packaging requirements (Kalantari et al., 2017). Due to these benefits, existing literature often advocates VFs as a sustainable food production system (Martin et al., 2023). However, the substantial electricity use for artificial light and climate control systems poses a significant challenge, amounting to approximately 15 kWh of electricity per kg of lettuce produced (Casey et al., 2022; Blom et al., 2022). This results in high operational costs and carbon emissions, which form a limiting factor for scaling up VFs (Sørensen et al., 2016), especially with the high energy prices at the moment of writing.

5.1.2 The carbon footprint of vertical farming

In the last years, several studies, including the study presented in Chapter 2, and those by Casey et al. (2022) and Martin et al. (2023), assessed the carbon footprint of VFs in comparison to conventional farming methods. These carbon footprints included the entire life cycles of both the farm and the crop, from cradle-to-grave, with a focus on lettuce production. The three studies reported varied carbon footprints. Chapter 2 studied a small-scale commercial VF in the Netherlands, while Casey et al. (2022) assessed a container farm in Great Britain, and Martin

et al. (2023) a large-scale commercial farm in Sweden. The carbon footprints were approximately 7.8[1], 8.9, and 1.0 kg $CO_{2\text{-eq}}$ per kg of fresh weight (FW) lettuce respectively.

The main difference in these findings is attributed to the energy system, particularly the grid-mix used for electricity production (Martin et al., 2023). While Sweden uses a great share of hydropower, the grid-mixes of the Netherlands and Great Britain are still significantly based on fossil fuels. Under renewable energy scenarios, all three VFs presented carbon footprints of approximately 1.00 kg $CO_{2\text{-eq}}$ per kg FW of lettuce. However, we found that this footprint remained higher than conventionally produced lettuce (Section 2.4.4, Fig. 2.11), in contrast to Martin et al. (2023) and Casey et al (2022), who did not consider renewable energy for the conventional farming methods.

Within the renewable energy scenario, in all three studies electricity usage still represents the largest share of the carbon footprint. Artificial lighting represented 65% of the total electricity input in the VF studied in Chapter 2. Casey et al. (2022) and Martin et al. (2023) did not provide sufficient data to determine the share of electricity used for artificial lighting, e.g., the Photosynthetic Photon Flux Density (PPFD) and photoperiod. Despite varying conclusions, all three studies agreed that the energy use of VFs needed to be reduced to decrease the carbon footprint of VFs.

5.1.3 Reducing the energy use of vertical farms

Advancements in LED lighting and climate control systems, and the improvement of crop cultivars for vertical production may reduce the energy use of VFs in the near future, and thereby increase their feasibility (Delden et al., 2021). One of the simplest ways to improve the energy efficiency of VFs is by enhancing the molar efficacy of the LEDs. Molar efficacy quantifies the micromoles reaching the crop per Joule of energy used by the LEDs (Pattison et al., 2018). In other words, the ratio between the PPFD and electricity use (Pennisi et al., 2019a). Currently, the maximum molar efficacy of LEDs for VF applications is 3.5 μmol J^{-1} (Weidner et al., 2021). Improving the molar efficacy not only decreases electricity use, but also reduces VF cooling demands, as approximately 90% of the LED electricity input dissipates as latent and sensible heat (Section 3.2.1.1).

1 Blom et al. (2022) polypropylene packaging scenario

A critical factor influencing VF feasibility is the sellable fresh weight (FW) produced per unit of incident light provided to the crop (Carotti et al., 2021; Janssen et al., 2019), also known as the light use efficiency (LUE_{FW}) in g FW mol^{-1}. The VF studied in Chapter 2 reported a LUE_{FW} of 18.7 g FW mol^{-1}; no data on LUE was available for the VFs studied by Casey et al. (2022) and Martin et al. (2023). The highest LUE_{FW} reported in lettuce producing VFs are 25.7 g FW mol^{-1} (Pennisi et al., 2019; 2020), and 44.0 g FW mol^{-1} (Carotti et al., 2021). These LUEs indicate a significant potential to reduce the carbon footprints of VFs. However, the application of these LUEs to the study in Chapter 2 requires further investigation due to the influence of several environmental factors on LUE, such as temperature, relative humidity and CO_2-concentration (Delden et al., 2021).

The use of artificial light in VFs generates significant quantities of residual heat (Blom et al., 2023). Martin et al. (2023) proposed to capture this heat for external usage to reduce the energy use of heating, ventilation, and air conditioning systems in VFs. This potential has been explored on building and urban scales in existing literature (Gentry et al., 2019; Martin et al., 2022) and in Chapter 3 and 4 of this dissertation respectively. In Chapter 4, potential energy savings of 15% were projected for a specific Dutch neighbourhood by implementing a district heat network (DHN) based on VF heat, replacing the current natural gas-based heating system. These savings were 64% when excluding the VF's energy use.

Furthermore, VFs can attune their electricity use to the availability of electricity in the grid. Given the intermittent nature of renewables, achieving a balance between energy generation and usage becomes challenging, leading to fluctuations in the day-ahead hourly electricity prices (Vandermeulen et al., 2018). Chapter 4 investigated alternative lighting schedules to align LED usage with lower electricity costs. This attuned electricity usage can potentially improve the balance between electricity supply and demand in the grid. Although a significant potential to reduce operation costs of LEDs in VFs was found, the study did not assess the impacts of these lighting schemes on the carbon footprint of VFs.

Therefore, Section 4.4.1.4 emphasised the need for a comprehensive carbon footprint assessment to fully evaluate the benefits of integrating VFs into energy systems. This assessment should include both the supply of residual heat delivery to local DHNs, and the effects of aligning lighting schedules with electricity price fluctuations. A crucial aspect of this assessment is a comparison between a city with these synergetically integrated VFs and a reference city that relies on natural gas for heating and crops produced through conventional farming systems.

5.1.4 Research aim

The primary objective of this study is to quantify the potential reduction in carbon emissions through the synergetic integration of VFs with urban energy systems, including the delivery of residual heat to local DHNs and attuning the electricity use according to the availability of renewable energy. The research will analyse different scenarios, comparing the carbon footprint of a synergetic VF that produces both heat and crops for the city with that of a city employing fossil-powered heating systems and conventional crop production systems in the Netherlands. To ensure comprehensive assessment, a diverse range of VFs will be included to incorporate the effects of optimised LUE and molar efficacy. This multifaceted analysis aims to provide insights into the potential environmental benefits of integrating VFs with energy systems, and to assess the potential for VFs in future sustainable food systems.

5.2 Methodology

This study builds upon the three preceding chapters of this dissertation, Chapter 2, 3, and 4. Chapter 2 defined the carbon footprint study of a lettuce-producing VF in comparison to conventional farming systems in the Netherlands. Chapter 3 assessed the potential to use residual heat from a VF for building heating purposes at building scale, and to reuse the building's wastewater and nutrient outputs as input for the VF. The scope of Chapter 3 was extended from the individual building to urban neighbourhood scale in Chapter 4, exploring the potential for VFs to contribute to local district heat networks by generating residual heat. In addition, Chapter 4 studied the potential for VFs to use electricity in a flexible manner, responding to the availability of electricity in the grid.

This fifth chapter aims to quantify the potential carbon savings achieved through this synergetic integration of VFs in an urban environment. To this aim, the study compares four scenarios for the city of Amsterdam, the Netherlands (Fig. 5.1–5.3):

1 Reference city: the vegetables and fruits consumed within the city are produced using conventional farming systems, including open-field farming and greenhouse horticulture. The energy needs are met using existing systems, a mixture of fossil- and renewable-powered systems.

2 VF city: the vegetables and fruits consumed within the city are produced using only VFs, while the energy systems remain unchanged.

3 Synergetic VF city: the vegetables and fruits consumed within the city are produced using only VFs that are in synergy with the city, using the farm's residual heat to replace the existing heating systems in the city.

4 Attuned Synergetic VF city: in addition to scenario III, the VF's electricity usage is attuned to the availability of renewable energy in the grid.

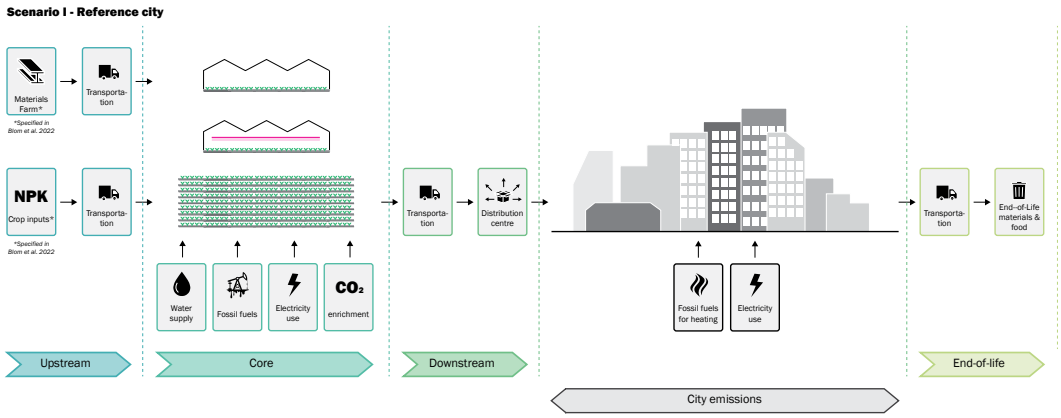

FIG. 5.1 Activities included within the carbon footprint of scenario I 'Reference city'. The vegetables and fruits consumed within the city are produced with conventional farming systems of which both activities within the life cycle of the farm and the crop are included in the carbon footprint. The energy needs of the city are met using existing systems.

TOC

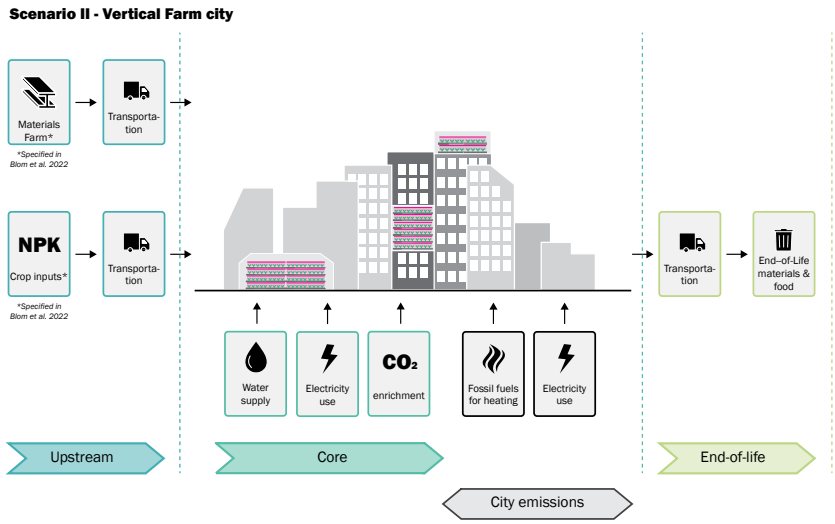

FIG. 5.2 Activities included within the carbon footprint of scenario II 'Vertical farm city'. The vegetables and fruits consumed within the city are produced with vertical farming systems of which both activities within the life cycle of the farm and the crop are included in the carbon footprint. The energy needs of the city are met using existing systems.

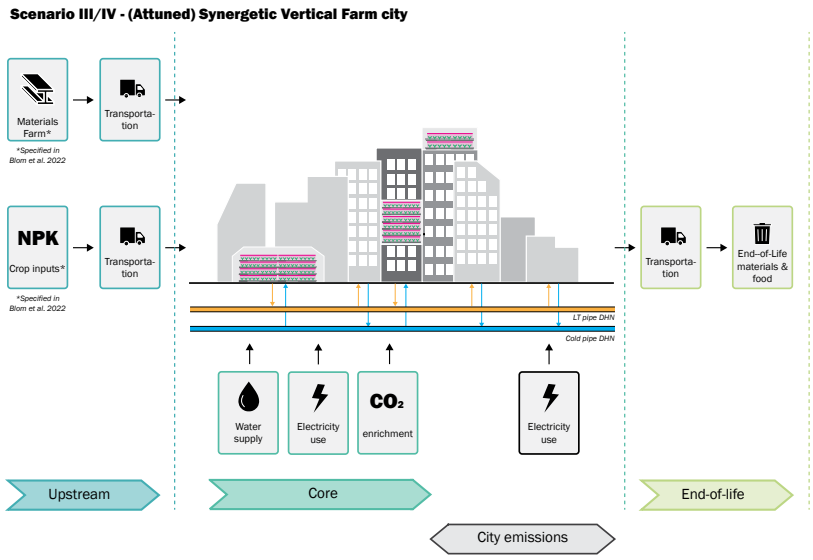

FIG. 5.3 Activities included within the carbon footprint of scenario III 'Synergetic Vertical farm city' and scenario IV 'Attuned Synergetic Vertical farm city'. The vegetables and fruits consumed within the city are produced with synergetic vertical farming systems of which both activities within the life cycle of the farm and the crop are included in the carbon footprint. The residual heat of the vertical farm is used to replace the existing fossil-based eating systems.

TOC

Table 5.1 presents the vegetable and fruit crop groups included in this study, and the recommended intake per person for a healthy diet. A representative crop was selected for each crop group using Righini et al. (2023). The crop groups 'whole grains' and 'legumes' were excluded from this study as these are primarily consumed in processed form. There is also no data available on legume production with conventional farming systems in the Netherlands, as this is not a common practice.

TABLE 5.1 Crop groups and their representative crop as included in this study, including the recommended intake of each crop group as presented by Righini et al. (2023).

Crop group	Representative crop	Recommended intake kg cap^{-1} y^{-1}
Leafy greens	Lettuce	29.20
Starchy vegetables	Potato	47.05
Red vegetables and fruits	Tomato	29.20
Berries	Strawberry	29.20
Other vegetables	Cucumber	29.20

Figure 5.4 presents the five methodological steps to define the carbon footprints of the four different scenarios. The first step calculates the carbon footprint of standalone farming systems producing each of the five selected crops (Table 5.1). This step does not include the supply of residual heat to the city. Step 1a collects the life cycle inventory (LCI) data required to determine the carbon footprints of vegetables and fruits produced with conventional farming systems in the Netherlands (Section 5.2.1).

Step 1b and 1c focus on the LCI data of the VF. The carbon footprints of three VFs are compared in step 1b to obtain a better insight into the carbon footprint of VFs (Section 5.2.1.2). The small-scale commercial farm assessed in Chapter 2 was referred to as VF_{I}. VF_{II} represents the VF described by Pennisi et al. (2019; 2020) which obtained the high LUE of 25.7 g FW mol^{-1}. The study of Carotti et al. (2021) was not included as not all inventory data was available to calculate the carbon footprint. VF_{III} uses the inventory data of the large-scale commercial VF studied by Martin et al. (2022). These three VFs produce lettuce and no full life cycle data was available for the other crops included in the research. Therefore, the life cycle data of the VFs producing lettuce (Step 1b) was used to approximate the carbon footprints of VFs when producing potato, tomato, strawberry and cucumber (Step 1c, Section 5.2.1.3).

Steps 2 to 5 discuss the calculations made to define the carbon emissions of the 4 different scenarios, including the emissions related to vegetable and fruit consumption and energy use in the city. The emissions for food consumption are based on the data collected in step 1, and the average intake per crop group defined in Table 5.1. The GHG emissions of the four scenarios are defined in kg $CO_{2\text{-eq}}$ per capita per year.

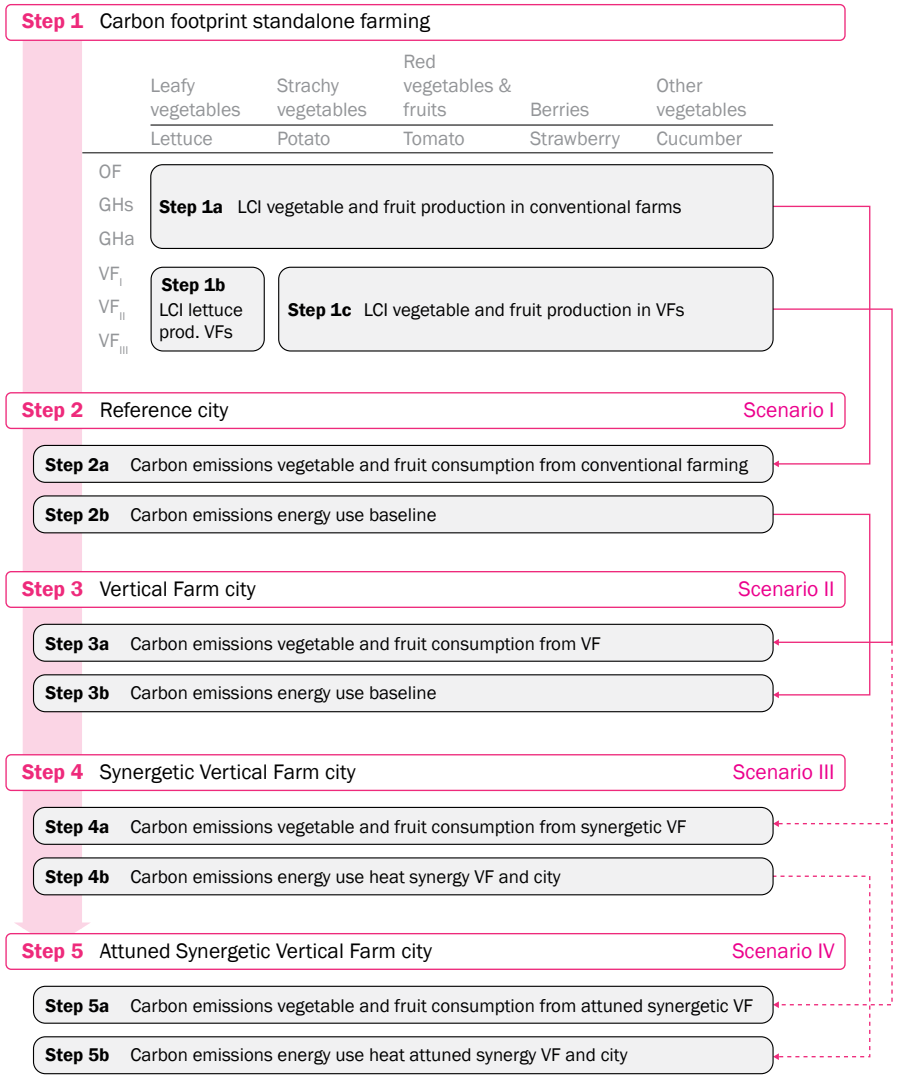

FIG. 5.4 Methodological steps.

TOC

5.2.1 Step 1: Carbon footprint of standalone farming systems

The carbon footprint assessments of standalone farming systems adopt a functional unit of 1 kg of fresh weight (FW) of crop produced, with emissions presented as kg of carbon dioxide equivalent ($CO_{2\text{-eq}}$) per kg FW crop (kg $CO_{2\text{-eq}}$ kg^{-1} FW). This assessment includes the entire life cycle of the farm and the crop, from cradle-to-grave, encompassing upstream, core, downstream and end-of-life emissions.

The activities included within each life cycle stage are detailed according to the system boundaries as described in Chapter 2. In contrast to this previous research, this study excludes seeds and seedlings from upstream emissions in the crop life cycle due to data limitations. In addition, the energy use for cooling in distribution centres was included as part of downstream emissions in the crop life cycle. It was assumed that crops produced in VFs are transported directly to local retailers. Product cooling in distribution centres is estimated at 0.100 kWh per kg product (Marchi et al., 2022).

To define the carbon footprint, the life cycle inventory (LCI) data for each of activity is collected and expressed in terms of the FU, per kg FW produced. The carbon footprint is calculated by multiplying the LCI data for each activity by the emission factor (EF) of that specific activity, measured in kg $CO_{2\text{-eq}}$ per unit of the activity data.

The EFs are assessed by the IPPC GWP100a characterisation method in SimaPro 9.0.0, based on the Ecoinvent 3.6 database. Appendix Table A.2 presents the references of each of the used EFs. Country-specific EFs for the Netherlands are used for energy-related EFs. Notably, the EF for the Dutch grid-mix decreased from 0.475 kg $CO_{2\text{-eq}}$ kWh^{-1} in 2021 (as used in Chapter 2) to 0.337 kg $CO_{2\text{-eq}}$ kWh^{-1} in 2023 (CO_2 emissiefactoren, 2023), reflecting an increased share of renewable energy. The EF of PV panels has improved by 14% due to efficiency increases (Ecoinvent, 2023).

5.2.1.1 Step 1a: LCI of vegetable and fruit production in conventional farms

The conventional farming methods include open-field farming (OF), soil-based greenhouse horticulture (GHs) and greenhouse horticulture using artificial light (GHa). In GHs natural sunlight exclusively serves as source for lighting, while natural light is supplemented with artificial lighting in GHa. Detailed descriptions of the three farming methods can be found in Chapter 2.

TOC

LCI data in Chapter 2 was primarily obtained from the KWIN database for open-field farming in the Netherlands (Schreuder et al., 2009), and the KWIN database for greenhouse horticulture in the Netherlands (Raaphorst and Benniga, 2019). Missing data were based on other literature or assumptions as described in Chapter 2. The KWIN database was also used to establish the carbon footprints of potato, tomato, strawberry, and cucumber production using conventional farming methods. No LCI data were available for open-field tomato and cucumber production, and for potato production in greenhouses. This lack of data is explained by the fact that growing tomatoes and cucumbers crops on open-fields, or potatoes in greenhouses is not a common practice in the Netherlands. The LCI data for lettuce production can be found in Appendix Tables A.3 (OF), A.4 (GHs) and A.5 (GHa), and that of the potato, tomato, strawberry and cucumber crops in Appendix D.1.

5.2.1.2 Step 1: LCI of lettuce production in vertical farms

In Chapter 2, we defined the carbon footprint of a small-scale commercial VF in the Netherlands. The studies conducted by Martin et al. (2023) and Pennisi et al. (2019; 2020) provided sufficient data to calculate the carbon footprint of lettuce producing VFs within system boundaries defined in Section 2.2.2.3. To minimise electricity use by LEDs without affecting yields, we applied the optimised molar efficacy of 3.5 µmol J^{-1} (Weidner et al., 2021) to the lighting systems of each farm.

VF_I

The operational small-scale VF studied in Chapter 2 cultivates lettuce within a stacked hydroponic system using individual plastic growth pots filled with nutrients and water. This VF uses artificial light exclusively, using a PPFD of 140 µmol m^{-2} s^{1} and a 20-hours photoperiod. By using the improved molar efficacy of 3.5 µmol J^{-1}, the electricity use for LEDs was reduced from 9.7 kWh kg^{-1} FW to 4.2 kWh kg^{-1} FW. The controlled environment of the VF had a temperature of 20 ºC and a relative humidity of 72%. The annual total yields were 68.9 kg FW lettuce per square metre of cultivation area.

In this study, we adopted the carbon footprint as defined within the alternative packaging scenario of Chapter 2, where polypropylene bags are used as packaging material. Further details on the VF can be found in Sections 2.2.1.4 and 2.2.3.4. The activity data of VF_I are presented in Appendix A.6.

TOC

VF_{II}

Pennisi et al. (2019a, b, c; 2020) conducted a series of studies on a research facility equipped with six growth chambers. Each of these compartments has a surface of 0.64 m^2, and a volume of 0.4 m^3. The compartments were enclosed with opaque and insulated walls (Pennisi et al., 2019a). Lettuce crops were cultivated in a hermetically sealed plastic pots of 1 L each, resembling a hydroponic deep-water culture system (Pennisi et al., 2019a;c). The crops were harvested 21 days after transplantation, yielding an average weight of 45 g (Pennisi et al., 2019a). The total annual yield was 108 kg FW m^{-2} (Pennisi et al., 2020).

Due to a high planting density of 100 plants per m^2, the fraction of light intercepted by the crops was substantial. As a result, the LUE_{FW} was 25.7 g FW mol^{-1} (Pennisi, 2020). The growth chambers were equipped with LEDs that use a PPFD of 215 µmol m^2 s^{-1}, and a 16-h photoperiod. The indoor conditions were maintained at approximately 24°C, with a relative humidity of 55–70%, and a CO_2 concentration of 450 ppm.

Due to a lack of data, some activity data relating to the crop life cycle stages were based on the assumptions made in Paper 1, including packaging, transportation, and food losses. For comparability, the farm materiality was assumed to be the same as that of Paper 1 per m^2 cultivation area. Appendix D.2 (Table D.4) presents the activity data of VF_{II}.

VF_{III}

Martin et al. (2023) conducted a life cycle assessment of 'Ljusgårda'; a large-scale commercial lettuce producing VF in Sweden. Data were collected throughout the year 2022. The VF produced 520,000 kg of lettuce using vertical growing tubes filled with plugs containing seedlings, peat and coconut coir, and irrigation through a drip system.

Martin et al. (2023) provides highly detailed data on the activities within the life cycle of both the farm and the crop. To increase comparability among the three case studies, we decided to employ the same farm materiality per square metre of cultivation area as in VF_I (Chapter 2). The transportation distances in the different life cycle stages were also taken from VF_I. No details were available on the lighting parameters used in VF_{III}, including photoperiod, PPFD and molar efficacy. It was, therefore, not possible to apply the improved molar efficacy of 3.5 µmol J^{-1}. The activity data used is presented in Appendix D.2 (Table D.5).

5.2.1.3 Step 1c: LCI of vegetable and fruit production in vertical farms

The activity data required to calculate the carbon footprints of VFs producing potatoes, tomatoes, strawberries, and cucumbers have been estimated based on data from the lettuce producing VFs and crop-specific data on electricity use, water consumption, and yields. This data was obtained from Righini et al. (2023) and presented in Table 5.2. The remaining life cycle inventory data required to define the carbon emissions in the crop life cycle were based on the VFs in step 2a, assuming the same inputs per kg of FW produced. The farm life cycle data were derived from the VF_I, assuming the identical materiality per m^2 of cultivation area. Appendix D.3 presents the activity data used for potato, tomato, strawberry, and cucumber production in VFs per kg FW in VFs.

TABLE 5.2 Life Cycle Inventory of the production of potato, tomato, strawberry, and cucumber in VFs based on Righini et al. (2023)

Crop group		Starchy vegetables	Red vegetables and fruits	Berries	Other vegetables
Representative crop	Unit	Potato	Tomato	Strawberry	Cucumber
Yields (FW)	kg m^{-2} y^{-1}	32.70	36.50	10.30	77.00
LUE	g FW mol^{-1}	0.24	0.23	0.29	0.23
PPFD	µmol m^{-2} s^{-1}	917	697	320	600
Photoperiod	h	12	14	14	17
Electricity use LED*	kWh kg^{-1} FW	35.09	27.88	45.36	13.81
Electricity use climate conditioning and other equipment	kWh kg^{-1} FW	10.24	8.13	13.17	4.03
Water use	L kg^{-1} FW	1.59	1.37	2.50	1.82

**Calculated with a molar efficacy of 3.5 µmol J^{-1}*

TOC

5.2.2 Step 2: Scenario I - Reference city

5.2.2.1 Step 2a: Carbon emissions of vegetable and fruit consumption

In Scenario I 'Reference City' (Fig. 5.1) the vegetables and fruits consumed per capita are produced using domestic conventional farming systems, which includes a mixture of open-field farming and greenhouse horticulture. The carbon footprints for these crops were calculated according to step 1a. For multiple conventional farming methods applicable to crops, it was assumed that the annual production was evenly distributed across these farming methods, using the average carbon emissions of the conventional farming methods for that specific crop.

5.2.2.2 Step 2b: Carbon emissions of energy use

The study is limited to the built environment, including the energy use of households, commercial services, and public services. In 2022, the total energy usage in the built environment of Amsterdam was 9,800,000 MWh (Table 5.3). In total, 40% of this energy use was electricity, the remaining energy use primarily derived from natural gas for heating. Additionally, some residential buildings were heated using district heating. These data are shown in Table 5.3, whilst the references of the EFs used to calculate the associated GHG emissions of the city of Amsterdam are presented in Appendix A.2.

TABLE 5.3 Energy use of the City of Amsterdam in 2022 (CBS, 2018a,b; Klimaatmonitor, 2023)

	Unit	Residential	Non-residential	Total
Natural gas	m^3	390,047,393	199,936,809	589,984,202
City heating	GJ	2,361,000	0	2,361,000
Electricity	MWh	940,278	3,016,944	3,957,222
Total energy	MWh	5,025,278	4,774,722	9,800,000

5.2.3 Step 3: Scenario II - Vertical Farm city

The vegetables and fruits consumed in scenario II are produced using only VFs (Fig. 5.2). The corresponding GHG emissions are calculated using the LCI data collected in step 1b and 1c. The energy use of the city of Amsterdam in scenario II is the same as in scenario I.

5.2.4 Step 4: Scenario III - Synergetic Vertical Farm city

5.2.4.1 Step 4a: Carbon emissions of vegetable and fruit consumption

In scenario III (Fig. 5.3), the vegetables and fruits are produced using only VFs that are in synergy with the city; i.e., the residual heat of these VFs is used for building heating using DHNs. The GHG emissions related to vegetable and fruit consumption of the inhabitants is calculated using the LCI data of step 1b and 1c. To enable heat exchange with the district heat network, the cooling and dehumidification systems in the VF will be adapted, changing the electricity use of the VFs (step 4b).

5.2.4.2 Step 4b: Carbon emissions of energy use

Decentralised energy system configuration

As outlined in the introduction, 90% of the electrical inputs in VFs must be cooled away as latent and sensible heat. Traditionally, this heat is expelled to the outside. An urban energy system that captures this waste heat from the VF and supplies it to local DHNs for building heating purposes (Fig. 5.5) was designed in Chapter 4. In this chapter, we refer to such a VF as a 'synergetic VF'. This synergy operates bidirectionally: the VF supplies heat to the DHN and utilises the cold from these networks to meet its cooling demands.

TOC

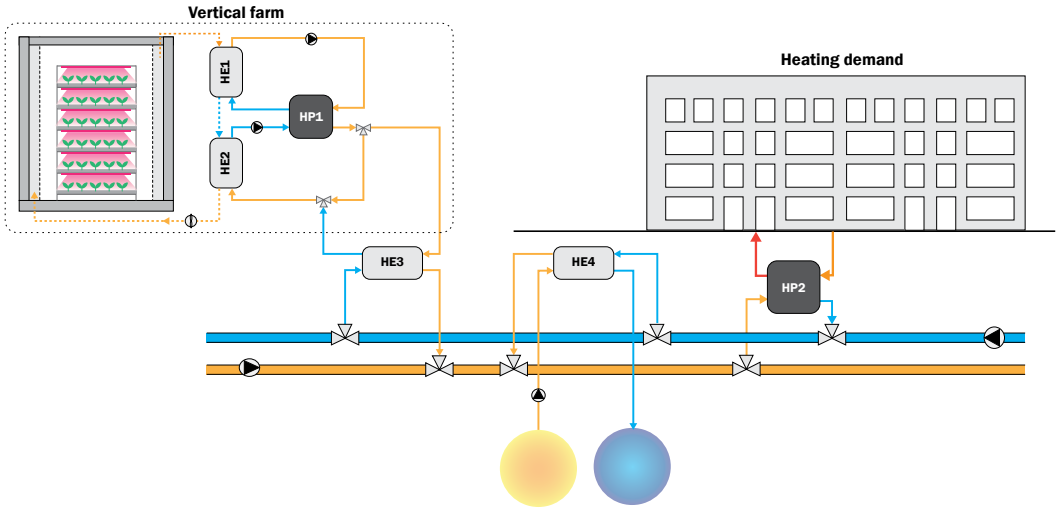

FIG. 5.5 Cooling and dehumidification system of the VF, and the energy systems required to supply the VF heat to the buildings.

Figure 5.5 schematically illustrates the energy systems required to facilitate the exchange of heat and cold between the VF and city. Firstly, the VF is cooled and dehumidified using a heat pump (HP1, Fig. 5.5). In this process, excess heat is generated, which is supplied to an ultra-low temperature DHN of approximately 20-30 °C, using a heat exchanger (HE3, Fig. 5.5). Additional details on the cooling and dehumidification system of the VF can be found in Sections 3.2.1.2 and 4.2.3. The heat in the DHN is supplied to individual heat pumps (HPs) at the building scale (HP2, Fig. 5.5). These HPs increase the ultra-low temperature VF heat to the temperature required for building heating: 40 °C for well-insulated buildings, 70 °C for buildings with lower energy performance, 90 °C for buildings with poor energy performance, and 55 °C for domestic hot water. In 2022, 67% of the buildings with an officially registered energy label in Amsterdam had energy label B or lower (RVO, 2022). Therefore, we used 70 °C space heating for all buildings for simplification. During this heating process, cold is generated by the individual HPs at the building scale, which is used for cooling by the VF. Finally, an aquifer thermal energy storage (ATES) system is connected to the DHN to address daily and seasonal timing issues between heat and cold demands and supplies. Further details concerning this energy system can be found in Section 4.3.2.2.

VF heat delivered to buildings

The amount of heat delivered to the building's heating systems depends on the waste heat produced by the VF, the losses within the DHN, and the coefficient of performance (COP) of the individual HPs. Given that 90% of the electrical inputs of the LEDs converts into sensible and latent heat (Section 3.2.1.1), the amount of waste heat produced was approximated for each crop type using Table 5.2. For simplification, we assumed that the indoor climate conditions for each crop aligns with that of Chapter 3 and 4, i.e., air supply temperature of 24 °C and relative humidity of 76%. When using the cooling and dehumidification system as specified in Section 3.2.1.2, every kWh of electricity used by the LEDs results in 1.4 kWh of low-temperature residual heat.

In a DHN, approximately 15% of the heat is lost through the associated infrastructures (Section 4.2.5). The individual HPs upgrade the remaining heat to the desired temperature. The quantity of heat delivered to the building heating systems ($Q_{supplied}$) is determined by:

$$Q_{supplied} = Q_{source} + (Q_{source} / COP) \quad \text{(Eq. 5.1)}$$

In which Q_{source} is the heat supplied by the DHN to the individual HPs in kWh, and the COP of the HPs is approximately 2.8 for the production of 70 °C space heating and 55 °C domestic hot water (Section 4.3.2.2).

The heat from the synergetic VF replaces the need for gas heating in scenarios III and IV (Fig. 5.3). The total heating demands were calculated using the energy use of Amsterdam in Table 5.3. Approximately 2% of the household natural gas consumption is used for cooking (CBS, 2018c), and a boiler efficiency of 90% was assumed. For the heating demands of the residences heated by the existing DHN in Amsterdam, the average residential natural gas use of 880 m^3 annually (CBS, 2023a) was extrapolated to the number of residences heated by city heating.

Energy use of the decentralised energy system

In order to calculate the GHG emissions associated with the energy system using VF heat, the electrical inputs of the energy system were calculated. These include the energy use of the decentralised HPs with a COP of 2.8, and the fans and pumps within the DHN and ATES system. The electricity use of the pumps were calculated using methods from Appendix B.2.6.2 and C.3.3. The energy use by the cooling and dehumidification system of the VF were calculated according to Appendix B.2, which replaces the emissions from climate control systems in scenario III and IV.

5.2.5 Step 5: Scenario IV - Attuned Synergetic Vertical Farm city

Scenario IV builds upon scenario III (Fig. 5.3). It uses residual heat from VFs to replace existing heating systems. In addition, scenario IV aligns the electricity usage for artificial light with the availability of renewable energy in the grid. As the electricity use by artificial light is the same for each lighting concept considered in this study, the quantity of residual heat produced remains constant. Any temporal differences between heat demand and supply are addressed through the ATES system (Section 5.2.4.2).

5.2.5.1 Alternative operation of the LEDs

The potential to reduce electricity cost for lettuce production in VFs by employing various lighting concepts was analysed in Chapter 4. In the baseline scenario of this study, LED lights operated under continuous light with a 16-hour photoperiod with a PPFD of 200 µmol m^{-2} s^{-1}. The photoperiod aligned with working hours, operating from 06:00 to 22:00. In paper 3 we found that shifting the continuous 16-h photoperiod to between 21:00 and 13:00 (C16/8) or employing two intermittent cycles of 8-h of light and 4-h of darkness (I8/4) with lights on from 04.00 to 08.00 and from 16.00 to 20.00, reduced the costs by 11% and 14%, respectively, when using the hourly day-ahead electricity prices of 2022. The lettuce yields were not affected by these strategies (Chen and Yang, 2018; Kondrateva et al., 2021). In the study presented here, we explored the potential to reduce GHG emissions by employing these three LED concepts.

The GHG emissions of these alternative LED operations were approximated for the 1st and 15th day of each month in 2022 by establishing the hourly EFs of the Dutch electricity grid-mix. Data on hourly electricity production per generation method was obtained from ENTSOE (2023). For simplification, we categorised generation methods into solar power, wind power, and 'other generation methods'. As no complete solar energy data is available in ENTSOE (2023), data from 'energieopwek.nl' was used. In 2022, 14% of the electricity was generated by PV panels, and 18% by wind turbines on sea and land (CBS, 2023b). The average EF of the 'other generation methods' was calculated using the EF for electricity in the Netherlands, along with the EFs for solar and wind energy (Appendix A.2). By combining these EFs with their respective hourly contributions, the hourly EFs for the Dutch electricity grid-mix was calculated for the 1st and 15th day of each month in 2022.

TOC

5.2.5.2 Flexible operation of the LEDs

Chapter 4 also explored the potential for electricity cost reduction in lettuce producing VFs by varying light intensities between 80 and 320 µmol s^{-1} m^{-2}. The photons received by the plants during each photoperiod remained constant to maintain yields (Bhuiyan and van Iersel, 2021). This flexible LED concept was applied to baseline, I8/4, and C16/8 lighting strategies, and the potential CO_2 reduction was calculated using the hourly EFs as defined in Section 5.2.5.1.

5.3 Results

5.3.1 Lettuce production in standalone vertical farming systems

The carbon footprints of the three VFs producing lettuce ranged between 3.087 and 3.750 kg $CO_{2\text{-eq}}$ kg^{-1} FW (Fig. 5.6 and Appendix Table D.7). The electricity use in VF_I, VF_{II} and VF_{III} accounted for 84%, 68%, and 89% of the total footprint, respectively.

We selected VF_I for the remainder of the study, as the electricity use represents a higher share of the overall footprint than VF_{II}, indicating a higher potential for reduction in scenario's III and IV. VF_{III} was not selected due to a lack of data on the share of lighting in the total electricity use.

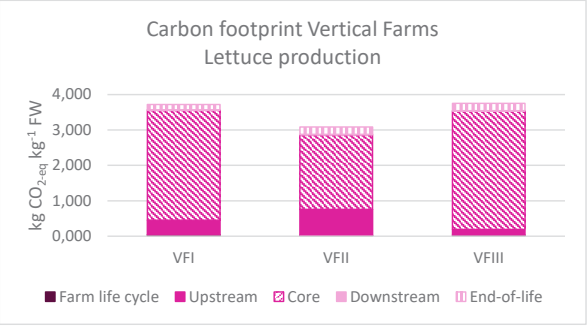

FIG. 5.6 Carbon footprints of three vertical farming systems producing lettuce.

TOC

5.3.2 Vegetable and fruit production in conventional and vertical farming systems

Figure 5.7 presents the carbon footprints per kg FW of each crop type when produced with open-field farming (OF), soil-based greenhouse horticulture (GHs), greenhouse horticulture using artificial light (GHa), and VF_I. The emissions of each activity within the life cycle of the crop and farm are provided in Appendix D.4 (Tables D.8 and D.9). The carbon footprints of the crop produced in VF_I are significantly higher than those produced by conventional farming systems. The carbon footprints of potato, tomato, lettuce, strawberry, and cucumber production in VF_I were respectively 50, 7, 4, 5, and 6 times greater than the average footprint of the conventional methods (Fig. 5.7, yellow bar). This is primarily explained by the electricity use, which represents 97%, 95%, 84%, 97%, and 89% of the carbon footprints of potato, tomato, lettuce, strawberry, and cucumber, respectively.

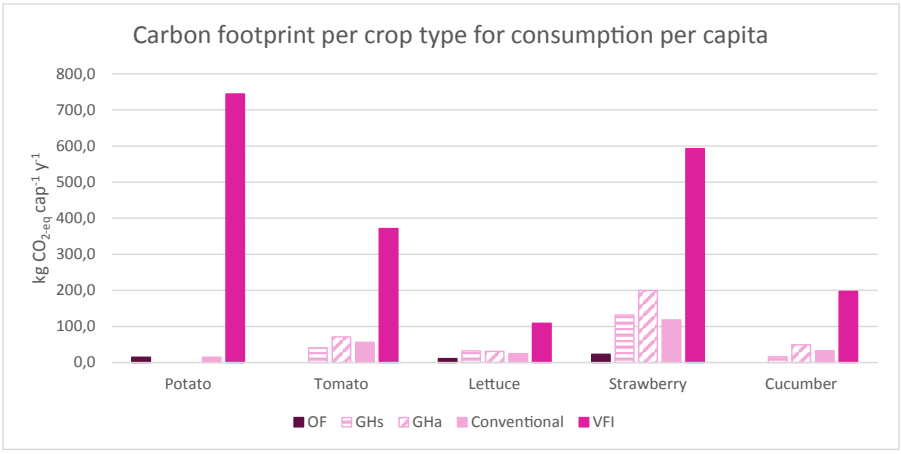

FIG. 5.7 Carbon footprints of potatoes, tomatoes, lettuce, strawberries, and cucumbers per kg FW when produced within open-field farming systems (OF), soil-based greenhouse horticulture (GHs), greenhouse horticulture using artificial light (GHa), and standalone vertical farming systems (VFI). 'Conventional' represents the average footprint of OF, GHs, and GHa production systems.

TOC

5.3.3 Carbon footprint for vegetable and fruit consumption and urban energy use

The carbon footprint of the Reference city (Scenario I), using the baseline energy systems and conventional farming systems for crop production, was 3115 kg $CO_{2\text{-}eq}$ per capita annually. This carbon footprint is 36% lower than that of the VF city (scenario II), i.e., 4883 kg $CO_{2\text{-}eq}$ per capita annually, where crops were produced with standalone VFs (Fig. 5.8). When replacing natural gas by residual heat produced within the VF (scenario III), the carbon footprint of scenario II was reduced by 13%, i.e., the Synergetic VF city had a carbon footprint of 4244 kg $CO_{2\text{-}eq}$ cap^{-1} y^{-1}.

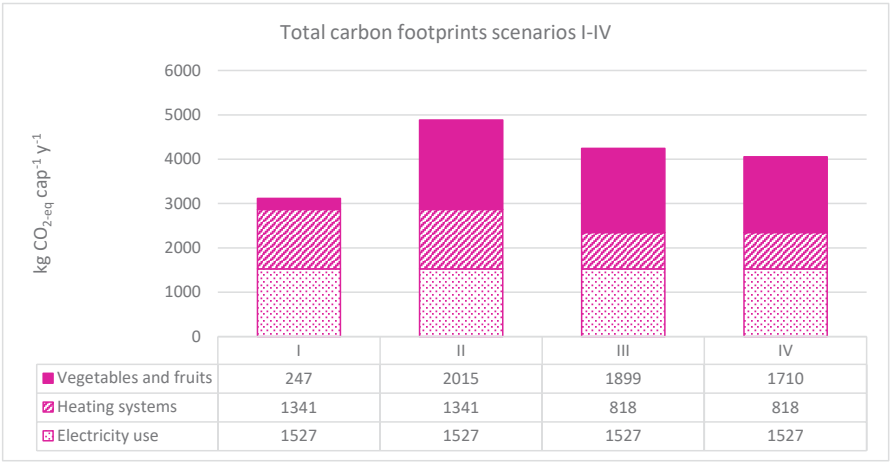

	I	II	III	IV
Vegetables and fruits	247	2015	1899	1710
Heating systems	1341	1341	818	818
Electricity use	1527	1527	1527	1527

FIG. 5.8 Carbon footprints per capita for the city of Amsterdam, including the energy use and the consumption of vegetables and fruits with scenario I-III.

The production of vegetables and fruits in a synergetic VF connected to the decentralised energy system resulted in the supply of 6.5 MWh cap^{-1} y^{-1} of mid-temperature heat energy to the buildings (Fig. 5.5). To enable the heat exchange between the VF and city, 5.3 MWh cap^{-1} y^{-1} of electricity is used for lighting and climate system of the VF, and 2.4 MWh cap^{-1} y^{-1} for the decentralised HPs and pumps within the DHN and ATES system (Table 5.4). The synergetic VFs in scenarios III and IV had an overproduction of 0.7 MWh cap^{-1} y^{-1} heat energy. This heat is exhausted into the atmosphere.

TOC

TABLE 5.4 The quantity of mid-temperature heat supplied to buildings using residual heat of VFs that produce different crops, and the energy use by the VF and decentralised energy system.

		Potato	Tomato	Lettuce	Strawberry	Cucumber	Total
Recommended consumption	kg cap^{-1} y^{-1}	47.1	29.2	29.2	29.2	29.2	163.9
Heat supply buildings	kWh_e kg FW^{-1}	56	38	2	72	22	
	kWh_{th} cap^{-1} y^{-1}	2629	1111	46	2109	642	6537
Electricity use LEDs VF	kWh_e kg FW^{-1}	35	24	1	45	14	
	kWh_e cap^{-1} y^{-1}	1651	698	29	1324	403	4106
Electricity use climate systems VF	kWh_e kg FW^{-1}	11	7	0	14	4	
	kWh_e cap^{-1} y^{-1}	495	209	9	397	121	1230
Electricity use decentralised HPs	kWh_e kg FW^{-1}	20	13	1	25	8	
	kWh_e cap^{-1} y^{-1}	925	391	16	742	226	2300
Electricity use pumps DHN and ATES	kWh_e kg FW^{-1}	1	1	0	1	0	
	kWh_e cap^{-1} y^{-1}	51	22	1	41	11	127
Total electricity use VF	kWh_e kg FW^{-1}	46	31	1	59	18	
	kWh_e cap^{-1} y^{-1}	2146	907	38	1721	524	5336
Total electricity use energy system	kWh_e kg FW^{-1}	21	14	1	27	8	
	kWh_e cap^{-1} y^{-1}	976	413	17	783	238	2428
Total energy use	kWh_e kg FW^{-1}	66	45	2	86	26	
	kWh_e cap^{-1} y^{-1}	3122	1319	55	2504	763	7764

To assess the potential carbon savings by scenario IV, the Attuned Synergetic VF city, lettuce crops were used as a reference. Three different lighting strategies were included for lettuce production: the baseline 16-h photoperiod between 06:00 and 22:00, C16/8, and I8/4. Under stable lighting intensity, the average carbon emissions for lighting increased from 0.30 kg $CO_{2\text{-eq}}$ per square meter cultivation area of a lettuce cultivating VF per day in the baseline strategy to 0.31 and 0.34 kg $CO_{2\text{-eq}}$ m^{-2} d^{-1} in concept C16/8 and I8/4, respectively.

The application of fluctuation lighting intensities to the baseline operation, ranging from 80 to 320 µmol s^{-1} m^{-2} while maintaining the total daily light integral, resulted in carbon emissions of 0.26 kg $CO_{2\text{-eq}}$ m^{-2} d^{-1}, representing a reduction of 13% in carbon emissions for lighting. However, further investigation into the impacts of alternative

and fluctuation lighting concepts on crop yields for different crops is needed, and savings will differ depending on the crop's photoperiod and PPFD. Nevertheless, the 13% reduction in carbon emissions for lighting was included to underscore the potential of fluctuating lighting intensities to reduce the carbon emissions of vertical farming. As a result, the total carbon emission in Scenario IV reduced by 5% compared to Scenario III, and the emissions for vegetable and fruit production by 10%.

5.4 Discussion

The following section discusses the results in more detail and in relation to other studies, identifies research limitations, and makes suggestions for further research. Section 5.4.1 discusses the effects of a high LUE and the electricity grid-mix on the carbon footprint of lettuce producing VFs. Section 5.4.2 focusses on the carbon footprint of other types of vegetables and fruits produced in VFs, and Section 5.4.3 on the carbon implications of integrating VFs with urban energy systems. Finally, Section 5.4.4 discusses sustainability indicators for VF systems other than the carbon footprint.

5.4.1 Lettuce production in standalone vertical farming

5.4.1.1 Light Use Efficiency

Given that the electricity use in VFs constitutes the largest share of the overall carbon footprint, enhancing LUE offers a significant potential to reduce the footprint. The LUE_{FW} of VF_I and VF_{II} were 18.7 g FW mol^{-1} (Section 2.4.5) and 25.7 g FW mol^{-1} (Pennisi et al., 2019; 2020), respectively. No data was available on the LUE of VF_{III}. As expected, the GHG emissions for electricity use were significantly smaller for VF_{II} compared to VF_I, with values of 2.105 kg $CO_{2\text{-eq}}$ kg^{-1} FW and 3.110 kg $CO_{2\text{-eq}}$ kg^{-1} FW, respectively (Appendix D.7).

The LUE is influenced by various environmental factors within the VF, including temperature, relative humidity, CO_2 concentration, crop density, and growth method (Delden et al., 2021). Electricity use in VF_I, VF_{II}, and VF_{III} accounted for 84%, 68%,

TOC

and 89% of the total carbon footprints of 3.721, 3.087 and 3.750 kg $CO_{2\text{-eq}}$ kg^{1} FW, respectively. The high impact of activities other than electricity use in VF_{II} can be attributed to the extensive use of growth materials. VF_{II} uses individual growth pots similar to VF_{I}. However, each crop produced has a significantly smaller fresh weight. These growth materials resulted in GHG emission of 0.596 kg $CO_{2\text{-eq}}$ kg^{-1} FW and increased the emissions for transportation and end-of-life processes.

The carbon footprint of VF_{II} draws attention to the potential to significantly reduce the carbon footprint of VFs by sufficiently increasing the LUE. However, consideration must be given to the impacts of crop inputs and material usage on the carbon footprint to avoid emissions that can potentially offset the carbon savings achieved by the optimising the LUE. Further research aimed at improving LUE holds the promise for even greater reductions in the carbon footprint of VFs. Carotti et al. (2021) obtained the highest LUE_{FW} in existing literature of 44.0 g FW mol^{-1} (Carotti et al., 2021), indicating an even smaller carbon footprint. However, the absence of sufficient LCI data made it impossible to define the carbon footprint of this VF.

5.4.1.2 Electricity grid-mix

The carbon emissions from electricity as calculated for VF_{I} and VF_{III} differed significantly from their original studies presented in Chapter 2 and Martin et al. (2023). This discrepancy is not only attributed to the increased LED molar efficacy of 3.5 µmol J^{-1}, but also to the Dutch EF for electricity. This EF has seen a 30% decrease between 2021 and 2023 due to an increased proportion of renewable electricity production, in contrast to the EF employed in Chapter 2. Consequently, the emissions from electricity usage were reduced from 6.963 kg $CO_{2\text{-eq}}$ kg^{-1} FW to 3.344 kg $CO_{2\text{-eq}}$ kg^{-1} FW in VF_{I}.

In the case of VF_{III}, Martin et al. (2023) did not provide specific details on the share of electricity used for lighting, making it impossible to apply the molar efficacy of 3.5 µmol J^{-1}. The total carbon footprint reported by Martin et al. (2023) was approximately 1.0 kg $CO_{2\text{-eq}}$ kg^{-1} FW, while this study calculated a value of 3.75 kg $CO_{2\text{-eq}}$ kg^{-1} FW. This difference can partly be attributed to the modification of farm materiality, transportation distances, and packaging materials to align with that of VF_{I}. However, the 89% contribution of electricity use to the carbon footprint of VF_{III} suggests that the primary factor driving the increased carbon footprint is the difference in EF for electricity usage between the Netherlands and Sweden, with Sweden relying heavily on hydropower.

If the electricity use of the VF was fully generated with photovoltaic panels, the emissions in scenario III 'Synergetic VF city' would be reduced by 34% to 2814 kg $CO_{2\text{-eq}}$ cap^{-1} y^{-1}. In this scenario, the carbon footprint per capita was lower than that of the 'Reference city'. With an energy use of 5366 kWh cap^{-1} y^{-1} for the climate systems of the VF, a total of 26.8 m^2 cap^{-1} of south facing PV panels under optimal angle of 36° would be needed to cover these demands (calculated according to methods presented in Appendix A.5.3), a significant area considering the unit per capita[2].

These findings indicate the potential to reduce the carbon footprint of VFs through the transition to renewable energy sources. However, it is essential to acknowledge that this transition may also diminish the carbon emissions, albeit not as significant, of the conventional farming methods as presented in Chapter 2 and may not necessarily result in lower GHG emissions for VFs than conventional methods. Furthermore, it suggests that the geographical location of a VF heavily affects its sustainability in terms of carbon footprint.

5.4.2 Vegetable and fruit production in vertical farms

Due to the unavailability of LCI data of VFs producing potatoes, tomatoes, strawberries, and cucumbers, the carbon footprints for these crops were approximated using data from VF_I and Righini et al. (2023). The latter included yields, electricity use, and water use. The molar efficacy of the LEDs was adjusted to 3.5 µmol J^{-1}. Although this approach might not perfectly resemble the LCI data, it provides a reasonable estimation of the carbon footprints, given that electricity use accounted for 97%, 95%, 97% and 89% of the total carbon footprint of potato-, tomato-, strawberry-, and cucumber-producing VFs, respectively.

The results showed that potato cultivation is currently not suitable for VF, as the carbon footprint was 50 times higher than that of potatoes produced on open-field farms in the Netherlands. The carbon footprints of lettuce, tomato, strawberry, and cucumber produced in VFs were 4.4, 6.6, 5.0, and 6.0 times greater than those produced using conventional production systems. This indicates that potato cultivation is currently not suitable for VFs.

2 Mind, in the northern hemisphere, solely south-oriented panels primarily produce electricity in the middle of the day, and most in summertime. Panels more diversely oriented would generate less electricity per m^2 of panel, but create a renewable production better spread over the day and seasons.

TOC

The differences in the carbon footprints of conventional farms and VFs are clearly visible in the carbon footprints per capita of the city. The carbon footprint of the Reference city (scenario I) was 36% smaller than the footprint of the VF city (scenario II), highlighting the significant environmental impacts when using VFs solely to replace conventional farming systems. When excluding potato production from the study, the Reference city had a 27% smaller carbon footprint than the VF city.

5.4.3 Synergetic integration of vertical farms with urban energy systems

5.4.3.1 Heat production for the built environment

The Synergetic VF city (scenario III) reduced the carbon emissions for city heating systems by 64% compared to the VF city (scenario II). This reduction was achieved by replacing natural gas with residual heat from VFs (Fig. 5.5). The total carbon footprint of scenario III amounted to 4244 kg $CO_{2\text{-eq}}$ cap^{-1} y^{-1}, including emissions from fruit and vegetable production in the VF, city electricity usage, and city heating systems. This total carbon footprint per capita was 13% lower than that of the VF city (scenario II).

When excluding potato production (Section 4.2), the reduction of the total carbon footprint in scenario III was limited to 5% compared to scenario II. This diminished reduction was attributed to the decreased production of residual heat by the exclusion of potatoes. As a result, 67% of the heating demands per capita were met with VF heat.

These findings indicate a significant potential to reduce the carbon footprint of VFs by using their residual heat for building heating, particularly when the VF fully meet the heating demands of a specific area. However, in comparison with the Reference city (scenario I), the total carbon footprint of the Synergetic VF city was 27% higher when including potato production, and 21% when excluding potato production. This suggests that, despite the supply of residual heat to buildings, VFs currently cannot sufficiently mitigate carbon emissions of cities due to their high electricity requirements for crop production compared to conventional farming methods.

The Synergetic VF presented in Chapter 4 decreased the annual energy consumption of the Westindische Buurt, a residential neighbourhood in Amsterdam, by 15%, accounting for the energy use of the VF. The Westindische Buurt uses VF residual heat for mid-temperature space heating and domestic hot water production through a decentralised energy system configuration. In contrast to the present study, Chapter 4 also includes residual heat from other functions in the neighbourhood beside VF heat, e.g., heat from cooling processes in supermarkets. Through the exchange of heat and cold among existing neighbourhood functions, the net heat demands of this area were significantly reduced. This approach minimising the required VF cultivation area to achieve thermal energy balance in the neighbourhood.

5.4.3.2 Attuned electricity usage of LEDs

The operation of LEDs in two intermittent cycles of 8-hour light and 4-hour dark (I8/4) a day could have reduced the annual electricity costs in a lettuce producing VF in the Netherlands by 14% in 2022 in comparison to a 16-hour photoperiod operated between 06:00 and 22:00 (Paper 3). Within both concepts the daily light integral remains the same, and the savings were obtained by attuning the light period to the hourly electricity prices. As these electricity prices reflect the (dis) balances between electricity generation and demands in the grid, it was suggested that operating the LEDs accordingly would contribute to a better-balanced electricity grid in addition to saving electricity costs for lighting.

However, this study showed that the adoption of light concept I8/4 also results in a 7% increase in carbon emissions for lighting compared to the baseline 16-hour photoperiod. This increase is attributed to the use of electricity during more cost-effective periods when electricity is abundant (I8/4) as opposed to the continuous 16-hour electricity usage between 06.00 and 22.00 when solar production energy peaks. The hourly electricity prices present two peaks around 06:00 and 17:00. Consequently, it is more cost effective to use electricity around noon and midnight. However, as the energy systems relies heavily on fossil fuels at night, attuning LEDs to address grid balancing issues has unintentionally elevated the carbon footprint of VFs. This raises a crucial dilemma regarding the primary focus of attuned electricity usage: should the emphasis lie in minimising (dis)balances in the electricity grid to avoid grid congestion, or in reducing carbon emissions to combat climate change?

When focussing on the flexible operation of LEDs with a 16-h photoperiod, i.e., adjusting light intensity based on hourly variations in carbon emissions of the electricity mix, emissions for lighting in a lettuce producing VF were reduced by 13% compared to fixed 16-h operation. However, further research on the effects of fluctuating light intensities on different crop types is necessary. Nevertheless, these savings were incorporated in the Attuned Synergetic VF City (scenario IV) as they underscore the potential for reduced VF emissions by attuning lighting intensities according to the availability of renewable energy in the grid.

5.4.4 Other sustainability indicators

In addition to the carbon footprint, several other life cycle indicators play a role in assessing the overall sustainability of VFs. Martin et al. (2023) evaluated the production of lettuces in VF in comparison to conventionally produced domestic and imported lettuces, considering indicators such as GHG emissions, land use, fresh water ecotoxicity, freshwater eutrophication, and water use.

VF significantly reduces land usage by increasing yields per cultivation area. The stacking of cultivation layers vertically increases the produce per square meter of land area (Casey et al., 2022; Martin et al., 2023). Furthermore, the year-round and high yields in VFs contribute to increased food security and self-sufficiency in urban areas. In that sense, crop production from open field farming was assumed at optimistic values, representing a 'good year' of harvest, which oftentimes can go wrong as well. Next to reduced food security, this also means a worse environmental performance per kg of FW crop.

According to Martin et al. (2023), VFs use lower quantities of fertilisers and no pesticides compared to the assessed conventional food systems, and VFs use water more efficiently. However, the ecotoxicity impacts are larger due to the high electricity use, which had double the impact of the fertilisers used. Eutrophication in VFs was observed to be lower than in open-field farming (Martin et al., 2023).

5.5 Conclusion

This study presents different strategies to reduce the carbon footprint of VFs, including enhanced light use efficiency and molar efficacy, the use of residual heat from VFs in urban district heat networks, and attuning light according to the availability of renewable energy in the grid. The performance of VFs, when compared to conventional farming methods, highly depends on the local electricity grid-mix, i.e., the share of renewable energy. Consequently, VFs may be less suitable for countries that heavily rely on fossil fuels.

In the context of the Netherlands, the use of residual heat from VFs in urban district heat networks has proven to be an effective strategy to reduce the carbon emissions of cities with VFs, as cities with these synergetic VFs had a 13% smaller total carbon footprint than cities that exclusively use non-synergetic VFs for crop production. However, compared to cities utilising natural gas heating and conventionally produced crops, the total carbon footprint of the synergetic VF city increased by 27%. Despite reductions in heating-related emissions, the overall emissions raised due to the carbon emissions associated with crop production in VFs compared to those from conventional farming. This disparity is mostly attributed to electricity use for artificial lighting in VFs. This highlights that in countries characterised by high fossil-based grid-mixes, such as the Netherlands, integrating VF into urban settings for vegetable and fruit production may not necessarily result in lower emissions, despite the notable reduction in city heating achieved through the replacement of fossil-based heating systems with VF heat.

Previous studies have identified the potential to lower electricity costs and enhance the electricity grid balance by attuning LED usage with real-time electricity prices, which reflect the (im)balances between supplies and demand in the electricity grid (Chapter 4). However, this study reveals that optimising lighting schedules based on the real-time electricity prices leads to an increase in GHG emissions. The question of whether VFs should prioritize attuning electricity use to balance the electricity grid to prevent grid congestion issues or focus on achieving carbon reduction to combat climate change is a complex debate that necessitates further investigation. The emissions could, however, be reduced by adjusting light intensities according to the real-time emission factor of the grid, reflecting the proportion of renewable energy production. When using lettuce as an example crop, the emissions by artificial lighting in VFs could be reduced by 13%. In comparison to the synergetic VF city (Scenario III), the attuned synergetic VF city had a 5% smaller total carbon footprint.

In conclusion, when establishing VFs in cities, careful consideration of the location, crop selection, LUE optimisation without increasing crop inputs, supplying residual heat to the city, and using electricity when the share of renewable energy production is high are crucial to minimise carbon emissions. The additional carbon emissions due to the use of (non-renewable) electricity for artificial lighting should be weighed against the benefits VFs can offer to a city, including food security, efficient land-use, residual heat supply, and attuned electricity usage to minimise grid imbalances.

References

Afvalfonds Verpakkingen. 2017. Bijlage 2: lijst van standaard gewichten verpakkingen. https://afvalfondsverpakkingen.nl/a/i/Bijlage-2-Lijst-met-standaardgewichten.xlsx. (Accessed October 25, 2023)

Baltussen, W., Janssens, S.R.M., Georgiev, E., Selten, M., Simmons, R.G.F. 2021. Monitor Voortgang Verduurzaming Voedselketens: Aardappelen, groenten en fruit. Wageningen Economic Research, Wageningen.

Barbosa, G.L., Almeida, G.F.D., Kublik, N., Proctor, A., Reichelm, L., Weissinger, L., Wohlleb, G.M., Halden, R.U. 2015. Comparison of land, water, and energy requirements of lettuce grown using hydroponic vs. conventional agricultural methods. Int. J. Environ. Res. Publ. Health. 12(6), 6879–6891. https://doi.org/ 10.3390/ijerph120606879.

Bougoul, S., Ruy, S., de Groot, F., Boulard, T. 2005. Hydraulic and physical properties of stone wool substrates in horticulture. Sci. Hortic. 104, 391–405. https://doi.org/ 10.1016/j.scienta.2005.01.018.

Breukers, A., Stokkers, R., Spruijt, J., Roelofs, P., de Haan, J. 2014. Teelt de grond uit in perspectief: prestaties van teeltsystemen op het gebied van integrale duurzaamheid. Praktijkonderzoek Plant & Omgeving, Wageningen University and Research, Wageningen.

Carotti, L., Graamans, L., Puksic, F., Butturini, M., Meinen, E., Heuvelink, E., Stanghellini, C. 2021. Plant factories are heating up: Hunting for the best combination of light intensity, air temperature and root-zone temperature in lettuce production. Front. Plant Sci. 11. https://doi.org/10.3389/fpls.2020.592171.

Casey, L., Freeman, B., Francis, K., Brychkova, G., McKeown, P., Spillane, C., Bezrukov, A., Zaworotko, M., Styles, D. 2022. Comparative environmental footprints of lettuce supplied by hydroponic controlled-environment agriculture and field-based supply chains. J. Clean. Prod. 369. https://doi.org/10.1016/j.jclepro.2022.133214.

CBS, 2018a. Aardgaslevering vanuit het openbare net: woningkenmerken. https://opendata.cbs.nl/statline (Accessed October 10, 2023)

CBS, 2018b. Elektriciteitslevering vanuit het openbare net: woningkenmerken, bewoners. https://opendata.cbs.nl/statline (Accessed October 10, 2023)

CBS, 2018c. Energieverbruik van particuliere huishoudens. https://www.cbs.nl/nl-nl/achtergrond/2018/14/energieverbruik-van-particuliere-huishoudens (Accessed October 10, 2023)

CBS. 2023a. Energieverbruik particuliere woningen; woningtype en regio's. opendata.cbs.nl (Accessed October 10, 2023)

CBS. 2023b. Hernieuwbare energy in Nederland 2022. https://www.cbs.nl/nl-nl/longread/rapportages/2023/hernieuwbare-energie-in-nederland-2022/2-algemene-overzichten (Accessed November 28, 2023)

Chen, X.L., Yang, Q.C. 2018. Effects of intermittent light exposure with red and blue light emitting diodes on growth and carbohydrate accumulation of lettuce. Sci. Hortic., 234, 220-226. https://doi.org/10.1016/j.scienta.2018.02.055.

Ciolkosz, D.E., Albright, L.D., Both, A.J. 1998. Characterizing evapotranspiration in a greenhouse lettuce crop. Acta Hortic. 456, 255–261.

CO_2 emissiefactoren, 2023. CO_2 emissiefactoren. https://www.co2emissiefactoren.nl (Accessed November 17, 2023).

Delden, S.H., van Sharath Kumar, M., Butturini, M., Graamans, L.J.A., Heuvelink, E.,Kacira, M., … Marcelis, L.F.M. 2021. Current status and future challenges in implementing and upscaling vertical farming systems. Nature food. https://doi.org/10.1038/s43016-021-00402-w.

[dataset] Ecoinvent 3.6, 2015. The Ecoinvent Database.

Energieopwek.nl. 2023. Nationaal Klimaat Platform https://energieopwek.nl/ (Accessed November 28, 2023)

ENTSOE. 2023. Actual Generation per Product Type: aggregated generation per type. Transparency.entsoe.eu (Accessed November 27, 2023).

Gentry, M. 2019. Local heat, local food: integration vertical hydroponic farming with district heating in Sweden. Energy 174, 191–197. https://10.1016/j. energy.2019.02.119.

Germer, J., Sauerborn, J., Asch, F., de Boer, J., Schreiber, J., Weber, G., Müller, J. 2011. Skyfarming an ecological innovation to enhance global food security. Journal für Verbraucherschutz und Lebensmittelsicherheit, 6(2), 237-251. https://10.1007/s00003-011-0691-6.

Graamans, L., Baeza, E., van den Dobbelsteen, A., Tsafaras, I., Stanghellini, C. 2018. Plant factories versus greenhouses: comparison of resource use efficiency. Agric. Syst. 160. 31-42. https://doi.org/10.1016/j.agsy.2017.11.003.

Janssen, R.J.P., Krijn, M.P.C.M., van den Bergh. T., van Elmpt, R.F.M., Nicole, C.C.S., van Slooten, U. 2019. Optimizing Plant Factory Performance for Local Requirements. In: Anpo, M., Fukuda, H., Wada, T. (Eds.), Plant Factory Using Artificial Light: Adapting to Environmental Disruption and Clues to Agriculture Innovation. pp. 281-293. https://doi.org/10.1016/C2017-0-00580-3.

Kalantari, F., Tahir, O. M., Joni, R. A., Fatemi, E. 2017. Opportunities and challenges in sustainability of vertical farming: A review. J. Landsc. Ecol., 11(1), 35-60. https://doi.org/10.1515/jlecol-2017-0016.

Khoshnevisan, B., Rafiee, S., Omid, M., Mousazadeh, H., Clark, S. 2014. Environmental impact assessment of tomato and cucumber cultivation in greenhouses using life cycle assessment and adaptive neuro-fuzzy inference system. J. Clean. Prod. 73, 183-192. http://dx.doi.org/10.1016/j.jclepro.2013.09.057.

Klimaatmonitor. 2023. Energieverbruik Amsterdam [dataset]. https://klimaatmonitor.databank.nl/dashboard. (Accesses October 2, 2023)

Kondrateva, N., Filatov, D., Bolshin, R., Krasnolutskaya, M., Shishov, A., Ovchukova, S., Mikheev, G. 2021. Determination of the effective operating hours of the intermittent lighting system for growing vegetables. International AgroScience Conference: Earth and Environmental Science, 935. https://dx.doi.org/10.1088/1755-1315/935/1/012004.

Kozai, T., Ohyama, K., Chun, C. 2006. Commercialized closed systems with artificial lighting for plant production. Acta Hortic. 711, 61-70. https://doi.org/10.17660/actahortic.2006.711.5.

Marchi, B., Zanoni, S. 2022. Energy efficiency in cold supply chains of the food and beverage sector. Transp. Res. Proc. 67, 56-62. https://doi.org/10.1016/j.trpro.2022.12.035.

Martin, M., Weidner, T., Gullström, C. 2022. Estimating the potential of building integration and regional synergies to improve the environmental performance of urban vertical farming. Front. Sustain. Food Sys. 6, 849304. https://doi.org/10.3389/fsufs.2022.849304.

Martin, M., Elnour, M., Sinol, A.C. 2023. Environmental life cycle assessment of a large-scale commercial vertical farm. Sustain. Prod. Consum. 40, 182-193. https://doi.org/10.1016/j.spc.2023.06.020.

Montero, J.I., Antón, A., Torrellas, M., Ruijs, M., Vermeulen, P., 2011a. Environmental and economic profile of present greenhouse production systems in Europe: EUPHOROS deliverable N 5 Final Report (No. Deliverable 5 Final Report). European Commission, Cabrils/Wageningen.

Montero, J.I., Antón, A., Torrellas, M., Ruijs, M., Vermeulen, P., 2011b. Environmental and economic profile of present greenhouse production systems in Europe: annex (No. Deliverable 5 Final Report). European Commission, Cabrils/Wageningen.

Pennisi, G., Orsini, F., Blasioli, S., Cellini, A., Crepaldi, A., Braschi, I., Spinelli, F., Nicola, S., Fernandez, J.A., Stanghellini, C., Gianquinto, G., Marcelis, L.F.M. 2019a. Resource use efficiency of indoor lettuce (Lactuca sativa L.) cultivation as affected by red:blue ratio provided by LED lighting. Sci. Rep. 9. 14127. https://doi.org/10.1038/s41598-019-50783-z.

Pennisi, G., Sanyé-Mengual, E., Orsini, F., Crepaldi, A., Nicola, S., Ochoa, J., Fernandez, J.A., Gianquinto, G. 2019b. Modelling Environmental Burdens of Indoor-Grown Vegetables and Herbs as Affected by Red and Blue LED lighting. Sustainability. 11(15), 4063. https://doi.org/10.3390/su11154063.

Pennisi, G., Blasioli, S., Cellini, A., Maia, L., Crepaldi, A., Braschi, I., Spinelli, F., Nicola, S., Fernandez, J.A., Stanghellini, C., Marcelis, L.F.M., Orsini, F., Gainquinto, G. 2019c. Unraveling the role of Red:Blue LED Lights on Resource Use Efficiency and Nutritional Properties of Indoor Grown Sweet Basil. Front. Plant Sci. 10. 305. https://doi.org/10.3389/fpls.2019.00305.

Pennisi., G., Pistillo, A., Orsini, F., Cellini, A., Spinelli, F., Nicola, S., Fernandez, J.A., Crepaldi, A., Gianquinto, G., Marcelis, L.F.M. 2020. Optimal light intensity for sustainable water and energy use in indoor cultivation of lettuce and basil under red and blue LEDs. Sci. Hortic. 272. https://doi.org/10.1016/j.scienta.2020.109508.

Pulselli, R.M., Marchi, M., Neri, E., Marchettini, N., Bastianoni, S. 2019. Carbon accounting for decarbonisation of European city neighbourhoods. J. Clean. Prod. 208, 850–868. https://doi.org/10.1016/j.jclepro.2018.10.102.

Raaphorst, M.G.M., Benninga, J. 2019. Kwantitatieve informatie voor de glastuinbouw 2019: kengetallen voor groenten-, snijbloemen-, pot- en perkplanten teelten. Wageningen University and Research, Wageningen.

Righini, I., Stangehellini, C., Hemming, S., Graamans, L., Marcelis, L.F.M. 2023. Resources for plant-based food: estimating resource use to meet the requirements of urban and peri-urban diets. Food Energy Secur. 12. https://doi.org/10.1002/fes3.462.

RVO. 2022. Registratiesysteem voor energielabels van woningen. Klimaatmonitor.databank.nl

Schreuder, R., van Leeuwen, M., Spruijt, J., van der Voort, M., van Asperen, P., Hendriks- Goossens, V. 2009. Kwantitatieve informatie akkerbouw en vollegrondsteelt 2009. Wageningen University and Research, Lelystad.

Sørensen, J.C., Kjaer, K.H., Ottosen, C.O., Jørgensen, B.N. 2016. DynaGow: Multi-Objective Optimization for Energy Cost-efficient Control of Supplemental Light in Greenhouses. Proceedings of the 8th International Joint Conference on Computational Intelligence, 1, 41-48. https://doi.org/10.5220/0006047500410048.

Vandermeulen, A., van der Heijde, B., Helsen, L. 2018. Controlling district heating and cooling network to unlock flexibility: A review. Energy, 151, 103-115. https://doi.org/10.1016/j/energy.2018.03.034.

Velden, N.J.A. van der, Smit, P.X., 2019. CO2-behoefte Glastuinbouw 2030. Research Report (2019-074). Wageningen University and Research, Wageningen.

Weidner, T., Yang, A., Hamm, M.W. 2021. Energy optimisation of plant factories and greenhouses for different climatic conditions. Energy Convers. Manag. 243. 114336. https://doi.org/10.1016/j.enconman.2021.114336.

TOC



Philips Horticulture LED solution by Signify

TOC

6 Conclusions

This dissertation was motivated around two global challenges. First, the need for innovative farming methods to deal with growing food demands, decreasing resource and land availability, and to reduce the environmental impacts of food production. Second, the urgency for cities to diminish greenhouse gas emissions by reducing energy and resource usage. Existing literature suggested vertical farming as a potential solution, emphasising its high yields and minimal land and resource usage. Moreover, the integration of vertical farms (VFs) in cities could potentially close energy and resource cycles to reduce the need for external inputs in both VFs and cities.

However, despite of the advocacy of VFs as sustainable food system, the carbon footprint of VFs was unknown. Furthermore, there was a need to understand the potential synergies between VFs and cities, and the energetic gains and carbon reductions brought about through symbiotic relationships.

This dissertation explored the potential to integrate vertical farming systems with the energy and resource systems of buildings (Chapter 3) and cities (Chapter 4). The potential reduction of greenhouse gas emissions that synergetic vertical farming systems in cities could provide were assessed in Chapter 5 which reflected on the initial carbon footprint of a non-synergetic VF as defined in Chapter 2. This chapter discusses the overall findings of the dissertation to answer the main research question:

Can the synergetic integration of vertical farms into cities reduce energy and resource usage, and carbon emissions of both entities collectively?

Firstly, the conclusions of the four sub-research questions are presented to thereafter answer the main research question. Furthermore, this chapter defines the research contributions, recaps the research limitations, and gives recommendations for future research regarding the integration of VFs in buildings and cities. The chapter concludes with a personal vision from the author on the role of vertical farming in sustainable cities.

6.1 Sub-research questions

6.1.1 The carbon footprint of vertical farming

Existing literature frequently advocates vertical farming as a sustainable food system as they offer significant benefits over conventional farming systems. These benefits include efficient land-use, high yields, minimal use of water, nutrients, pesticides and herbicides, and the ability to be located near or within cities where the food demands are the highest. At the start of this research project, the current carbon footprint of vertical farming was unknown. This assessment was, however, crucial to understand the potential contribution of vertical farms (VFs) to future sustainable food production and cities, as well as evaluating their current performance. Consequently, the first sub-research question of this dissertation was:

How does the current carbon footprint of vertical farming system compare to that of open-field farming and greenhouse horticulture in the Netherlands?

Chapter 2 addressed this question by conduction a quantitative carbon footprint assessment of lettuce produced in an operational commercial VF and comparing this with conventional farming systems in the Netherlands. The latter included open-field farming (OF), soil-based greenhouse horticulture (GHs), and greenhouse horticulture using artificial light (GHa). This assessment incorporated the greenhouse gas emissions throughout the entire life cycles of both the farm and the crop, from cradle-to-grave (Fig. 2.3). The initial assessment used the electricity grid-mix in the Netherlands as of 2022. Additionally, three alternative scenarios were formulated to enhance comparability between the four farming systems and to include the effects of the energy transition: the inclusion of the lost carbon sequestration potential resulting from land-use change by conventional farming systems (1), the adoption of identical packaging for all farming systems (2), and the use of renewable energy (3).

Collectively, the alternative scenarios resulted in a VF carbon footprint of 1.797 kg $CO_{2\text{-eq}}$ per kg fresh weight (FW) lettuce. This footprint was significantly higher than those of the OF, GHs and GHa, which were 0.544 kg $CO_{2\text{-eq}}$ kg^{-1} FW, 0.788 kg $CO_{2\text{-eq}}$ kg^{-1} FW, and 0.751 kg $CO_{2\text{-eq}}$ kg^{-1} FW, respectively. The electricity usage of the VF accounted for 66% of the emissions, with artificial light representing 65% of the total electricity use. These findings indicate that, despite of the potential benefits that VFs offer over conventional farming methods, the substantial energy

use outweighs these advantages. In their current state, VFs cannot compete with conventional farming systems in the Netherlands from a carbon footprint perspective. To become a sustainable and secure solution for future food systems and cities, VFs must significantly decrease their energy use to reduce their carbon footprint.

6.1.2 Vertical farms integrated into buildings

The substantial use of artificial light to promote photosynthesis results, in addition to the high carbon footprint of VFs (RQ1), in the production of residual heat. This heat can be used for building heating purposes by creating energy synergy between the VF and its host building. Literature suggested that the exchange of energy and other resources between VFs and buildings could potentially reduce the need for external inputs. Therefore, the second sub-research question addressed in this dissertation was:

How can the integration of vertical farms into the energy and resource systems of a building reduce the energy and resource use of both entities?

Chapter 3 explored the potential to integrate VFs within various building typologies in the Netherlands, including apartments, offices, restaurants, supermarkets, and swimming pools. Several integration strategies were defined to facilitate the exchange of heat and cold between the VF and building, distinguishing between direct integration and integration with aquifer thermal energy storage (ATES) systems (Section 3.2.3). The use of ATES systems enabled the option to seasonally store VF heat produced outside of the building's heating systems for use in winter.

The bidirectional exchange of thermal energy between the VF and building reduced the annual energy use for climate control systems of both entities collectively by 12% to 51%. The highest savings were obtained when using a heat exchanger to directly supply VF heat to an indoor swimming pool. This swimming pool requires heating throughout the entire year, eliminating to need for seasonal storage of VF heat. The integration of VFs with apartments or restaurants benefits from ATES systems as it minimised the cultivation area needed to meet the heating demands. Office buildings with substantial cooling demands do not benefit from the integration with VFs when using ATES systems. In this scenario, heat produced during summer office cooling is stored for winter usage, establishing a balanced energy system without the need for VF heat.

To conclude, Chapter 3 revealed that the exchange of energy between VFs and buildings offers a significant potential to reduce the energy use for climate systems in VFs and buildings collectively. In addition, waste flows of grey water and nutrients from buildings can minimise the need for external inputs of water and nutrient in VFs.

6.1.3 Vertical farms integrated into urban energy systems

The third sub-research question was formulated as follows:

How can the integration of vertical farms into urban energy systems establish a thermal energy equilibrium within local district heat networks, while responding to fluctuations in electricity supplies by the electricity grid?

Chapter 4 adopted a stepped approach to design two energy system configurations for year-round thermal energy balance through heat and cold exchange between VFs and the buildings of a specific neighbourhood, using the Westindische buurt in Amsterdam as a case study. The two configurations included a 4-pipes DHN with a centralised heat pump (HP), and a 2-pipe district heat network (DHN) with decentralised HPs. Aquifer thermal energy storage (ATES) systems were added to address timing issues between heat and cold supplies and demands. The decentralised configuration proved most effective in terms of VF cultivation area to reach energy equilibrium, energy storage needs, annual energy use, and future-readiness. However, spatial integration of the individual HPs and buffer tanks might be challenging at building level.

For this specific neighbourhood, energy savings of 15% were achieved compared to the existing heating systems using natural gas. These savings also included the energy use of the VF. The ratio between VF electricity use and low-temperature heat production resembles that of datacentres, which are frequently promoted as heat source for DHNs. However, in contrast to datacentres, VF can provide flexibility to the electricity grid by adjust their electricity usage to the hourly electricity prices, e.g., by using intermittent lighting schedules or flexible light intensities in response to real-time price fluctuations. Due to the integration of the ATES system and the constant diurnal LED electricity use, intermittent or flexible lighting did not affect the quantity of heat supplied to the DHN.

In conclusion, the integration of VFs into urban energy systems can establish thermal energy equilibrium in local DHNs by using VF heat, while enhancing grid stability by aligning LED operation with real-time electricity prices. Through these contributions, VFs can offer additional benefits to cities aside from the production of fresh vegetables and fruits.

6.1.4 The carbon footprint of synergetic vertical farms

As presented in RQ1, VFs have a significantly higher carbon footprint than conventional farming systems in the Netherlands. However, synergetic integration of VFs in cities can reduce the energy use of a neighbourhood by supplying residual VF heat to local DHNs and enhance grid stability by attuning the LED according to the real-time electricity prices (RQ3). Consequently, the fourth sub-research question of this dissertation was:

What carbon reductions can be achieved through the synergetic integration of vertical farms with urban energy systems?

Chapter 5 assessed the carbon footprint per capita for the city of Amsterdam in four different scenarios. The carbon footprint included the greenhouse gas (GHG) emissions related to the consumed vegetables and fruits and the energy use of the built environment. The scenarios included: the Reference city relying on conventional farming and natural gas-based energy systems (1), the VF city maintaining the reference energy systems, while using VFs exclusively for vegetable and fruit production (2), the Synergetic VF city in which VFs also produce heat for the city (3), and the Attuned VF city using VF heat and attuning VF electricity use to minimise grid imbalances (4).

The use of VF heat in DHNs (Scenario 3) effectively reduced the carbon footprint of cities with VFs when compared to scenario 2. However, despite of replacing the fossil-based heating systems with VF heat, the substantial GHG emissions for crop production in VFs increases the carbon footprint in comparison to that of a city relying on conventional farming and energy systems (Scenario 1). Furthermore, the study revealed that the carbon footprint of VFs increases when attuning LEDs to minimise grid imbalances using real-time electricity prices. This prompts a complex debate on whether vertical farmers should prioritise balancing the electricity grid or achieving carbon reductions. Carbon reductions could, however, be achieved when attuning LEDs according to the availability of renewable energy in the grid.

To conclude, when integrating VFs in cities, careful considerations of location, crop selection, light use efficiency optimisations, and residual heat use are crucial to minimise the additional carbon emissions from vertical farming for the city. These emissions should be weighed against the benefits VFs can bring to a city, including food security, self-sufficiency, efficient land-use, and attuned electricity usage to minimise grid imbalances.

6.2 Main research question

These four sub-research questions were formulated to address the overarching research question of this dissertation:

How can the synergetic integration of vertical farms into cities reduce energy and resource usage, and carbon emissions of both entities collectively?

This research was conducted within the context of the Netherlands, with a primary focus on the energy synergy, i.e., the exchange of residual heat produced by VFs with the cold generated when heating city buildings using heat pumps.

The findings revealed that the synergetic integration of VFs in cities effectively reduces the collective energy use of both the VF and the city, lowering the carbon footprint of VFs in cities. However, despite the carbon savings achieved by replacing fossil-based heating systems with VF heat, the overall carbon footprint of such synergetic cities surpassed that of cities relying on fossil-based heating and conventional farming for vegetable and fruit consumption. This increase was attributed to the substantial energy use for artificial light to cultivate crops in VFs.

Furthermore, the study highlighted the crucial need for careful consideration of location, crop selection, light use efficiency, and the use of residual heat to minimise the additional carbon emissions by the integration of VFs into cities. The observed increase in greenhouse gas emissions should be weighed against the potential benefits VFs bring to cities, including enhanced food security, self-sufficiency, replacement of fossil-based heating systems, efficient land-use, and the flexibility offered to the electricity grid by attuning the LEDs.

At the building scale, the maximum energy savings occurs when integrating VFs into building functions that require year-round, non-seasonal, heating, such as swimming pools or wellness centres. The heating demands of these facilities align with the consistent year-round heat production of the VF, eliminating the need for complex seasonal storage systems.

Another key insight from this study is the trade-off between minimising the carbon footprint and the present essential need for flexible electricity operations in cities. While crucial for cities, attuning the LEDs in a VF to enhance grid stability currently increases the carbon emissions of VFs. This is because the low demand of electricity at night results in an abundance of electricity in the grid, while the hourly emission

factor of this grid-mix is the highest at midnight. Avoiding electricity use at midnight would thus reduce the carbon footprint of vertical farming but does not contribute to a better-balanced electricity grid. This debate exemplifies the complexity of accessing VFs either as a sustainable or non-sustainable alternative for conventional farming systems. For instance, prioritising carbon savings over considerations as food security or land-usage is a complex matter of debate.

In conclusion, the synergetic integration of VFs offers substantial benefits for cities, including food production, land-use, flexible electricity utilisation, and heat supply. However, when exclusively focussing on carbon footprints, VFs face a significant challenge in competing with conventional farming systems. This challenge arises primarily from to the absence of natural light (direct sunlight and diffuse daylight) resulting from the objectives to minimise land-use and maximise yields by stacking crops in a uniform growth environment.

6.3 Research contribution

In addition to addressing the specific research questions, the primary research contributions of this dissertation were the baseline carbon footprint assessment of vertical farming systems, the determination of potential synergetic technical systems at the building and urban scale, and the quantification of energy, water and nutrient synergies between vertical farming systems and the built environment. The carbon footprint assessment undertaken in this research represents one the initial comprehensive analyses of a running commercial vertical farming system. Although specifically focussed on the Netherlands, the output fed into the ongoing debate regarding the sustainability of vertical farming systems and underscored the need for energy reduction within this field.

Furthermore, previous studies identified urban agriculture as a strategy to reduce energy and resource usage of both farming systems and the city by creating symbiosis between both entities. However, few studies focussed on exploring the potential synergies when integrating vertical farming systems into urban environments and more specifically, the energetic gains and carbon savings resulting from such integration were unknown. This dissertation addressed this gap by investigating and quantifying the potential synergies that arise when integrating VFs into buildings and cities.

Moreover, this dissertation introduced a novel approach by using one single system, the VF, to address two challenges associated with the urban energy transition: the demand for alternative fossil-free heat sources and grid congestion issues. As a result, this dissertation provided cross-disciplinary approach to define potential energy and resource synergies between VFs and cities to enhance the understanding of the environmental and energetic gains from such symbiotic relationship.

6.4 Research limitations

Several limitations within the scope of this research (Section 1.2.2) need to be addressed as a consequence of the limited access to data regarding vertical farming systems; the most significant constraint within this research. Horticulture is a highly protective sector regarding data sharing. This lack of data sharing is not only reflected in the amount data provided by commercial parties but also in research papers. Researchers in the field of vertical farming can often not publish all data used in their studies due to restrictions imposed by data owners. Additionally, relatively few studies on VFs existed due to the novelty of the vertical farming industry. This lack of data resulted in several research limitations.

Firstly, the carbon footprint assessment in Chapter 2 (RQ1) included only one case study: a commercial lettuce-producing VF located in the Netherlands (VF_{I} in Chapter 5). This VF might not be the most optimal representation of existing VFs due to the absence of carbon enrichment, the use of individual growth pots, and its small scale. Therefore, the electricity use for artificial lighting, the most significant contributor to the carbon footprint, was compared to that of other VF studied by literature. However, data on lighting characteristics and yields were often incomplete, and most of the published data was based on simulated VFs. Towards the end of the research project, new vertical farming studies were published, including the carbon footprints of a small research facility (Chapter 5, VF_{II}) and a commercial large-scale VF (Chapter 5, VF_{III}). These footprints were compared to that of VF_{I} in Chapter 5 (RQ4), using the electricity grid-mix of the Netherlands. However, a complete comparison in terms of electricity use for artificial light was hindered as VF_{III} did not publish data on lighting characteristics.

TOC

Secondly, not all life cycle inventory data was available to define the carbon emissions in the entire life cycle of both the farm and the crop (Chapter 2). Due to this lack of data, emissions such as the materials used in machinery, climate systems, and auxiliary equipment, the energy used to construct and disassemble the farm, and energy use of retail were not included in the carbon footprint.

Thirdly, it was not possible to define a typical VF layout due to the novelty of the vertical farming sector. Various VF approaches for food production exist, including growth methods, number of growth layers, cultivation height, and automation levels. Although this study discussed the integration of VF in buildings and cities, spatial integration beyond the cultivation area was, therefore, not addressed (Chapters 3 and 4). To maximise replicability of the results we chose to specify the results in terms of the square meters of one VF production layer required to, for example, supply the heat demands of a certain building (Chapter 3) or neighbourhood (Chapter 4).

Fourthly, complete life cycle inventory data on crops other than leafy greens were not available for cultivation in VFs. Although an assorted range of vegetables is required to provide a healthy diet, Chapters 2, 3 and 4 (RQ1–RQ3) only studied butterhead lettuce due to this lack of data. Although Chapter 5 (RQ4) included the production of crops other than lettuce, only data on yields, electricity use, and water use of these crops was available and the remaining life cycle inventory data had to be approximated using data of lettuce-producing VFs.

Finally, the carbon footprint calculated in Chapter 2 (RQ1) was based on measured data of an existing VF, while the calculations for RQ2 and RQ3 (Chapter 3 and 4) rely on simulated VF data. This decision was made as the VF studied in Chapter 2 used a cooling and dehumidification system that was not optimal for the recovery of residual heat and was not representative for other VFs. To incorporate the use of residual heat in the carbon footprint of Chapter 5 (RQ4), the measured data of the climate systems in the VFs were replaced by the energy use for climate systems as in the simulated synergetic VF (RQ3).

6.5 Recommendations for further research

Several recommendations for further study relating to the integration of vertical farming systems in buildings and cities emerge from this research. The main challenge in advancing VFs lies in sustainability and profitability, primarily due to the high electricity use for artificial light and climate systems. Further research aimed at enhancing light use efficiency (LUE) in VFs, measured as moles of light supplied per kg fresh weight produced, holds the potential for significant reductions of the carbon footprint (Chapter 5). Studies focussed on LUE should avoid increasing crop inputs and material usage, preventing emissions that might offset carbon savings. In addition, these studies should explore lighting concepts that slightly reduce yields, but significantly reduce electricity consumption, particularly in the context of rising electricity prices.

Furthermore, alternative strategies for lighting should be explored, which were not investigated in this study. These strategies may include adjusting lighting intensities according to the specific needs of each growth phase of the crop, such as using lower light intensities during growth phases where it is feasible in terms of yields. Another strategy could be the adoption of hybrid lighting strategies, which involve both natural and artificial light to reduce electricity use, carbon emissions and residual heat production. Future studies should examine the extent to which these approaches impact the uniformity of lighting in the vertical farm and the trade-off between reduced yields and electricity usage.

In line with these recommendations, experiments focussed on alternating LEDs either to the real-time electricity prices or the share of renewable energy in the grid (Chapter 5) are needed, including the effects of intermittent photoperiods and fluctuating light intensities on the yields of various crop types. In the broader urban energy system perspective, the use of thermal inertia of buildings or battery systems can provide additional flexibility in energy systems, which requires further investigation in terms of cost savings, enhanced grid stability, or carbon reductions.

Furthermore, the study only included one configuration for cooling and dehumidification of the VF (Chapter 3 and 4). A comprehensive study of different cooling and dehumidification strategies, including energy use and residual heat production, is needed to enhance energy efficiency. Such configuration may include passive use of outdoor air for cooling or water-cooled LEDs (Chapter 3).

Apart from the potentials to reduce the energy use of the VF to reduce GHG emissions and costs, this study also explored options to reduce resource usage by leveraging synergies between the VF and cities. Besides the use of grey water and nutrient outputs from buildings in VFs (Chapter 3), other potential synergies may be identified in future studies. On the building scale, Chapter 3 suggested exploring the use of evapotranspiration to purify grey water and rainwater, and the use of CO_2 from human respiration to replace the pressurised CO_2 in VFs in a sustainable manner. In cities, the integration of VFs may also unlock synergies as a wider range and quantity of resources will be available.

Finally, as discussed in Section 6.4, the inability to define a typical VF layout was a significant research limitation. Therefore, further research towards optimal VF configurations is necessary to advance studies on the integration of VFs in buildings and cities. Such studies should address the minimum cultivation area of a VF to maximise energy efficiency and profitability.

6.6 Personal reflection on urban vertical farms

This final section of this dissertation provides a personal vision on the role of vertical farms in sustainable cities, beyond the scientific research done within the previous chapters of the dissertation.

Vertical farming is often promoted as a sustainable food production system by addressing pressing agricultural issues such as limited availability of arable land, resource scarcity, and the need for low carbon systems to mitigate greenhouse gas emissions. Throughout this dissertation, one of the central focus points has been to critically evaluate the claims of vertical farming as a sustainable food system.

This task, however, proved more challenging than anticipated when writing the research proposal, primarily due to the lack data from operation vertical farms (VFs). The industry's evolving nature resulted in relatively scarce literature. Furthermore, the hesitance of vertical farmers to share data, driven by competition within the sector and ongoing developments concerns, has created a closed environment. This attitude necessitates researchers and companies to reinvent the wheel and hinders the overall improvement of the sector's performance.

In spite of these obstacles, data from a small-scale VF in the Netherlands was successfully collected. While the representability of this farm was difficult to verify due to the abovementioned challenges, new literature and data that became available towards the final stages of the PhD allowed for a comparative analysis of VF carbon footprints. Results indicated a significant carbon footprint, primarily driven by the electricity use needed to maintain indoor climate conditions in stacked systems for high year-round produce with limited land use. Future improvements, such as water-cooled LEDs and light intensity adjustment according to crop growth stages, are envisioned, but competing with carbon footprints of conventional farming systems in the Netherlands which make better use of natural resources, such as solar energy, will remain a challenge.

Using renewable energy would significantly reduce this carbon footprint of vertical farming. However, this energy will need to be generated offsite, either through wind turbines or at a large-scale photovoltaic production site, as the building envelope of the VF itself will not be able to accommodate sufficient panels to meet the electricity needs of a VF.

Setting aside the high carbon footprint, the potential to offer a reliable year-round food supply, enhancing food security, and the ability to alleviate pressure from agricultural soils creating opportunities for rewilding, makes vertical farming an interesting proposition in the light of rising food demands, urbanisation, and climate change. However, the current focus on a limited range of crops with low nutritional value, sold at a high price, making them inaccessible to the general public, highlights a mismatch between real urban food demands and VF production. A tremendous shift is required to make vertical farming accessible and to contribute to future food security in a meaning full way.

In addition, despite the benefits of reducing transportation distances, the connectivity of citizens with food production in other forms of urban agricultural is overlooked by the closed-box environment of VFs. Although vertical farming can be agriculture in proximity to citizens, the expensive crop production in a high-tech and invisible environment might feel more distant than ever before.

Furthermore, when discussing the contribution of vertical farming to food security it should be questioned whether we should try to produce the increasing food demands or change our diets. As food production for animals takes up a significant portion of agricultural land, switching to mostly plant-based diets could be a more effective pathway to meet the global food demands, while reducing carbon emissions of the food system overall.

The second element of the dissertation emphasised a multi-disciplinary approach, advocating vertical farming as an integral element of a broader urban strategy. By addressing interconnected challenges of agriculture, cities, and energy systems, a more impactful approach is proposed compared to the narrow focus on each of these problems individually. The research suggested that, when integrating VFs in urban energy and resource systems, VFs can offer benefits beyond stable food supplies. These include using the light required to produce food in VFs as a heat source that can replace fossil-based heating systems in cities, aligning their usage with the needs of the electricity grid. Furthermore, VFs could be used to reuse nutrients from black water and reuse grey water for irrigation, limiting waste outputs of the city and inputs of farming. These synergies also reduce the carbon footprint of VFs in cities. However, VFs do add a substantial electricity demand to the city, adding even more difficulties to the significant challenge of meeting the electricity demands sustainably while ensuring stable supplies.

In conclusion, a multi-disciplinary approach of integrating VFs with the urban energy and resource systems can make a valuable contribution to closing resource and energy cycles in cities, balancing energy systems, and alleviating some of the pressure on agricultural lands. However, substantial challenges of vertical farming including economic accessibility, production of nutritious crops, and most importantly reducing energy use, must be addressed first. For now, it remains questionable if VFs can address these challenges.

TOC

Appendices

TOC

APPENDIX A

Chapter 2

A.1 Energy use and lighting characteristics of VFs in literature

TABLE A.1 Data on electricity use and artificial light characteristics of CBVF in literature and the studied VF.

#	Location	Crop	Yields	LED	PFFD	DLI	photoperiod
			kg m^{-2} y^{-1}	W m^{-2}	µmol m^{-2} s^{-1}	mol m^{-2} d^{-1}	h d^{-1}
1	Lisbon, Portugal	Tomato	74	47	427	20.0	13
2	Singapore	Leafy vegetable	-	-	735	29.1	11
3	Kashiwa, Japan	Lettuce and herbs	-	364	-	-	-
4	Aarhus, Denmark	Basil	50	176	243	14.0	16
5	The Netherlands	Lettuce	74.1	199	500	28.8	16
6	Beijing, China	Lettuce	-	-	250	14.4	16
7	Japan	Lettuce	-	-	-	-	-
8a	Stockholm, Sweden	Vegetable basket	38	104	272	13.7	14-16
8b	Stockholm, Sweden	Lettuce	52.6		200	11.5	16
9a	Netherlands	Lettuce	68.9	91	140	10.1	20
9b	Netherlands	Basil	36.9	106	150	10.8	20

>>>

TABLE A.1 Data on electricity use and artificial light characteristics of CBVF in literature and the studied VF.

#	Total electricity use	Electricity use LED	Method		Reference
	kWh kg^{-1}	kWh kg^{-1}	simulated	measured	
1	3.3	3.1	X		Benis et al., 2017
2	-	26.4	X		Li et al., 2020
3	-	30.3		X	Kikuchi et al., 2018
4	20.8	20.6	X		Avgouastaki & Xydis, 2020; 2021
5	17.3	15.7	X		Graamans et al. 2018
6	-	31.5		X	Zhang et al., 2018
7	7.1-9.1	-			Kozai, 2019
8a	15-17.5	14	X		Weidner et al., 2021
8b	-	-	X		Weidner et al., 2021
9a	14.8	9.7		X	CBVF studied
9b	30.7	21		X	CBVF studied

A.2 List of emission factors used within this research

TABLE A.2 TReferences used per EF

Activity	Unit	Reference	Notes & IPPC GWP100a EF reference
Seeds and seedlings			
Seeds	$kgCO_{2\text{-}eq}/kg$	Ecoinvent v3.6	Wheat seed taken as reference, for sowing {GLO}| market for | Alloc Rec, U
Seedlings	$kgCO_{2\text{-}eq}/n$	Ecoinvent v3.6	Strawberry seedlings taken as reference, for planting {GLO}| market for | Cut-off, U
Water and nurturing			
Water (irrigation)	$kgCO_{2\text{-}eq}/m^3$	Ecoinvent v3.6	Tap water {Europe without Switzerland}| market for | Alloc Rec, U
Nitrogen Fertilisers*	$kgCO_{2\text{-}eq}/kg$	Ecoinvent v3.6	Nitrogen fertiliser, as N {GLO}| market for | Alloc Rec, U
Phosphate Fertilisers	$kgCO_{2\text{-}eq}/kg$	Ecoinvent v3.6	Phosphate fertiliser, as P2O5 {GLO}| market for | Alloc Rec, U
Potassium Fertilisers	$kgCO_{2\text{-}eq}/kg$	Ecoinvent v3.6	Potassium fertiliser, as K2O {GLO}| market for | Alloc Rec, U
Lime – Calcium oxide	$kgCO_{2\text{-}eq}/kg$	Ecoinvent v3.6	Lime, packed {GLO}| market for | Alloc Rec, U
Sulphur trioxide (SO_3)	$kgCO_{2\text{-}eq}/kg$	Ecoinvent v3.6	Sulfur trioxide {RER}| production | Alloc Rec, U
Magnesium	$KgCO_{2\text{-}eq}/kg$	Ecoinvent v3.6	Magnesium oxide {GLO}| market for | Alloc Rec, U
Pesticide	$kgCO_{2\text{-}eq}/kg$	Ecoinvent v3.6	Pesticide unspecified, at regional storehouse/RER U
Herbicides	$kgCO_{2\text{-}eq}/kg$	Ecoinvent v3.6	Herbicides, at regional storehouse/RER U
Potting/garden soil	$kgCO_{2\text{-}eq}/kg$	Ecoinvent v3.6	Peat potting soils 20L = 7.5 kg (Pokon) Peat {GLO}| market for | Cut-off, U
CO_2 enrichment	$kgCO_{2\text{-}eq}/kg$	Ecoinvent v3.6	Pressurised liquid carbon dioxide, liquid {RER}| market for | Alloc Rec, U
N_2O from soils	$kgCO_{2\text{-}eq}/kg$	Foster et al., 2021	kg N_2O-N * (44/28) = kg N_2O (Klein et al., 2006) 1 kg N_2O emission refers to 273 $kgCO_{2\text{-}eq}$
Operating energy			
Electricity	$kgCO_{2\text{-}eq}/kWh_e$	Emissiefactoren NL	Dutch electricity mix
Electricity production with PV	$kgCO_{2\text{-}eq}/kWh_e$	Ecoinvent v3.6	EcoInvent GWP100a (CML-IA) - Electricity, low voltage {IT}| electricity production, photovoltaic, 3kWp slanted-roof installation, multi-Si, panel, mounted | Cut-off, U
Natural gas	$kgCO_{2\text{-}eq}/m^3$	Emissiefactoren NL	Groningen gas
Diesel	$kgCO_{2\text{-}eq}/kg$	Ecoinvent v3.6	z_diesel con emissioni

>>>

TABLE A.2 TReferences used per EF

Activity	Unit	Reference	Notes & IPPC GWP100a EF reference
Bio-diesel	$kgCO_{2\text{-}eq}/kg$	Emissiefactoren NL	Vegetable oil methyl ester {GLO}| market for | Alloc Rec, U
Biogas	$kgCO_{2\text{-}eq}/m^3$	Ecoinvent v.3.6	Biogas {RoW}| market for biogas | Cut-off, U // density 1.15 kg/m^3
Lubricants	$kgCO_{2\text{-}eq}/kg$	Ecoinvent v3.6	Lubricating oil {GLO}| market for | Alloc Rec, U
Disposable materials			
Bamboo with PE coating	$kgCO_{2\text{-}eq}/kg$	(-)	Calculated by material composition, PE: 15% of total mass (Ligthart and van den Oever, 2018).
Polyethylene (PE)	$kgCO_{2\text{-}eq}/kg$	Ecoinvent v3.6	Polyethylene, low density, granulate {GLO}| market for | Alloc Rec, U
Bamboo paper	$kgCO_{2\text{-}eq}/kg$	Ecoinvent v3.6	Kraft paper taken as reference, unbleached {GLO}| market for | Alloc Rec, U
Bioplastic (PLA)	$kgCO_{2\text{-}eq}/kg$	Ecoinvent v3.6	Polyester-complexed starch biopolymer {GLO}| market for | Alloc Rec, U
Polypropylene (PP)	$kgCO_{2\text{-}eq}/kg$	Ecoinvent v3.6	Polypropilene, granulate {GLO}| market for | Alloc Rec, U
Rockwool	$kgCO_{2\text{-}eq}/kg$	Ecoinvent v3.6	Rock wool {GLO}| market for | Alloc Rec, U
Materiality: structure, equipment and machinery			
Steel	$kgCO_{2\text{-}eq}/kg$	Ecoinvent v3.6	Steel, unalloyed {GLO}| market for | Alloc Rec, U
Aluminium	$kgCO_{2\text{-}eq}/kg$	Ecoinvent v3.6	Aluminium, cast alloy {GLO}| market for | Alloc Rec, U
Reinforced concrete	$kgCO_{2\text{-}eq}/m^3$	Ecoinvent v3.6	Concrete, normal {GLO}| market for | Alloc Rec, U
Glass	$kgCO_{2\text{-}eq}/kg$	Ecoinvent v3.6	Flat glass, uncoated {GLO}| market for | Alloc Rec, U
PVC	$kgCO_{2\text{-}eq}/kg$	Ecoinvent v3.6	Polyvinylchloride, emulsion polymerised {GLO}| market for | Alloc Rec, U
Polyester	$kgCO_{2\text{-}eq}/kg$	Ecoinvent v3.6	
Polyethylene (PE)	$kgCO_{2\text{-}eq}/kg$	Ecoinvent v3.6	Polyethylene, low density, granulate {GLO}| market for | Alloc Rec, U
Polycarbonate (PC)	$kgCO_{2\text{-}eq}/kg$	Ecoinvent v3.6	Polycarbonate {GLO}| market for | Cut-off, U
Transportation			
Lorry	$kgCO_{2\text{-}eq}/ton\ km$	Ecoinvent v3.6	Transport, freight, lorry 3.5-7.5 metric ton, EURO5 {GLO}| market for | Alloc Rec, U
End-of-life			
waste-to-energy	$kgCO_{2\text{-}eq}/kg$	Pulselli et al., 2019	incineration
organic waste-to-compost	$kgCO_{2\text{-}eq}/kg$	Pulselli et al., 2019	
Carbon sequestration			
Forestry	$kgCO_2/m^2\ yr^{-1}$	COM, 2021	Young European forest

** The specific emission factors for the two different fertilisers used in the VF were calculated based on their nutrient composition. Within this research, only the macronutrients were included to calculate these specific emission factors. In this case, the macronutrients N, P, K, Ca, Mg, and S (Wada, 2019), which represent the largest share of the minerals.*

A.3 Activity data

TABLE A.3 Activity data for butterhead lettuce production in an open-field farm per kg FW.

Activity	Activity data FU	Unit	Note
FARM LIFE CYCLE			
Upstream			
Steel	1.08E-03	kg	structure, corrugated steel roof and façade panels, lifespan 50 y (Appendix A.4)
Polycarbonate (PC)	7.22E-05	kg	Windows, lifespan 50 y (Appendix A.4)
Reinforced concrete	4.23E-05	m3	Floor, lifespan 50 y (Appendix A.4)
Insulation Rockwool	1.13E-04	kg	Façade insulation, lifespan 50 y (Appendix A.4)
Transportation	1.00E-02	kg km	Section 2.2.3
End-of-life			
Transportation	5.00E+01	km kg	Section 2.2.3
CROP LIFE CYCLE			
Upstream			
Seedlings	3.36E+00	n	(Schreuder et al., 2009)
Fertiliser			
– Nitrogen (N)	3.90E-03	kg	(Schreuder et al., 2009)
– Potassium (K_2O)	6.81E-03	kg	(Schreuder et al., 2009)
Pesticides & herbicides			
– Pesticides	4.32E-04	kg	(Schreuder et al., 2009)
– Herbicides	0	kg	(Schreuder et al., 2009)
Packaging materials			
– Polypropylene bags	1.14E-02	kg	4 g per crop (Afvalfonds verpakkingen, 2017)
Transportation inputs	1.00E+02	km kg	Section 2.2.3
Core			
Watering	1.51E+01	L	5.3 m^3 per 1000 lettuce heads, excluding rainfall (Breukers et al., 2014)
N_2O from soils (direct and indirect)	3.90E0-05	kg	Calculated for synthetic fertiliser application according to Klein et al., 2006 (TIER 1). *1
Fuel use	3.11E-02	kg	Diesel used for machinery (Schreuder et al., 2009)
Lubricants	1.93E-04	kg	Lettuce production OF Italy taken as reference (Ecoinvent 3.6)

>>>

TABLE A.3 Activity data for butterhead lettuce production in an open-field farm per kg FW.

Activity	Activity data FU	Unit	Note
Downstream			
Transportation	1.60E+02	km kg	Section 2.2.3
End-of-life			
Cultivation phase			
– Cultivation losses	1.50E-01	kg	15% losses, 85% production yields (Schreuder et al., 2009)
Supply chain			
– Food losses	5.87E-03	kg	Section 2.2.3
Consumer			
– Food losses	9.50E-02	kg	Section 2.2.3
– Packaging	1.14E-02	kg	Polypropylene bags
Transportation	5.00E+01	km kg	Section 2.2.3

1. *Both direct and indirect N_2O emissions from managed soils were calculated according to Klein et al (2006), using tier 1 as no specific data was available. This case study only includes synthetic fertilisers. For direct N_2O emissions the following formulae were applied:*

$$N_2O_{direct}\text{-}N = N_2O\text{-}N_{N\text{-}inputs} \quad \textit{(Eq. A.1)}$$

in which $N_2O\text{-}N_{N\text{-}inputs}$ represents the annual direct N_2O-N emissions from N inputs to managed soils in kg N_2O-N y^{-1}.

$$N_2O\text{-}N_{N\text{-}inputs} = F_{sn} * EF_1 \quad \textit{(Eq. A.2)}$$

in which F_{sn} is the annual amount of synthetic N fertiliser applied to soils in kg N y^{-1} and EF_1 the emission actor for N_2O from N inputs of 0.01 kg $N_2O\text{-}N_N$ (kg N input)$^{-1}$.

The indirect N_2O-N emissions from managed soils were calculated by summing the N_2O emissions from atmospheric deposition of N volatised ($N_2O_{(ATD)}$-N) and the N_2O emissions from leaching and runoff ($N_2O_{(L)}$-N), using formulae A.3. and A.4:

$$N_2O_{(ATD)}\text{-}N = (F_{sn} * Frac_{GASF}) * EF_4 \quad \textit{(Eq. A.3)}$$

In which $Frac_{GASF}$ is the fraction of synthetic fertiliser N that volatilises as NH_3 and NO_x in kg N volatilised of 0.10 kg NH_3 + NO_x-N (kg N)$^{-1}$ and EF_4 the activity's emission factor of 0.010 kg $N_2O\text{-}N_N$ (kg NH_3 + NO_x-N volatilised)$^{-1}$.

$$N_2O_{(L)}\text{-}N = (F_{sn} * Frac_{leach\text{-}(H)}) * EF_5 \quad \textit{(Eq. A.4)}$$

In which $Frac_{leach\text{-}(H)}$ is the fraction of N added to managed soils that is lost through leaching and runoff of 0.30 kg N (kg N)$^{-1}$ applied and EF_5 the activity's emission factor of 0.075 (kg $N_2O\text{-}N_N$ (kg N)$^{-1}$.

N_2O-N emissions were converted into N_2O-emissiosn using:

$$N_2O = N_2O\text{-}N * (44/28) \quad \textit{(Eq. A.5)}.$$

TOC

TABLE A.4 Activity data for butterhead lettuce production in a soil-based greenhouse horticulture per kg FW.

Activity	Activity data FU	Unit	Note
FARM LIFE CYCLE			
Upstream			
Steel	2.53E-02	kg	Roof bars, girders, stability braces, rails, posts, tie beams, foundations, reinforcements, high wire system, ventilation opening mechanism, 15 y lifespan (Montero et al., 2011a, 2011b)
Aluminium	6.48E-03	kg	Gutters, ridges, bars, ventilator opening mechanism, energy screens (Montero et al., 2011a, 2011b)
Reinforced concrete	1.05E-05	m^3	Foundations and path / 15 y lifespan (Montero et al., 2011a, 2011b)
Glass	2.74E-02	kg	Covering and walls / 15 y lifespan (Montero et al., 2011a, 2011b)
Polyester	3.35E-04	kg	Floor material and screens / 15 y lifespan (Montero et al., 2011a, 2011b)
Transportation	1.00E+02	km kg	Section 2.2.3
End-of-life			
Transportation	5.00E+01	km kg	Section 2.2.3
CROP LIFE CYCLE			
Upstream			
Seedlings	3.00E+00	n	(Raaphost and Benninga, 2019)
Fertiliser			
– Nitrogen (N)	3.14E-03	kg	Lettuce production in Italian GH taken as reference (Ecoinvent 3.6)
– Phosphate (P_2O_5)	2.00E-03	kg	Lettuce production in Italian GH taken as reference (Ecoinvent 3.6)
– Potassium (K_2O)	4.29E-03	kg	Lettuce production in Italian GH taken as reference (Ecoinvent 3.6)
– Magnesium	1.44E-04	kg	Lettuce production in Italian GH taken as reference (Ecoinvent 3.6)
Pesticides & herbicides			
– Pesticides	1.44E-04	kg	Lettuce production in Italian GH taken as reference (Ecoinvent 3.6)
– Herbicides	-	kg	Lettuce production in Italian GH taken as reference (Ecoinvent 3.6)
Growth materials			
– Potting soil	3.80E-01	L	Peat potting soil, 20 L = 7.52 kg (Pokon), (Raaphorst and Benninga, 2019)
Packaging materials			
– Polypropylene bags	1.14E-02	kg	4 g per crop (Afvalfonds verpakkingen, 2017)
Transportation inputs	1.00E+02	km kg	Section 2.2.3

>>>

TABLE A.4 Activity data for butterhead lettuce production in a soil-based greenhouse horticulture per kg FW.

Activity	Activity data FU	Unit	Note
Core			
Watering	1.90E+01	L	(Raaphost and Benninga, 2019)
N_2O from soils (direct and indirect)	6.45E-05	Kg	Calculated for synthetic fertiliser application according to Klein et al., 2006 (TIER 1), see subscript table A.1.
Fuel use	3.67E-01	m^3	Natural gas for heating and steaming (Raaphost and Benninga, 2019)
Electricity use	1.38E-01	kWh	(Raaphost and Benninga, 2019)
Total carbon enrichment	3.46E-01	kg	10 kg m^{-2} (Velden and Smit, 2019)
Downstream			
Transport	1.60E+02	km kg	Section 2.2.3
End-of-life			
Cultivation phase			
– Cultivation losses	5.00E-02	kg	5% cultivation losses (Raaphorst and Benninga, 2019)
Supply chain			
– Food losses	6.00E-03	kg	Section 2.2.3
Consumer			
– Food losses	9.50E-02	kg	Section 2.2.3
– Packaging	1.14E-02	kg	Polypropylene bags
Transportation	5.00E+01	km kg	Section 2.2.3

TOC

TABLE A.5 Activity data for butterhead lettuce production in a hydroponic greenhouse per kg FW.

Activity	Activity data FU	Unit	Note
FARM LIFE CYCLE			
Upstream			
Steel	1.38E-02	kg	Section 2.2.3.2
Aluminium	3.52E-03	kg	Section 2.2.3.2
Reinforced concrete	5.70E-06	m^3	Section 2.2.3.2
Glass	1.49E-02	kg	Section 2.2.3.2
Polyester	1.82E-04	kg	Section 2.2.3.2
PVC	9.08E-03	kg	CropKing Classic NFT channel of 3.7m with 24 plant spaces per channel, 2mm PVC thickness (CropKing 2022), PVC density 1420kg/m^3, lifespan 8 y
Transportation	1.00E+02	km kg	Section 2.2.3
End-of-life			
Transportation	5.00E+01	km kg	Section 2.2.3
CROP LIFE CYCLE			
Upstream			
Seedlings	4.72E+00	n	(Raaphost and Benninga, 2019)
Fertiliser			43% of the fertilisers used in GHs (Raaphost and Benninga, 2019)
– Nitrogen (N)	1.33E-03	kg	
– Phosphate (P_2O_5)	8.60E-04	kg	
– Potassium (K_2O)	1.84E-03	kg	
– Magnesium	6.19E-05	kg	
Pesticides & herbicides			41% of the pesticides used in GHs (Raaphost and Benninga, 2019)
– Pesticides	5.92E-05	kg	
– Herbicides	-	kg	
Growth materials			
– Substrate	1.14E-02	kg	(Raaphorst and Benninga, 2019); Rockwool 0.0675 kg/dm^3 (Bougoul et al., 2005)
Packaging materials			
– Polypropylene bags	1.14E-02	kg	polystryne bag, same weight per kg FW as OF and GHs
Transportation inputs	1.00E+02	km kg	Section 2.2.3

>>>

TABLE A.5 Activity data for butterhead lettuce production in a hydroponic greenhouse per kg FW.

Activity	Activity data FU	Unit	Note
Core			
Watering	1.540E+00	L	1.4 L per 5 g DW lettuce (Ciolkosz et al., 1998) multiplied by 110% to include nutrient flushing (Barbosa et al. 2015)
Fuel use	8.84E-02	m^3	Natural gas for heating (Raaphost and Benninga, 2019)
Electricity use	1.37E+00	kWh	(Raaphost and Benninga, 2019)
Total carbon enrichment	3.52E-01	kg	(Raaphost and Benninga, 2019)
Downstream			
Transport	1.60E+02	km kg	Section 2.2.3
End-of-life			
Cultivation phase			
– Cultivation losses	4.00E-02	kg	4% cultivation losses (Raaphorst and Benninga, 2019)
– Growth materials	1.14E-02	kg	Rockwool
Supply chain			
– Food losses	6.00E-03	kg	Section 2.2.3
Consumer			
– Food losses	9.50E-02	kg	Section 2.2.3
– Packaging	9.09E-03	kg	Polystyrene bags
Transportation	5.00E+01	km kg	Section 2.2.3

TABLE A.6 Activity data for butterhead lettuce production in a VF per kg FW.

Activity	Activity data FU	Unit	Note
FARM LIFE CYCLE			
Upstream			
Steel	4.23E-03	kg	Leaf carriers and propagation, lifespan 8 y
Steel	3.60E-03	kg	Tables and cable trays, lifespan 10 y
Aluminium	6.70E-03	kg	Leaf carrier and propagation, lifespan 8 y
Transportation	1.00E+02	km kg	Section 2.2.3
End-of-life			
Transportation	5.00E+01	km kg	Section 2.2.3
CROP LIFE CYCLE			
Upstream			
Seeds	1.21E-05	kg	
Fertiliser			Supplied in tablet form (2 per pot), 20% discarded end of growth phase
– Nutrients NPK	1.39E-02	kg	NPK fertiliser
– Nutrients N Ca0	1.86E-02	kg	Nitrogen and calcium fertiliser
Pesticides & herbicides	-		Not applied
Growth & culture materials			
– Polypropylene	1.15E-01	kg	Growth container and lid used for 5 growth cycles on average
– Bioplastic	3.06E-02	kg	Plug holder, assumed PLA material: polyester-complexed starch biopolymer
– Rockwool	6,69E-03	kg	
Packaging materials			
– Bamboo with PE coating	2.88E-01	kg	15% polyethylene film, 75% bamboo of total weight (Ligthart and van den Oever, 2018)
Transportation inputs	1.00E+02	km kg	Section 2.2.3
Core			
Watering	1.68E+01	L	per crop: 700 mL + 550 mL (refill) growth pot, of which 248 mL left and discharged before moving to selling pot filled with 600 mL water.
Electricity use	1.47E+01	kWh	66% LED lighting with 20 h photoperiod, 22% cooling and fans, 12% dehumidification, 0% propagation light
Carbon enrichment			Not applied
Downstream			
Transport	1.50E+01	km kg	Sold at local supermarket, including water the product weighs 6.45 kg per kg lettuce

>>>

TABLE A.6 Activity data for butterhead lettuce production in a VF per kg FW.

Activity	Activity data FU	Unit	Note
End-of-life			
Cultivation phase			
– cultivation losses	2.00E-02	kg	2% cultivation losses
– Growth materials	1.15E-01	kg	Polypropylene growth containers and lid; plugs and Rockwool moved to selling pot after growth phase
– Discharged nutrients	6.49E-03	kg	20% of nutrients applied
Supply chain			
– Food losses	5,87E-03	kg	Section 2.2.3
Consumer			
– Food losses	9.50E-02	kg	Section 2.2.3
– Plant debris	1.82E-01	kg	Non consumable part of the crop
– Packaging	3.26E-01	kg	Bamboo pot and lid, plugs and Rockwool
Transportation	5.00E+01	km kg	Section 2.2.3

A.4 Theoretical model materiality open-field farm

To define the materiality of agricultural buildings on an average open-field farm in The Netherlands, a theoretical model was created as no reference data were available. Nine case studies of open-field farms were studied to determine the type and number of buildings that an average farm has. These case studies were collected from the Dutch property sales website: 'Funda in Business'. This website provided information on the total plot size, and the number, dimensions and materiality of the agricultural buildings present. The average farm size of the analysed case studies was 13.9 hectare per farm, close to the national average open-field farm size of 15 hectares (CBS, 2021). On average, the studied farms had two agricultural buildings with an average total floor area of 1,400 m^2, for the storage of fertilizers, pesticides, herbicides, machinery, and crops. The materiality of agricultural buildings is described in Figure A.1 and Table A.1. Approximately half of the agricultural buildings studied were insulated. The structural steel was sized using structural rules of thumb (table D.1). The lifespan of the two agricultural buildings was set at 50 years (Nemecek and Kägi, 2007).

TOC

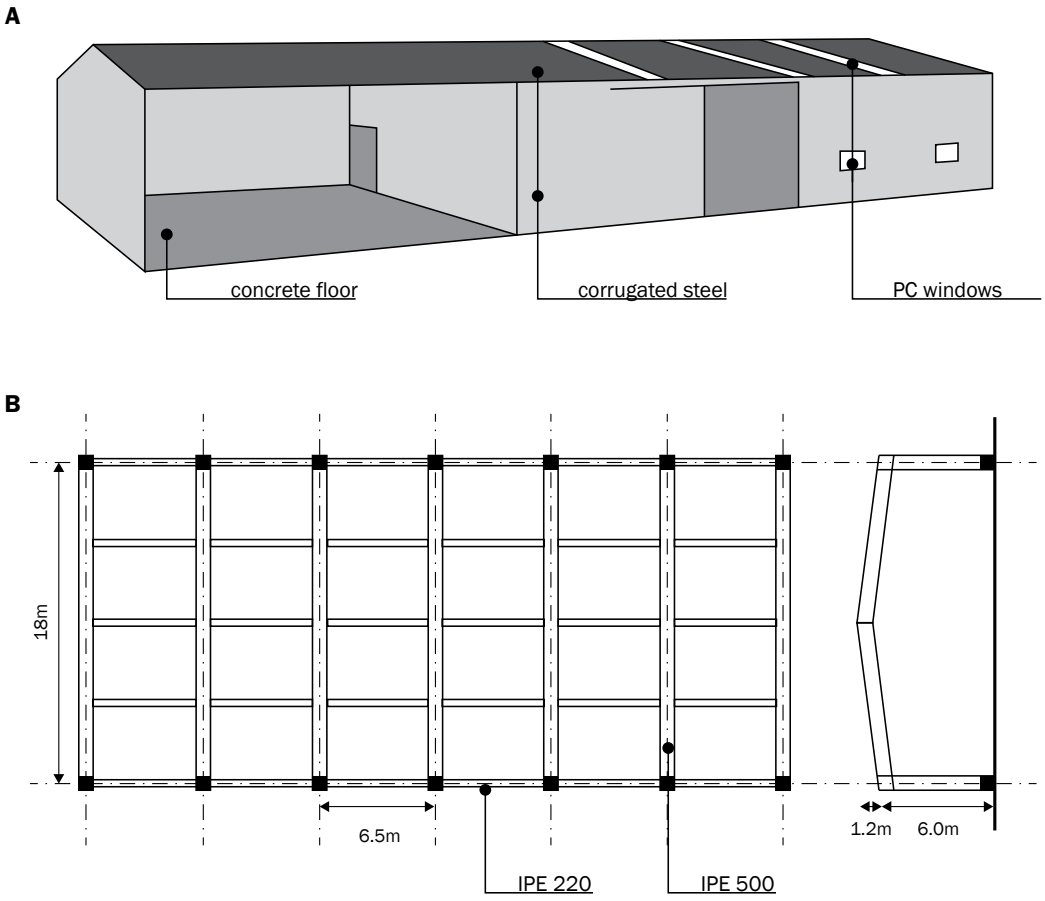

FIG.A.1 (A) 3D model of one of two 700 m2 agricultural buildings used in the theoretical model.
(B) Typical structural arrangement of the agricultural building using a steel columns and beams.

TOC

TABLE A.7 Material characteristics of the agricultural storage building as included in the theoretical model for the open-field farm. Two of these buildings are included in the model of which one of the two buildings is insulated.

Element	Materials	Dimension	Density	Number or area	Quantity materials	Note
Structure						
Portal frame	Steel	Total length frame (s) 30.2 m, IPE 500	92.5 kg/m	7 x	19.5 ton	Rule of thumb portal h =1/30 * s (Boveldt, 1999)
Beam	Steel	Length 6.5m, IPE 240	26.7 kg/m	35 x	6 ton	Rule of thumb roof beam single field h = 1/30 * length (Boveldt, 1999)
Rails and purlins	Steel				3.8 ton	Estimated additional 15% of structure weight
Façade						
Cladding	Corrugated steel sheets	Thickness 0.4mm	3.8 kg/m2	745 m^2	2.8 ton	(HGM Benelux, 2021)
Insulation	PIR insulation	Thickness 400mm	34 kg/m3	550 m^2	7.5 ton	1 of the 2 sheds insulated (Unilin, 2021)
Cladding interior side insulation	Corrugated steel sheets	Thickness 0.4mm	3.8 kg/m2	550 m^2	2.1 ton	Only applied to the insulated shed
Roof						
Roof panels	Corrugated steel plates	Thickness 0.4mm	3.8 kg/m2	702 m^2	2.7 ton	(HGM Benelux, 2021)
Windows						
Windows & sky Lights	PC	Thickness 6mm	2 kg/m2	120 m^2	0.2 ton	(DaglichtDirect, 2021)
Floor						
Concrete floor	Reinforced concrete	Thickness 20mm	-	700 m^2	140 m^3	

TOC

A.5 Renewable energy scenario

Table A.8 presents the fossil fuels used within the baseline scenario of the case studies and the alternative renewable technologies and fuels used in the renewable energy scenario. Table A.9 represents the core emissions of each farming typology in the renewable energy scenario. To determine the carbon footprint of the renewable energy scenario, the electricity demands for GH heating and steaming first had to be calculated.

A.5.1 Greenhouse heating

In the renewable energy scenario heating with a closed loop ground source heat pump was considered as these are identified as an effective and efficient alternative for greenhouse heating (Anifantis et al., 2016; Benli, 2013). A COP of 4 for estimated for the ground-source HP using Baetschmann and Leibundgut (2012, p. 1054) and the following characteristics for the ground-source HP system: a heating temperature of 8 °C above ambient for GHs and 10 °C for GHa (Raaphorst and Benninga, 2019), an average ground temperature of 4°C at 2-4 m depth (Ligget and Milne, 2018), and an exergy coefficient of 0.4 for the ground-source HP (Maivel and Kurnitski, 2015). A thermal efficiency of 90% was used for the natural gas boiler in the baseline scenario, resulting in a heat demand of 1.7 kWh kg^{-1} for GHs and 0.8 kWh kg^{-1} for GHa and a electricity demand of 0.43 kWh kg $^{-1}$and 0.19 kWh kg^{-1}.

A.5.2 Greenhouse steaming

Aside from heating, 5 m^3 m^{-2} of natural gas was used to steam the soil of GHs (Raaphorst and Benninga, 2019). A water output temperature of 100°C was assumed and an average water input temperature of 15°C. With this information, the baseline water volume for steaming was calculated using the following formula:

$$q = m * Cw * \Delta T, \quad \text{(Eq. A.1)}$$

where q is the energy required to heat the volume of water in the boiler with ΔT in KJ, m is the heated volume (L), Cw is the specific heat capacity of water (J/g°C), and ΔT is the temperature difference between the supply water and the steamed water. An efficiency of 90% for the gas boiler was assumed. This resulted in a water volume of 15 L kg^{-1}. By using the same formulae and a COP of 1 for the electric boiler in the renewable energy scenario an electricity demand of 1.52 kWh kg^{-1} was calculated.

TABLE A.8 Fossil fuel sources within the baseline scenario and the alternative renewables in the renewable energy scenario.

Farm	Purpose	Baseline scenario	Renewable energy scenario
Open-field	Machinery	Diesel	Bio-diesel
Soil-based greenhouse	Heating	Natural gas boiler	GSHP
	Steam	Natural gas boiler	Electric boiler
	Electricity	National grid-mix	PV panels
	CO_2	On-site natural gas combustion	CO_2 from biogas
Greenhouse with artificial light	Heating	Natural gas boiler	GSHP
	Electricity	National grid-mix	PV panels
	CO_2	1) on-site natural gas combustion 2) Liquefied CO_2	CO_2 from biogas
Vertical farm	Electricity	National grid-mix	PV panels

TABLE A.9 Core missions in the renewable energy scenario

Activity	OF	GHs	GHa	VF
	kg $CO_{2\text{-eq}}$ kg^{-1}	kg $CO_{2\text{-eq}}$ kg^{-1}	kg $CO_{2\text{-eq}}$ kg^{-1}	kg $CO_{2\text{-eq}}$ kg^{-1}
Watering	0.006	0.008	0.001	0.007
Bio-diesel	0.083			
N_2O from soils	0.022	0.018		
Electricity use		0.167	0.125	1.188
Total emissions	**0.111**	**0.192**	**0.126**	**1.194**

A.5.3 PV panel production

The kWh of electricity produced per m^2 PV is calculated with the following formula:

$$E_{pv} = \eta_{pv} * \eta_{or} * q_{sun} \quad \text{(Eq. A.2)}$$

Where η_{pv} is the efficiency of the PV panels which is approximately 20% (Delden et al., 2021), η_{or} the orientation efficiency and q_{sun} the solar radiation in the Netherlands of 1000 kWh m^{-2}. The orientation efficiency can be determined with a radiation diagram for the Netherlands (Induurzaam, n.d.). The production for south facing PV panels under an optimal angle of 40° for placement on flat surfaces and those for 90° for façade panels at east, west and south orientation are presented in Table A.10. Each m^2 of cultivation area requires 1013 kWh y^{-1} of electricity to be produced by 5.1 m^2 south-orientated 40° PV cell area. Assuming a land area

efficiency of 75% for these PV panels (Delden et al., 2020) results in 6.8 m^2 of land area. If the vertical farm was a standalone building 13500 kWh of electricity could be produced on its roof and 18826 kWh on the east, west and south facades. According to the allocation of electricity (Section 2.3.4), 51% of the total electricity is used for lettuce cultivation. Therefore, 51% of the PV panels are allocated to lettuce, resulting in a total production of 251 kWh per m^2 lettuce cultivation. The remaining electricity required for the production of lettuce still requires 3.8 m^2 of south facing PVs under a 40° angle per m^2 cultivation area.

TABLE A.10 Yearly production of PV panels in the Netherlands

PV orientation and angle	η_{or}	E_{pv}
	%	kWh m^{-2}
South, 40°	100%	200
South, 90°	75%	150
East, 90°	60%	120
West, 90°	55%	110

TOC

References

Afvalfonds Verpakkingen. 2017. Bijlage 2: lijst van standaard gewichten verpakkingen. https://afvalfondsverpakkingen.nl/a/i/Bijlage-2-Lijst-met-standaardgewichten.xlsx.

Anifantis, A.S., Pascuzzi, S., Scarascia-Mugnozza, G. 2016. Geothermal source heat pump performance for a greenhouse heating system: an experimental study. J. Agric. Eng. 47(3), 164–170. https://doi.org/10.4081/jae.2016.544.

Avgoustaki, D.D., Xydis, G. 2020. Indoor vertical farming in the urban Nexus content: business growth and resource savings.

Avgoustaki, D.D., Xydis, G. 2021. Energy cost reduction by shifting electricity demand in indoor vertical farms with artificial lighting. Biosyst. Eng. 211, 219–229. https://doi. org/10.1016/j.biosystemseng.2021.09.006.

Baetschmann, M., Leibundgut, H. 2012. LowEx solar building system: integration of PV/ T collectors into low exergy building systems. Energy Proc. 1052–1059. https://doi. org/10.1016/j.egypro.2012.11.118.

Barbosa, G.L., Almeida, G.F.D., Kublik, N., Proctor, A., Reichelm, L., Weissinger, L., Wohlleb, G.M., Halden, R.U. 2015. Comparison of land, water, and energy requirements of lettuce grown using hydroponic vs. conventional agricultural methods. Int. J. Environ. Res. Publ. Health 12 (6), 6879–6891. https://doi.org/ 10.3390/ijerph120606879.

Benis, K., Reinhart, C., Ferrao, P. 2017. Development of a simulation-based decision support workflow for the implementation of building-integrated agriculture (BIA) in urban contexts. J. Clean. Prod. 147, 589–602. https://doi.org/10.1016/j. jclepro.2017.01.130.

Benli, H. 2013. A performance comparison between a horizontal source and a vertical source heat pump systems for a greenhouse heating in the mild climate Elazig. Turkey. Appl. Therm. Eng 50 (1), 197–206. https://doi.org/10.1016/j. applthermaleng.2012.06.005.

Bougoul, S., Ruy, S., de Groot, F., Boulard, T. 2005. Hydraulic and physical properties of stone wool substrates in horticulture. Sci. Hortic. 104, 391–405. https://doi.org/ 10.1016/j.scienta.2005.01.018.

Boveldt, A. te, 1999. Jellema Hogere Bouwkunde Deel 7: Bouwmethodiek. Thiememeulenhoff, Utrecht/ Zutphen.

Breukers, A., Stokkers, R., Spruijt, J., Roelofs, P., de Haan, J. 2014. Teelt de grond uit in perspectief: prestaties van teeltsystemen op het gebied van integrale duurzaamheid. Praktijkonderzoek Plant & Omgeving, WUR, Wageningen.

DaglichtDirect. 2021. Polycarbonaat golfplaat 177/51 driewandig 275x110cm. https://d aglichtdirect.nl/. (Accessed February 3, 2022).

Delden, S.H. van, SharathKumar, M., Butturini, M., Graamans, L.J.A., Heuvelink, E., Kacira, M., Marcelis, L.F.M. 2021. Current status and future challenges in implementing and upscaling vertical farming systems. Nature food. https://doi. org/10.1038/s43016-021-00402-w.

Centraal Bureau voor de Statistiek. 2021. Landbouw: gewassen, dieren en grondgebruik naar bedrijfstype, nationaal. https://opendata.cbs.nl/statline/#/CBS/nl/dataset/ 80782ned/table?ts=1642524024433.

Ciolkosz, D.E., Albright, L.D., Both, A.J. 1998. Characterizing evapotranspiration in a greenhouse lettuce crop. Acta Hortic. 456, 255–261.

CO_2 emissiefactoren. 2021. CO2 emissiefactoren. https://www.co2emissiefactoren.nl/. (Accessed December 6, 2021).

COM. 2021. Commission staff working document: the 3 billion tree planting pledge for 2030 (651 final). European Commission, Brussel. https://ec.europa.eu/environment/3-billion-trees_en.

CropKing. 2022. CropKing. https://cropking.com/sites/default/files/2022-02/Catalo g_Web.pdf. (Accessed 25 April 2022).

Ecoinvent. 2015. The Ecoinvent Database. V3.6

Graamans, L., Baeza, E., van den Dobbelsteen, A., Tsafaras, I., Stanghellini, C. 2018. Plant factories versus greenhouses: comparison of resource use efficiency. Agric. Syst. 160, 31–42. https://doi.org/10.1016/j.agsy.2017.11.003.

HGM Benelux. 2021. Damwandplaat PS20/1100TR. https://www.hmg-benelux-shop. com/damwandplaat-ps201100tr-2e-keus-dak-staal-040-mm-7016–antracietgrijs- 500076w20lr.html. (Accessed 3 February 2022).

Induurzaam. n.d. Zoninstraling en orientatie. http://www.induurzaam.nl/2-energie-o pwekken/zonnepanelen/zoninstraling-en-orientatie (accessed 16 June, 2022).
Klein, C. de, Novoa, R.S.A., Ogle, S., Smith, K.A., Rochette, P., Wirth, T.C., McConkey, B. G., Mosier, A., Rypdal, K. 2006. N2O emission from managed soils, and CO2 emissions from lime and urea application. In: Eggleston, S., Buendia, L., Miwa, K.,
Ngara, T., Tanabe, K. (Eds.), IPPC Guidelines for National Greenhouse Gas Inventories Volume 4: Agriculture, Forestry and Other Land Use. IPPC, pp. 11.1–11.54.
Kozai, T. 2019. Towards sustainable plant factories within artificial lighting (PFALs) for achieving SDGs. Int. J. Agric. Biol. Eng. 12, 28–37. https://doi.org/10.25165/j. ijabe.20191205.5177.
Li, Y., Ding, Y., Li, D., Miao, Z. 2018. Automatic carbon dioxide enrichment strategies in the greenhouse: a review. Biosyst. Eng. 171, 101–119. https://doi.org/10.1016/j. biosystemseng.2018.04.018.
Ligget, R., Milne, M. 2018. Climate consultant 6.0. https://climate-consultant.informer. com/6.0/.
Ligthart, T., Oever, M., van den, 2018. Milieu-impact van twee verwerkingsroutes voor warme drankenbekers: vergisting en papierrecycling van karton-PLA koffiebekers. Wageningen Food Biobased Res. https://doi.org/10.18174/434835.
Maivel, M., Kurnitski, J. 2015. Heating system return temperature efficiency effect on heat pump performance. Energy Build. 94, 71–79. https://doi.org/10.1016/j. enbuild.2015.02.048.
Montero, J.I., Anton, A., Torrellas, M., Ruijs, M., Vermeulen, P. 2011a. Environmental and Economic Profile of Present Greenhouse Production Systems in Europe: EUPHOROS Deliverable N 5 Final Report (No. Deliverable 5 Final Report). European Commission, Cabrils/Wageningen.
Montero, J.I., Anto´n, A., Torrellas, M., Ruijs, M., Vermeulen, P. 2011b. Environmental and Economic Profile of Present Greenhouse Production Systems in Europe: Annex (No. Deliverable 5 Final Report). European Commission, Cabrils/Wageningen.
Nemecek, T., Kägi, T. 2007. Life Cycle Inventories of Agricultural Production Systems: Data v2.0. Agroscope Reckenholz-Tänikon Reseach Station ART. https://db.ecoinve nt.org/reports/15_Agriculture.pdf.
Pulselli, R.M., Marchi, M., Neri, E., Marchettini, N., Bastianoni, S. 2019. Carbon accounting for decarbonisation of European city neighbourhoods. J. Clean. Prod. 208, 850–868. https://doi.org/10.1016/j. jclepro.2018.10.102.
Raaphorst, M.G.M., Benninga, J. 2019. Kwantitatieve informatie voor de glastuinbouw 2019: kengetallen voor groenten-, snijbloemen-, pot- en perkplanten teelten. Wageningen UR, Wageningen, 26.
Schreuder, R., van Leeuwen, M., Spruijt, J., van der Voort, M., van Asperen, P., Hendriks- Goossens, V. 2009. Kwantitatieve informatie akkerbouw en vollegrondsteelt 2009. Wageningen UR, Lelystad.
Unilin Insulation. 2021. Why PIR? https://www.unilininsulation.com/en/all-about-ins ulation/why-pir. (Accessed February 3, 2022).
Velden, N.J.A. van der, Smit, P.X. 2019. CO2-behoefte Glastuinbouw 2030: Research Report (2019-074). Wageningen UR, Wageningen.
Voutsinos, O., Mastoraki, M., Ntatsi, G., Liakopoulos, G., Savvas, D. 2021. Comparative assessment of hydroponic lettuce production either under artificial lighting, or in a Mediterranean greenhouse during wintertime. Agriculture 11 (503). https://doi. org/10.3390/agriculture11060503.
Weidner, T., Yang, A., Hamm, M.W. 2021. Energy optimisation of plant factories and greenhouses for different climatic conditions. Energy Convers. OR Manag. 243 (114336) https://doi.org/10.1016/j. enconman.2021.114336.
Zhang, X., He, D., Niu, G., Yan, Z., Song, J., 2018. Effects of environmental lighting on the growth, photosynthesis, and quality of hydroponic lettuce in a plant factory. Int. J. Agric. Biol. Eng. 11 (2), 33–40. https://doi.org/10.25165/j.ijabe.20181102.3420.

APPENDIX B

Chapter 3

These supplementary materials provide additional information to the calculations supporting the study in Chapter 3 and the therefore created dataset. This dataset can be downloaded via the 4TU.ResearchData repository: https://doi.org/10.4121/adca348c-49a6-4e2f-a1c7-6f2b3d40c16b. Within the following chapters the calculations made in this dataset will be explained step-by-step.

Section B.1 provides further details on the climate set points of the vertical farm (VF), the calculated cooling demands of the VF, and the cooling and dehumidification system of the VF. Section B.2 presents the required calculations to define the energy use of the cooling and dehumidification system, and the residual heat produced by the system. Section B.3 describes the baseline conditions of the selected building typologies, including the heating and cooling demands, the baseline energy use for heating and cooling, and the inputs and outputs of vegetables, water, and nutrients. Finally, section B.4 presents the calculations made to define the energy savings obtained by creating bidirectional synergies between the VF and various building typologies.

B.1 Cooling and dehumidification of the vertical farm

B.1.1 Climate setpoints

Current cooling and dehumidification systems for VFs were discussed with five VF companies in The Netherlands. These conversations indicated a preference for dehumidification by cooling the air below the dewpoint temperature (DPT). In VFs, air-cooled systems are applied commonly as 100% direct liquid cooling is not possible due to the significant quantity of latent heat (Graamans, 2021). Fig. B.1 presents a simplification of the selected dehumidification strategy. At the DPT the air is 100% saturated. When cooling below the DPT the air starts to condense, rejecting moisture and heat from the air (Q_{out}). The temperature achieved at point 2 is lower than the desired return temperature needed at point 3. Therefore, reheating is required (Q_{in}).

TOC

During the photoperiod (16h), the exhaust air temperature of the VF was 26 °C, and a relative humidity (RH) 72% (Fig. B.1 point 1). The return air (Fig. B.1 point 3), after cooling and dehumidification, was 24 °C and 76% RH. These climate set points were based on an commercial VF located in The Netherlands. For simplification, this research only includes the photoperiod. By plotting the temperatures and associated RH of the supply (point 1) and return air (point 3) on a psychrometric chart, a DPT of 20.6°C (100% RH) and a cooling temperature of 19.5°C and 100% RH (point 2) were found (see Fig. B.2).

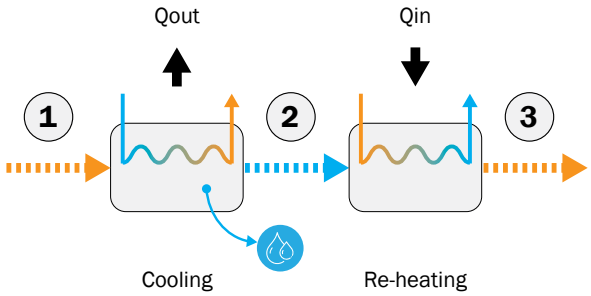

FIG.B.1 Schematic representation of the cooling and dehumidification strategy. The exhaust air (1) is cooled below DPT (2) to reject heat and moist (Qout), and re-heated (Qin) to reach the desired return temperature (3).

B.1.2 Heat production within the VF

The total heat produced within the vertical farm (Q_{vf}), Q_{out}, and Q_{in} were calculated using the following formulae:

$$Q_t = Q_s + Q_l$$
$$Q_t = \dot{m} * \Delta h \quad \text{(Eq. B.2)}$$

In which Q_t is the total cooling or heating demand including both sensible (Q_s) and latent heat (Q_l) in kJ s^{-1}, $\dot{m}$ is the flowrate of the heat transfer media (water or air) in kg s^{-1}, and Δh is the enthalpy difference in kJ kg^{-1}. The air flowrate ($\dot{m}_a$) is constant throughout whole process and was 0.004 kg s^{-1} for one m^2 cultivation area. Q_{vf} is equal to 90% of the electricity used for LED. Sensible and latent heat were calculated as follows:

$$Q_s = \dot{m} * C_p * \Delta T \quad \text{(Eq. B.3)}$$
$$Q_l = \dot{m} * h_w * \Delta w \quad \text{(Eq. B.4)}$$
$$T_w = (T_{dpt} + T_2) / 2 \quad \text{(Eq. B.5)}$$

TOC

In which C_p is the specific heat capacity in J kg^{-1} K^{-1}, ΔT the temperature difference, Δw the difference in humidity ratio, h_w the enthalpy of latent heat of evaporation water at T_w (water) in kJ kg^{-1}, T_{dpt} the DPT, and T_2 the temperature at point 2 (Fig. B.1). The specific heat capacity of water ($C_{p,water}$) is 4184 J kg^{-1} K^{-1}, that of air ($C_{p,air}$) is 1005 J kg^{-1} K^{-1}. When reheating the air, the latent heat is zero as no dehumidification takes place. The enthalpy and humidity ratio were obtained from the psychrometric chart (Fig. B.2).

The total heat produced within the VF (Q_{vf}), the heat rejected when cooling below DPT (Q_{out}) and the heat added to reheat the VF air to the desired temperature and RH before returning into the VF (Q_{in}) are presented in Table B.1. These values were calculated using Equations B.1–B.5.

TABLE B.1 Sensible and latent heat production per m^2 cultivation area of the VF (Q_{vf}), heat removal by cooling and dehumidification (Q_{out}), and re-heating (Q_{in}).

	Q_s J s^{-1} m^{-2}	Q_l J s^{-1} m^{-2}	Q_{tot} J s^{-1} m^{-2}
Q_{vf}	+24.2	+27.2	+51.4
Q_{out}	-76.2	-27.2	-103.4
Q_{in}	+52.0	0.0	+52.0

TOC

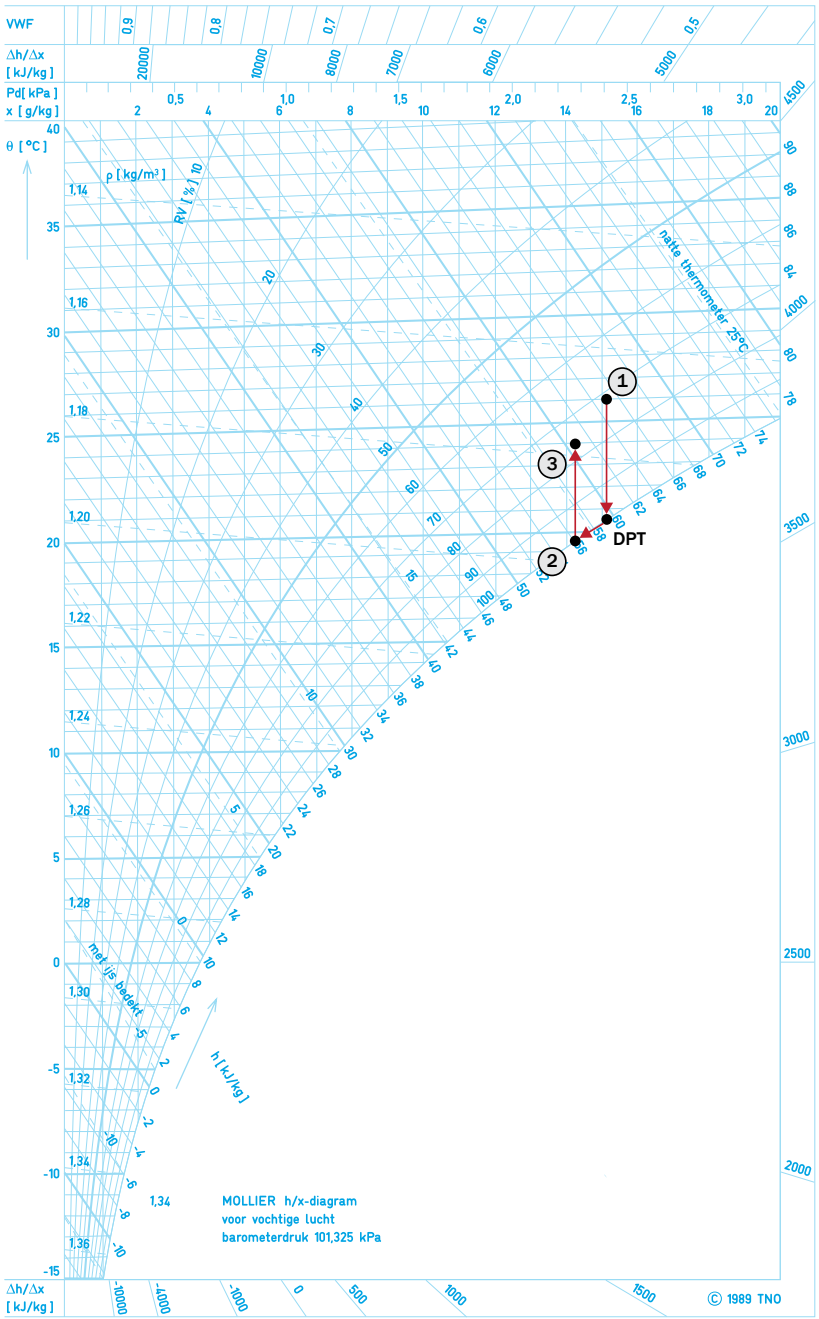

FIG.B.2 Psychrometric chart by TNO. Vertical left axis represents the temperature of the air (°C), horizontal the absolute humidity (g/kg), RV is the relative humidity, wet bulb temperature is presented by "natte thermometer".

TOC

B.1.3 Cooling an dehumidification of the baseline vertical farm

A cooling and dehumidification system was selected for the baseline VF that uses one water-to-water heat pump (HP1) for cooling, dehumidification, and reheating (Fig. 3.2). The evaporator of HP1 is used to cool the exhaust air from the VF below the DPT in heat exchanger 1 (HE1). The condenser HP1 reheats the air in heat exchanger 2 (HE2). In this system, Q_{in} is smaller than Q_{out} as the ΔT between points 2 and 3 is smaller than the ΔT of points 2 and 1, and the latent heat produced when reheating the air is zero. Q_{out} is equal to the heat removed by the evaporator (Q_e).

$$Q_{out} > Q_{in} \quad \text{(Eq. B.6)}$$
$$Q_e = Q_{out} \quad \text{(Eq. B.7)}$$

According to the first law of thermodynamics the energy balance in this system is as follows:

$$Q_e + Q_c + W_{in} = 0 \quad \text{(Eq. B.8)}$$
$$Q_c = Q_e + W_{in} \quad \text{(Eq. B.8a)}$$

where Q_c is the heat produced by the condenser, and W_{in} the electricity input of the HP's compressor. By combining equations B6, B7 and B8a, it was found that the condenser produces more heat than required by HE2. This abundance of heat is rejected to the atmosphere via HE3. A cold and warm buffer tank are included together with mixing values to allow temperature variations within the system whilst keeping uniform VF conditions.

B.2 Energy use of the baseline cooling and dehumidification strategy of the VF

B.2.1 Air-to-water heat exchanger 1 (cooling and dehumidifying)

As first step the temperatures within cooling and dehumidifying HE1 were calculated. The total latent and sensible cooling by the dehumidifying heat exchanger (HE1, Fig. 3.2) is equal to Q_{out} (Table B.1) and calculated using the following equations:$Q_{tot} = \dot{m} * \Delta h$ (Eq. B.9)

TOC

$$Q_s = \dot{m} * C_p * \Delta T \quad \text{(Eq. B.10)}$$

$$Q_l = \dot{m} * h_w * \Delta w \quad \text{(Eq. B.11)}$$

We assumed no heat losses occur within all heat exchangers by using insulation. Therefore:

$$Q_{tot,side\ 1} = Q_{tot,\ side\ 2} \quad \text{(Eq. B.12)}$$

In this case $Q_{tot,air\text{-}side} = Q_{tot,water\text{-}side}$ in which the water-side of the HE is heated and thereby only includes sensible heat, which is equal to the sum of both latent and sensible heat at the air-side.

The temperatures at the air-side of the HE were determined in Section B.1.1 of the supplementary materials; the air entering HE1 is 26 ºC VF air ($T_{air,in}$) and the air leaving HE1 is 19.5 ºC ($T_{air,out}$). The effectiveness (ε) of an air-to-water dehumidifying and cooling HE was be calculated using the following formula (Mansour and Fath, 2016):

$$\varepsilon \approx (T_{air,out} - T_{air,in}) / (T_{water,in} - T_{air,in}) \quad \text{(Eq. B.13)}$$

In which $T_{water,in}$ is the temperature of the water entering HE1. The effectiveness of a HE can be determined by using the effectiveness NTU (ε-NTU) method:

$$\varepsilon = Q_{actual} / Q_{max} \quad \text{(Eq. B.14)}$$

ε is the heat transfer effectiveness of the HE, Q_{actual} is the actual heat transfer, and Q_{max} the maximum heat transfer. The effectiveness of a HE can be found by using effectiveness relation diagrams which are developed for various HEs. Within these diagrams the effectiveness is determined with the outcome of C_{min} / C_{max} and the number of transfer units (NTU). The larger the NTU, the larger the dimensions of the HE (Chaware, 2016.):

$$NTU = (A * U) / C_{min} \quad \text{(Eq. B.15)}$$

A is the area of the HE in m^2, U the overall heat transfer coefficient of the HE in W/m^2 °C, C_{min} is $C_p * \dot{m}$ of the hot or cold side of the HE. The highest outcome of $C_p * \dot{m}$ gives C_{max}, the lowest C_{min}. We excluded HE sizing from research, therefore, NTU remains unknown.

The effectiveness of a counter flow HE can be found by using Figure 11. of Ezgi (2017). With the maximum NTU value, the effectiveness of the counter flow HE

is 90%. The overall heat transfer coefficient of air-to-water HEs is significantly smaller than for water-to-water HEs. Therefore, a large HE area is required to obtain the same NTU value and thus the effectiveness of air-to-water HEs was set at 70%. By using a 70% effectiveness, the air-temperatures in the HE, and equation B.5, the required water temperature to cool the air below DPT was calculated ($T_{water,in}$).

B.2.2 Air-to-water heat exchanger 2 (re-heating)

As for HE1, the temperatures of the water entering and leaving re-heating HE2 had to be determined. Within counter flow air-to-water HE2 the air of the VF is reheated to the desired supply temperature (Fig. 3.2). When (re)heating the air, the latent heat is zero. The effectiveness was calculated with the ε-NTU method where Q_{actual} and Q_{max} were calculated as follows:

$$Q_{actual} = \dot{m}_w * C_{pw} * (T_{h,o} - T_{h,i}) = \dot{m}_a * C_{pa} * (T_{c,o} - T_{c,i}) \quad \text{(Eq. B.16)}$$

$$Q_{max} = C_{min} * \Delta T_{max} \quad \text{(Eq. B.17)}$$

In this HE C_{min} is $\dot{m}_w * C_{pw}$ and ΔT_{max} is $T_{h,i} - T_{c,i}$. This gives the following equation for the effectiveness of this specific counter flow air-to-water HE without dehumidification:

$$\varepsilon = (T_{h,o} - T_{h,i}) / (T_{h,i} - T_{c,i}) \quad \text{(Eq. B.18)}$$

As for HE1, we assumed an effectiveness of 70% for the counter flow air-to-water HE. By combining equation B18 with the air temperatures determined in Section 3.2.1, the water temperatures of HE2 were calculated.

B.2.3 Heat pump 1

The calculated temperatures of the water flow through HE1 are equal to the required input and output temperatures of the evaporator of HP. The cooling required by HE1 has to be produced by the evaporator of HP1, thus Qhe1 is equal to Qev HP1. As explained within Section 3.2.3, an abundance of heat will be produced by the condenser. This heat will be removed using water-to-air heat exchanger 3 (Fig. 3.2). This section will explain the calculations made to define the quantity of heat produced by the condenser and removed via HE3, together with the total energy use of the cooling and dehumidification system. This includes the energy use by HP1, the fans, and pumps.

TOC

B.2.3.1 Temperatures of the condenser and evaporator

The effectiveness of the condenser and evaporator of a heat pump were calculated with the following equation (Ezgi, 2017):

$$\varepsilon = 1 - EXP(-NTU) \quad \text{(Eq. B.19)}$$

Within evaporators and condensers C_{min} / C_{max} is zero, as $C_p * \dot{m}$ in of the refrigerant within the evaporator and condenser is infinite. Using the graphs of Ezgi (2017), we assumed an effectiveness of 90% for counter flow evaporators and condensers and 80% for parallel flow.

In the baseline vertical farming system, $T_{h,i}$ and $T_{h,o}$ of the evaporator were equal to the water temperatures of HE1 (Fig. 3.2). $T_{h,o}$ of the evaporator was equal to $T_{water,in}$ of HE1 as calculated in Section B.2.1. According to RVO (2015) the temperature difference (TD) between the two media of the evaporator is 2 to 8 °C for both water- and air-source evaporators; which is the difference between $T_{c,i}$ and $T_{h,i}$. Within the evaporator the temperature (T_{ev}) is constant and thus $T_{c,i} = T_{c,o}$. Using a TD of 6 °C, $T_{h,o}$, and an effectiveness of 90%, we calculated $T_{h,i}$ and $T_{saturated}$.

The temperature within the condenser is also constant (T_{con}), and thus $T_{h,i} = T_{h,o}$. TD is the difference between $T_{c,i}$ and $T_{saturated}$ of condenser and is around 8 °C higher than $T_{c,i}$ for water-sources, and around 10 °C higher for air-sources (RVO, 2015). As C of the condenser and evaporator where infinite, C_{min} is $C_{pw} * \dot{m}_w$ for water-sources and $C_{p,air} * \dot{m}_{air}$ for air-sources. When applying this finding to equation B.7 this results in the following equiations to calculate the effectiveness.

$$\text{Evaporator: } \varepsilon = (T_{h,i} - T_{h,o}) / (T_{h,i} - T_{sat}) \quad \text{(Eq. B.20)}$$

$$\text{Condenser: } \varepsilon = (T_{c,o} - T_{c,i}) / (T_{sat} - T_{c,i}) \quad \text{(Eq. B.21)}$$

For the cooling and dehumdification system selected for the VF specifically, the water temperature entering the condenser of HP1 were determined by that of mixing valve 1 (Fig B.3, v1), and should be selected somewhere between the water temperature leaving and entering HE2. We have selected a T_{sat} for the condenser of 32 °C, $T_{c,i}$ and $T_{c,o}$ were calculated using a TD of 8 °C, and equation B21.

B.2.3.2 Coefficient of performance

After the temperatures of the refrigerant in the condenser and evaporator were determined the coefficient of performance of the HP could be calculated. Refrigerant R134A was selected for all HPs included in this study, and steady state operation for assumed. Figure B.3 schematizes the refrigeration cycle.

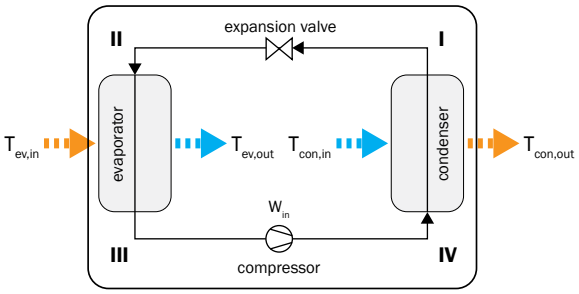

FIG.B.3 HP refrigeration cycle.

In Figure B.3, the T_I is the condenser temperature (T_{con}) at saturated liquid state and T_{III} is the evaporator temperature (T_{ev}) at saturated vapour state. T_{con} and T_{ev} were calculated according to Section B.2.3.1. To find the coefficient of performance (COP) of the HP the T_{II} and T_{IV} had to be determined using the following steps.

Step 1: Draw T_{con} (T_I) on saturated liquid line of the pressure enthalpy (P/H) diagram of selected refrigerant R134a to find $Pbar_I$ (pressure) and $Hbar_I$ (enthalpy).

Step 2: Draw T_{ev} (T_{III}) on saturated vapour line to find P_{III}, H_{III} and S_{III} (entropy) in the P/H diagram.

Step 3: Determine point II as $T_{II} = T_{III}$, $P_{II} = P_{III}$ and $H_I = H_{II}$

Step 4: From point III follow the constant entropy (s) line ($S_{III} = S_{IV}$) to P_I ($=P_{IV}$), to find H_{IV} and T_{IV}. Within the refrigerant cycle $T_I > T_{II}$; $T_{III} < T_{IV}$ and $T_{IV} > T_I$

Step 5: Point IV presents the ideal compression cycle, to determine the actual compression IV' an isentropic efficiency (E) of 0.7 was assumed. This means that 30% more power is required in actual compression than in an ideal cycle.

$$E = (h_{IV} - h_{III}) / (h_{IV}' - h_{III}) \quad \text{(Eq. B.22)}$$

TOC

Step 6: As P_{IV}' = $P_{IV,}$ T_{IV}' was found using the P/H diagram. From h_{IV}' we find h_{III}' and T_{III}' with the P/H diagram, as S_{III}' = S_{IV}' and P_{III}' = P_{III}. T_{III}' – T_{III} is called superheat which should be 4 to 10 °C (RVO, 2015).

To define the heat produced by the condenser first the flow rate of the refrigerant had to be determined. This flow rate is the same throughout the full refrigerant cycle and was calculated using:

$$Q_{ev} = \dot{m}_r * (h_{III} - h_{II}) \quad \text{(Eq. B.23)}$$

Therefore, the heat produced by the condenser was calculated using:

$$Q_{con} = \dot{m}_r * (h_I - h_{Iv}') \quad \text{(Eq. B.24)}$$

Finally, the efficiency (COP) of the heat pump for refrigeration (COP_r) and heating (COP_h) and the energy input of the compressor (W_{in}) were calculated using:

$$COP_r = Q_{ev} / W_{in} \quad \text{(Eq. B.25)}$$
$$COP_r = (h_{III}-h_{II})/(h_{IV}'-h_{III}) \quad \text{(Eq. B.26)}$$
$$COP_h = Q_{con} / W_{in} \quad \text{(Eq. B.27)}$$
$$COP_h = (h_{IV}'-h_I)/(h_{IV}'-h_{III}) \quad \text{(Eq. B.28)}$$

B.2.4 Mixing valves

The flow rates and temperatures entering and leaving a mixing valve were calculated using the following equation:

$$\dot{m}_l = ((T_h - T_f) / (T_h - T_l)) * \dot{m}_f \quad \text{(Eq. B.29)}$$

In which $\dot{m}_l$ is the mass flow rate of the flow entering the valve with lowest temperature (T_l) in kg s^{-1}, T_h the highest temperature entering the valve and T_f the temperature leaving the valve with flow rate $\dot{m}_f$. Flow rate $\dot{m}_f$ is equal to the sum of the two entering flows T_l and T_h.

B.2.5 Heat exchanger outdoor air

The amount of heat removed via HE3 was calculated by subtracting the heat required by HE2 (Qout, Section B.1.2) from the heat produced by the condenser (using equation B24). The temperature within this heat exchanger will be determined in this section. Counter flow air-to-water HE3 uses outdoor air, which is year-round on average 11 °C in the Netherlands (KNMI, 2021), to remove the abundant heat

TOC

produced by the condenser of the HP. The temperatures and heat transfer were calculated in the same way as HE2 using equations B15-B17. The effectiveness of this counter flow air-to-water HE is also 70%. Using equation B29 the temperatures towards mixing valve 2 could be calculated.

B.2.6 Total system performance

Finally, the total energy use of the system had to be calculated. The overall system performance, the coefficient of system performance (COSP), was determined by including the energy use of the heat pump(s), and the necessary fans (E_{fans}) and pumps (E_{pumps}) within the system.

$$E_{tot} = W_{in,tot} + E_{tot,fans} + E_{tot,pumps} \quad \text{(Eq. B.28)}$$

$$COSP = Q_{vf} / E_{tot} \quad \text{(Eq. B.29)}$$

B.2.6.1 Energy use pumps

The energy use of pumps was calculated with the following equations:

$$E_{pump}\,[kW] = (\Delta p * C) / (36 * \eta) \quad \text{(Eq. B.30)}$$

$$C = \dot{m}_w / p_{water} \quad \text{(Eq. B.31)}$$

In which Δp is the pressure difference in bar, C the capacity of the pump in $m^3\,s^{-1}$, η the overall efficiency of the pump, $\dot{m}_w$ the flowrate through the pump in kg s^{-1}, and p_{water} the water density in kg m^{-3}. According to Kaya et al., (2021) the efficiency of an optimised pump is 72%, this includes the efficiencies of the motor, motor-to-pump coupling, pump, piping, and the variable speed drive. The pressure differences were calculated by:

$$\Delta p = 0{,}981 * h * SG \quad \text{(Eq. B.32)}$$

In which h is the head in m, and SG the specific gravity of the fluid, which is 1 for water. The head is the height difference between the fluid being moved and the discharge point. We assumed that HE1 and HE2 were located on top of the VF unit, therefore, a head of 3m was used between the evaporator and condenser and the discharge points, i.e. HE1 and HE2. To obtain yearly energy use the energy use of the pumps in kW was multiplied by the hours the pumps are active, which we set equal to the photoperiod in the farm.

TOC

The pumping energy required to transport the produced heat (or cold) towards the floor heating/cooling system of the baseline or host-building was excluded from this study. This pumping energy would depend on the head, i.e. the height difference between the location of the HP and the discharge point (floor heating or cooling system). This height difference depends on the design of the building which is unknown. A head difference of 100m for pumping energy required for the ATES system in integration strategy E2 was used.

B.2.6.2 Energy use fans

The energy use of the fans within the system is calculated according to the method described by Graamans et al. (2020), using the following equations:

$$E_{fan} = (V_{air} / \eta) * \Delta P \quad \text{(Eq. B.33)}$$

$$\Delta P = ((\mu_{air}^2 * \rho_{air})/2) + \Delta P_{fl} \quad \text{(Eq. B.34)}$$

$$\Delta P_{fl} = 3{,}4 * \mu_{air}^2 + 4{,}9 * \mu_{air} \quad \text{(Eq. B.35)}$$

In which E_{fan} is the power usage of the fans in W, V_{air} the flow rate in $m^3\ s^{-1}$, ΔP the pressure difference in Pa, η overall the fan efficiency of 65% (Graamans et al., 2020), μ_{air} the air velocity in $m\ s^{-1}$, ρ_{air} the density of air in $kg\ m^{-3}$, and ΔP_{fl} the friction loss. The air velocity within the main supply and extraction ducts of industrial functions is 6-12 $m\ s^{-1}$, that of air intake from the outside within industrial functions is 5-6 $m\ s^{-1}$, and that of air intake from outside within public functions is max. 4.5 $m\ s^{-1}$ (Engineering Toolbox, 2003). Air velocities of 8 and 6 $m\ s^{-1}$ were selected respectively for the VF, an air velocity of 4.5 $m\ s^{-1}$ was used for the air intake from the outside within the baseline of the studied building functions, i.e. apartments, offices, restaurants, and swimming pools. Within real designs the flow rates will be split over multiple fans to limit duct sizes.

B.3 Baseline conditions host buildings

This research included apartments, offices, restaurants, swimming pools and supermarkets. For each function, data were collected on the average thermal energy demands (heat and cold), and the inputs and outputs of water, nutrients and food. To determine the energy savings achieved with building-integration the baseline energy use for heating and cooling the host-building was calculated.

B.3.1 Baseline thermal energy demands

The measured on-the-meter natural gas and electricity consumption of the A- and C-label apartments were collected from CBS (2018a; b) together with those of restaurants and supermarkets (CBS, 2018d). For non-residential functions CBS did not provide insight into the energy use per energy label, therefore, the energy use data of A- and C-label offices were collected from Sipma et al. (2017). Stimular (2022a) provided the measured energy use of both indoor and outdoor swimming pools. To convert on-the-meter natural gas consumption into heating demands, the share of gas used for heating, domestic hot water (DHW), and cooking was determined for each function using CBS (2018c), ECW (2022) and Sipma (2019). A boiler efficiency of 90% was assumed for space heating. The heating demands were corrected using the heat degree day method for the period 2011-2020 (KWA, 2022). The heating and cooling demands of BENG-labelled apartments and offices were based on simulated data from ECW (2022).

The share of the total electricity consumption used to cooling offices, restaurants and supermarkets in the Netherlands is respectively 17%, 15% and 88% (KWA, 2016). The cooling demands were calculated by using an air-conditioner coefficient of performance (COP) of 4 in offices and restaurants, and a COP of 3 in supermarkets (KWA, 2016). These cooling demands were corrected using the cooling degree day method for the period 2011-2020 (KWA, 2022). According to CBS (2018c) only 1% of the electricity consumption in apartments is used for cooling. Although air-conditioner units are growing in number, cooling systems are not common in residential buildings in the Netherlands (Hooff et al., 2016). With climate change, air-conditioners are expected to become more standard, especially for new buildings. According to Hooff et al. (2016), residential buildings with an average thermal resistance (R_c) of 6.5 for closed surfaces and solar shading systems have a cooling demand of 2.5 kWh m^{-2}. Less insulated buildings (R_c = 4.0) without solar shading have a cooling demand of 4.5 kWh m^{-2}.

TABLE B.2 Heating and cooling demands per m2 floor area per year for an apartment, small office, larger office, restaurant, outdoor swimming pool, indoor swimming pool and a supermarket.

Building function	Energy label	Heat demand kWh m^{-2} y^{-1}	Cooling demand kWh m^{-2} y^{-1}
Apartment	BENG*[1]	40.9	2.5
	A-label	55.5	2.5
	C-label	75.6	4.5
Office small (250-2500 m^2)	BENG*[1]	22.8	11.4
	A-label	95.3	51.0
	C-label	108.5	48.3
Office larger (2500-5000 m^2)	BENG*[1]	34.3	17.2
	A-label	68.9	59.2
	C-label	86.5	57.1
Restaurant	Average	191.9	58.7
Swimming pool[2]	Indoor	2022.3	
	Outdoor[3]	141.6	
Supermarket (1000-2500 m^2)	Average	99.0	407.0

1. BENG data are based on simulated data, all other data are measured;
2. Energy use swimming pool is indicated per m^2 water surface;
3. The outdoor pool is opened 5 months per year, the indoor pool year-round.

B.3.2 Baseline energy use

The baseline energy use was calculated for BENG, A- and C-label apartments (80 m^2), BENG, A- and C-label offices (250-2500 m^2 and 2500-5000 m^2), restaurants, and indoor and outdoor swimming pools. We included a reversible HP system that uses ambient air as baseline heating and cooling system. In this research, we focus on heating and cooling only, domestic hot water (DHW) production was excluded. In general, low temperature space heating was supplied with a floor heating system of 40°C supply. The C-label apartment and offices used radiators with a supply temperature of 70°C. The return temperature of floor heating was 10°C lower than the supply temperature, and the return temperature of radiators decreased by 20°C (Maivel and Kurnitski, 2015). To avoid condensation, we used LT floor cooling with a supply temperature of 18°C and a return temperature of 23°C for all typologies. The average temperature of the swimming pool was 23°C (Koppejan, 2016). The energy use in heating and cooling modus were calculated according to the methods described in Section B.1 and by including the following assumptions.

Heating of the apartments, offices and restaurants took place somewhere in the 5-month heating season when the average ambient temperature is 4.5°C (1). Residential buildings were cooled when the outdoor temperature reaches 24°C,

TOC

which is about 265 h y^{-1} (Warmtepomp tips, 2022) with an average outdoor temperature of 26.4°C (2). Modern offices start cooling when the outdoor temperature exceeds 12°C (Tillie et al., 2009). Between 2012-2020 the outdoor temperature was 12°C or higher for 4315 h y^{-1} (3), with an average temperature of 17.7°C (KNMI, 2022) (4). For the apartments, offices, and restaurant, the evaporator's exhaust air temperature was set at -2.3°C when heating (5). The exhaust air temperature of the condenser was set at 35°C when cooling an apartment, and 25°C for the office, and 33°C for the restaurant (6). The indoor swimming pool was heated year-round. The outdoor pool was open, and heated, for 5 months between May and September (7). The heat installation of a Dutch indoor pool has about 3648 full load hours a year (8) and an outdoor pool about 1500 h y^{-1} (Koppejan, 2016) (9).

B.3.2.1 Reversible heat pumps

Reversible HPs can switch from one modus into the other, e.g. switch between cooling and heating modus. This was not applicable to the baseline vertical farming system, but will be for buildings that need to be heated and cooled. When heating a building by using outdoor air as the source, the condenser is located at building-side. This can change by reversing the direction of the refrigerant so that the evaporator is located at building side and building is cooled. The direction of flow in the secondary fluid (water or air) is constant. The heat exchange within the condenser and evaporator of a reversible HP will thus be in counter flow for the most prevalent operation and in parallel for the other operation, i.e. heating or cooling (SWEP, 2019). Parallel operation results in a lower HE effectiveness, therefore an evaporator and condenser effectiveness of 80% was assumed for parallel mode.

The energy use of the heat pumps that heat and cool the buildings was calculated in the following way. First the temperature of the evaporator and condenser had to be determined. In the heating season, the temperature entering the condenser is equal to the return temperature of the heating system, and the temperature leaving the condenser is equal to the required supply temperature of the heating system. The condenser temperature is calculated using these values, Equation B21, and a condenser effectiveness of 90%. The evaporator temperature is calculated using Equation B20 and an evaporator effectiveness of 90%. The supply temperature of the evaporator is equal to that of the outdoor air, the return temperature is calculated using a TD of 2 to 8 °C (Section B.2.3.1). In summer, the evaporator temperature is calculated using the floor cooling return and supply temperature. The condenser temperature is calculated using the outdoor temperature and a TD of 8 °C. For the summer calculations, Equations B20 and B21 are used and a effectiveness of 80%.

To define the energy use and COP of the HP the steps described in Section B.2.3.1 are followed. In winter, the heat produced by the condenser is equal to the building's heating demands. In summer, the cold produced by the evaporator is equal to the building's cooling demands.

B.3.3 Food

A Dutch person consumes about 3.1 kg of food per day, and 1 kg when excluding beverages. The vegetable intake is on average 0.131 kg d^{-1} (RIVM, 2018). As a vegetable intake of 250 g d^{-1} is recommended this quantity was used as vegetable demand in this research. About 6% of the daily vegetable intake is consumed during lunch and 83% during dinner (RIVM, 2020). To provide healthy lunches, we assumed the average vegetable intake during dinner to be applicable for office lunches.

B.3.4 Water

An average Dutch person uses 120.1 L d^{-1} water of which 33.7 L is used for toilet flushing (Samenwerkende Drinkwaterbedrijven, 2011). The average toilet usage is 6 times a day (Blokker & Vloerbergh, 2011). We assumed the toilet was used 4 out of 6 times a day at home, once a day at the office, and once per restaurant visit. On average, a full time employee (FTE) in the Netherlands works 228 days y^{-1}. Per FTE, an average Dutch office uses 7.1 (Stimular, 2022b) to 7.3 m^3 water y^{-1} (Samenwerkende Drinkwaterbedrijven, 2011). For restaurants, the water usage is about 20 L per visitor (Samenwerkende Drinkwaterbedrijven, 2011). The water use of swimming pools was collected from Stimular (2022a) and included the water required to fill up any water losses in the pool. The water use in swimming pools was presented per visitor. Table B.3 presents the water inputs and outputs for one visitor visiting the pool each day, 6 days a week. There were no data available on toilet usage in swimming pools and it was assumed that the water used for toilet flushing was negligible in comparison to the total water use of the swimming pools. The buildings in this research reuse grey water for toilet flushing to reduce tap water demands.

B.3.5 Nutrients

Nutrients leave the human body via faeces and urine. Nutrients can be recovered from black water to replace synthetic fertilisers. Urine consists most nutrients (D'Ostuni et al., 2023). When only including the macro (e.g. C, H, O, N, P, K, Ca, S and Mg) and micro (e.g. Fe, Cl, Mn, B, Zn, Cu and Mo) nutrients required for plant growth (Goddek et al., 2015) this results in a total of at least 65 g p.p. d^{-1} (calculated with Rose et al., 2015). To match the commercial fertiliser recipes 46% of these nutrients will used. The quantity of nutrients for each building were calculated according to the toilet usage, e.g. $^{4}/_{6}$ of the nutrients from human excreta were recovered per inhabitant of the apartment, and $^{1}/_{6}$ per FTE or restaurant visitor.

TABLE B.3 Inputs and outputs of water, vegetables and nutrients per person per year of the different functions. The restaurant and swimming pool data include 1 visitor per day of the year the facility is opened. The restaurant is opened 4 days a week, the indoor pool 7 days a week and the outdoor pool 7 days a week for 5 months. The supermarket represents the food bought by customer.

		Apartment		Office		Restaurant		Supermarket		Swimming pool indoor		Swimming pool outdoor	
		1 persons		1 person (fte)		1 visitor		1 visitor		1 visitor		1 visitor	
Resource	Unit	In	Out	In	Out	In	Out	In	Out	In	Out	In	Out
Water													
Drink water	kg y^{-1}	31536	0	1281	0	2992	0	n/a	n/a	35880	0	14950	0
Grey water	kg y^{-1}	0	23336	0	0	0	1823	n/a	n/a	0	24960	0	10400
Black water	kg y^{-1}	0	8200	0	1281	0	1168	n/a	n/a	n/a	n/a	n/a	n/a
Biomass													
Vegetables	kg y^{-1}	91		57		52		91		n/a		n/a	
Nutrients*	kg y^{-1}		7		1		1		n/a		n/a		n/a

**Share of nutrients recovered from black water to match the commercial fertiliser recipe.*

TOC

B.4 Energy synergies

This section presents the calculations related to the energy use of the selected integration strategies to create bidirectional exchange of thermal energy between the vertical farm and the buildings. The selected strategies included: direct integration with a HE (A1), direct integration with a HP (B1), and integration with ATES using two HPs (E2).

B.4.1 Direct integration with HE (A1)

Within direct integration strategy A1, HE3 of the baseline cooling and dehumidification system of the VF (Fig. 3.2) is replaced by a water-to-water HE connecting the vertical farm to the building (Fig. 3.3). Due to the low-temperature characteristic of the heat produced by the VF this integration strategy was only applicable for swimming pools. The return and supply temperature of the swimming pool were determined in Section B.3.2, i.e., 23 °C supply and 30 °C return. These temperatures determined $T_{c,i}$ and $T_{c,o}$ of HE3. When using an effectiveness of 80% and equation S18, $T_{h,i}$ and $T_{h,o}$ of HE3 were calculated. QHE3 was equal to the amount of heat produced at HE3 by one m^2 cultivation area of the VF in the baseline cooling and dehumidification strategy. The water surface of the swimming pool that could be heated with this bidirectional thermal energy exchange was calculated using the heating demands per m^2 water surface as determined in Section B.3.1.

B.4.2 Direct integration with HP (B1)

By direct integration of vertical farms in buildings using a HP (B1), higher temperatures could be provided to the building as HE3 (Fig. 3.2) was replaced by HP2 (Fig. 3.3). HP2 upgrades the residual heat of the vertical farm to the temperatures required for low- and mid-temperature heating (Section B.3.2). HP2 cannot provide cooling for the VF and building at the same time, therefore, this bidirectional thermal energy exchange is only applicable in winter. Outside the building's heating system, both vertical farm and building switch to their baseline energy systems as defined in Sections B.1.3 and B.3.1.

$T_{c,i}$ and $T_{c,o}$ of the condenser were equal to the supply and return temperatures of the low-temperature floor heating system or mid-temperature radiator. The condenser temperature was calculated using equation B21 and a 90% effectiveness.

TOC

The evaporator temperature was calculated using $T_{h,i}$ and $T_{h,o}$ as determined for HE3 in the baseline vertical farming system, a 90% effectiveness, and equation B20. Using the methods described in Section B.2.3.2, the energy use of the heat pump was calculated. The energy produced by the evaporator (Qev) was set equal to the cooling demands of one m^2 cultivation area of the VF at air-to-water HE3 in the baseline cooling and dehumidification system of the VF.

B.4.3 Integration with ATES using two HPs (E2)

The integration of the VF and building using an ATES system and two heat pumps made it possible to have a year-round bidirectional exchange of thermal energy. The energy performance of this system had to be calculated for both the buildings heating season, and the intermediate and cooling season. In the latter, HP3 was in cooling modus. In winter, HP3 is in heating modus. Therefore, HP3 is a reversible HP and the condenser and evaporator have a effectiveness of 80% in summer, and 90% in winter (Section B.3.2.1).

B.4.3.1 Heating season

The temperatures in the water circuit between HP2 and HP3 were determined by the storage temperatures within the ATES system. These temperatures were set at 25 °C for the hot source, and 5 °C for the cold source, and also defined $T_{h,i}$ and $T_{h,o}$ in HE4. Using equation B18 and a 80% efficiency for the water-to-water HE4, we could calculate $T_{c,i}$ and $T_{c,o}$ of HE4. These were equal to $T_{c,i}$ and $T_{c,o}$ of the condenser of HP2, and $T_{h,i}$ and $T_{h,o}$ of the evaporator of HP3.

The condenser temperature of HP2 was thus calculated using equation B21, and an effectiveness of 90%. The evaporator $T_{h,i}$ and $T_{h,o}$ were equal to that of HE3 in the baseline cooling and dehumidification strategy of the VF. The same applied to the cooling demands of the evaporator (Q_{ev}). The evaporator temperature was calculated using equation B20, and an effectiveness of 90%. $T_{c,i}$ and $T_{c,o}$ of the HP3's condenser were equal to the supply and return temperature of the low-temperature floor heating system or the mid-temperature radiators of the building. The evaporator and condenser temperature of HP3 were again calculated with an effectiveness of 90%, and equations B20 and B21. The cold produced by the evaporator of HP3 was equal to the amount of heat supplied by the vertical farm and the heat extracted from the ATES hot source. Using the methods in Section B.2.3.2 the energy use of HP2 and HP3 was calculated.

B.4.3.2 Cooling and intermediate season

Outside of the building's heating season, the cold produced by the vertical farm was stored within the ATES hot source. Furthermore, the cold produced by HP3 when cooling the building was also stored in the ATES hot source during summer. The calculations follow a similar approach as those for the heating season. However, the temperatures in the water circuit between HP2 and HP3 were different as the ATES system works the other way around. The temperature of the ATES is still 25 °C for the hot source and 5 °C for the cold source, however, cold is extracted and heat is stored. Therefore, these temperatures now define $T_{c,o}$ and $T_{c,o}$ HE4, affecting the temperatures between HP2 and HP3. Furthermore, HP3 will be in cooling mode, and is thus a reversed HP. This results in a condenser and evaporator effectiveness of 80% when in cooling mode. $T_{h,o}$ and $T_{h,i}$ of the evaporator of HP3 are determined by the return and supply temperature of the floor cooling system.

References

Blokker, E.J.M., Vloerbergh, I.N. 2011. Kwantitatieve toekomstscenario's waterverbruik: DIMDEUM ingezet voor het berekenen van totaal en piekverbruik. https://edepot.wur.nl/450924.

CBS. 2018a. Aardgaslevering vanuit het openbare net: woningkenmerken. https://opendata.cbs.nl/statline.

CBS. 2018b. Elektriciteitslevering vanuit het openbare net: woningkenmerken, bewoners. https://opendata.cbs.nl/statline.

CBS. 2018c. Energieverbruik van particuliere huishoudens. https://www.cbs.nl/nl-nl/achtergrond/2018/14/energieverbruik-van-particuliere-huishoudens

CBS. 2018d. Energiekentallen utiliteitsbouw dienstensector: oppervlakte klasse. https://opendata.cbs.nl/statline/#/CBS/nl/dataset/83374NED/table?ts=1642090250137.

Chaware, P. 2016. Multiple pass and cross flow heat exchangers. Cummins College of Engineering. https://paragchaware.files.wordpress.com/2016/08/ntu.pdf.

D'Ostuni, M., Stanghellini, C., Boedijn, A., Zaffi, L., Pennisi, G., Orsini, F. 2023. Evaluating the impacts of nutrient recovery from urine in wastewater in Building-Integrated Agriculture: a test case study in Amsterdam. Sustain. Cities and Soc. 91. https://doi.org/10.1016/j.scs.2023.104449.

Engineering Toolbox. 2003. Air Duct Velocities. https://www.engineeringtoolbox.com/flow-velocity-air-ducts-d_388.html

Expertise Centrum Warmte. 2022. Uniforme maatlat gebouwde omgeving 5.03 [dataset]. https://www.expertisecentrumwarmte.nl/themas/technische+oplossingen/de+uniforme+maatlat+gebouwde+omgeving/default.aspx.

Ezgi, C. 2017. Basic design methods of heat exchanger. In: Murshed, S.S., Lopes, M.M. (Eds.), Heat exchangers – design, experiment and simulation. IntechOpen. https://doi.org/10.5772/67888.

Goddek, S., Delaide, B., Mankasingh, U., Ragnarsdottir, K.V., Jijakli, H., Thorarinsdottir, R. 2015. Challenges of sustainable and commercial aquaponics. Sustain. 7(4), 4199-4224. https://doi.org/10.3390/su7044199.

Graamans, L., Tenpierik, M., van den Dobbelsteen, A., Stanghellini, C. 2020. Plant factories: reducing energy demand at high internal heat loads through façade design. Appl. Energy. 262. https://doi.org/10.1016.j.apenergy.2020.11454.

Graamans, L.J.A. 2021. Stacked: the building design, systems engineering and performance analysis of plant factories for urban food production [Doctoral dissertation, Delft University of Technology]. A+BE | Architecture and the Built Environment. https://doi.org/10.7480/abe.2021.05.

Hooff, van T., Blocken, B., Timmermans, H.J.P., Hensen, J.L.M. 2016. Analysis of the predicted effect of passive climate adaptation measures on energy demand for cooling and heating in a residential building. Energy. 94, 811-820. https://doi.org/10.1016/j.energy.2015.11.036.

Kaya, D., Çanka Kılıç, F., Öztürk, H.H. 2021. Energy efficiency in pumps. In: Kaya, D., Çanka Kılıç, F., Öztürk, H.H. (Eds.), Energy management and energy efficiency in industry. Green energy and technology. Springer, Chambridge, pp. 329-374. https://doi.org/10.1007/978-3-030-25995-2_11.

KNMI 2021. De Bilt, langjarige gemiddelde, tijdvak 1991-2020 [dataset]. http://www.knmi.nl/klimaat-viewerKNMI 2022. De Bilt, uurwaarnemingen, tijdvlak 2012-2022 [dataset]. https://daggegevens.knmi.nl/klimatologie/uurgegevens.

Koppejan, J. 2016. Inventarisatie van markttoepassingen van biomassaketels en bio-wkk. https://www.rvo.nl/sites/default/files/2017/04/Rapportage-Marktkansen-bioketels.pdf

KWA. 2016. Het elektrisch energieverbruik en het warmteaanbod van koelinstallaties voor een veertigtal bedrijfssectoren. KWA, Amersfoort.

KWA. 2022. Graaddagen_11-20 [dataset]. https://www.kwa.nl/diensten/graaddagen-en-koeldagen. Maivel, M., Kurnitski, J. 2015. Heating system return temperature efficiency effect on heat pump performance. Energy and Build. 94, 71-79. https://doi.org/10.1016/j.enbuild.2015.02.048.

Mansour, M.K., Fath, H.E. 2016. A new and practical ε-NTU correlation for the humidification process under different Lewis number. Desalination. 395, 72-28. https://doi.org/10.1016/j.desal.2016.05.025.

RIVM. 2018. Voedselconsumptie 2012-2016: wat, waar en wanneer. https://www.rivm.nl/sites/default/files/2018-11/Factsheet%20Voedselconsumptie%202012%20-%202016%20Wat%2C%20waar%20en%20wanneer.pdf.

RIVM. 2020. DNFCS 2012-2016: mean distribution (%) of moment of a food group [dataset]. https://statline.rivm.nl/#/RIVM/nl/dataset/50070NED/table?ts=1583415567279.
Rose, C., Parker, A., Jefferson, B., Cartmell, E. 2015. The characterization of feces and urine: a review of the literature to inform advanced treatment technology. Crit. Rev. Reviews in Environ. Sci. and Technol. 1827-1879. https://doi.org/10.1080/10643389.2014.1000761.
RVO. 2015. Best practice koudetechniek. https://www.rvo.nl
Samenwerkende drinkwaterbedrijven. 2011. Waterwerkblad: berekeningsgrondslagen gemiddeld waterverbruik per etmaal voor mens, dier en plant. https://www.infodwi.nl/IDWI/media/infodwi/WB-2-1-B-dec-2015.pdf.
Sipma, J.M., Kremer, A., Vroom, J. 2017. Energielabels en het daadwerkelijk energieverbruik van kantoren. https://www.publicaties.ecn.nl.
Sipma, J.M. 2019. Het daadwerkelijk energieverbruik van gelabelde en niet-gelabelde restaurants. https://www.rvo.nl.
Stimular. 2022a. Gemiddelde milieubelasting zwembaden. https://www.milieubarometer.nl/voorbeelden/zwembad/
Stimular. 2022b. Milieubarometer kantoor. Retrieved https://www.milieubarometer/nl/voorbeeld/kantoor
SWEP. 2019. Refrigeration handbook. https://www.swep.net/refrigerant-handbook/refrigerant-handbook/
Tillie, N., van den Dobbelsteen, A., Doepel, D., de Jager, W., Joubert, M., Mayenburg, D. 2009. Towards CO2 neutral urban planning: introducing the Rotterdam energy approach and planning (REAP). J. Green Build. 4, 103-112. https://doi.org/10.3992/JGB.4.3.103.
Warmtepomp tips. 2022. Kengetallen voor een woning. https://warmtepomp-tips.nl/warmtepomp/kengetallen.

APPENDIX C

Chapter 4

C.1 Energy profiles neighbourhood

C.1.1 Baseline energy profile

In 2022, the buildings in the Westindische Buurt primarily relied on natural gas for heating, using individual boilers (96%) or block heating systems (2%) (CBS, 2022a). On average, the apartments consumed 900 m^3 of natural gas (CBS, 2021a). Approximately 8.8% of this energy was used for cooking (CBS, 2018a). The non-residential buildings collectively consumed 455,000 m^3 natural gas annually (Klimaatmonitor, 2023), which averages 365 m^3 per company registration. As we focus on the year 2025, we do not include for energy retrofitting measures. Therefore, the energy demands were based on the consumption patterns observed in 2022 (Table C.1).

TABLE C.1 Baseline energy use of the Westindische buurt.

	Residential	Non-residential	Total
	MWh y^{-1}	MWh y^{-1}	MWh y^{-1}
Heating and DHW	29,124	4,445	33,569
Electricity	7,046	3,773	10,819
Total	36,170	8,218	44,388

C.1.2 Heating and domestic hot water demands

The hourly fraction of the total annual natural gas consumption is made publicly available by MMFBAS (2023). These figures present the expected percentage of the total natural gas consumption per hour for small connections (G1A) with a maximum annual consumption of 5,000 m^3, and for larger consumers (G2A) with a maximum annual consumption of 170,000 m^3 for the year 2023. Based on the average gas consumption of households and companies in the Westindische Buurt, we assumed that all natural gas connections fall under the G1A category.

To derive heating and domestic hot water (DHW) use profiles, we converted the natural gas use profiles based on MMFBAS using the heating value of Dutch Groningen gas (31.65 MJ m^{-3}) and a 90% efficiency for high-efficiency natural gas boilers. With the current energetic performance, mid-temperature heating of 70 °C will be provided using the existing radiators. The return temperature is approximately 50 °C (Maivel and Kurnitski, 2015). DHW is supplied at 55 °C.

C.1.3 Cooling demands

Since no data were available on the cooling demands of the Westindische Buurt, assumptions had to be made to estimate these demands. The cooling demands of the neighbourhood are categorized as supermarket cooling (i.e., product cooling), and space cooling of residential and non-residential purposes. There are four large supermarkets located in the neighbourhood with respective floor areas of 988, 987, 1,255 and 1,379 m^2 (maps.amsterdam.nl). On average, 88% of the electricity use by supermarkets is used for product cooling with a coefficient of performance (COP) of 3 (KWA, 2016). The average electricity use per m^2 floor area was obtained from CBS (2018b). We assumed that the product cooling requirements were evenly distributed throughout the year.

The total electricity use of the non-residential functions amounts 5,435 MWh annually (Klimaatmonitor, 2023), including that of the supermarkets. The electricity use for space cooling of hospitality, retail, and office functions averages 14% of their total electricity use, using a COP of 3 of the cooling installations (KWA, 2016). KoWaNet provides insight into the average cooling demands per square meter apartment in the Netherlands based on their energy labels (Jansen et al., 2021b). The energy labels were obtained from allecijfers.nl. Space cooling will be supplied through the existing radiators at about 12 °C supply, and 22 °C return. Daily and monthly space cooling demand profiles were generated using cooling degree days (KWA, 2022). We assumed that no non-residential cooling takes place after 19.00.

C.1.4 Electricity use

The user-related electricity use of the Westindische Buurt includes the energy consumed by the buildings in the neighbourhood, excluding energy for heating, cooling and DHW production. Additionally, we included the expected electricity use for electric vehicle charging in 2025.

On average, the households within the Westindische buurt use 1940 kWh of electricity per household, excluding electricity use for cooling (CBS, 2021b). In total, the non-residential functions use 5,435 MWh annually (Klimaatmonitor, 2023), including electricity use for cooling, which should be subtracted when calculated according to Section C.1.3. The monthly and daily (January 18th, and July 24th) user-related energy profiles of residential and non-residential functions are generated using the 15 minute profile fractions provided by MMFBAS (2023). These fractions represent the share of the annual electricity used every 15 minutes of the year. Different profile fractions are developed for various electricity grid connections sizes. We assumed that the households use E1 connections, which are suitable for households with standard appliances, including solar panels, induction cooking, heat pumps, and electric vehicle charging. Non-functions employ E2 connections, designed for larger residences and small businesses (Enexis, n.d.).

Currently, households within the Westindische Buurt own an average of 0.37 cars per household (CBS, 2022b). According to Refa et al. (2019), 5% to 10% of the passenger cars in the municipality of Amsterdam will be electric by 2025. The yearly energy use for charging these electric vehicles is calculated using the following assumptions. Electric cars in the Netherlands cover a distance of 15,144 to 16,890 km annually (CBS, 2022b; Refa et al., 2023) (1). Charging these vehicles requires about 0.2 kWh km^{-1} (2), with approximately 75% of the charging occurring within the neighbourhood (3) (Refa et al., 2023). To define monthly electricity profiles we assumed that the total daily electricity use for electric vehicles charging in the neighbourhood remains consistent throughout the year. The daily profile is generated using the grid-conscious public charging profile for 100 electric vehicles as defined by Refa et al. (2023). Since all residences are apartment buildings, we assumed that only public charging points are available within the neighbourhood. Refa et al. (2023) provides both standard and grid conscious profiles for electric vehicle charging. When employing grid conscious charging, the total daily electricity use remains constant, but the charging power is reduced in the evening to minimise additional electricity peaks in the grid.

C.2 Temperatures in the grid

The temperatures in the grid depend on the temperatures of the connected heat exchangers for passive heating or cooling, and the heat and cold extracted from the aquifer thermal energy storage (ATES) systems. For active heating and cooling with heat pumps (HPs), the HP can produce the desired temperature in the grid. The following section describes how temperatures within heat exchangers (HE) are calculated. HP calculations are discussed in Section C.3.1.

C.2.1 Heat exchangers

The effectiveness of a counter flow water-to-water HE is set at 80%. The effectiveness is calculated using the following formulas:

$$\varepsilon = (T_{c,o} - T_{c,i}) / (T_{h,i} - T_{c,i}) \quad \text{(Eq. C.1)}$$

$$\varepsilon = (T_{h,i} - T_{h,o}) / (T_{h,i} - T_{c,i}) \quad \text{(Eq. C.2)}$$

Where $T_{c,i}$ is the incoming temperature of the cold liquid, $T_{c,o}$ the increased temperature of the cold fluid leaving the heat exchanger, $T_{h,I}$ is the temperature of the hot fluid entering the heat exchanger, and $T_{h,o}$is the reduced temperature of the hot fluid leaving the heat exchanger. In this study, we assumed no heat losses occurred within the heat exchangers. The heat exchanged within the HE (Q) is calculated using Equation B16.

C.2.2 Building heating temperatures

The buildings required both space heating at 70 °C, and domestic hot water of 55 °C (Section C.1.2). This heat is provided passively with a HE, or actively with individual HPs. In both cases these temperatures define $T_{c,o}$ of the HE or the HPs condenser. The return temperature $T_{c,i}$ are defined by the radiator return temperature of 50 °C (Section C.1.2), and the tap water supplies of 12 °C. By using the following formula the $T_{c,i}$ and $T_{c,o}$ are simplified to one temperature each (Conrad and Greif, 2019):

$$T_{fl} = (T_{heating} * \%_{heating}) + (T_{dhw} * \%_{dhw}) \quad \text{(Eq. C.3)}$$

TOC

T_{fl} represents the resulting supply or return temperature for space heating and domestic hot water combined in Kelvin, $T_{heating}$ is the space heating supply or return temperature in Kelvin, $\%_{heating}$ is the fraction of the space heating demands in the total heat demands, T_{dhw} is the supply or return temperature of DHW in Kelvin, and $\%_{heating}$ is the share of the DHW in the total heat demands.

C.3 Energy use by the energy systems

This section explains how the energy use of the different district heat network configurations are calculated, these include the energy used by the centralised or decentralised HPs to produce MT heat (Section C.3.1), energy used for active space or product cooling using a HP (Section C.3.2), electricity used by the pumps of the DHN (Section C.3.3), and pumps in the ATES system (Section B.2.6.1). The electricity used to distribute heat or cold within the buildings is excluded.

C.3.1 Heat pump in heating modus

C.3.1.1 Centralised HP

The effectiveness (ε) of the condenser and evaporator of the centralised HP was set at 90% for counter flow evaporators and condensers (Section B.2.3.1). The supply and return temperatures towards the condenser are equal to those of the mid-temperature DHN, i.e., $T_{c,i}$ as the temperature of the colder return pipe, and $T_{c.o}$ as the temperature of the mid-temperature warm pipe. The condenser temperature (T_1) is calculated using Equation B21.

The supply and return temperatures of the evaporator are defined by the temperatures in the ultra-low temperature grid. The supply temperature ($T_{h,i}$) is equal to the ultra-low temperature pipe, and the return temperature ($T_{h,o}$) to the temperature of the cold pipe. The evaporator temperature (T_3) is calculated using Equation B20.

To define the electricity use of the HP, its coefficient of performance (COP) should be calculated.

TOC

We have selected refrigerant R134A for all HPs included in this research. The temperature of the condenser ($T_{con} = T_1$) and that of the evaporator ($T_{ev} = T_3$) were calculated using equations B20 and B21. T_1 is the condenser temperature (T_{con}) at saturated liquid state and T_3 is the evaporator temperature (T_{ev}) at saturated vapour state. To find the coefficient of performance (COP) of the HP the temperature of the refrigerant entering the evaporator (T_2) and entering the condenser (T_4) within the HP cycle had to be determined using the steps described in Section B.2.2.

C.3.1.2 Decentralised HPs

When the mid-temperature heat is generated using decentralised HPs connected the ultra-low temperature grid, the input temperature of the evaporator ($T_{h,i}$) is equal to that of the ultra-low temperature grid, and the return temperature ($T_{h,o}$) to that of the cooling grid. The input temperature of the condenser ($T_{c,i}$) is equal to the return temperature of the building's heating and DHW systems, the condenser's output temperature to that of the required supply temperature of the heating demand ($T_{c,o}$). As the input and output temperature of the condenser depend on the temperatures for heating and DHW equation C.3 is used. The COPs of the decentralised HPs are calculated following the calculation method described in Section B.2.2.

C.3.2 Heat pump in cooling modus

The electricity use of the HPs in cooling modus are calculated in the same way as the HP in heating modus (Section B.2.2) when they are continuously operating in cooling mode. If a HP is in heating mode for a part of its operation time, a reversible HP is used (Section B.3.2.1). The evaporator temperature for supermarket product cooling was set at -5 °C supply ($T_{h,o}$), and 5 °C return ($T_{h,i}$). The evaporator temperatures for space cooling are set at 12 °C supply ($T_{h,o}$), and 22 °C return ($T_{h,i}$). The condenser uses the temperature from the cold grid ($T_{c,i}$) and supplies the heat produced to the uLT grid ($T_{c,o}$) for both product and space cooling. This applies both to the centralised and the decentralised configurations.

C.3.3 Electricity use of DHN pumps

The energy use (E_{pump}) of a DHN can be simplified using the following formulae (Jansen et al., 2021b):

$$E_{pump} = 0.2 * C \quad \text{(Eq. C.4)}$$

$$C = \dot{m}_w * p_{water} \quad \text{(Eq. C.5)}$$

$$Q = \dot{m}_w * C_{pw} * \Delta T \quad \text{(Eq. C.6)}$$

Where E is the pump energy in kWh, C is the required capacity of the pump in $m^3\ y^{-1}$, p_{water} the water density of 977.0 kg m^{-3}, Q is the total heat or cold distributed by the DHN in MJ, C_{pw} the specific heat capacity of water of 4184 J/ kg K, and ΔT the temperature difference between the warm and cold pipe of the DHN.

C.4 Additional results

C.4.1 Step 1 and 2: Daily energy profiles of the neighbourhood

Figure C.1 illustrates the daily profiles created for heating, cooling and electricity at January 18th and July 24th, 2025. Heating and DHW result in a double peak, with the first peak occurring around 8.00 and the second peak around 19.00, both in winter and summer. In winter, these two peaks are of a similar height, while in summer, the evening peak is notably higher than the morning peak.

The cooling demand has a flat profile during winter, as it solely includes product cooling within the four supermarkets (Section C.1.3). During the summer, a distinctive peak emerges between 13.00 and 19.00, reaching its maximum at 16.00. The electricity profile, which includes user-related electricity and electric vehicle charging, is similar to that of the heating demands, featuring a double peak at 09.00 and 19.00.

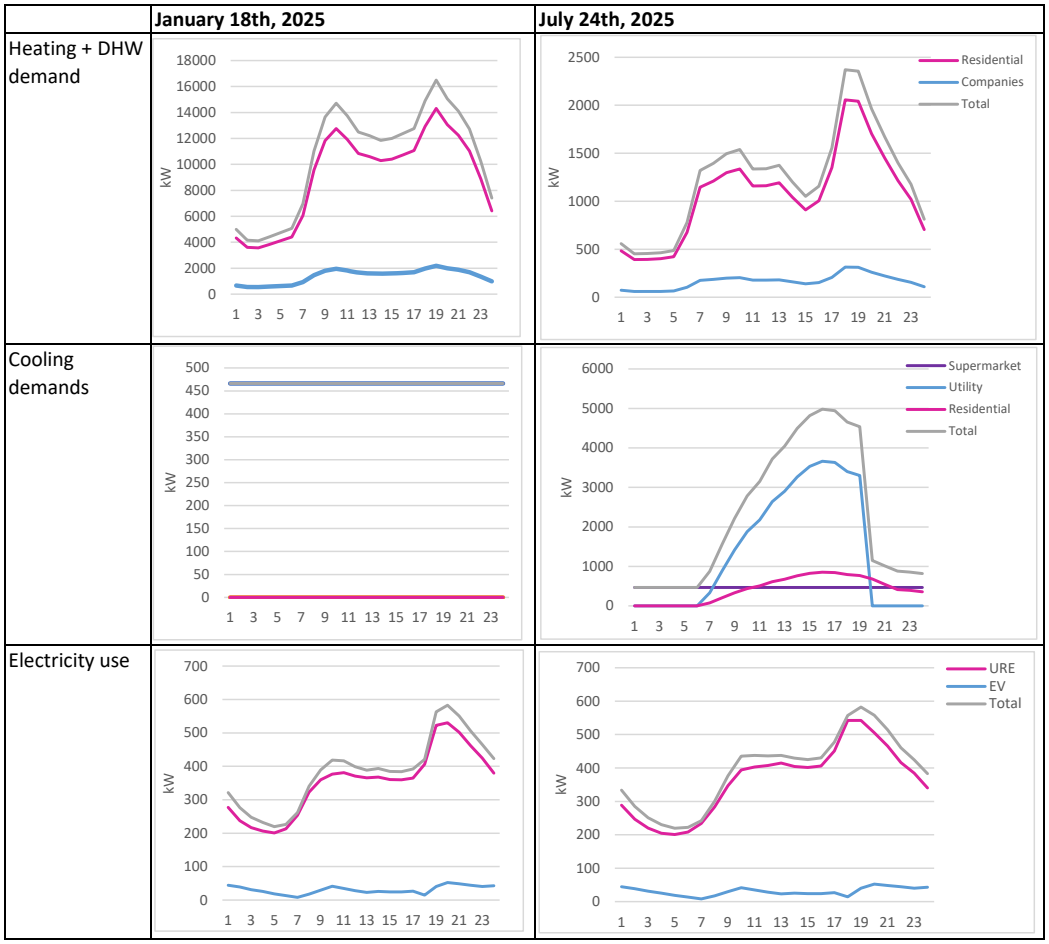

FIG.C.1 Daily heating, cooling and electricity profiles for January 18th and July 24th 2025 of the Westindische Buurt.

TOC

C.4.2 Step 3: Energy profile vertical farm

As defined in step 4 (Section 4.2.4), the aquifer's warm source is 24 °C, and its cold source is 7 °C. For both centralised and decentralised configuration, this results in temperatures of 20 °C and 3 °C in the ultra-low temperature and cold temperature pipes in winter, and 28 °C and 11 °C in summer. The VF consumes 434 kWh m^{-2} y^{-1} of electricity, and produces 462 kWh m^{-2} y^{-1} of residual heat. In summer, the heat pump consumes more energy as the COP is lower due to the higher temperatures in the DHN. The daily electricity profile and residual heat production for January 18th and July 24th 2025 are presented in Figure C.2. Both electricity consumption and residual heat production drop during the 8 hour dark period.

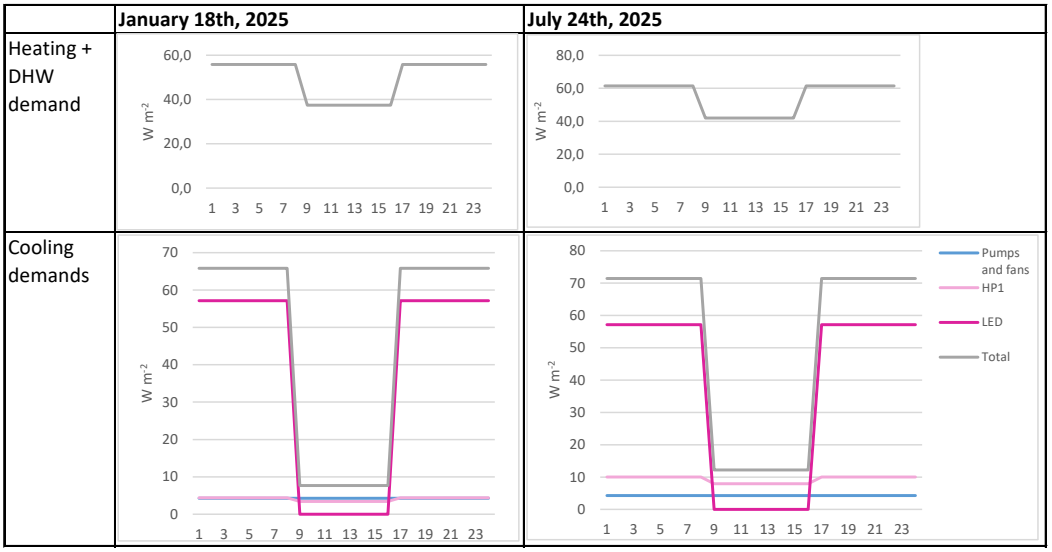

FIG.C.2 Daily residual heat production and electricity profile on January 18th and July 24th 2025 of one square meter cultivation area of a vertical farm with a 16h photoperiod and PPFD of 200 µmol s^{-1} m^{-2}. The dark period in this profile is between 09.00-16.00.

TOC

C.4.3 Step 4 and 5: District heat network configurations and energetic performance

C.4.3.1 Centralised: 4-pipe DHN with central heat pump

This section presents additional figures on the centralised configuration consisting of a 4-pipe district heat network with a centralised heat pump as described in Section 4.3.2.1. Figure C.3 presents the centralised configuration in summer mode. The annual heat and cold balance of the centralised configuration applied to the Westindische Buurt are presented in Figures C.4 and C.5.

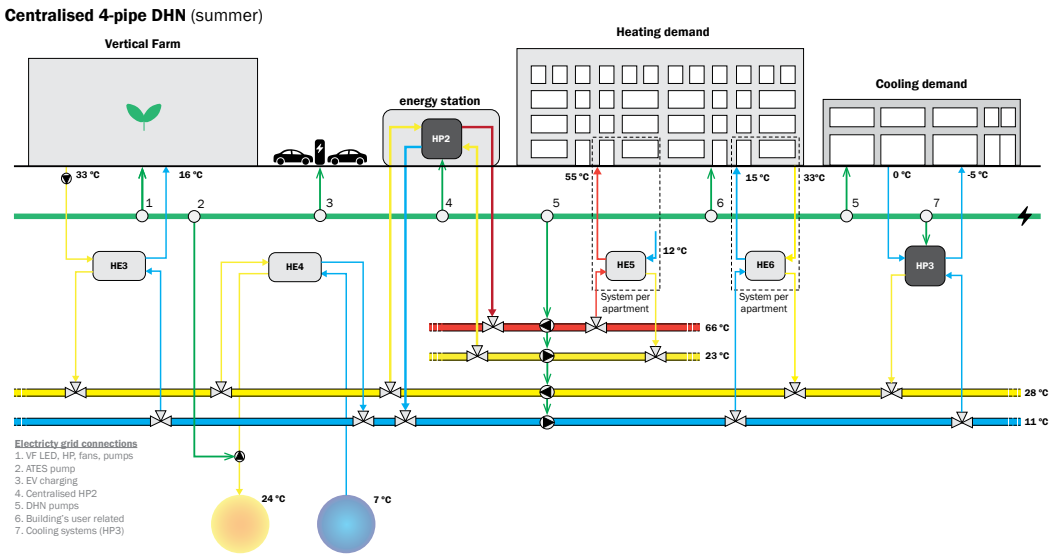

FIG.C.3 Centalised energy system configuration with 4-pipe DHN in summer mode.

TOC

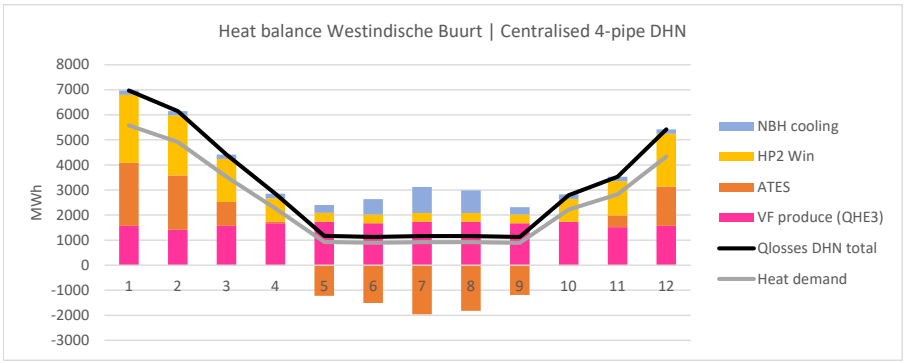

FIG.C.4 Annual heat balance of the Westindische Buurt with integrated using the centralised 4-pipe DHN configuration. The stacked lines present the heat demands of the buildings in the neighbourhood, and the heat losses within the 4-pipe DHN. The stacked columns represent the heat supplies in positive axis. The abundance of heat produced in summer is stored in the ATES hot source, and presented in negative axis.

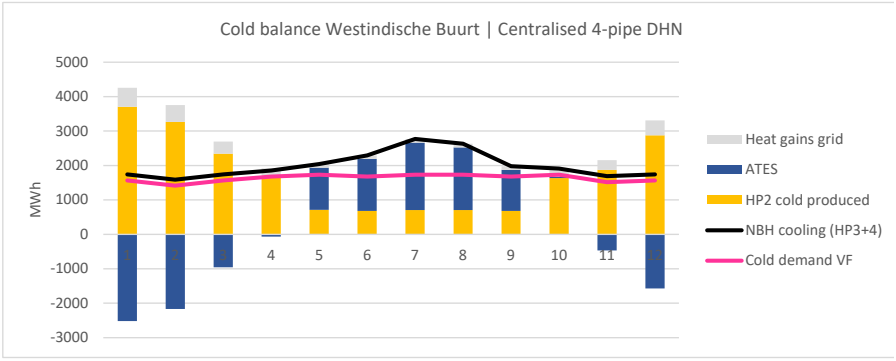

FIG.C.5 Annual cold balance of the Westindische Buurt with integrated using the centralised 4-pipe DHN configuration. The stacked lines present the cooling demands of the vertical farm buildings in the neighbourhood, and the heat gains within the cold pipe. The stacked columns represent the cold generation in positive axis. The abundance of cold produced in winter is stored in the ATES cold source, and presented in negative axis.

TOC

C.4.3.2 Decentralised: 2-pipe DHN with decentral heat pumps

The following section presents additional figures on the decentralised configuration consisting of a 2-pipe district heat network with a decentralised heat pump described in Section 4.3.2.2. Figure C.6 presents the decentralised configuration in summer mode. The annual heat and cold balance of the decentralised configuration applied to the Westindische Buurt are presented in Figures C.7 and C.8.

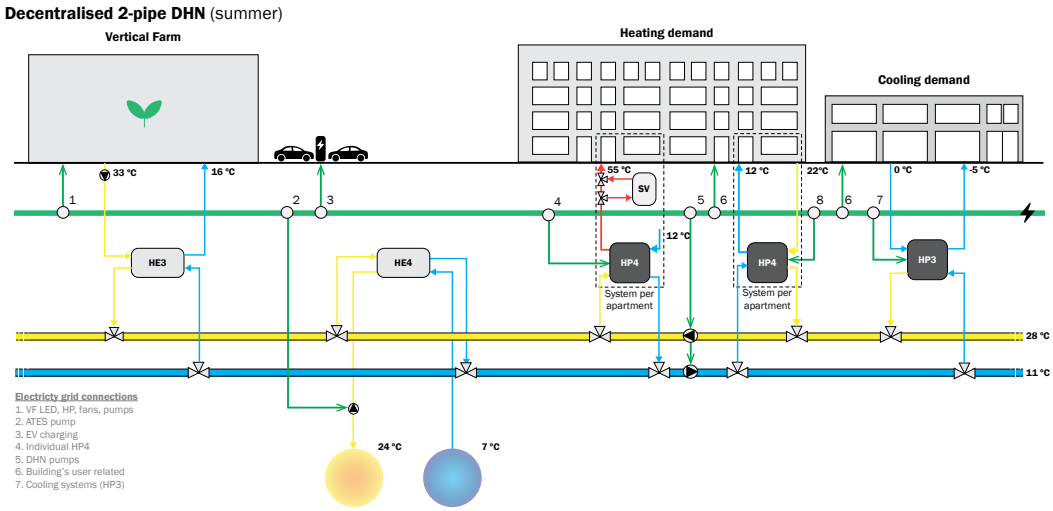

FIG.C.6 Decentralised energy system configuration with 2-pipe DHN in summer mode.

TOC

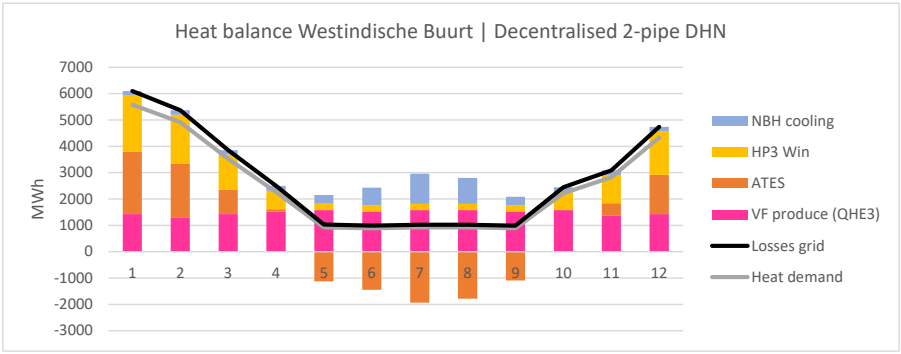

FIG.C.7 Annual heat balance of the Westindische Buurt with integrated using the decentralised 2-pipe DHN configuration. The stacked lines present the heat demands of the buildings in the neighbourhood, and the heat losses within the 2-pipe DHN. The stacked columns represent the heat supplies in positive axis. The abundance of heat produced in summer is stored in the ATES hot source, and presented in negative axis.

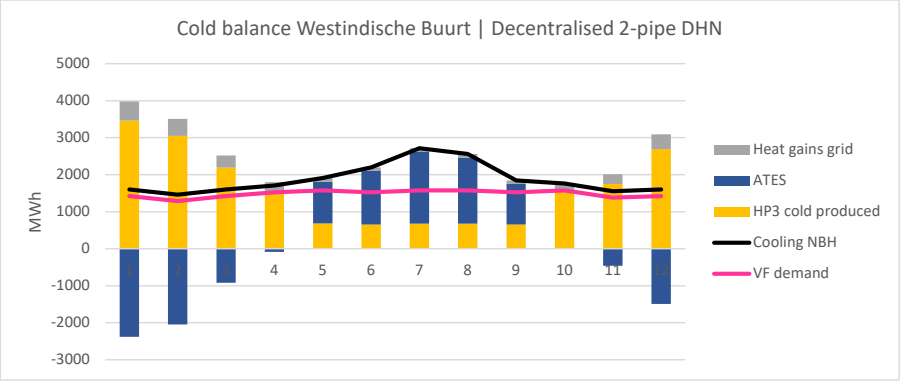

FIG.C.8 Annual cold balance of the Westindische Buurt with integrated using the decentralised 2-pipe DHN configuration. The stacked lines present the cooling demands of the vertical farm buildings in the neighbourhood, and the heat gains within the cold pipe. The stacked columns represent the cold generation in positive axis. The abundance of cold produced in winter is stored in the ATES cold source, and presented in negative axis.

TOC

References

CBS, 2018a. Energieverbruik van particuliere huishoudens. https://www.cbs.nl/nl-nl/achtergrond/2018/14/energieverbruik-van-particuliere-huishoudens.

CBS, 2018b. Energiekentallen utiliteitsbouw dienstensector: oppervlakte klasse. https://opendata.cbs.nl/statline/#/CBS/nl/dataset/83374NED/table?ts=1642090250137.

CBS Statline. 2021a. Elektriciteitslevering vanuit het openbare net; woningkenmerken, bewoners, 2019. Opendata.cbs.nl/statline

CBS Statline. 2021b. Energieverbruik particuliere woningen; woningtype, wijken en buurten, 2020. Opendata.cbs.nl/statline

CBS Statline. 2022a. Woningen; hoofdverwarmingsinstallaties, wijken en buurten, 2020. Opendata.cbs.nl/statline

CBS. 2022b. Gemiddeld aantal personenauto's per huishouden naar wijk, 1 januari 2020. https://www.cbs.nl/nl-nl/maatwerk/2022/12/autobezit-per-huishouden-januari-2020

Conrad, J., Greif, S. 2019. Modelling Load Profiles of Heat Pumps. Energies, 12(4). https://doi.org/10.3390/en12040766.

Enexis. https://www.enexis.nl/aansluitingen/welke-aansluiting-heb-ik-nodig

Jansen, S., Verhoeven, R., Elswijk, M. 2021b. KoWaNet: Technisch handboek koele warmtenetten.

Klimaatmonitor. 2023. Gemeente Amsterdam: rapportage wijken en buurten. Klimaatmonitor.databank.nl

KWA, 2016. Het elektrisch energieverbruik en het warmteaanbod van koelinstallaties voor een veertigtal bedrijfssectoren. KWA, Amersfoort.

KWA, 2022. Graaddagen_11-20 [dataset]. https://www.kwa.nl/diensten/graaddagen-en-koeldagen

Maivel, M., Kurnitski, J., 2015. Heating system return temperature efficiency effect on heat pump performance. Energy and Build. 94, 71–79. https://doi.org/10.1016/j.enbuild.2015.02.048.

MFFBAS. 2023. https://www.mffbas.nl/documenten/

Ommen, T., Throsen, J.E., Markussen, W.B., Elmegaard, B., 2017. Performance of ultra low temperature district heating systems with utility plant and booster heat pumps. Energy, 137, 544–555. https://doi.org/10.1016/j.energy.2017.05.165.

Refa, N., Hammer, D., Slobben, T., Broos, P., van Zanten, E., Oude Weernink, F., de Croon, R. 2023. Analyse van laadprofielen voor EV's bij thuis-, publiek-, werk- en snelladen in 2030. http://elaad.nl.

Refa, N., Speel, P., van Bokhoven, P., van der Poel, G., Noordijk, R., de Croon, R. 2019. Waar rijden en laden EV's in de toekomst?: de ontwikkeling van elektrische voertuigen en laadpunten in Nederland t/m 2035. http://elaad.nl.

APPENDIX D

Chapter 5

D.1 Activity data vegetable and fruit production with conventional farms

TABLE D.1 Activity data for potato and strawberry production in an open-field farm per kg FW.

Activity	Potato Activity data	Strawberry Activity data	Unit	Note
FARM LIFE CYCLE				
Upstream				
Steel	2.27E-03	5.62E-03	kg	Materiality per m^2 area equal to OF lettuce (Table A.3)
Polycarbonate (PC)	1.52E-05	3.76E-05	kg	Materiality per m^2 area equal to OF lettuce (Table A.3)
Reinforced concrete	8.91E-06	2.20E-05	m3	Materiality per m^2 area equal to OF lettuce (Table A.3)
Insulation Rockwool	2.37E-04	5.86E-04	kg	Materiality per m^2 area equal to OF lettuce (Table A.3)
Transportation	1.00E-02	1.00E-02	kg km	Section 2.2.3
End-of-life				
Transportation	5.00E+01	5.00E+01	km kg	Section 2.2.3

>>>

TABLE D.1 Activity data for potato and strawberry production in an open-field farm per kg FW.

Activity	Potato Activity data	Strawberry Activity data	Unit	Note
CROP LIFE CYCLE				
Upstream				
Fertiliser				
– Nitrogen (N)	6.07E-03	5.88E-03	kg	(Schreuder et al., 2009)
– Phosphate (P_2O_5)	2.79E-03	8.82E-03	Kg	(Schreuder et al., 2009)
– Potassium (K_2O)	5.00E-03	-	kg	(Schreuder et al., 2009)
Pesticides	3.33E-04	1.94E-03	kg	Potato 14 kg ha^{-1} y^{-1}, fruit 33 kg ha^{-1} y^{-1} (Baltussen et al., 2021);
Growth materials				
– Straw	-	5.88E-01		(Schreuder et al., 2009)
Packaging materials				
– Polypropylene bags	2.80E-03	4.20E-02	kg	(Afvalfonds verpakkingen, 2017)
Transportation inputs	1.00E+02	1.00E+02	km kg	Section 2.2.3
Core				
Watering	4.80E+01	5.00E+01	L	Potato 0.4 m^3/1000 EUR (Baltussen et al., 2021); strawberry 50m^3 ton^{-1} (Breukers et al., 2014)
N_2O from soils	1.26E-04	1.22E-04	kg	Calculated according to input N fertiliser (Chapter 2)
Fuel use	5.37E-03	7.93E-02	kg	Diesel used for machinery (Schreuder et al., 2009)
Lubricants	-	-	kg	Included in fuel use (Schreuder et al., 2009)
Electricity use	2.00E-02	-	kWh	(Schreuder et al., 2009)
Downstream				
Product cooling distribution	1.00E-01	1.00E-01	kWh	(Marchi et al., 2022)
Transportation	1.60E+02	1.60E+02	km kg	Section 2.2.3
End-of-life				
Cultivation phase				
– Cultivation losses	3,00E-02	2.00E-01	kg	Potato 3% (Schreuder et al., 2009), strawberry assumption 20%
Supply chain				
– Food losses	5.87E-03	5.87E-03	kg	Section 2.2.3
Consumer				
– Food losses	1.40E-01	8.00E-02	kg	Potato 14%, fruits 8% (Baltussen et al., 2021)
– Packaging	2.80E-03	4.20E-02	kg	
Transportation	5.00E+01	5.00E+01	km kg	Section 2.2.3

TOC

TABLE D.2 Activity data for tomato, strawberry, and cucumber production in a soil-based greenhouse per kg FW

Activity	Tomato Activity data	Strawberry Activity data	Cucumber Activity data	Unit	Note
FARM LIFE CYCLE					
Upstream					
Steel	9.93E-03	5.51E-02	1.06E-02	kg	Materiality per m^2 equal to GHs lettuce (Table A.4)
Aluminium	2.54E-03	1.41E-02	2.71E-03	kg	Materiality per m^2 equal to GHs lettuce (Table A.4)
Reinforced concrete	4.11E-06	2.28E-05	4.38E-06	m3	Materiality per m^2 equal to GHs lettuce (Table A.4)
Glass	1.08E-02	5.96E-02	1.15E-02	kg	Materiality per m^2 equal to GHs lettuce (Table A.4)
Polyester	1.31E-04	7.28E-04	1.40E-04	kg	Materiality per m^2 equal to GHs lettuce (Table A.4)
Transportation	1.00E-02	1.00E-02	1.00E-02	kg km	Section 2.2.3
End-of-life					
Transportation	5.00E+01	5.00E+01	5.00E+01	km kg	Section 2.2.3
CROP LIFE CYCLE					
Upstream					
Fertiliser					Tomato (Montero et al. 2011b); Strawberry (Breukers et al., 2014); Cucumber (Khoshnevisan et al 2014)
– Nitrogen (N)	2.99E-03	5.80E-03	4,30E-03	kg	
– Phosphate (P_2O_5)	7.20E-04	5.00E-04	4,20E-03	kg	
– Potassium (K_2O)	3.29E-03		4,90E-03	kg	
– Sulfur			1,10E-03	kg	
Pesticides	1.77E-05	1.94E-03	1.60E-03	1.60E-03	Tomato (Montero et al. 2011a); Strawberry ratio cost with OF (Breukers et al., 2014); Cucumber (Khoshnevisan et al 2014)
Growth materials					
– Potting soil	5.61E-02	4.52E-01	7.61E-02	kg	(Raaphorst and Benninga, 2019)
Packaging materials					
– Polypropylene bags	-	4.20E-02	-	kg	(Afvalfonds verpakkingen, 2017)
– Cardboard	3.40E-02	-	9.62E-02	kg	(Afvalfonds verpakkingen, 2017)
Carbon enrichment	1.89E-01	1.22E+00	2.37E-01	kg	(Raaphorst and Benninga, 2019)
Transportation inputs	1.00E+02	1.00E+02	1.00E+02	km kg	Section 2.2.3

>>>

TOC

TABLE D.2 Activity data for tomato, strawberry, and cucumber production in a soil-based greenhouse per kg FW

Activity	Tomato Activity data	Strawberry Activity data	Cucumber Activity data	Unit	Note
Core					
Watering	1.02E+01	5.50E+01	1.57E+02	L	Tomato (Raaphorst and Benninga, 2019); Strawberry (Breukers et al., 2014); Cucumber (Khoshnevisan et al 2014)
N_2O from soils	6,23E-08	1.21E-04	8,95E-05	kg	Calculated according to input N fertiliser (Chapter 2)
Fuel use	4.67E-01	1.41E+00	1.03E-01	m^3	(Raaphorst and Benninga, 2019)
Electricity use	1.36E-05	4.51E-01	1.45E-01	kWh	(Raaphorst and Benninga, 2019)
Downstream					
Product cooling distribution	1.00E-01	1.00E-01	1.00E-01	kWh	(Marchi et al., 2022)
Transportation	1.60E+02	1.60E+02	1.60E+02	km kg	Section 2.2.3
End-of-life					
Cultivation phase					
– Cultivation losses	6.78E-02	7.52E-02	5.78E-02	kg	(Raaphorst and Benninga, 2019)
Supply chain					
– Food losses	5.87E-03	5.87E-03	5.87E-03	kg	Section 2.2.3
Consumer					
– Food losses	9.00E-02	8.00E-02	9.00E-02	kg	Vegetables 9%, fruits 8% (Baltussen et al., 2021)
– Packaging	3.40E-02	4.20E-02	9.62E-02	kg	
Transportation	5.00E+01	5.00E+01	5.00E+01	km kg	Section 2.2.3

TOC

TABLE D.3 Activity data for tomato, strawberry, and cucumber production in a greenhouse with artificial light per kg FW

Activity	Tomato Activity data	Strawberry Activity data	Cucumber Activity data	Unit	Note
FARM LIFE CYCLE					
Upstream					
Steel	7.85E-03	5.38E-02	7.22E-03	kg	Materiality per m^2 equal to GHs lettuce (Table A.5)
Aluminium	2.01E-03	1.38E-02	1.85E-03	kg	Materiality per m^2 equal to GHs lettuce (Table A.5)
Reinforced concrete	3.25E-06	2.23E-05	2.99E-06	m3	Materiality per m^2 equal to GHs lettuce (Table A.5)
Glass	8.50E-03	5.83E-02	7.81E-03	kg	Materiality per m^2 equal to GHs lettuce (Table A.5)
Polyester	1.04E-04	7.12E-04	9.54E-05	kg	Materiality per m^2 equal to GHs lettuce (Table A.5)
Transportation	1.00E-02	1.00E-02	1.00E-02	kg km	Section 2.2.3
End-of-life					
Transportation	5.00E+01	5.00E+01	5.00E+01	km kg	Section 2.2.3
CROP LIFE CYCLE					
Upstream					
Fertiliser					Tomato (Montero et al. 2011b); Strawberry (Breukers et al., 2014); Cucumber (Khoshnevisan et al 2014)
– Nitrogen (N)	2.99E-03	2.30E-03	4,30E-03	kg	
– Phosphate (P_2O_5)	7.20E-04	5.00E-04	4,20E-03	kg	
– Potassium (K_2O)	3.29E-03		4,90E-03	kg	
– Sulfur			1,10E-03	kg	
Pesticides	1.77E-05	1.94E-03	1.60E-03	kg	Tomato (Montero et al. 2011a); Strawberry ratio cost with OF (Breukers et al., 2014); Cucumber (Khoshnevisan et al 2014)
Growth materials					
– Potting soil		4.42E-01	5.19E-02	kg	(Raaphorst and Benninga, 2019)
– Plastic	2.00E-05				Tomato (Montero et al. 2011b)
– Rockwool	6.00E-05				Tomato (Montero et al. 2011b)
Packaging materials					
– Polypropylene bags	-	4.20E-02	-	kg	(Afvalfonds verpakkingen, 2017)
– Cardboard	3.40E-02	-	9.62E-02	kg	(Afvalfonds verpakkingen, 2017)
Carbon enrichment	1.40E-01	1.19+00	1.54E-01	kg	(Raaphorst and Benninga, 2019)
Transportation inputs	1.00E+02	1.00E+02	1.00E+02	km kg	Section 2.2.3

>>>

TABLE D.3 Activity data for tomato, strawberry, and cucumber production in a greenhouse with artificial light per kg FW

Activity	Tomato Activity data	Strawberry Activity data	Cucumber Activity data	Unit	Note
Core					
Watering	8.04E+00	1.40E+01	1.57E+02	L	Tomato (Raaphorst and Benninga, 2019); Strawberry (Breukers et al., 2014); Cucumber (Khoshnevisan et al 2014)
N_2O from soils	6,23E-08	1.21E-04	8,95E-05	kg	Calculated according to input N fertiliser (Chapter 2)
Fuel use	4.67E-01	1.49E+00	1.08E-02	m^3	(Raaphorst and Benninga, 2019)
Electricity use	3.88E+00	7.13+00	3.00E+00	kWh	(Raaphorst and Benninga, 2019)
Downstream					
Product cooling distribution	1.00E-01	1.00E-01	1.00E-01	kWh	(Marchi et al., 2022)
Transportation	1.60E+02	1.60E+02	1.60E+02	km kg	Section 2.2.3
End-of-life					
Cultivation phase					
– Cultivation losses	5.36E-02	2.94E-02	3.94E-02	kg	(Raaphorst and Benninga, 2019)
Supply chain					
– Food losses	5.87E-03	5.87E-03	5.87E-03	kg	Section 2.2.3
Consumer					
– Food losses	9.00E-02	8.00E-02	9.00E-02	kg	Vegetables 9%, fruits 8% (Baltussen et al., 2021)
– Packaging	3.40E-02	4.20E-02	9.62E-02	kg	
Transportation	5.00E+01	5.00E+01	5.00E+01	km kg	Section 2.2.3

TOC

D.2 Activity data lettuce production within standalone vertical farms

TABLE D.4 Activity data for lettuce production in VFII per kg FW (Pennisi et al., 2019a,b,c; 2020)

Activity	Activity data FU	Unit	Note
FARM LIFE CYCLE			
Upstream			
Steel	5.00E-03	kg	Materiality per m^2 cultivation area VF equal to VF_I (Table A.6)
Aluminium	4.27E-03	kg	Materiality per m^2 cultivation area VF equal to VF_I (Table A.6)
Transportation	1.00E+02	km kg	Section 2.2.3
End-of-life			
Transportation	5.00E+01	km kg	Section 2.2.3
CROP LIFE CYCLE			
Upstream			
Fertiliser	4.32E-02	kg	0.25L per growth pot (Pennisi et al., 2020), nutrient uptake 12.9 L kg^{-1} FW (Pennisi et al., 2019B), composition addressed in Penissi et al., 2019b
Pesticides & herbicides	-		Not applied
Growth & culture materials			
– Polypropylene	4.35E-01	kg	Plastic growth pot per crop (Pennisi et al., 2019a,c) assumed same pots as VF_I
Packaging materials			
– Polypropylene	1.14E-02	kg	Section 2.4.2.1
Carbon enrichment	8.40E-02	kg	450 ppm (Pennisi et al., 2019a), 2.1 kg CO_2 kg^{-1} DW to maintain those CO_2 concentrations (Graamans et al., 2018). DM content 4.0% (Pennisi et al., 2020)
Transportation inputs	1.00E+02	km kg	Section 2.2.3
Core			
Watering	1.33+01	L	Water use efficiency 60 g FW L^{-1} (Pennisi et al., 2020)
Electricity use	6.25E+00	kWh	Energy use efficiency LED 91 g FW kWh^{-1} (Pennisi et al., 2020) with molar efficacy 3.5 µmol J^{-1}· and electricity use for cooling, dehumidification, fans , and pumps (Pennisi et al., 2020)
Downstream			
Transport	1.50E+01	km kg	Sold at local supermarket (Table A.6)

>>>

TOC

TABLE D.4 Activity data for lettuce production in VFII per kg FW (Pennisi et al., 2019a,b,c; 2020)

Activity	Activity data FU	Unit	Note
End-of-life			
Cultivation phase			
– cultivation losses	2.00E-02	kg	2% cultivation losses (VF_1)
– Growth materials	4.35E-01	kg	Polypropylene growth
Supply chain			
– Food losses	5,87E-03	kg	Section 2.2.3
Consumer			
– Food losses	9.50E-02	kg	Section 2.2.3
– Packaging	1.14E-02	kg	Plastic bag
Transportation	5.00E+01	km kg	Section 2.2.3

TABLE D.5 Activity data for lettuce production in VF_{III} per kg FW (Martin et al. 2023)

Activity	Activity data FU	Unit	Note
FARM LIFE CYCLE			
Upstream			
Steel	6.13E-03	kg	Materiality per m^2 cultivation area VF equal to VF_I (Table A.6)
Aluminium	5.25E-03	kg	Materiality per m^2 cultivation area VF equal to VF_I (Table A.6)
Transportation	1.00E+02	km kg	Section 2.2.3
End-of-life			
Transportation	5.00E+01	km kg	Section 2.2.3
CROP LIFE CYCLE			
Upstream			
Fertiliser	5.30E-02	kg	(Martin et al., 2023)
Pesticides & herbicides	-		Not applied
Growth & culture materials			
– Peat	1.17E-01	kg	(Martin et al., 2023)
– Coir	1.17E-01	kg	(Martin et al., 2023)
– Binding agent	2.31E-04	kg	(Martin et al., 2023)
– Growth pipes	1.05E-02		Ethyne Hexene, lifespan 8y (Martin et al., 2023)
Packaging materials			
– Polypropylene	8.09E-02	kg	(Martin et al., 2023)
Carbon enrichment	1.04E-01	kg	(Martin et al., 2023)
Transportation inputs	1.00E+02	km kg	Section 2.2.3
Core			
Watering	9.08E+00	L	(Martin et al., 2023)
Electricity use	9.92E+00	kWh	(Martin et al., 2023)
Downstream			
Transport	1.50E+01	km kg	Sold at local supermarket (Table A.6)
End-of-life			
Cultivation phase			
– cultivation losses	8.00E-02	kg	8% cultivation losses (Martin et al., 2023)
– Growth materials	2.44E-01	kg	(Martin et al., 2023)
Supply chain			
– Food losses	5,87E-03	kg	Section 2.2.3
Consumer			
– Food losses	3.00E-02	kg	(Martin et al., 2023)
– Packaging	8.08E-2	kg	(Martin et al., 2023)
Transportation	5.00E+01	km kg	Section 2.2.3

TOC

D.3 Activity data vegetable and fruit production within standalone vertical farms

TABLE D.6 Activity data for vegetable and fruit production using VFI per kg FW, with three times reuse of growth materials.

	Activity data FU	Potato	Tomato	Strawberry	Cucumber	Note
Input data						
Yields (FW)	kg	1.00	1.00	1.00	1.00	(Righini et al. 2023)
Yields (FW)	kg m^2 y^{-1}	32.70	36.50	10.30	77.00	(Righini et al. 2023)
Growth cycles	n y^{-1}	3.48	2.90	1.68	3.07	(Righini et al. 2023)
LUE	g FW mol^{-1}	0.24	0.23	0.29	0.23	(Righini et al. 2023)
PPFD	µmol m^{-2} s^{-1}	917	697	320	600	(Righini et al. 2023)
Photoperiod	h	12	14	14	17	(Righini et al. 2023)
Electricity use LED	kWh kg^{-1} FW	35.09	27.88	45.36	13.81	(Righini et al. 2023)
molar efficacy	µmol J^{-1}	3.50	3.50	3.50	3.50	(Weidner et al 2021)
FARM LIFE CYCLE						
Upstream						
Steel	kg	1.51E-03	1.69E-03	4.76E-04	3.56E-03	Materiality per m^2 cultivation area VF equal to VF_I (Table A.6)
Aluminium	kg	1.29E-03	1.44E-03	4.08E-04	3.05E-03	Materiality per m^2 cultivation area VF equal to VF_I (Table A.6)
Transportation	km kg	1.00E+02	1.00E+02	1.00E+02	1.00E+02	Section 2.2.3
End-of-life						
Transportation	km kg	5.00E+01	5.00E+01	5.00E+01	5.00E+01	Section 2.2.3
CROP LIFE CYCLE						
Upstream						
Fertiliser	kg	3.25E-02	3.25E-02	3.25E-02	3.25E-02	Per kg FW produced equal to lettuce production VF_I (Table A.6)
Growth materials						
Polypropylene	kg	1.51E-01	1.51E-01	1.51E-01	1.51E-01	Per kg FW produced equal to lettuce production VF_I. but 3x reused (Table A.6)
Packaging materials						
Polypropylene bags	kg	2.80E-03		4.20E-02		(Afvalfonds verpakkingen. 2017)
Cardboard	Kg		3.40E-02		9.62E-02	(Afvalfonds verpakkingen. 2017)
Transportation inputs	km kg	1.00E+02	1.00E+02	1.00E+02	1.00E+02	Section 2.2.3

>>>

TABLE D.6 Activity data for vegetable and fruit production using VFI per kg FW, with three times reuse of growth materials.

	Activity data FU	Potato	Tomato	Strawberry	Cucumber	Note
Core						
Watering	L	1.59E+00	1.37E+00	2.50E+00	1.82E+00	(Righini et al. 2023)
Electricity use	kWh	4.54E+01	3.60E+01	5.83E+01	1.79E+01	(Righini et al. 2023)
Downstream						
Transport	km kg	1.50E+01	1.50E+01	1.50E+01	1.50E+01	Section 2.2.3
End-of-life						
Cultivation phase						
– Cultivation losses	kg	2.00E-02	2.00E-02	2.00E-02	2.00E-02	Same percentage as lettuce production VF_I (Table A.6)
– Growth materials	kg	1.53E-01	1.53E-01	1.53E-01	1.53E-01	
Supply chain						
– Food losses	kg	5.87E-03	5.87E-03	5.87E-03	5.87E-03	Section 2.2.3
Consumer						
Food losses	kg	9.50E-02	9.50E-02	9.50E-02	9.50E-02	(Baltussen et al.. 2021)
Packaging	kg	2.80E-03	3.40E-02	4.20E-02	9.62E-02	
Transportation	km kg	5.00E+01	5.00E+01	5.00E+01	5.00E+01	Section 2.2.3

TOC

D.4 Carbon footprints standalone farming

TABLE D.7 Carbon footprints of the three vertical farming systems for the production of lettuce in kg $CO_{2\text{-eq}}$ kg^{-1}.

Activity	VF_I	VF_{II}	VF_{III}
Life cycle farm	**0.042**	**0.027**	**0.033**
Upstream	0.042	0.027	0.032
End-of-life	0.000	0.000	0.000
Life cycle farm	**3.679**	**3.060**	**3.716**
Upstream	**0.409**	**0.730**	**0.157**
Nutrients	0.052	0.021	0.026
Carbon enrichment	-	0.071	0.087
Packaging material	0.024	0.024	0.024
Growth materials	0.322	0.596	0.003
Transport	0.010	0.018	0,018
Core	**3.114**	**2.110**	**3.348**
Water	0.005	0.005	0.004
Electricity	3.110	2.105	3.344
Downstream	**0.008**	**0.008**	**0.008**
Transportation	0.008	0.008	0.008
End-of-life	**0.147**	**0.213**	**0.204**
Compost	0.028	0.011	0.024
Incineration	0,107	0.191	0.167
Transport to treatment facility	0.012	0.011	0.014
Total carbon footprint	**3.721**	**3.087**	**3.750**

TOC

TABLE D.8 Carbon footprints per kg fresh weight produce for different crops produced in a standalone vertical farm

	Potato	Tomato	Strawberry	Cucumber
	$kgCO_{2\text{-eq}}\ kg^{-1}$ FW	$kgCO_{2\text{-eq}}\ kg^{-1}$ FW	$kgCO_{2\text{-eq}}\ kg^{-1}$ FW	$kgCO_{2\text{-eq}}\ kg^{-1}$ FW
FARM LIFE CYCLE	0.008	0.009	0.003	0.019
Upstream	**0.008**	**0.009**	**0.003**	**0.019**
Steel	0.003	0.003	0.001	0.007
Aluminium	0.005	0.006	0.002	0.012
Transportation	0.000	0.000	0.000	0.000
End-of-life	**0.000**	**0.000**	**0.000**	**0.000**
Transportation	0.000	0.000	0.000	0.000
CROP LIFE CYCLE	15.797	12.715	20.356	6.718
Upstream	**0.390**	**0.429**	**0.475**	**0.511**
Fertiliser	0.052	0.052	0.052	0.052
Pesticides & herbicides	-	-	-	-
Growth materials	0.322	0.322	0.322	0.322
Packaging materials	0.006	0.043	0.089	0.122
Transportation inputs	0.010	0.011	0.012	0.015
Core	**15.280**	**12.137**	**19.726**	**6.015**
Watering	0.001	0.001	0.001	0.001
Electricity use	15.279	12.136	19.725	6.015
Downstream	**0.008**	**0.008**	**0.008**	**0.009**
Transport	0.008	0.008	0.008	0.009
End-of-life	**0.120**	**0.141**	**0.146**	**0.183**
Compost	0.011	0.011	0.011	0.011
Incineration	0.101	0.122	0.127	0.162
Transportation	0.007	0.008	0.008	0.010
TOTAL	**15.805**	**12.721**	**20.145**	**6.737**

TOC

TABLE D.9 Carbon footprints per kg fresh weight produce for different crops produced by conventional farms.

	OF Lettuce	GHs Lettuce	GHa Lettuce	OF Potato	GHs Tomato	GHa Tomato
	kg $CO_{2\text{-eq}}$ kg^{-1} FW	$kgCO_{2\text{-eq}}$ kg^{-1} FW	$kgCO_{2\text{-eq}}$ kg^{-1} FW	$kgCO_{2\text{-eq}}$ kg^{-1} FW	$kgCO_{2\text{-eq}}$ kg^{-1} FW	$kgCO_{2\text{-eq}}$ kg^{-1} FW
FARM LIFE CYCLE	0.005	0.114	0.086	0.010	0.045	0.045
Upstream	**0.005**	**0.112**	**0.085**	**0.010**	**0.044**	**0.044**
Steel	0.002	0.050	0.027	0.004	0.019	0.019
Aluminium	0.000	0.025	0.014	0.000	0.010	0.010
Reinforced concrete	0.002	0.004	0.002	0.004	0.002	0.002
Glass	0.000	0.028	0.015	0.000	0.011	0.011
Polycarbonate (PC)	0.000	0.000	0.000	0.000	0.000	0.000
Polyester	0.000	0.001	0.000	0.000	0.000	0.000
PVC	0.000	0.000	0.024	0.000	0.000	0.000
Rockwool Insulation	0.000	0.000	0.000	0.000	0.000	0.000
Transportation	0.001	0.004	0.002	0.001	0.002	0.002
End-of-life	**0.000**	**0.000**	**0.000**	**0.000**	**0.000**	**0.000**
Transportation	0.000	0.000	0.000	0.000	0.000	0.000
CROP LIFE CYCLE	0.378	0.992	0.985	0.307	1.356	2.384
Upstream	**0.077**	**0.085**	**0.207**	**0.086**	**0.247**	**0.200**
Fertiliser	0.046	0.041	0.018	0.075	0.036	0.036
Pesticides & herbicides	0.005	0.002	0.001	0.004	0.000	0.000
Growth materials	0.000	0.010	0.000	0.000	0.004	0.000
Packaging materials	0.024	0.024	0.024	0.006	0.043	0.043
Carbon enrichment		0.000	0.164		0.159	0.118
Transportation inputs	0.001	0.009	0.001	0.001	0.005	0.002
Core	**0.146**	**0.763**	**0.630**	**0.081**	**0.946**	**2.022**
Watering	0.006	0.008	0.001	0.019	0.004	0.003
N_2O from soils	0.022	0.018	0.000	0.035	0.017	0.017
Fuel use	0.117	0.691	0.166	0.020	0.879	0.695
Lubricants	0.000					
Electricity use	0.000	0.047	0.462	0.007	0.046	1.308

>>>

TABLE D.9 Carbon footprints per kg fresh weight produce for different crops produced by conventional farms.

	OF Lettuce	GHs Lettuce	GHa Lettuce	OF Potato	GHs Tomato	GHa Tomato
	kg $CO_{2\text{-eq}}$ kg^{-1} FW	$kgCO_{2\text{-eq}}$ kg^{-1} FW	$kgCO_{2\text{-eq}}$ kg^{-1} FW	$kgCO_{2\text{-eq}}$ kg^{-1} FW	$kgCO_{2\text{-eq}}$ kg^{-1} FW	$kgCO_{2\text{-eq}}$ kg^{-1} FW
Downstream	**0.119**	**0.119**	**0.119**	**0.118**	**0.121**	**0.121**
Cooling distribution centre	0.034	0.034	0.034	0.034	0.034	0.034
Transport	0.085	0.085	0.085	0.084	0.087	0.087
End-of-life	**0.037**	**0.025**	**0.030**	**0.023**	**0.042**	**0.041**
Compost	0.023	0.014	0.013	0.016	0.015	0.014
Incineration	0.007	0.007	0.013	0.002	0.022	0.022
Transportation	0.007	0.004	0.004	0.005	0.005	0.005
TOTAL	**0.383**	**1.106**	**1.071**	**0.317**	**1.401**	**2.428**

TOC

TABLE D.10 : Carbon footprints per kg fresh weight produce for different crops produced in a standalone conventional farms.

	OF Strawberry	GHs Strawberry	GHa Strawberry	GHs Cucumber	GHa Cucumber
	kg $CO_{2\text{-eq}}$ kg^{-1} FW	$kgCO_{2\text{-eq}}$ kg^{-1} FW	$kgCO_{2\text{-eq}}$ kg^{-1} FW	$kgCO_{2\text{-eq}}$ kg^{-1} FW	$kgCO_{2\text{-eq}}$ kg^{-1} FW
FARM LIFE CYCLE	0.025	0.249	0.243	0.005	0.033
Upstream	**0.024**	**0.244**	**0.239**	**0.005**	**0.032**
Steel	0.011	0.108	0.105	0.002	0.014
Aluminium	0.000	0.054	0.053	0.001	0.007
Reinforced concrete	0.009	0.009	0.009	0.000	0.001
Glass	0.000	0.062	0.060	0.001	0.008
Polycarbonate (PC)	0.000	0.000	0.000	0.000	0.000
Polyester	0.000	0.002	0.002	0.000	0.000
PVC	0.000	0.000	0.000	0.000	0.000
Rockwool Insulation	0.001	0.000	0.000	0.000	0.000
Transportation	0.003	0.010	0.009	0.000	0.001
End-of-life	**0.001**	**0.005**	**0.005**	**0.000**	**0.001**
Transportation	0.001	0.005	0.005	0.000	0.001
CROP LIFE CYCLE	0.760	4.273	6.584	0.539	1.664
Upstream	**0.225**	**1.248**	**1.186**	**0.225**	**0.339**
Fertiliser	0.083	0.064	0.026	0.059	0.059
Pesticides & herbicides	0.021	0.021	0.021	0.017	0.017
Growth materials	0.028	0.022	0.021	0.000	0.002
Packaging materials	0.089	0.089	0.089	0.122	0.122
Carbon enrichment		1.026	1.003	0.020	0.129
Transportation inputs	0.003	0.026	0.026	0.006	0.009
Core	**0.352**	**2.856**	**5.234**	**0.111**	**1.118**
Watering	0.020	0.022	0.006	0.063	0.063
N_2O from soils	0.033	0.033	0.013	0.024	0.024
Fuel use	0.299	2.649	2.812	0.019	0.020
Lubricants					
Electricity use	0.000	0.152	2.404	0.005	1.010
Downstream	**0.121**	**0.121**	**0.121**	**0.126**	**0.126**

>>>

TABLE D.10 : Carbon footprints per kg fresh weight produce for different crops produced in a standalone conventional farms.

	OF Strawberry	GHs Strawberry	GHa Strawberry	GHs Cucumber	GHa Cucumber
	kg $CO_{2\text{-eq}}$ kg^{-1} FW	$kgCO_{2\text{-eq}}$ kg^{-1} FW	$kgCO_{2\text{-eq}}$ kg^{-1} FW	$kgCO_{2\text{-eq}}$ kg^{-1} FW	$kgCO_{2\text{-eq}}$ kg^{-1} FW
Cooling distribution centre	0.034	0.034	0.034	0.034	0.034
Transport	0.088	0.088	0.088	0.092	0.092
End-of-life	**0.062**	**0.047**	**0.042**	**0.077**	**0.081**
Compost	0.026	0.015	0.010	0.009	0.012
Incineration	0.027	0.027	0.027	0.063	0.063
Transportation	0.009	0.005	0.004	0.005	0.006
TOTAL	**0.785**	**4.522**	**6.827**	**0.544**	**1.696**

TOC

References

Afvalfonds Verpakkingen. 2017. Bijlage 2: lijst van standaard gewichten verpakkingen. https://afvalfondsverpakkingen.nl/a/i/Bijlage-2-Lijst-met-standaardgewichten.xlsx. (Accessed October 25, 2023)

Baltussen, W., Janssens, S.R.M., Georgiev, E., Selten, M., Simmons, R.G.F. 2021. Monitor Voortgang Verduurzaming Voedselketens: Aardappelen, groenten en fruit. Wageningen Economic Research, Wageningen.

Breukers, A., Stokkers, R., Spruijt, J., Roelofs, P., de Haan, J. 2014. Teelt de grond uit in perspectief: prestaties van teeltsystemen op het gebied van integrale duurzaamheid. Praktijkonderzoek Plant & Omgeving, Wageningen University and Research, Wageningen.

Graamans, L., Baeza, E., van den Dobbelsteen, A., Tsafaras, I., Stanghellini, C. 2018. Plant factories versus greenhouses: comparison of resource use efficiency. Agric. Syst. 160. 31–42. https://doi.org/10.1016/j.agsy.2017.11.003.

Khoshnevisan, B., Rafiee, S., Omid, M., Mousazadeh, H., Clark, S. 2014. Environmental impact assessment of tomato and cucumber cultivation in greenhouses using life cycle assessment and adaptive neuro-fuzzy inference system. J. Clean. Prod. 73, 183–192. http://dx.doi.org/10.1016/j.jclepro.2013.09.057.

Marchi, B., Zanoni, S. 2022. Energy efficiency in cold supply chains of the food and beverage sector. Transp. Res. Proc. 67, 56–62. https://doi.org/10.1016/j.trpro.2022.12.035.

Martin, M., Elnour, M., Sinol, A.C. 2023. Environmental life cycle assessment of a large-scale commercial vertical farm. Sustain. Prod. Consum. 40, 182–193. https://doi.org/10.1016/j.spc.2023.06.020.

Montero, J.I., Antón, A., Torrellas, M., Ruijs, M., Vermeulen, P., 2011a. Environmental and economic profile of present greenhouse production systems in Europe: EUPHOROS deliverable N 5 Final Report (No. Deliverable 5 Final Report). European Commission, Cabrils/Wageningen.

Montero, J.I., Antón, A., Torrellas, M., Ruijs, M., Vermeulen, P., 2011b. Environmental and economic profile of present greenhouse production systems in Europe: annex (No. Deliverable 5 Final Report). European Commission, Cabrils/Wageningen.

Pennisi, G., Orsini, F., Blasioli, S., Cellini, A., Crepaldi, A., Braschi, I., Spinelli, F., Nicola, S., Fernandez, J.A., Stanghellini, C., Gianquinto, G., Marcelis, L.F.M. 2019a. Resource use efficiency of indoor lettuce (Lactuca sativa L.) cultivation as affected by red:blue ratio provided by LED lighting. Sci. Rep. 9. 14127. https://doi.org/10.1038/s41598-019-50783-z.

Pennisi, G., Sanyé-Mengual, E., Orsini, F., Crepaldi, A., Nicola, S., Ochoa, J., Fernandez, J.A., Gianquinto, G. 2019b. Modelling Environmental Burdens of Indoor-Grown Vegetables and Herbs as Affected by Red and Blue LED lighting. Sustainability. 11(15), 4063. https://doi.org/10.3390/su11154063.

Pennisi, G., Blasioli, S., Cellini, A., Maia, L., Crepaldi, A., Braschi, I., Spinelli, F., Nicola, S., Fernandez, J.A., Stanghellini, C., Marcelis, L.F.M., Orsini, F., Gainquinto, G. 2019c. Unraveling the role of Red:Blue LED Lights on Resource Use Efficiency and Nutritional Properties of Indoor Grown Sweet Basil. Front. Plant Sci. 10. 305. https://doi.org/10.3389/fpls.2019.00305.

Pennisi., G., Pistillo, A., Orsini, F., Cellini, A., Spinelli, F., Nicola, S., Fernandez, J.A., Crepaldi, A., Gianquinto, G., Marcelis, L.F.M. 2020. Optimal light intensity for sustainable water and energy use in indoor cultivation of lettuce and basil under red and blue LEDs. Sci. Hortic. 272. https://doi.org/10.1016/j.scienta.2020.109508.

Raaphorst, M.G.M., Benninga, J. 2019. Kwantitatieve informatie voor de glastuinbouw 2019: kengetallen voor groenten-, snijbloemen-, pot- en perkplanten teelten. Wageningen University and Research, Wageningen.

Righini, I., Stangehellini, C., Hemming, S., Graamans, L., Marcelis, L.F.M. 2023. Resources for plant-based food: estimating resource use to meet the requirements of urban and peri-urban diets. Food Energy Secur. 12. https://doi.org/10.1002/fes3.462.

Schreuder, R., van Leeuwen, M., Spruijt, J., van der Voort, M., van Asperen, P., Hendriks- Goossens, V. 2009. Kwantitatieve informatie akkerbouw en vollegrondsteelt 2009. Wageningen University and Research, Lelystad.

Weidner, T., Yang, A., Hamm, M.W. 2021. Energy optimisation of plant factories and greenhouses for different climatic conditions. Energy Convers. Manag. 243. 114336. https://doi.org/10.1016/j.enconman.2021.114336.

Curriculum Vitae



Education

07/2020 – Current	PhD Candidate, Department of Architectural Engineering and Technology, Climate Design and Sustainability, Delft University of Technology
09/2015 – 01/2018	MSc Building Technology, Delft University of Technology
09/2011 – 07/2014	BSc Architecture and the Built Environment, Delft University of Technology

Work Experience

05/2018 – 07/2020	Researcher Climate Design and Sustainability, Delft University of Technology
11/2016 – 05/2017	Building Physics Consultant, Nieman Utrecht

Tess Blom was born on March 31st 1993 in Breda, the Netherlands. In September 2011, she started with the Bachelor of Architecture and the Built Environment at Delft University of Technology, where she successfully completed her Bachelor's degree in July 2014. In September 2015, she started with the Master's programme Building Technology at the same institution. In 2016, Tess took a temporary break from her Master's studies by taking on the role of Building Physics Consultant at Nieman, located in Utrecht, the Netherlands. Throughout her MSc studies she developed deep interest in the urban energy transition, which resulted in her thesis entitled "Delft in Transition: towards sustainable energy systems for Dutch Municipalities".

Following her graduation in 2018, Tess embarked on an academic career as researcher within the Climate Design and Sustainability chair at Delft University of Technology. In this role, she was involved in various research projects related to the energy transition of the built environment, ranging from urban to building scales. Notably, she contributed to the development of the MOOC (Massive Open Online Course) titled "Zero-Energy Design: an approach to make your building sustainable", and its professional counterpart, the ProfED Zero-Energy Design. The MOOC Zero-Energy Design received the edX Prize for Exceptional Contributions in Online Teaching and Learning in 2020. Tess was also involved as tutor in the campus course "Zero-Energy Design".

In July 2020, her research position led to a PhD position within the same chair, of which the results are presented in this dissertation. Beyond her research duties, Tess continued to participate as tutor in the campus course "Zero-Energy design", and provided guidance to students as Building Physics tutor for the bachelor course "Design and Engineering" and as graduation mentor for students of the Amsterdam Metropolitan Solutions Institute's Master programme MADE, and the Master Track in Building Engineering at Delft University of Technology.

List of publications

[*Under review*] Blom, T., Jenkins, A., Pulselli , R.M., van den Dobbelsteen, A.A.J.F. 2024. Synergetic Urban Agriculture: Life cycle based design of vertical farms integrated in urban energy systems. Frontiers in Built Environment and Urban Science.

Blom, T., Jenkins, A., van den Dobbelsteen, A.A.J.F. 2024. Synergetic urbanism: a theoretical exploration of a vertical farm as local heat source and flexible electricity user. Sustainable Cities and Society, 103.

Blom, T., Jenkins, A., van den Dobbelsteen, A.A.J.F. 2023. Synergetic integration of vertical farms in buildings: reducing the use of energy, water, and nutrients. Frontiers in Sustainable Food Systems, 2023, 29.

Blom, T., Jenkins, A., Pulselli, R.M., van den Dobbelsteen, A.A.J.F. 2022. The embodied carbon emissions of lettuce production in vertical farming, greenhouse horticulture, and open-field farming in the Netherlands. Journal of Cleaner Production, 337.

TOC



24#17

Synergetically integrated vertical farms

Reducing energy and resource use through synergies between vertical farms and cities

Tess Blom

Over the past decades, various farming methods have evolved to address global challenges of increasing food demands, decreasing availability of arable land, and climate change. One such method is vertical farming, which uses active climate systems and artificial lighting in stacked systems, enabling year-round, stable yields with minimal land-use. Vertical farms (VFs) are often advocated as sustainable, offering benefits such as efficient land-use, high yields, minimal water and nutrient use, no pesticides, and proximity to urban food demands. However, substantial electricity use for lighting and climate control poses a major challenge.

This study assesses the potential to integrate VFs in cities to reduce energy and resource use, and carbon emissions of both entities collectively. It compares the carbon footprint of VFs and conventional farming in the Netherlands, revealing that the substantial electricity use in VFs outweighs their benefits from a carbon footprint perspective. Additionally, it explores reusing residual heat from VFs for building heating at both building and urban scales. It also examines synergies such as reusing water and nutrients outputs from buildings in VFs, and attuning lighting with grid electricity availability.

Findings indicate that synergetic integration of VFs in cities can reduce collective energy use and carbon footprints of both VFs and cities. However, the overall carbon footprint of these cities surpasses that of cities relying on fossil-based heating and conventional farming. These increased emissions should be weighed against the benefits VFs bring to cities, including enhanced food security, self-sufficiency, replacement of fossil-based heating, efficient land-use, and grid flexibility. In conclusion, while VFs offer significant urban benefits, their high carbon footprint due to artificial lighting remains a challenge.

A+BE | Architecture and the Built Environment | TU Delft BK